CANCER AND BONE METASTASIS

EDITED BY: Chandi C. Mandal and Julie A. Sterling
PUBLISHED IN: Frontiers in Endocrinology

frontiers Research Topics

frontiers

ISSN 1664-8714
ISBN 978-2-88963-408-8
DOI 10.3389/978-2-88963-408-8

About Frontiers

Frontiers is more than just an open-access publisher of scholarly articles: it is a pioneering approach to the world of academia, radically improving the way scholarly research is managed. The grand vision of Frontiers is a world where all people have an equal opportunity to seek, share and generate knowledge. Frontiers provides immediate and permanent online open access to all its publications, but this alone is not enough to realize our grand goals.

Frontiers Journal Series

The Frontiers Journal Series is a multi-tier and interdisciplinary set of open-access, online journals, promising a paradigm shift from the current review, selection and dissemination processes in academic publishing. All Frontiers journals are driven by researchers for researchers; therefore, they constitute a service to the scholarly community. At the same time, the Frontiers Journal Series operates on a revolutionary invention, the tiered publishing system, initially addressing specific communities of scholars, and gradually climbing up to broader public understanding, thus serving the interests of the lay society, too.

Dedication to Quality

Each Frontiers article is a landmark of the highest quality, thanks to genuinely collaborative interactions between authors and review editors, who include some of the world's best academicians. Research must be certified by peers before entering a stream of knowledge that may eventually reach the public - and shape society; therefore, Frontiers only applies the most rigorous and unbiased reviews.
Frontiers revolutionizes research publishing by freely delivering the most outstanding research, evaluated with no bias from both the academic and social point of view. By applying the most advanced information technologies, Frontiers is catapulting scholarly publishing into a new generation.

What are Frontiers Research Topics?

Frontiers Research Topics are very popular trademarks of the Frontiers Journals Series: they are collections of at least ten articles, all centered on a particular subject. With their unique mix of varied contributions from Original Research to Review Articles, Frontiers Research Topics unify the most influential researchers, the latest key findings and historical advances in a hot research area! Find out more on how to host your own Frontiers Research Topic or contribute to one as an author by contacting the Frontiers Editorial Office: researchtopics@frontiersin.org

CANCER AND BONE METASTASIS

Topic Editors:
Chandi C. Mandal, Central University of Rajasthan, India
Julie A. Sterling, Vanderbilt University, United States

Citation: Mandal, C. C., Sterling, J. A., eds. (2020). Cancer and Bone Metastasis. Lausanne: Frontiers Media SA. doi: 10.3389/978-2-88963-408-8

Table of Contents

frontiers in Endocrinology

EDITORIAL
published: 04 December 2019
doi: 10.3389/fendo.2019.00852

Editorial: Cancer and Bone Metastasis

*Chandi C. Mandal**

Department of Biochemistry, Central University of Rajasthan, Ajmer, India

Keywords: cancer, microenvironment, bone metastases, osteolysis, stromal

Editorial on the Research Topic

Cancer and Bone Metastasis

INTRODUCTION

In spite of great efforts, cancer continues to be a leading cause of mortality and morbidity nationwide. Recent advances through innovation and discoveries in cancer biology have largely improved overall survival as well as quality of life in cancer patients. This is through the treatment of primary tumors, when the tumors are diagnosed at an early stage. The development of cancer metastases is still a deadly threat to cancer patients. Metastases frequently occur in bone tissue since it provides fertile nutrients to those disseminated tumor cells which had already traveled to bone environment. Bone is an active and dynamic tissue which is continuously remodeled by balanced and coordinated action of bone forming osteoblast and bone resorbing osteoclast cells. Dispersed tumor cells growing in the bone microenvironment often supply various cytokines/chemokines to bone resident cells. This eventually disrupts the balanced action between these two types of bone resident cells. Here, excess osteoclast activity leads to develop osteolytic lesions, whereas abnormal osteoblast activity drives to develop osteoblastic metastases. Indeed, cancer cells derive various cytokines (e.g., CSF-1, RANKL, DKK-1, JAGGED 1, etc.) either directly or indirectly which promote bone metastasis. Thus, the detailed mechanism for understanding the influence of bone microenvironment and adjacent stromal cells in the development of metastases is of urgent need. Understanding this process might identify targets in which one could design therapies for metastatic bone disease. Articles published on the topic "cancer and bone metastasis" have described important mechanisms and cellular interaction involved in bone metastasis.

INTERACTION BETWEEN CELLS AT METASTATIC NICHE

Osteolytic metastasis increases fracture risk and leads to develop cachexia. Guise TA research group described herein that this osteolytic metastasis also causes skeletal muscle weakness (Regan et al.). Increased oxidative stress caused by disseminated cancer cells might accelerate the pathological process of the sarcoplasmic Ca^{++} release from muscle cells to make the muscle weak. This would further potentiate fracture risk. In depth studies have found an involvement of TGF-β/NOX4/RyR1 signaling in breast cancer osteolyitc induced muscle weakness. In fact, disseminated cancer cells present in bone environment disrupts bone remodeling by altering the activity of osteoblast and osteoclast cells. Mechanical loading prevents bone metastasis. Lynch ME research

OPEN ACCESS

Edited and reviewed by:
Jonathan H. Tobias,
University of Bristol, United Kingdom

***Correspondence:**
Chandi C. Mandal
chandicmandal@gmail.com

Specialty section:
This article was submitted to Bone Research, a section of the journal Frontiers in Endocrinology

Received: *15 October 2019*
Accepted: *21 November 2019*
Published: *04 December 2019*

Citation:
Mandal CC (2019) Editorial: Cancer and Bone Metastasis. Front. Endocrinol. 10:852. doi: 10.3389/fendo.2019.00852

work suggested that in bone metastasis, mechanical loading increases osteocyte dendrite formation and downstream resorption (Wang et al.). This study further suggested that loading condition might increase and/or alter soluble factors (which are yet to be identified) to enhance osteocyte E11 expression and remodeling RANKL/OPG ratio along with decreasing osteocyte cells. Beside bone cells, various stromal cells including immune, endothelial, fibroblast, and adipocytes (directly or indirectly) modulate survival, dormancy, growth of disseminated cancer cells, and metastatic activity by supplying various factors and modulating intracellular signals, in addition to cell-cell interaction. Lynch research team highlighted the impact of bone resident macrophages on bone metastasis and cancer cell progression at metastatic sties. The factors CSF-1 and CCL2 released by disseminated cancer cells, recruit macrophages to the metastatic environment (Lo and Lynch). However, these recruited macrophages may polarize into pro-inflammatory and/or anti-inflammatory depending on the molecular and cellular components present at the metastatic niche. These polarized macrophages seem to have various roles in cancer progression and osteoblast/osteoclast activity. Uma Sankar research group also emphasized the recruitment of macrophages to the site of bone metastases by prostate cancer cells (Dadwal et al.).

CELLULAR SIGNALING FOR TARGET IDENTIFICATION AND THERAPY

Dadwal et al. outlined how androgen-deprivation therapy (ADT) not only affects bone health, but promote cancer resistance probably because of mutations in the androgen receptor (AR). Such mutations activate downstream CaMKK2 signaling even in the presence of very low androgen levels. Thus, targeting AR-CaMKK2 seems to be a therapeutic strategy for metastatic bone disease. Similarly, Suvannasankha group pointed out that blocking semaphoring 4D (Sema4D) may prevent osteolytic deposits along with inhibition of cancer progression both at the primary and metastatic sites (Lontos et al.). Both Sema4D and its receptor, Plexin B1 are often deregulated in various cancers. In addition, Sema4D expressed in mature osteoclast binds to Plexin B1 present on the osteoblast cell surface. This receptor ligand interaction not only inhibits osteoblast differentiation, but it also promotes angiogenesis. Galson DL research team reported that small molecule inhibitor, XRK3F2, reduced osteoclast activity along with the suppression of multiple myeloma (MM) growth (Adamik et al.). Moreover, this inhibitor blocks P62-ZZ domain signaling to rescue MM-suppressed osteoblast differentiation by reducing the transcriptional epigenetic repressor of RunX2, a key osteoblast differentiation factor. Martin TJ research study suggests that PTHrP might work differentially in disseminated cancer cells, and in bone osteoblast/osteocyte cells to promote metastases (Johnson et al.). They suggest that PTHrP potentiates the growth of cancer cells at the site of osteolytic deposits by reducing expression of tumor dormancy genes presumably via PTHR1/cyclic AMP-independent manner; whereas it can alter bone homeostasis by acting with osteoblast/osteocyte cells following canonical PTHR1/cyclic AMP signaling pathway.

The bone microenvironment also modulates the level of various microRNAs and could be targeted by specific metastatic therapy. In this context, Haider MT research group emphasized the role of various microRNAs in regulation of metastatic growth (Haider and Taipaleenmaki). For example; miR-34a, miR-133a, miR-141, and miR-219 inhibit osteoclast activity, whereas miR-135 and miR-203 prevent macrometastases. Similarly, miR-218 and miR-296 increase osteoblast and osteoclast activity, respectively. Thus, delivery of these microRNAs or antagomiRs can be used to limit disease progression in metastatic bone disease. Similarly, Reagah MR research team suggested that the use of proteasome inhibitors (PI) in controlling multiple myeloma induced bone disease will be more effective if PI resistance is overcome (Farrell and Reagan).

ADVANCED IMAGING AND SURGICAL PERSPECTIVE FOR METASTATIC BONE DISEASE

However, it is quite difficult to diagnose metastatic bone disease at an early stage. Silbermann R group suggested that various advanced imaging techniques including (i) skeletal survey (SS), (ii) whole body computed tomography (WBCT), and (iii) positron emission tomography-CT (PET-CT) could be used for the detection of very small sized osteolytic lesions. They also emphasized the improved combination of WBCT and 18F fluoro-deoxyglucose (FDG) PET-CT for visualizing bone marrow infiltration along with whole body tumor burden (Hansford and Silbermann). Similarly, both surgical and non-surgical multimodal treatment strategies are required to deal with metastatic bone disease. Choong PF research group emphasized that orthopedic surgeons have a critical role in the decision making to choose the most effective treatment strategy. This may depend on the site (e.g., femur, humerus, etc.) and bone metastasis type (e.g., breast, lung, etc.), since type of implants and surgical options available will influence the outcome (Soeharno et al.).

CONCLUSION

In brief, the articles published on the Research Topic "cancer and bone metastasis" emphasized the importance of various molecules, different cell types, and crucial signaling pathways working in various bone metastatic niches, and how they influence our understanding of metastatic bone disease. This is in addition to advancing imaging diagnostic techniques and various surgical options in dealing with such devastating disease. The Research Topic also suggested various non-surgical treatment options including proteasome inhibitors, small molecule inhibitors and microRNAs. Being an editor, I would like to express my gratitude to all the contributing

authors for providing valuable research manuscripts to this Research Topic.

AUTHOR CONTRIBUTIONS

CM has formulated and written the editorial.

FUNDING

CM was supported by Department of Biotechnology [6242-P9/RGCB/PMD/DBT/CCML/2015], University Grant Commissions [30-49/2014 (BSR)], and Department of Science and Technology (India)-Russian Foundation for Basic Research (INT/RUS/RFBR/P-256).

Conflict of Interest: The author declares that the research was conducted in the absence of any commercial or financial relationships that could be construed as a potential conflict of interest.

frontiers in Endocrinology

ORIGINAL RESEARCH
published: 19 December 2017
doi: 10.3389/fendo.2017.00358

Osteolytic Breast Cancer Causes Skeletal Muscle Weakness in an Immunocompetent Syngeneic Mouse Model

Jenna N. Regan[1], Carter Mikesell[1], Steven Reiken[2], Haifang Xu[3], Andrew R. Marks[2], Khalid S. Mohammad[1], Theresa A. Guise[1] and David L. Waning[3]**

[1] Department of Medicine, Indiana University School of Medicine, Indianapolis, IN, United States, [2] Department of Physiology and Cellular Biophysics, Columbia University College of Physicians and Surgeons, New York, United States, [3] Department of Cellular and Molecular Physiology, College of Medicine, Pennsylvania State University, Hershey, PA, United States

OPEN ACCESS

Edited by:
Julie A. Sterling, Vanderbilt University, United States

Reviewed by:
Antonia Sophocleous, University of Edinburgh, United Kingdom
Han Qiao, Shanghai Jiao Tong University, China

***Correspondence:**
Theresa A. Guise
tguise@iu.edu;
David L. Waning
dwaning@psu.edu

Specialty section:
This article was submitted to Bone Research, a section of the journal Frontiers in Endocrinology

Received: *31 October 2017*
Accepted: *07 December 2017*
Published: *19 December 2017*

Citation:
Regan JN, Mikesell C, Reiken S, Xu H, Marks AR, Mohammad KS, Guise TA and Waning DL (2017) Osteolytic Breast Cancer Causes Skeletal Muscle Weakness in an Immunocompetent Syngeneic Mouse Model. Front. Endocrinol. 8:358. doi: 10.3389/fendo.2017.00358

Muscle weakness and cachexia are significant paraneoplastic syndromes of many advanced cancers. Osteolytic bone metastases are common in advanced breast cancer and are a major contributor to decreased survival, performance, and quality of life for patients. Pathologic fracture caused by osteolytic cancer in bone (OCIB) leads to a significant (32%) increased risk of death compared to patients without fracture. Since muscle weakness is linked to risk of falls which are a major cause of fracture, we have investigated skeletal muscle response to OCIB. Here, we show that a syngeneic mouse model of OCIB (4T1 mammary tumor cells) leads to cachexia and skeletal muscle weakness associated with oxidation of the ryanodine receptor and calcium (Ca^{2+}) release channel (RyR1). Muscle atrophy follows known pathways *via* both myostatin signaling and expression of muscle-specific ubiquitin ligases, atrogin-1 and MuRF1. We have identified a mechanism for skeletal muscle weakness due to increased oxidative stress on RyR1 *via* NAPDH oxidases [NADPH oxidase 2 (Nox2) and NADPH oxidase 4 (Nox4)]. In addition, SMAD3 phosphorylation is higher in muscle from tumor-bearing mice, a critical step in the intracellular signaling pathway that transmits TGFβ signaling to the nucleus. This is the first time that skeletal muscle weakness has been described in a syngeneic model of OCIB and represents a unique model system in which to study cachexia and changes in skeletal muscle.

Keywords: breast cancer, osteolytic disease, muscle weakness, immune competent, syngeneic tumor model

INTRODUCTION

Breast cancer is the most common cancer in women (1) and frequently metastasizes to bone in advanced disease (2). Healthy bone has endocrine functions that are achieved both by active signaling from bone cells such as osteoblasts and osteocytes as well as passive release of cytokines and minerals stored in the bone matrix. However, in the tumor–bone microenvironment, breast cancer cells secrete factors that stimulate osteoclast-mediated bone resorption. The increased resorption, in turn, greatly increases the release of signaling factors from the mineralized matrix, including TGFβ. This further promotes cancer cell invasion, growth, and osteolytic factor production to fuel a feed-forward vicious cycle that induces more bone destruction (3–6). Increased bone resorption

also causes skeletal complications such as bone pain, fractures, hypercalcemia, and nerve compression syndromes (6).

Skeletal muscle weakness is a debilitating consequence of many advanced malignancies. Muscle is one of the organ systems responsive to bone-derived signals. Thus, conditions such as osteolytic cancer in bone (OCIB) that disrupt the balance of normal bone resorption (7, 8) may also have detrimental effects on skeletal muscle. We have recently shown that a significant reduction in skeletal muscle function occurs in mice with osteolytic bone metastases from breast, prostate, and lung cancer and in multiple myeloma (9).

In normal muscle contraction, the ryanodine receptor calcium (Ca^{2+}) release channel (RyR1) is activated, leading to the release of Ca^{2+} from the sarcoplasmic reticulum (SR) and causing muscle contraction. Ca^{2+} is then pumped back into the SR during relaxation by the sarcoplasmic/endoplasmic reticulum Ca^{2+} ATPase. Physiological oxidation is a normal signaling mediator in skeletal muscle whereas pathological oxidation of RyR1 leads to channel Ca^{2+} leak and muscle weakness (10, 11). We have previously shown that RyR1 oxidation and loss of its stabilizing subunit, calstabin1 (also known as FKBP12), is a biochemical signature of RyR1 channel Ca^{2+} leak in OCIB (9). This biochemical signature was also present in skeletal muscle samples taken from patients with breast cancer that had metastasized to bone, validating the clinical importance of our model systems. NADPH oxidase 4 (Nox4), a constitutively active oxidase and TGFβ target gene, is the source of reactive oxygen species in our models of OCIB that lead to skeletal muscle weakness. These data collectively describe a novel TGFβ-Nox4-RyR1 axis responsible for skeletal muscle weakness in OCIB (9).

The studies described above used human tumor cells, which made it necessary to perform the experiments in immunocompromised mice. Thus, we wondered whether the presence of a functional immune system would alter the TGFβ-Nox4-RyR1 axis that we identified. The present study addresses this question using a syngeneic murine model of breast cancer that is osteolytic in bone (4T1 cells). We have found that mice with 4T1 OCIB develop profound skeletal muscle weakness and cachexia within 4 weeks of tumor cell inoculation to bone. SMAD3 phosphorylation, the relative expression of Nox4 mRNA, and Nox4-RyR1 binding were higher in muscle from mice with 4T1 OCIB, consistent with disruption of the TGFβ-Nox4-RyR1 axis (9). In addition, skeletal muscle fiber diameter was reduced, and mRNA expression of the atrophy-related muscle-specific ubiquitin ligases, atrogin-1 and MuRF1, were higher in mice with OCIB than non-tumor control animals. The relative expression of myostatin mRNA, a strong mediator of muscle atrophy, was also higher in mice with OCIB. These data indicate that a syngeneic model of OCIB shows both muscle weakness due to Ca^{2+} mishandling and activation of a muscle atrophy program.

RESULTS

Weight Loss in Mice with 4T1 OCIB

To investigate skeletal muscle changes in an immune competent model of OCIB, we used 4T1 mouse stage IV breast cancer cells (12). We inoculated 100,000 cells (non-tumor mice received PBS), directly into the right tibia of 5-week old female Balb/c mice. Mice with 4T1 cells in bone exhibit osteolytic lesions as detected by X-ray (13–15). In our study, we confirmed this result at 4-week postinoculation (**Figure 1A**). We also found that mice with 4T1 OCIB had progressive weight loss starting at approximately 14-day postinoculation (**Figure 1B**). At 4-week postinoculation, mice with 4T1 OCIB had lower individual skeletal muscle weights measured following dissection. The extensor digitorum longus (EDL), tibialis anterior (TA), soleus (SOL), and gastrocnemius (Gastroc) muscles were dissected from hindlimb contralateral to the site of inoculation and weighed intact (**Figure 1C**). Mice with 4T1 OCIB also had lower lean (**Figure 1D**) and fat (**Figure 1E**) content as measured by dual energy X-ray absorptiometry (DXA). Lean and fat mass was measured both as absolute value at 4-week postinoculation and as the percentage change over the baseline reading (**Figures 1D,E**).

4T1 Osteolytic Bone Lesions Cause Skeletal Muscle Atrophy

Because mice with 4T1 OCIB lost lean mass, we investigated known mechanisms of skeletal muscle atrophy. Skeletal muscle fiber cross-sectional area was lower in mice with 4T1 OCIB than in non-tumor control mice (**Figure 2A**). We measured cross-sectional area from H&E stained histological sections from the Gastroc muscle dissected from the side contralateral to tumor cell inoculation. At least 200 fibers were measured from histological sections taken from three samples from each group. Mice with 4T1 OCIB also had higher relative mRNA expression of myostatin, a strong negative regulator of skeletal muscle mass (16), compared to non-tumor controls (**Figure 2B**). In addition to myostatin, we also measured the relative expression of FOXO3a and its downstream targets atrogin-1 and MuRF1. The muscle-specific ubiquitin ligases atrogin-1 and MuRF1 are induced by FOXO3a by two distinct mechanisms during skeletal muscle atrophy (17–19). We found that the relative mRNA expression of FOXO3a, atrogin-1, and MuRF1 were all increased in mice with 4T1 OCIB compared to non-tumor control mice (**Figure 2C**).

Skeletal Muscle Weakness in Mice with 4T1 OCIB

To determine skeletal muscle function in mice with 4T1 OCIB, we measured *in vivo* forelimb grip strength over the course of the experiment and at 4-week postinoculation we measured whole muscle contractility of the excised EDL muscle. Mice with 4T1 OCIB developed muscle weakness measured by forelimb grip strength starting at approximately 3-week postinoculation (**Figure 3A**). Whole muscle contractility of the excised EDL muscle showed lower muscle-specific force in tumor-bearing mice compared to non-tumor control animals (**Figure 3B**). Specific force corrects for differences in muscle size between individual animals and test groups (20). We also observed higher EDL fatigability in mice with 4T1 OCIB. Fatigue was tested by repeated whole muscle tetanic stimulation (**Figure 3C**). Finally, from our whole muscle contractility studies we determined the half-relaxation time of twitch stimulation of the EDL from mice with 4T1 OCIB. Tumor mice had a slower relaxation time compared

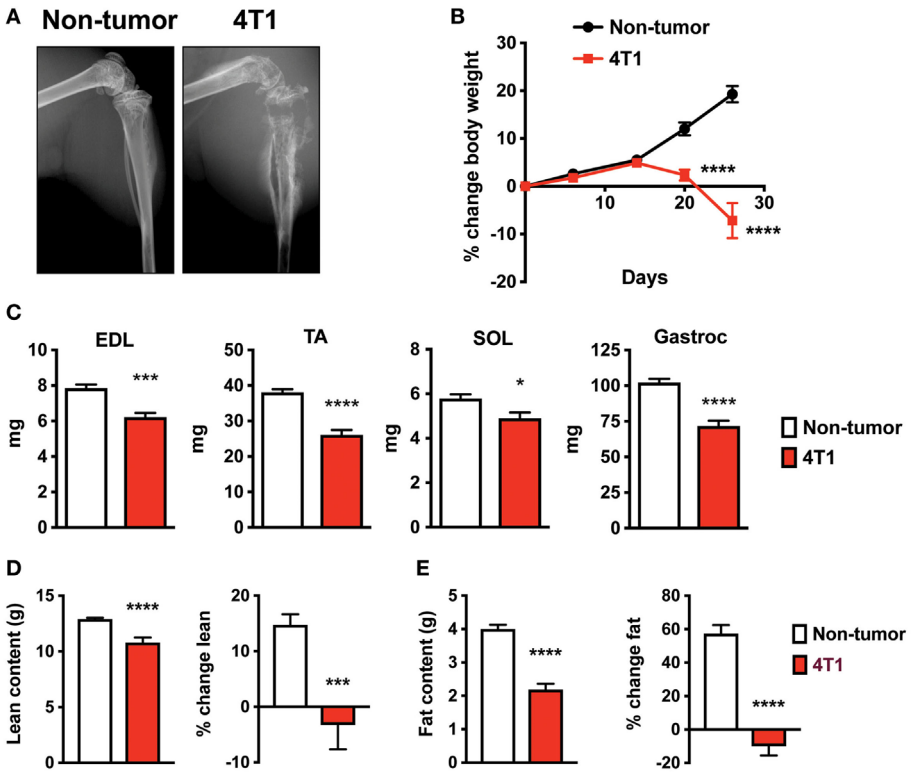

FIGURE 1 | Mouse breast cancer 4T1 osteolytic cancer in bone (OCIB) leads to osteolysis and body weight loss. **(A)** X-ray analysis revealed large osteolytic lesions in mice receiving 4T1 cell *via* intratibial injection at 4-week postinjection. **(B)** Body weight loss in mice with 4T1 OCIB (percentage change in total body weight over baseline) ($n = 10$). **(C)** Weight loss of individual muscles dissected from the lower hindlimb ($n = 10$) of mice with 4T1 OCIB; extensor digitorum longus (EDL), tibialis anterior (TA), soleus (SOL), and gastrocnemius (Gastroc) compared to non-tumor control mice. Dual energy X-ray absorptiometry (DXA) scan revealed loss of both **(D)** lean content and **(E)** fat content in mice with 4T1 OCIB at 4-week postinjection ($n = 10$). Data are mean ± SEM, **(B)** two-way analysis of variance with Bonferroni post-test; **(C–E)** *t*-test. $^{*}p < 0.05$, $^{***}p < 0.001$, and $^{****}p < 0.0001$.

to non-tumor control mice (**Figure 3D**) indicating dysfunctional Ca^{2+} handling in muscle.

RyR1 Oxidation in Skeletal Muscle of Mice with 4T1 OCIB

Increased oxidative stress is a characteristic of advanced breast cancer (21). Oxidation of RyR1 channels and reduced binding of the stabilizing subunit, calstabin1, in skeletal muscle result in pathological SR Ca^{2+} leak that is associated with muscle weakness (9–11). Indeed, skeletal muscle RyR1 channels from mice with 4T1 OCIB were oxidized, nitrosylated, and depleted of calstabin compared to non-tumor control mice (**Figure 4A**). We have previously shown that a major source of oxidative stress in OCIB is expression of Nox4 (9), a constitutively active Nox protein. Nox4 is a TGFβ target gene that is upregulated following the release of TGFβ from the bone matrix during OCIB (9). Mice with 4T1 OCIB showed higher SMAD3 phosphorylation, indicative of TGFβ signaling, compared to non-tumor control mice (**Figure 4B**). We also found higher relative mRNA expression of Nox4 and higher levels of direct Nox4-RyR1 binding compared to non-tumor control mice (**Figures 4C,D**). Our data also indicate an upregulation of NADPH oxidase 2 (Nox2) (**Figure 4E**) which could serve as another source of oxidative stress in muscle from mice with 4T1 OCIB. Nox2 and Nox4 are both induced in response to TGFβ in certain cell types (22), but interestingly, we did not observe upregulation of Nox2 mRNA in muscle in our previous studies using human tumor cells in athymic nude mice (9). The regulation of Nox2 gene expression in muscle represents a difference between immunocompetent and immunosuppressed mouse models of OCIB. Nox2 is thought to predominantly function in phagocytes (23) and activity of these cells in athymic nude mice may actually be enhanced (24). Thus, the role of Nox2 and Nox4 in OCIB-induced oxidative stress still needs to be determined.

DISCUSSION

Muscle weakness and cachexia are significant paraneoplastic syndromes of many advanced cancers. In the present study, we have investigated skeletal muscle weakness in a syngeneic mouse model of OCIB. Primary mouse 4T1 breast cancers are highly metastatic, including an affinity for bone, where the cells are aggressively osteolytic (14). Inoculating 4T1 tumor cells directly into the bone recapitulates the bone destruction (**Figure 1A**), while limiting metastasis to other organs and allowing investigation of bone to muscle signaling in the setting of OCIB. While we did observe metastases of 4T1 cells to lung,

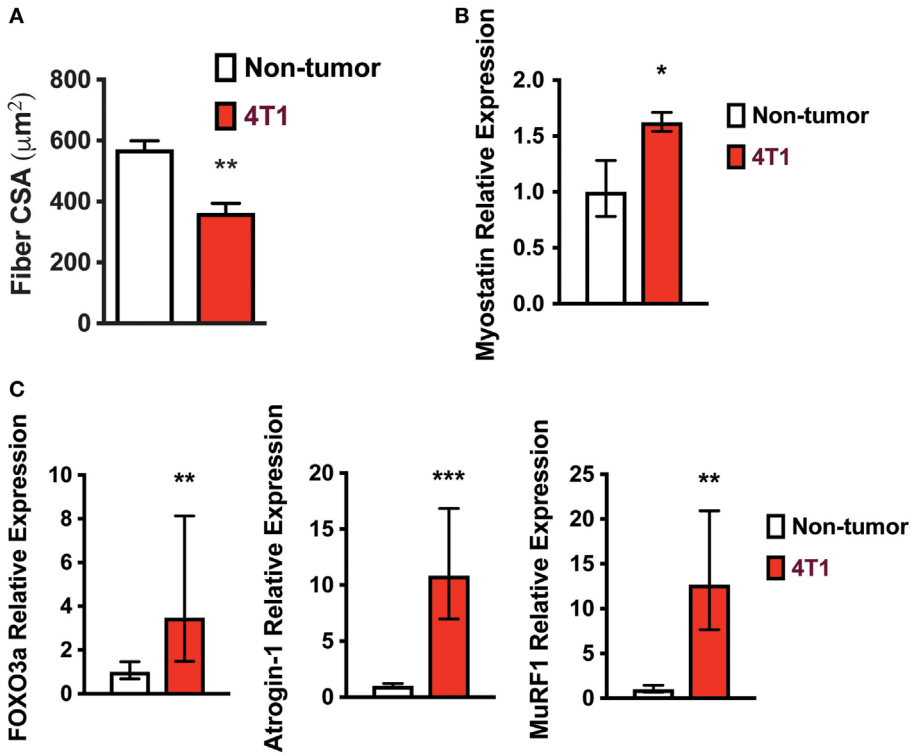

FIGURE 2 | Skeletal muscle fiber size is lower in mice with 4T1 osteolytic cancer in bone (OCIB). **(A)** Gastrocnemius muscle fiber diameter was lower in mice with 4T1 OCIB ($n = 3$ histological sections) compared to non-tumor control mice. **(B)** Relative myostatin mRNA expression in tibialis anterior (TA) muscle from non-tumor mice and mice with 4T1 OCIB ($n = 6$). **(C)** Relative FOXO3, atrogin-1, and MuRF1 mRNA expression in TA muscle from non-tumor mice and mice with 4T1 OCIB ($n = 6$). **(A)** Data are mean ± SEM, error bars in **(B,C)** represent ddCt ± SD propagated to fold change, **(A–C)** *t*-test. $^{*}p < 0.05$, $^{**}p < 0.01$, and $^{***}p < 0.001$.

the number of cells inoculated and the time postinoculation were optimized for assessment of skeletal muscle changes in response to osteolytic lesion development. Importantly, this syngeneic system allows for the study of pathways important for changes in both muscle mass and muscle function in animals with an intact immune system and mimics the bone destruction and bone–muscle crosstalk that occur in humans with breast cancer bone metastases (9).

We have previously shown that TGFβ released from the bone matrix during osteolysis due to breast cancer bone metastases causes oxidative stress and skeletal muscle Ca^{2+} leak and weakness *via* the TGFβ-Nox4-RyR1 axis (9). This mechanism was elucidated in athymic nude mice to accommodate the use of human breast cancer cells (MDA-MB-231, ZR-75-1, and MCF-7), human lung cancer cells (RWGT2 and A549), human prostate cancer cells (PC-3), and human multiple myeloma cells (JJN-3). In addition, mice with MDA-MB-231, MCF-7, A549, or PC-3 bone metastases also develop cachexia that is independent of the reduction in skeletal muscle function.

While our previous studies strongly implicate bone-to-muscle signaling as the root cause of the skeletal muscle weakness, we felt it was important to investigate whether the presence of a functional immune system significantly alters OCIB-driven muscle weakness since this represents a major difference between the mouse models and human patients. In the present study, we have shown that mice with 4T1 OCIB develop both cachexia and skeletal muscle weakness. Myostatin expression and activation of the ubiquitin ligases atrogin-1 and MuRF1 downstream of FOXO3a are hallmarks of skeletal muscle atrophy (16–19) and are likely responsible for the cachexia in the 4T1 OCIB model. In addition, we determined that these immune competent mice display the same biochemical signature of RyR1 oxidation leading to skeletal muscle SR Ca^{2+} leak as immunodeficient mice with human tumor cells (9). The TGFβ signal mediator SMAD3 is phosphorylated in mice with 4T1 OCIB and that the relative expression of Nox4 mRNA and Nox4-RyR1 binding is higher than in non-tumor control mice. Overall, these data recapitulate those described in athymic nude mice and suggest that immune functionality does not significantly alter OCIB-induced cachexia or muscle weakness.

MATERIALS AND METHODS

Animals

Female Balb/c mice were obtained from Harlan (Indianapolis, IN, USA) at 5 weeks of age. All experiments with animals were performed at the Indiana University School of Medicine (IUSM) and approved by Indiana University's Institutional Animal Care and Use Committee (IACUC).

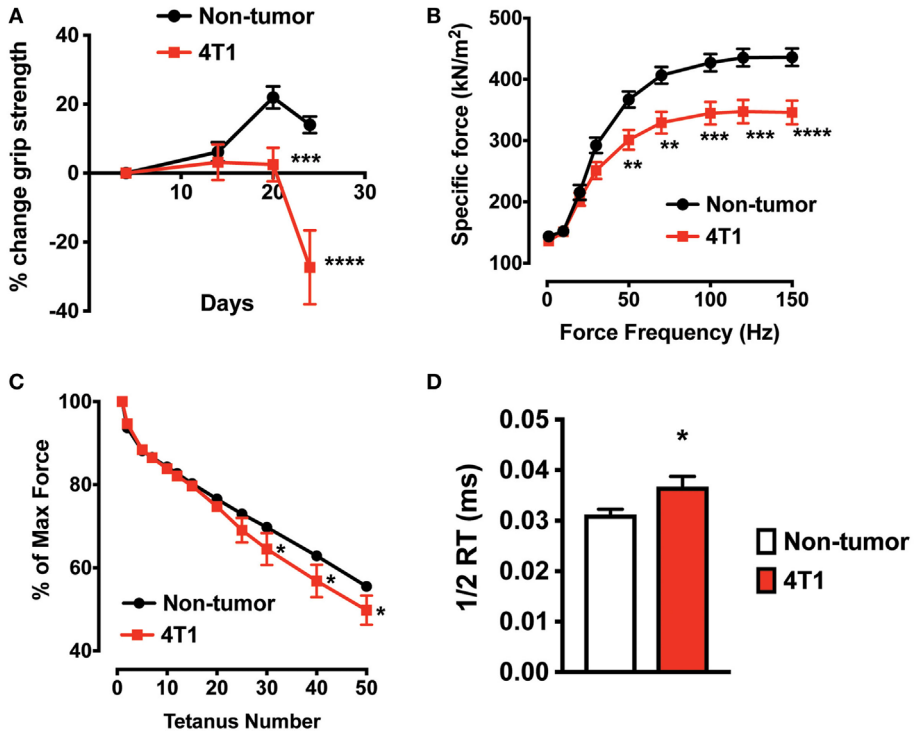

FIGURE 3 | Skeletal muscle weakness in mice with 4T1 osteolytic cancer in bone (OCIB). **(A)** *In vivo* forelimb grip strength ($n = 10$) and **(B)** excised whole muscle contractility of the extensor digitorum longus (EDL) muscle ($n = 10$) were lower in mice with 4T1 OCIB. **(C)** Skeletal muscle fatigue was higher in mice with 4T1 cells in bone (percent of maximum force) ($n = 10$). **(D)** Half-relaxation time (1/2 RT) was higher in EDL from mice with 4T1 OCIB compared to non-tumor control mice. Data are mean ± SEM, **(A,B,C)** two-way analysis of variance with Bonferroni post-test, **(D)** *t*-test. $^{*}p < 0.05$, $^{**}p < 0.01$, $^{***}p < 0.001$, and $^{****}p < 0.0001$.

Ethics Statement

In all studies, mice were handled and euthanized in accordance with approved institutional and national guidelines set forth by the Indiana University IACUC and the Laboratory Animal Resource Center at the IUSM. This facility is fully accredited by the American Association for the Accreditation of Laboratory Animal Care, International and is registered with the USDA as a Research Facility.

Materials

Antibodies: Anti-RyR (Affinity Bioreagents, cat. no. MA3-916, Golden, CO, USA; 1:2,000), anti-RyR1 5029 (custom rabbit polyclonal antibody raised against the C-terminus of human RyR1, Yenzyme, South San Francisco, CA, USA; 1:250 for IP), anti-Cys NO antibody (Sigma, cat. no. N0409, St. Louis, MO, USA; 1:2,000), anti-calstabin antibody (Santa Cruz Biotechnology, cat. no. sc-6173, Santa Cruz, CA, USA, 1:2,500), anti-DNP (Oxyblot, cat. no. S7150, Millipore, Darmstadt, Germany; 1:250), anti-pSMAD3 (Abcam, cat. no. ab40854, Cambridge, UK; 1:1,000), anti-SMAD3 (Abcam, cat. no. 52903, Cambridge, UK; 1:1,1000), and anti-Nox4 (Abcam, cat. no. 109225, Cambridge, UK; 1:1,000).

Cell Culture

4T1 breast cancer cells (ATCC, CRL-2539, Manassas, VA, USA) were cultured in Dulbecco's modified Eagle's media (Hyclone, Logan, UT, USA) containing 10% heat-inactivated fetal bovine serum. Cells were maintained at 37°C with 5% CO_2 in a humidified chamber.

In Vivo Models

Intratibial inoculation of tumor cells was performed on 5-week old female Balb/c mice. Tumor cells were trypsinized, washed twice in sterile ice cold PBS, and resuspended in ice cold PBS to a final concentration of 10^5 cells in 20 µl. Mice were anesthetized (ketamine and xylazine) and inoculated in the proximal tibia using a 27-gauge needle. 100,000 cells (or PBS for non-tumor controls) were inoculated into the right tibia of each animal. Measurements of muscle weight and muscle function were done using the hindlimb contralateral to the side of tumor cell inoculation.

Radiography

The presence of osteolytic lesions was visualized by radiography on a Kubtec digital X-ray imager (Kubtec, Milford, CT, USA). Mice were placed in a prone position and imaged at 2.7× magnification. The investigators were blinded to treatment subjects.

Dual Energy X-ray Absorptiometry

Body composition (lean and fat content) was determined using a PIXImus mouse densitometer (GE Lunar II, Faxitron Corp., Tucson, AZ, USA). Mice were anesthetized and placed with limbs spread on an adhesive tray in a prone position. Measurements

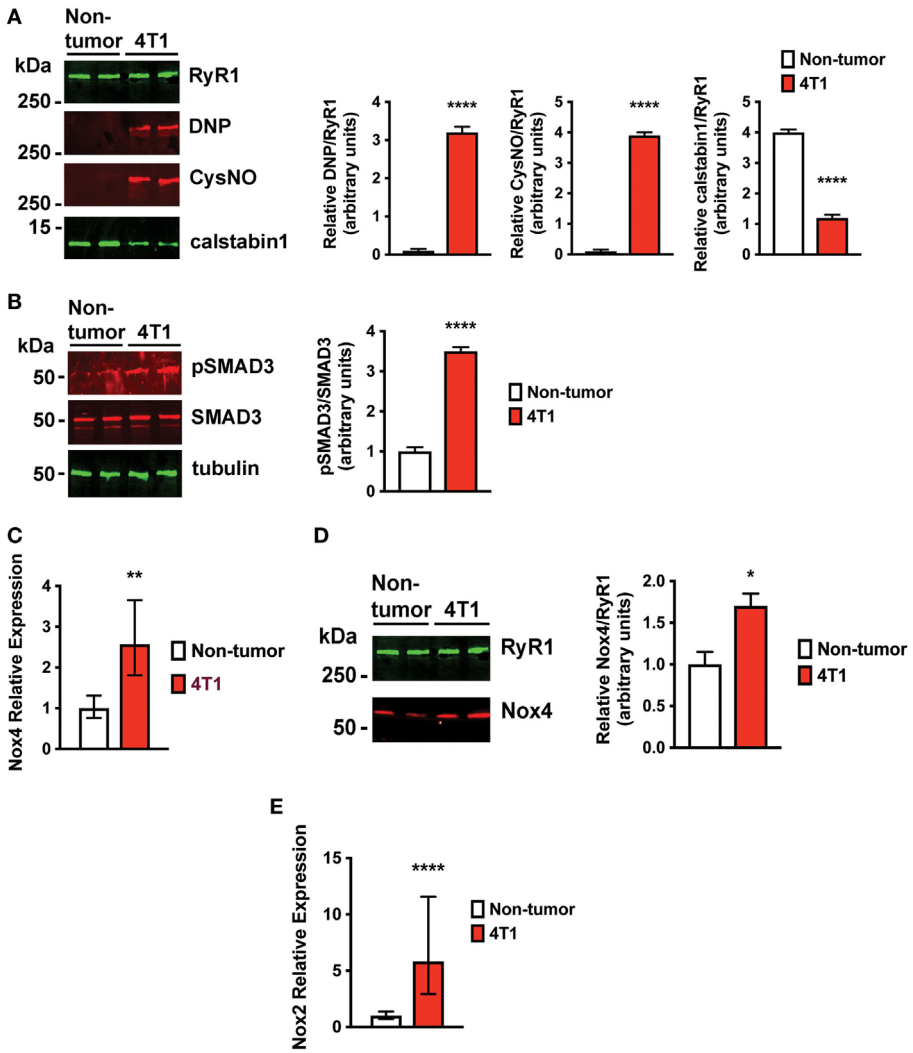

FIGURE 4 | Skeletal muscle ryanodine receptor oxidation and SMAD3 phosphorylation are higher in mice with 4T1 osteolytic cancer in bone (OCIB). **(A)** Immunoblot (left) and quantification (right) of RyR1 oxidation (DNP) and nitrosylation (CysNO) and of RyR1-calstabin1 binding, as measured by coimmunoprecipitation, from extensor digitorum longus (EDL) muscle ($n = 4$). RyR1 was oxidized and depleted of calstabin1 in mice with 4T1 OCIB. **(B)** Immunoblot of SMAD3 phosphorylation (left) and quantification (right) from muscle revealed increased phosphorylation in mice with 4T1 OCIB compared to non-tumor control mice ($n = 4$). **(C)** Relative NADPH oxidase 4 (Nox4) mRNA expression was higher in tibialis anterior (TA) muscle from mice with 4T1 OCIB than in non-tumor control mice ($n = 6$). **(D)** Immunoblot (left) and quantification (right) of Nox4 coimmunoprecipitation with RyR1 from EDL muscle revealed higher Nox4 interaction with RyR1 in muscle from mice with 4T1 OCIB ($n = 4$). **(E)** Relative NADPH oxidase 2 (Nox2) mRNA expression was higher in TA muscle from mice with 4T1 OCIB than in non-tumor control mice ($n = 6$). **(A,B,D)** Data are mean ± SEM, error bars in **(C,E)** represent ddCt ± SD propagated to fold-change, **(A,B,D)** *t*-test. $^{*}p < 0.05$, $^{**}p < 0.01$, and $^{****}p < 0.0001$.

were performed and analyzed excluding the calvarium, mandible, and teeth. Values for lean and fat content were expressed as both a final absolute value and as a percentage change over the baseline scan. The investigators were blinded to treatment of subjects.

Grip Strength

Forelimb grip strength was assessed by allowing each mouse to grab a wire mesh attached to a force transducer (Bioseb, Vitrolles, France) that records the peak force generated as the mouse is pulled by the tail horizontally away from the mesh. The investigators were blinded to treatment of subjects.

Muscle Function

Whole muscle contractility of the EDL muscles was determined as previously described (9). EDL was dissected from hind limbs, and stainless steel hooks were tied to the tendons of the muscles using 4-0 silk sutures, and the muscles were mounted between a force transducer (Aurora Scientific, Aurora, ON, Canada) and an adjustable hook. The muscles were immersed in a stimulation chamber containing O_2/CO_2 (95/5%) bubbled Tyrode solution (121 mM NaCl, 5.0 mM KCl, 1.8 mM $CaCl_2$, 0.5 mM $MgCl_2$, 0.4 mM NaH_2PO_4, 24 mM $NaHCO_3$, 0.1 mM EDTA, and 5.5 mM glucose). The force–frequency

relationships were determined by stimulation of 0.5 ms pulses at 1–150 Hz for 350 ms with rest for 3 min between stimulations. Fatigue of the muscle was determined by calculating the percentage of maximum force generated at repeated tetanic stimulations. To quantify the specific force, the absolute force was normalized to the muscle size (20). The half-relaxation time was determined during muscle stimulations during twitch stimulation. The investigators were blinded to treatment of subjects.

RyR1 Immunoprecipitation and Immunoblotting

RyR1 oxidation and nitrosylation and calstabin1 binding were determined from EDL muscles as previously described (9). Immunoblots were developed and quantified using the Odyssey Infrared Imaging System (LI-COR Biosciences, Lincoln, NE, USA) and infrared-labeled secondary antibodies. Detection of Nox4 (Abcam, Cambridge, UK; 1:1,000) was from immunoprecipitated RyR1 as described above. Detection of pSMAD3, SMAD3 (Abcam, Cambridge, UK; 1:1,000 each), and tubulin (Sigma, St. Louis, MO, USA; 1:500 each) from mouse muscle was *via* lysis in NP-40 buffer, and detection and quantification of immobilized proteins using the Odyssey Infrared Imaging System. The investigators were blinded to treatment of subjects.

Semi-Quantitative RT-PCR

Tibialis anterior muscle was lysed by dounce homogenization in Trizol (Invitrogen) for RNA extraction. One-fifth volume chloroform was added to lysates and vortexed vigorously for 15 s and incubated at room temperature for 3 min. Samples were loaded onto GenElute mammalian total RNA mini columns (Sigma). DNase I treatment was performed to remove genomic DNA contamination (Qiagen), and RNA integrity was assessed on agarose gels. RNA was reverse transcribed using Superscript II (Invitrogen) with anchored oligo(dT) (Promega) for priming. The cDNAs were prepared for semiquantitative real-time PCR using HotStart-IT SYBR Green PCR Kit (Affymetrix) and analyzed in a CFX96 Real-Time PCR Detection System (BioRad) for 40 cycles (95°C for 15 s, 58°C 30 s, and 72°C for 30°s) after an initial 2 min incubation at 95°C. Target gene expression (Nox2 and Nox4), FOXO3a, atrogin-1, MuRF1, and myostatin were normalized against the housekeeping gene β2-microglobulin (B2M), and data were analyzed using the ΔΔCt method. Primers: B2M forward: 5′-CTG ACC GGC CTG TAT GCT AT-3′; B2M reverse 5′-CAG TCT CAG TGG GGG TGA AT-3′; Nox2 forward 5′-CCC TTT GGT ACA GCC AGT GAA GAT-3′; Nox2 reverse 5′-CAA TCC CGG CTC CCA CTA ACA TCA-3′; Nox4 forward 5′-GGA TCA CAG AAG GTC CCT AGC AG-3′; Nox4 reverse 5′-GCG GCT ACA TGC ACA CCT GAG AA-3′; FOXO3 forward 5′-CAG GCT CCT CAC TGT ATT CAG CTA-3′; FOXO3 reverse 5′-CAT TGA ACA TGT CCA GGT CCA A-3′, atrogin-1 forward 5′-GCA GAG AGT CGG CAA GTC-3′, atrogin-1 reverse 5′-CAG GTC GGT GAT CGT GAG-3′, MuRF1 forward 5′- GCT GGT GGA AAA CAT CAT TGA CAT-3′, and MuRF1 reverse 5′-ACT GGA GCA CTC CTG CTT GTA GAT-3′.

Statistical Analysis

The data are presented as mean ± SEM. Differences among experimental groups were analyzed by *t*-tests or analysis of variance (ANOVA) with appropriate *post hoc* and multiple comparison tests. For single time point measures of any sample size, a two-sided *t*-test was used (25). When more than two groups were compared simultaneously ANOVA, followed by Bonferroni *post hoc* tests, was used (e.g., force–frequency comparison between control and tumor bearing groups). *p*-Values less than 0.05 were considered significant ($^{*}p < 0.05$; $^{**}p < 0.01$; $^{***}p < 0.0005$; and $^{****}p < 0.0001$). Statistical analyses were performed with Prism 6.0 software (GraphPad Prism, La Jolla, CA, USA). The number of mice required to assess muscle function in mice with OCIB was determined by power analysis using previous data on improvement in muscle function in mice with bone metastases. From the mean difference in specific force production with OCIB vs vehicle was 42% (275 vs 390 kN/m^2) with SD = 64 kN/m^2. Assuming α error rate = 0.05 and β error rate = 0.20, and a more conservative 30% mean difference (275–360), the minimum number of animals per group needed is $n = 8$ for a two-sided Student's *t*-test. Based on the experience of the Investigators, approximately 80% of mice injected develop tumors; so 10 mice per group were used. Exclusion plan: EDL-specific force data were excluded in cases where there was evidence of damage to the muscle fibers. This exclusion plan was pre-established. Female Balb/c mice received from Harlan (Indianapolis, IN, USA) were randomized into groups upon arrival.

ETHICS STATEMENT

In all studies, mice were handled and euthanized in accordance with approved institutional and national guidelines set forth by the Indiana University Institutional Animal Care and Use Committee and the Laboratory Animal Resource Center (LARC) at the Indiana University School of Medicine (IUSM). This facility is fully accredited by the American Association for the Accreditation of Laboratory Animal Care, International (AAALAC) and is registered with the USDA as a Research Facility.

AUTHOR CONTRIBUTIONS

All contributing authors have agreed to submission of this manuscript for publication. JR, AM, KM, TG, and DW conceived of the study. JR, AM, KM, TG, and DW designed experiments, analyzed data, and interpreted results. JR, KM, CM, SR, HX, and DW performed experiments. JR, KM, TG, and DW wrote the manuscript.

ACKNOWLEDGMENTS

This work was supported by the US National Institutes of Health (NIH) (grant CA205437 (DW) from the National Cancer Institute (NCI) Research Answers to NCI's Provocative Questions, and grant CA143057 (TG) from the National Cancer Institute (NCI) Tumor Microenvironment Network), the American Cancer Society and Indiana University Simon Cancer Center (grant IRG-84-002-28;

DW), the Indiana University Health Strategic Research Initiative in Oncology (DW), the Phi Beta Psi National Project (DW), The Pennsylvania State University College of Medicine (DW), the Susan G. Komen Foundation (grant SAC110013; TG), the Jerry and Peggy Throgmartin Endowment of the Indiana University Simon Cancer Center Breast Cancer Program (TG), and the Indiana University School of Medicine Student Research Program in Academic Medicine (SPRinAM) (CM).

REFERENCES

1. Howlader N, Noone AM, Krapcho M, Garshell J, Miller D, Altekruse SF, et al. *SEER Cancer Statistics Review, 1975–2011*. Bethesda, MD: National Cancer Institute (2014). Available from: http://seer.cancer.gov/csr/1975_2011/
2. Coleman RE. Metastatic bone disease: clinical features, pathophysiology and treatment strategies. *Cancer Treat Rev* (2001) 27(3):165–76. doi:10.1053/ctrv.2000.0210
3. Coleman RE, Lipton A, Roodman GD, Guise TA, Boyce BF, Brufsky AM, et al. Metastasis and bone loss: advancing treatment and prevention. *Cancer Treat Rev* (2010) 36(8):615–20. doi:10.1016/j.ctrv.2010.04.003
4. Kang Y, He W, Tulley S, Gupta GP, Serganova I, Chen CR, et al. Breast cancer bone metastasis mediated by the Smad tumor suppressor pathway. *Proc Natl Acad Sci U S A* (2005) 102(39):13909–14. doi:10.1073/pnas.0506517102
5. Korpal M, Yan J, Lu X, Xu S, Lerit DA, Kang Y. Imaging transforming growth factor-beta signaling dynamics and therapeutic response in breast cancer bone metastasis. *Nat Med* (2009) 15(8):960–6. doi:10.1038/nm.1943
6. Weilbaecher KN, Guise TA, McCauley LK. Cancer to bone: a fatal attraction. *Nat Rev Cancer* (2011) 11(6):411–25. doi:10.1038/nrc3055
7. Waning DL, Guise TA. Molecular mechanisms of bone metastasis and associated muscle weakness. *Clin Cancer Res* (2014) 20(12):3071–7. doi:10.1158/1078-0432.CCR-13-1590
8. Waning DL, Guise TA. Cancer-associated muscle weakness: what's bone got to do with it? *Bonekey Rep* (2015) 4:691. doi:10.1038/bonekey.2015.59
9. Waning DL, Mohammad KS, Reiken S, Xie W, Andersson DC, John S, et al. Excess TGF-beta mediates muscle weakness associated with bone metastases in mice. *Nat Med* (2015) 21(11):1262–71. doi:10.1038/nm.3961
10. Andersson DC, Betzenhauser MJ, Reiken S, Meli AC, Umanskaya A, Xie W, et al. Ryanodine receptor oxidation causes intracellular calcium leak and muscle weakness in aging. *Cell Metab* (2011) 14(2):196–207. doi:10.1016/j.cmet.2011.05.014
11. Bellinger AM, Reiken S, Carlson C, Mongillo M, Liu X, Rothman L, et al. Hypernitrosylated ryanodine receptor calcium release channels are leaky in dystrophic muscle. *Nat Med* (2009) 15(3):325–30. doi:10.1038/nm.1916
12. Aslakson CJ, Miller FR. Selective events in the metastatic process defined by analysis of the sequential dissemination of subpopulations of a mouse mammary tumor. *Cancer Res* (1992) 52(6):1399–405.
13. Rose AA, Pepin F, Russo C, Abou Khalil JE, Hallett M, Siegel PM. Osteoactivin promotes breast cancer metastasis to bone. *Mol Cancer Res* (2007) 5(10):1001–14. doi:10.1158/1541-7786.MCR-07-0119
14. Yoneda T, Michigami T, Yi B, Williams PJ, Niewolna M, Hiraga T. Actions of bisphosphonate on bone metastasis in animal models of breast carcinoma. *Cancer* (2000) 88(12 Suppl):2979–88. doi:10.1002/1097-0142(20000615)88:12+<2979::AID-CNCR13>3.0.CO;2-U
15. Wright LE, Ottewell PD, Rucci N, Peyruchaud O, Pagnotti GM, Chiechi A, et al. Murine models of breast cancer bone metastasis. *Bonekey Rep* (2016) 5:804. doi:10.1038/bonekey.2016.31
16. McPherron AC, Lawler AM, Lee SJ. Regulation of skeletal muscle mass in mice by a new TGF-beta superfamily member. *Nature* (1997) 387(6628):83–90. doi:10.1038/387083a0
17. Bollinger LM, Witczak CA, Houmard JA, Brault JJ. SMAD3 augments FoxO3-induced MuRF-1 promoter activity in a DNA-binding-dependent manner. *Am J Physiol Cell Physiol* (2014) 307(3):C278–87. doi:10.1152/ajpcell.00391.2013
18. Sandri M, Sandri C, Gilbert A, Skurk C, Calabria E, Picard A, et al. Foxo transcription factors induce the atrophy-related ubiquitin ligase atrogin-1 and cause skeletal muscle atrophy. *Cell* (2004) 117(3):399–412. doi:10.1016/S0092-8674(04)00400-3
19. Senf SM, Dodd SL, Judge AR. FOXO signaling is required for disuse muscle atrophy and is directly regulated by Hsp70. *Am J Physiol Cell Physiol* (2010) 298(1):C38–45. doi:10.1152/ajpcell.00315.2009
20. Yamada T, Place N, Kosterina N, Ostberg T, Zhang SJ, Grundtman C, et al. Impaired myofibrillar function in the soleus muscle of mice with collagen-induced arthritis. *Arthritis Rheum* (2009) 60(11):3280–9. doi:10.1002/art.24907
21. Vera-Ramirez L, Sanchez-Rovira P, Ramirez-Tortosa MC, Ramirez-Tortosa CL, Granados-Principal S, Lorente JA, et al. Free radicals in breast carcinogenesis, breast cancer progression and cancer stem cells. Biological bases to develop oxidative-based therapies. *Crit Rev Oncol Hematol* (2011) 80(3):347–68. doi:10.1016/j.critrevonc.2011.01.004
22. Bondi CD, Manickam N, Lee DY, Block K, Gorin Y, Abboud HE, et al. NAD(P)H oxidase mediates TGF-beta1-induced activation of kidney myofibroblasts. *J Am Soc Nephrol* (2010) 21(1):93–102. doi:10.1681/ASN.2009020146
23. Cheers C, Waller R. Activated macrophages in congenitally athymic "nude mice" and in lethally irradiate mice. *J Immunol* (1975) 115(3):844–7.
24. Segal AW. The function of the NADPH oxidase of phagocytes and its relationship to other NOXs in plants, invertebrates, and mammals. *Int J Biochem Cell Biol* (2008) 40(4):604–18. doi:10.1016/j.biocel.2007.10.003
25. Mohammad KS, Chen CG, Balooch G, Stebbins E, McKenna CR, Davis H, et al. Pharmacologic inhibition of the TGF-beta type I receptor kinase has anabolic and anti-catabolic effects on bone. *PLoS One* (2009) 4(4):e5275. doi:10.1371/journal.pone.0005275

Conflict of Interest Statement: The authors declare that the research was conducted in the absence of any commercial or financial relationships that could be construed as a potential conflict of interest.

frontiers in Endocrinology

MINI REVIEW
published: 27 April 2018
doi: 10.3389/fendo.2018.00202

Targeting the Metastatic Bone Microenvironment by MicroRNAs

*Marie-Therese Haider and Hanna Taipaleenmäki**

Molecular Skeletal Biology Laboratory, Department of Trauma, Hand and Reconstructive Surgery, University Medical Center Hamburg-Eppendorf, Hamburg, Germany

Bone metastases are a common and devastating feature of late-stage breast cancer. Metastatic bone disease is a consequence of disturbed bone remodeling due to pathological interactions between cancer cells and the bone microenvironment (BME). In the BME, breast cancer cells severely alter the balanced bone formation and bone resorption driven by osteoblasts and osteoclasts. The complex cellular cross talk in the BME is governed by secreted molecules, signaling pathways and epigenetic cues including non-coding RNAs. MicroRNAs (miRNAs) are small non-coding RNAs that reduce protein abundance and regulate several biological processes, including bone remodeling. Under pathological conditions, abnormal miRNA signaling contributes to the progression of diseases, such as bone metastasis. Recently miRNAs have been demonstrated to regulate several key drivers of bone metastasis. Furthermore, miRNAs are implicated as important regulators of cellular interactions within the metastatic BME. As a consequence, targeting the BME by miRNA delivery or antagonism has been reported to limit disease progression in experimental and preclinical conditions positioning miRNAs as emerging novel therapeutic tools in metastatic bone disease. This review will summarize our current understanding on the composition and function of the metastatic BME and discuss the recent advances how miRNAs can modulate pathological interactions in the bone environment.

Keywords: breast cancer, bone metastases, microRNA, bone microenvironment, osteoclast, osteoblast

OPEN ACCESS

Edited by:
Julie A. Sterling, Vanderbilt University, United States

Reviewed by:
Graziana Colaianni, University of Bari, Italy
Jennifer Tickner, University of Western Australia, Australia

***Correspondence:**
Hanna Taipaleenmäki
h.taipaleenmaeki@uke.de

Specialty section:
This article was submitted to Bone Research, a section of the journal Frontiers in Endocrinology

Received: *07 February 2018*
Accepted: *11 April 2018*
Published: *27 April 2018*

Citation:
Haider M-T and Taipaleenmäki H (2018) Targeting the Metastatic Bone Microenvironment by MicroRNAs. Front. Endocrinol. 9:202. doi: 10.3389/fendo.2018.00202

INTRODUCTION

Breast cancer is one of the most common malignancies in the world. Approximately 12% of women are diagnosed with breast cancer during their lifetime (1). After successful treatment of the primary tumor that often comprises surgery, adjuvant chemo- and radiation therapy, and the administration of anti-hormonal drugs, patients frequently suffer from distant metastases even decades after a disease-free interval (2). Bone is the most common site for breast cancer metastases, and approximately 70% of patients with advanced breast cancer suffer from osteolytic bone metastases (3). Osteolytic metastases are frequently associated with skeletal-related events (SREs), including fractures and spinal cord compression, that are often accompanied by severe pain and hypercalcemia (4).

In a physiological context, bone mass is maintained by the balanced activities of matrix-producing osteoblasts (OBs) that originate from mesenchymal cells and can become matrix-entrapped osteocytes (OCYs), and bone-resorbing osteoclasts (OCs) that arise from the hematopoietic lineage (5). OC function and bone resorption is stimulated by the receptor activator of NFκB ligand (RANKL) that is expressed in membrane-bound and soluble forms by OBs and OCYs (**Figure 1**). The activity is restricted by osteoprotegerin, which is a soluble decoy receptor against RANKL (6). Under

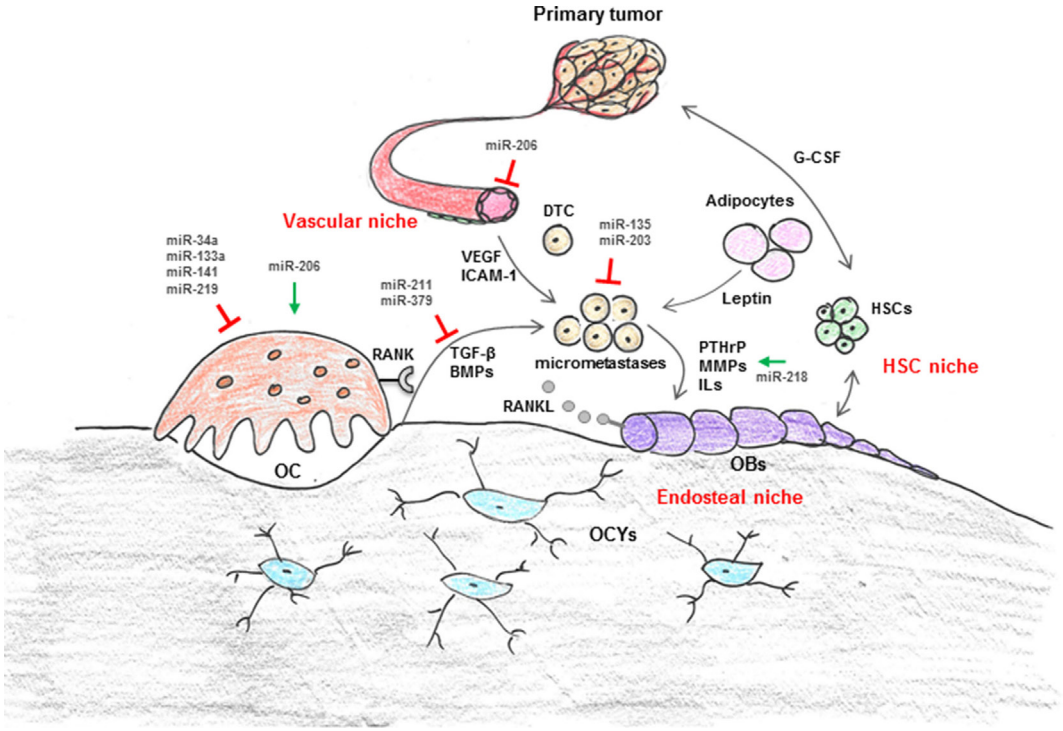

FIGURE 1 | Regulation of cellular interaction in breast cancer bone metastasis by microRNA (miRNAs). The bone microenvironment (BME) is composed of cellular entities, including hematopoietic stem cells (HSC niche), osteoblasts (OBs), osteoclasts (OCs), and adipocytes (endosteal niche) as well as vascular endothelial cells and pericytes (vascular niche). These niches are suggested to control survival, dormancy, and growth of disseminated tumor cells (DTCs) through production of cytokines (i.e., leptin, G-CSF, VEGF, etc.) and intracellular signals in addition to cell-to-cell contact. In a physiological context, the highly coordinated cross talk between bone-forming OBs and bone-resorbing OCs maintains bone mass. OC function is regulated *via* OB and osteocyte (OCYs) derived RANKL. In the context of metastatic breast cancer disease, breast cancer cells severely disturb the balance between bone formation and resorption through secretion of various growth factors and cytokines [i.e., interleukins (ILs), parathyroid hormone-related protein (PTHrP), matrix metalloproteinases (MMPs), RANKL]. Recently, it has also been suggested that cells from the primary tumor themselves modify the distant microenvironment, for example through systemic factors (i.e., VEGF, TGF-β, G-CSF, miRNAs), in order to make it more attractive for DTCs. Several components of the BME are negatively (red blocks) or positively (green arrows) regulated by miRNAs.

pathological conditions, for instance in the context of metastatic breast cancer disease, breast cancer cells colonize the bone marrow microenvironment and severely disturb the balance between bone formation and bone resorption (7). This multi-directional process termed "vicious cycle" perpetuates metastatic bone destruction (8).

MicroRNAs (miRNAs) are small non-coding RNAs and key regulators of various biological processes including bone remodeling and cancer progression (9, 10). miRNAs bind to the 3′UTR of their target mRNAs, and depending on the degree of complementarity interfere with the mRNA stability and/or by block protein translation (9). Abnormal miRNA expression has been implicated in the pathology of osteoporosis, primary bone tumors, and bone metastases of various cancers (11–14). Furthermore, *in vivo* delivery of miRNA mimics or miRNA antagonists has been established as an attractive therapeutic approach to reverse bone degeneration, or to prevent cancer-induced bone diseases (15, 16). Thus, miRNAs can be used as therapeutic targets and may provide a novel tool to treat breast cancer-induced osteolytic disease.

Several miRNAs have been identified to regulate breast cancer cell-intrinsic oncogenic properties, such as proliferation, migration, and invasion (17–19). However, how miRNAs regulate non-cell autonomous interactions in the bone microenvironment (BME) remains largely unknown. This review highlights the recent understanding of the role of miRNAs in the metastatic BME and their potential use as therapeutic targets to modulate the pathological environment and limit disease progression.

METASTATIC BONE DISEASE

Bone is the most prevalent metastatic site for breast cancer cell colonization and growth. Bone metastasis is a complex multistep process starting from the dissemination of malignant cells into bloodstream, survival of these circulating tumor cells (CTCs) in the circulation, homing to distant organs and eventually metastases formation in the distant site (2). Disseminated tumor cells (DTCs) can be detected in the bone marrow of approximately 30% of breast cancer patients and predict for poor overall survival, breast cancer-specific survival, and disease-free survival compared to patients without DTCs (20).

Once bone metastases occur, the disease is incurable, and treatment remains palliative (21). The standard of care for patients with bone metastases comprises anti-resorptive drugs that reduce

the progression of bone destruction and increase survival (22). For instance, bisphosphonates are well established in the treatment of osteolytic disease. Bisphosphonates are incorporated into the bone matrix and taken up by OCs during bone resorption, leading to OC apoptosis and a consecutive reduction of bone resorption (22). An alternative therapeutic approach is the use of the human monoclonal antibody Denosumab (Xgeva®) that inhibits RANKL and has been shown to delay the time to first and subsequent SRE in breast cancer patients (23). Although breast cancer patients greatly benefit from the use of bisphosphonates and Denosumab, a better understanding of the control of the "vicious cycle" in the BME and the underlying cellular and molecular mechanisms is needed as it is likely to help identifying novel therapeutic concepts to restrict SREs.

TUMOR MICROENVIRONMENT (TME)—THE BME IN BREAST CANCER BONE METASTASIS

Over the last decade, a variety of preclinical studies have emphasized the contribution of the TME to disease progression (24–28). The TME comprises the cellular environment in which the tumor exists, the surrounding extracellular matrix, and signaling molecules. Several aspects of how the TME impacts cancer growth are well established such as the role of endothelial cells in tumor angiogenesis (29, 30). However, others including the role of the TME in mediating tumor cell invasion, dissemination, and metastasis remain poorly defined (31).

Circulating tumor cells have a high affinity for bone, in particular areas of active bone remodeling (32). The highly balanced cross talk between OBs and OCs, the presence of various other bone marrow-derived cell populations and soluble factors including osteopontin (OPN) and matrix metalloproteinases (MMPs) make bone an attractive site ("soil") for DTCs ("seeds"). Nearly almost a century ago Steven Pagets' "seed and soil theory" proposed that therapies to modify the TME might be of equal importance as therapies targeted against the tumor cells themselves (33). Hence, cells of the BME are becoming increasingly recognized as potential therapeutic targets for breast cancer bone metastasis (24–27, 34, 35).

Upon their arrival in bone, DTCs encounter a heterogeneous BME, which is composed of various cells originating from either hematopoietic or mesenchymal stem cells (HSCs, MSCs, respectively) (**Figure 1**). These include lymphoid and myeloid lineage cells (e.g., immune cells, megakaryocytes, erythrocytes, and macrophages such as OCs) as well as adipocytes and bone and connective tissue-forming cells (e.g., chondrocytes and OBs). In addition, the BME contains a dense, interconnected vascular system which maintains hematopoiesis and osteogenesis (36, 37). Within bone, these various cellular entities form supporting microenvironments, "niches," which are thought to regulate tumor cell homing, survival, and dormancy (28, 38–41) (**Figure 1**). The most well-studied niches are the HSC-, endosteal- (OBs, OCs), and vascular niche (vascular endothelial cells, pericytes). Both, the endosteal and the vascular niche control self-renewal, differentiation, and proliferation of HSCs through cell-to-cell contacts as well as by producing a variety of cytokines and intracellular signals (42–45). It is thought that tumor cells respond, similar like HSCs, to these signals. Among the most well studied pathways is the CXCL12/CXCR4 axis. CXCL12 or stromal cell-derived factor-1 (SDF-1) is produced and secreted by bone marrow stromal cells, primarily the OB, endothelial, and epithelial cells (46) (**Figure 1**). Its cognate receptor CXCR4 is expressed in high levels on various cancer cell lines, including MDA-MB-231 (47). Overexpression of CXCR4 in MDA-MB-231 cells increases bone metastasis, and very recently, it has been demonstrated that both newly and established metastases were anchored in the bone marrow by CXCR4/CXCL12 interactions (48, 49). Further niche signals are suggested to include OPN, vascular adhesion molecule-1, intercellular adhesion molecule-1, chemokines such as Interleukins (ILs) and various growth factors, including bone morphogenetic proteins, Transforming growth factor-β1 (TGF-β), and Vascular endothelial growth factor (VEGF) (50–52) (**Figure 1**). Emerging data also implicate the importance of the immune- and bone marrow adipocyte niche in bone metastasis (28, 53, 54). Studies by Templeton et al. highlighted the role of adipocytes, one of the most abundant stromal components in the BME, in breast cancer cell osteotropism and early colonization by demonstrating that adipokines, including leptin, promote the migration of MDA-MB-231 breast cancer cells to human bone tissue fragments *in vitro* (28). Nevertheless, exact mechanisms that guide DTCs toward the metastatic site in bone remain to be established. Recently, it was proposed that cells from the primary tumor themselves modify the distant (bone) microenvironment, for example through systemic factors (i.e., VEGF, TGF-β, LOX, G-CSF, miRNAs), in order to make it more attractive for DTCs (27, 55, 56).

Given the heterogeneity of the BME, the fate of DTCs might be determined by the nature of their arrival site within bone. A recent review by Croucher et al. suggests that long-term dormancy might be supported when tumor cells face quiescent/static microenvironments (e.g., endosteal surfaces covered by bone lining cells or stable vasculature), whereas active, dynamic BMEs including areas of osteoclastic bone resorption and sprouting vasculature foster proliferation and/or reactivation of dormant tumor cells (26, 57).

Once activated, breast cancer cells secrete growth factors, such as Parathyroid hormone-related protein (*PTHrP*), ILs, and MMPs, which stimulate OBs to produce excessive amounts of RANKL and other cytokines (58–60). RANKL increases OCs activity and subsequent bone degradation. During bone resorption, matrix-derived growth factors, e.g., TGF-β1 are released into the metastatic microenvironment and further stimulate cancer cell proliferation (7). This "vicious cycle" perpetuates metastatic bone destruction leading to osteolytic disease (8). Therefore, targeting the BME, for instance by miRNAs, to disable this cycle is not only scientifically interesting but also clinically relevant approach.

TUMOR-DERIVED miRNAs INFLUENCING THE BME

MicroRNAs have been recently recognized as key regulators of various biological processes, including cancer progression and

metastasis. miRNAs are small (20–22 nucleotides in length), endogenous non-coding RNAs which posttranscriptionally regulate mRNA stability and protein translation (9). More than 1,800 miRNAs are expressed in humans and according to prediction tools, each miRNA regulates numerous target genes (61–63). An important feature of miRNAs is that miRNAs can be encapsulated in extracellular vehicles and released to bloodstream (64–66), which makes them attractive minimal or non-invasive source of biomarkers of various diseases, including bone disorders (67, 68).

MicroRNAs expressed by tumor cells can act as master regulators of bone metastases formation by targeting metastasis-driving factors and consequently altering cancer cell behavior (17–19). In addition, tumor-derived miRNAs can exert their oncogenic or tumor-suppressive action by altering the BME. A specific feature of bone metastatic breast cancer cells is that they exhibit pathologically elevated expression of bone-related genes [e.g., Runt-related transcription factor 2 (Runx2)] and signaling pathways, including the Wnt pathway (69–71). Runx2 is necessary for normal bone formation but often dysregulated in bone metastatic breast cancer cells due to a downregulation of Runx2-targeting miRNAs, including miR-135 and miR-203 (72). Runx2 promotes tumor growth in bone and knocking down Runx2 in cancer cells protects from breast cancer-induced osteolytic disease, positioning Runx2 as an attractive target to reduce bone metastatic burden (73). Indeed, pharmacological delivery of synthetic miR-135 and miR-203 mimics into metastatic breast cancer cells reduces Runx2 protein abundance and consequently, diminishes tumor growth and spontaneous metastasis to bone (72). Furthermore, reconstitution of miR-135 and miR-203 greatly impairs tumor growth in the BME and alleviates osteolytic disease. The bone protecting effect occurred through downregulation of several metastasis-promoting Runx2 target genes, including IL-11, MMP-13, and PTHrP, and subsequent inhibition of OC activity (72).

Similarly, Wnt signaling promotes OB differentiation and function under physiological conditions but a hyper activation of the signaling pathway is implicated in numerous cancers, including metastatic breast cancer (70, 74). In bone metastatic breast cancer cells, Wnt signaling induces the expression of PTHrP thus aggravating the vicious cycle (75). In OBs, Wnt signaling and miR-218 create a positive feed-forward loop through targeting of Wnt inhibitors, such as Dkk1 and sFRP1 by miR-218 (76). Similarly, miR-218 activates Wnt signaling in metastatic breast cancer cells (76). Consequently, miR-218 enhances MDA-MB-231 cell proliferation and increases the expression of Wnt target genes in a Wnt-dependent manner (76, 77). Furthermore, miR-218 promotes PTHrP secretion in cancer cells and subsequent activation of RANKL in OBs, leading to an enhanced OB-mediated OC differentiation. Importantly, antagonizing miR-218 reversed these effects *in vitro* and prevented the formation of cancer-induced osteolytic lesions *in vivo* (77). Tumor-derived osteolytic cytokines are also regulated by miR-211 and miR-379 (78). Both miRNAs prevented TGF-β-induced upregulation of IL-11 and downregulated several genes involved in TGF-β pathway (78). Thus, miR-211 and miR-379 block the vicious cycle by preventing breast cancer cells from receiving signals from the metastatic BME.

Besides regulating the vicious cycle of bone metastasis, tumor-derived miRNAs, including miR-126, have been established in pathological angiogenesis in the BME (79). miR-126, which is silenced in breast cancer cells with bone metastatic potential, suppresses endothelial recruitment and metastatic angiogenesis in a non-cell autonomous manner and, importantly, inhibits bone metastatic colonization of breast cancer cells. The underlying mechanism involves a coordinated targeting of two newly identified pro-metastatic genes; insulin-like growth factor binding protein 2 (IGFPB2) and c-Mer tyrosine kinase (MERTK). Metastatic breast cancer cells secrete IGFPB2 that acts on insulin-like growth factor (IGF1) type I receptor on endothelial cells and modulates IGF1 activation and subsequently endothelial recruitment. In addition, endothelial recruitment is promoted upon cleavage of cMERTK receptor from the breast cancer cells, which antagonizes the binding of GAS6 to endothelial MERTK receptors. A series of elegant loss-of-function and replacement experiments revealed individual components of the pro-angiogenic IGFPB2/IGF1/IGF1R and GAS6-MERTK signaling pathways as direct targets of miR-126 and establish miR-126 as a crucial factor regulating endothelial interactions in the metastatic BME (79).

Recently, miRNAs released from cancer cells in microvesicles or exosomes have been shown to directly control cell–cell interactions in the BME. For instance, miR-192, which is highly abundant in metastatic lung cancer, can be secreted from the cancer cells in extracellular vesicles and transferred to endothelial cells (80). Cancer cell-derived miR-192 is efficiently taken up by endothelial cells *in vitro* and *in vivo,* and inhibits tumor-induced angiogenesis leading to reduced metastatic burden and decreased osteolytic disease in mice.

TARGETING THE BME BY miRNAs

Since OC activity is a hallmark of metastatic bone disease, the current treatment as well as the majority of basic research is focusing on restricting OC activity and attenuating pathological bone resorption. Along these lines, several studies have established miRNAs as crucial regulators of pathological OC differentiation. Especially miRNAs that suppress bone resorption provide an attractive approach to limit disease progression (81, 82). For instance, miR-34a was recently reported to inhibit physiological and pathological OC differentiation and to block osteoporosis and cancer-induced bone destruction (83). Using several genetic mouse models, Krzezinski et al. demonstrated that OC-targeted overexpression of miR-34a impairs bone resorption resulting in resistance of bone metastases. Conversely, deletion of miR-34a activated OCs leading to reduced bone mass and exacerbated bone metastasis burden. Mechanistically, miR-34a targets a homeodomain protein TG-interacting factor 2, a novel positive regulator of osteoclast differentiation and function. In a therapeutically relevant setting, systemic delivery of miR-34a mimic oligonucleotides *via* chitosan nanoparticles diminished bone metastatic burden and osteolysis (83). Since miR-34a had no direct effect of cancer cell proliferation these effects are likely mediated by osteoclasts and possibly other cells in the BME emphasizing the importance of the TME in disease progression.

In another comprehensive study, a group of miRNAs was shown to regulate tumor-induced osteoclast differentiation. Five miRNAs, miR-33a, miR-133a, miR-141, miR-190, and miR-219 were downregulated during osteoclast differentiation under physiological and pathophysiological conditions (84). Among them, miR-133a, miR-141, and miR-219 impaired osteoclast differentiation *in vitro* by targeting important osteoclast-promoting factors Mitf, Mmp14, Calcitonin receptor, and Traf5. *In vivo* administration of synthetic miR-141 and miR-219 oligonucleotides reduced physiological bone resorption, impaired tumor growth in bone and prevented pathological bone destruction. In this study, two miRNAs, miR-16 and miR-378 secreted in exosomes by osteoclasts were found to be increased in patients with bone metastases compared to healthy controls and the expression correlated with bone metastasis burden (84). Interestingly, miR-378 promotes tumor growth, angiogenesis, and tumor cell survival through the repression of tumor suppressors SuFu and Fus-1 (85). Although beyond this review, it is important to emphasize that miRNA signatures are being pursued as novel clinical diagnostic targets for predicting metastasis or therapeutic resistance (1, 4).

miR-214 is strongly increased in bone specimen of breast cancer patients with osteolytic bone metastases compared to healthy controls and patients without bone involvement (86). Consistently, osteoclasts isolated from mice with bone metastases express significantly higher levels of miR-214 compared to controls. In addition, miR-214 is elevated in bone tissue and serum of aged patients with fractures and miR-214 expression is accompanied with increased osteoclast activity and bone resorption, indicating that miR-214 regulates bone remodeling in health and disease (87, 88). Indeed, miR-214 is expressed and has a functional role in both OBs and osteoclasts. In OBs, miR-214 inhibits differentiation *in vitro* and bone formation *in vivo* by targeting the activating transcription factor 4. As a consequence, delivery of OB-targeted antagomiR-214 in osteoporotic mice increased bone formation and restored bone mass (87). In contrast, in osteoclasts, miR-214 promotes osteoclast function and bone resorption through inhibition of the phosphatase and tensin homolog and Traf3, a negative regulator of NFkB signaling and osteoclast differentiation (86, 89). As a consequence, osteoclast-targeted deletion of miR-214 reduced bone resorption and prevented the development of osteolytic lesions in mice (86). The number and size of non-bone metastases was not changed in mice lacking miR-214 in the osteoclast lineage indicating that the tumor-suppressive effect of bone metastases is mediated by the BME. Importantly, pharmacological delivery of osteoclast targeted (D-Asp8)-liposome conjucated antimiR-214 oligonucleotides reduced physiological and pathological bone resorption and protected from osteolytic bone metastases, suggesting that inhibition of miR-214 could provide an attractive therapeutic strategy to prevent pathological bone destruction (86).

Intriguingly, miR-214 is secreted from osteoclasts in exosomes into circulation and acts on local and distant OBs (88). Treatment of wild-type mice with exosomes isolated from mice with osteoclast-targeted overexpression of miR-214 reduced bone formation demonstrating that the osteoclast-derived miR-214 is fully functional in OBs. This was further supported by an increased bone formation after systemic administration of antagomiR-214 encapsulated in osteoclast-targeted (D-Asp)8-liposomes (88). Given the dual bone anabolic and anti-catabolic effect of antago-miR-214, a systemic delivery of antago-miR-214 might provide a potent strategy to not only prevent osteolytic disease but also reverse existing lesions.

PERSPECTIVES

MicroRNAs play a pivotal role in tissue development and homeostasis. Therefore, dysregulation of individual miRNAs is implicated in several pathological conditions, including the onset and progression of metastatic bone disease. While the role of miRNAs regulating oncogenic properties of tumor cells is relatively well established, the direct or indirect regulation of TME by miRNAs has only recently started to be uncovered. In particular, miRNAs that mediate cell–cell interactions in the BME provide a novel therapeutic approach to disable the pathological cross talk in the bone marrow. For instance, identifying and targeting miRNAs that are pathologically elevated in osteoclasts and promote the vicious cycle could offer novel strategies for diagnosis and treatment of bone metastases. Although the evidence is thus far exclusively based on preclinical data, the applications of using miRNAs as adjuvant tools in bone metastases targets are very promising. Therefore, a better understanding of the complex miRNA-mediated cellular interactions is not only scientifically interesting but also critical in transmitting the knowledge from the bench to bedside.

AUTHOR CONTRIBUTIONS

M-TH and HT reviewed literature and wrote the manuscript.

FUNDING

M-TH is supported by a post-doctoral fellowship from the Humboldt Foundation. HT received funding from the Deutsche Forschungsgemeinschaft (TA1154/1-1).

REFERENCES

1. McGuire A, Brown JAL, Kerin MJ. Metastatic breast cancer: the potential of miRNA for diagnosis and treatment monitoring. *Cancer Metastasis Rev* (2015) 34:145–55. doi:10.1007/s10555-015-9551-7
2. Pantel K, Brakenhoff RH. Dissecting the metastatic cascade. *Nat Rev Cancer* (2004) 4:448–56. doi:10.1038/nrc1370
3. Roodman GD. Mechanisms of bone metastasis. *Discov Med* (2004) 4:144–8.
4. D'Oronzo S, Brown J, Coleman R. The role of biomarkers in the management of bone-homing malignancies. *J Bone Oncol* (2017) 9:1–9. doi:10.1016/j.jbo.2017.09.001
5. Baron R, Hesse E. Update on bone anabolics in osteoporosis treatment: rationale, current status, and perspectives. *J Clin Endocrinol Metab* (2012) 97:311–25. doi:10.1210/jc.2011-2332
6. O'Brien CA, Nakashima T, Takayanagi H. Osteocyte control of osteoclastogenesis. *Bone* (2013) 54:258–63. doi:10.1016/j.bone.2012.08.121

7. Weilbaecher KN, Guise TA, McCauley LK. Cancer to bone: a fatal attraction. *Nat Rev Cancer* (2011) 11:411–25. doi:10.1038/nrc3055
8. Mundy GR. Metastasis to bone: causes, consequences and therapeutic opportunities. *Nat Rev Cancer* (2002) 2:584–93. doi:10.1038/nrc867
9. Lian JB, Stein GS, van Wijnen AJ, Stein JL, Hassan MQ, Gaur T, et al. MicroRNA control of bone formation and homeostasis. *Nat Rev Endocrinol* (2012) 8:212–27. doi:10.1038/nrendo.2011.234
10. Drusco A, Croce CM. MicroRNAs and cancer: a long story for short RNAs. *Adv Cancer Res* (2017) 135:1–24. doi:10.1016/bs.acr.2017.06.005
11. Taipaleenmäki H. Regulation of bone metabolism by microRNAs. *Curr Osteoporos Rep* (2018) 16(1):1–12. doi:10.1007/s11914-018-0417-0
12. Browne G, Taipaleenmäki H, Stein GS, Stein JL, Lian JB. MicroRNAs in the control of metastatic bone disease. *Trends Endocrinol Metab* (2014) 25:320–7. doi:10.1016/j.tem.2014.03.014
13. van der Deen M, Taipaleenmäki H, Zhang Y, Teplyuk NM, Gupta A, Cinghu S, et al. MicroRNA-34c inversely couples the biological functions of the runt-related transcription factor RUNX2 and the tumor suppressor p53 in osteosarcoma. *J Biol Chem* (2013) 288:21307–19. doi:10.1074/jbc.M112.445890
14. Iorio MV, Croce CM. MicroRNA dysregulation in cancer: diagnostics, monitoring and therapeutics. A comprehensive review. *EMBO Mol Med* (2012) 4:143–59. doi:10.1002/emmm.201100209
15. Taipaleenmäki H, Bjerre Hokland L, Chen L, Kauppinen S, Kassem M. Mechanisms in endocrinology: micro-RNAs: targets for enhancing osteoblast differentiation and bone formation. *Eur J Endocrinol* (2012) 166:359–71. doi:10.1530/EJE-11-0646
16. Krzeszinski JY, Wan Y. New therapeutic targets for cancer bone metastasis. *Trends Pharmacol Sci* (2015) 36:360–73. doi:10.1016/j.tips.2015.04.006
17. Zoni E, van der Pluijm G. The role of microRNAs in bone metastasis. *J Bone Oncol* (2016) 5:104–8. doi:10.1016/j.jbo.2016.04.002
18. Zhao Q, Luo F, Ma J, Yu X. Bone metastasis-related microRNAs: new targets for treatment? *Curr Cancer Drug Targets* (2015) 15:716–25. doi:10.2174/1568009615666150629102408
19. Croset M, Kan C, Clézardin P. Tumour-derived miRNAs and bone metastasis. *Bonekey Rep* (2015) 4:688. doi:10.1038/bonekey.2015.56
20. Fontanella C, Fanotto V, Rihawi K, Aprile G, Puglisi F. Skeletal metastases from breast cancer: pathogenesis of bone tropism and treatment strategy. *Clin Exp Metastasis* (2015) 32:819–33. doi:10.1007/s10585-015-9743-0
21. Coleman R. Bone targeted treatments in cancer – the story so far. *J Bone Oncol* (2016) 5:90–2. doi:10.1016/j.jbo.2016.03.002
22. Coleman RE. Impact of bone-targeted treatments on skeletal morbidity and survival in breast cancer. *Oncology (Williston Park)* (2016) 30:695–702.
23. Stopeck AT, Lipton A, Body J-J, Steger GG, Tonkin K, de Boer RH, et al. Denosumab compared with zoledronic acid for the treatment of bone metastases in patients with advanced breast cancer: a randomized, double-blind study. *J Clin Oncol* (2010) 28:5132–9. doi:10.1200/JCO.2010.29.7101
24. Haider M-T, Holen I, Dear TN, Hunter K, Brown HK. Modifying the osteoblastic niche with zoledronic acid in vivo-potential implications for breast cancer bone metastasis. *Bone* (2014) 66:240–50. doi:10.1016/j.bone.2014.06.023
25. Ubellacker JM, Haider M-T, DeCristo MJ, Allocca G, Brown NJ, Silver DP, et al. Zoledronic acid alters hematopoiesis and generates breast tumor-suppressive bone marrow cells. *Breast Cancer Res* (2017) 19:23. doi:10.1186/s13058-017-0815-8
26. Ghajar CM, Peinado H, Mori H, Matei IR, Evason KJ, Brazier H, et al. The perivascular niche regulates breast tumour dormancy. *Nat Cell Biol* (2013) 15:807–17. doi:10.1038/ncb2767
27. Cox TR, Rumney RMH, Schoof EM, Perryman L, Høye AM, Agrawal A, et al. The hypoxic cancer secretome induces pre-metastatic bone lesions through lysyl oxidase. *Nature* (2015) 522:106–10. doi:10.1038/nature14492
28. Templeton ZS, Lie W-R, Wang W, Rosenberg-Hasson Y, Alluri RV, Tamaresis JS, et al. Breast cancer cell colonization of the human bone marrow adipose tissue niche. *Neoplasia* (2015) 17:849–61. doi:10.1016/j.neo.2015.11.005
29. Bissell MJ, Radisky D. Putting tumours in context. *Nat Rev Cancer* (2001) 1:46–54. doi:10.1038/35094059
30. Folkman J. Role of angiogenesis in tumor growth and metastasis. *Semin Oncol* (2002) 29:asonc02906q0015. doi:10.1053/sonc.2002.37263
31. Hanahan D, Weinberg RA. Hallmarks of cancer: the next generation. *Cell* (2011) 144:646–74. doi:10.1016/j.cell.2011.02.013
32. Brown HK, Ottewell PD, Evans CA, Holen I. Location matters: osteoblast and osteoclast distribution is modified by the presence and proximity to breast cancer cells in vivo. *Clin Exp Metastasis* (2012) 29:927–38. doi:10.1007/s10585-012-9481-5
33. Paget S. The distribution of secondary growths in cancer of the breast. 1889. *Cancer Metastasis Rev* (1989) 8:98–101.
34. Zheng H, Bae Y, Kasimir-Bauer S, Tang R, Chen J, Ren G, et al. Therapeutic antibody targeting tumor- and osteoblastic niche-derived jagged1 sensitizes bone metastasis to chemotherapy. *Cancer Cell* (2017) 32:731–47.e6. doi:10.1016/j.ccell.2017.11.002
35. Haider M-T, Hunter KD, Robinson SP, Graham TJ, Corey E, Dear TN, et al. Rapid modification of the bone microenvironment following short-term treatment with cabozantinib in vivo. *Bone* (2015) 81:581–92. doi:10.1016/j.bone.2015.08.003
36. Kusumbe AP, Ramasamy SK, Adams RH. Coupling of angiogenesis and osteogenesis by a specific vessel subtype in bone. *Nature* (2014) 507:323–8. doi:10.1038/nature13145
37. Itkin T, Gur-Cohen S, Spencer JA, Schajnovitz A, Ramasamy SK, Kusumbe AP, et al. Distinct bone marrow blood vessels differentially regulate haematopoiesis. *Nature* (2016) 532:323–8. doi:10.1038/nature17624
38. Zalucha JL, Jung Y, Joseph J, Wang J, Berry JE, Shiozawa Y, et al. The role of osteoclasts in early dissemination of prostate cancer tumor cells. *J Cancer Stem Cell Res* (2015) 3:e1005. doi:10.14343/JCSCR.2015.3e1005
39. Wang H, Yu C, Gao X, Welte T, Muscarella AM, Tian L, et al. The osteogenic niche promotes early-stage bone colonization of disseminated breast cancer cells. *Cancer Cell* (2015) 27:193–210. doi:10.1016/j.ccell.2014.11.017
40. Shiozawa Y, Pedersen EA, Havens AM, Jung Y, Mishra A, Joseph J, et al. Human prostate cancer metastases target the hematopoietic stem cell niche to establish footholds in mouse bone marrow. *J Clin Invest* (2011) 121:1298–312. doi:10.1172/JCI43414
41. Shiozawa Y, Havens AM, Pienta KJ, Taichman RS. The bone marrow niche: habitat to hematopoietic and mesenchymal stem cells, and unwitting host to molecular parasites. *Leukemia* (2008) 22:941–50. doi:10.1038/leu.2008.48
42. Taichman RS. Blood and bone: two tissues whose fates are intertwined to create the hematopoietic stem-cell niche. *Blood* (2005) 105:2631–9. doi:10.1182/blood-2004-06-2480
43. Psaila B, Lyden D, Roberts I. Megakaryocytes, malignancy and bone marrow vascular niches. *J Thromb Haemost* (2012) 10:177–88. doi:10.1111/j.1538-7836.2011.04571.x
44. Calvi LM. Osteoblastic activation in the hematopoietic stem cell niche. *Ann N Y Acad Sci* (2006) 1068:477–88. doi:10.1196/annals.1346.021
45. Adams GB, Chabner KT, Alley IR, Olson DP, Szczepiorkowski ZM, Poznansky MC, et al. Stem cell engraftment at the endosteal niche is specified by the calcium-sensing receptor. *Nature* (2006) 439:599–603. doi:10.1038/nature04247
46. Ponomaryov T, Peled A, Petit I, Taichman RS, Habler L, Sandbank J, et al. Induction of the chemokine stromal-derived factor-1 following DNA damage improves human stem cell function. *J Clin Invest* (2000) 106:1331–9. doi:10.1172/JCI10329
47. Müller A, Homey B, Soto H, Ge N, Catron D, Buchanan ME, et al. Involvement of chemokine receptors in breast cancer metastasis. *Nature* (2001) 410:50–6. doi:10.1038/35065016
48. Kang Y, Siegel PM, Shu W, Drobnjak M, Kakonen SM, Cordón-Cardo C, et al. A multigenic program mediating breast cancer metastasis to bone. *Cancer Cell* (2003) 3:537–49. doi:10.1016/S1535-6108(03)00132-6
49. Price TT, Burness ML, Sivan A, Warner MJ, Cheng R, Lee CH, et al. Dormant breast cancer micrometastases reside in specific bone marrow niches that regulate their transit to and from bone. *Sci Transl Med* (2016) 8:340ra73. doi:10.1126/scitranslmed.aad4059
50. McAllister SS, Gifford AM, Greiner AL, Kelleher SP, Saelzler MP, Ince TA, et al. Systemic endocrine instigation of indolent tumor growth requires osteopontin. *Cell* (2008) 133:994–1005. doi:10.1016/j.cell.2008.04.045
51. Lu X, Mu E, Wei Y, Riethdorf S, Yang Q, Yuan M, et al. VCAM-1 promotes osteolytic expansion of indolent bone micrometastasis of breast cancer by engaging α4β1-positive osteoclast progenitors. *Cancer Cell* (2011) 20:701–14. doi:10.1016/j.ccr.2011.11.002
52. Butler JM, Kobayashi H, Rafii S. Instructive role of the vascular niche in promoting tumour growth and tissue repair by angiocrine factors. *Nat Rev Cancer* (2010) 10:138–46. doi:10.1038/nrc2791
53. Malladi S, Macalinao DG, Jin X, He L, Basnet H, Zou Y, et al. Metastatic latency and immune evasion through autocrine inhibition of WNT. *Cell* (2016) 165:45–60. doi:10.1016/j.cell.2016.02.025

54. Monteiro AC, Leal AC, Gonçalves-Silva T, Mercadante ACT, Kestelman F, Chaves SB, et al. T cells induce pre-metastatic osteolytic disease and help bone metastases establishment in a mouse model of metastatic breast cancer. *PLoS One* (2013) 8:e68171. doi:10.1371/journal.pone.0068171
55. Kaplan RN, Psaila B, Lyden D. Bone marrow cells in the "pre-metastatic niche": within bone and beyond. *Cancer Metastasis Rev* (2007) 25:521–9. doi:10.1007/s10555-006-9036-9
56. Costa-Silva B, Aiello NM, Ocean AJ, Singh S, Zhang H, Thakur BK, et al. Pancreatic cancer exosomes initiate pre-metastatic niche formation in the liver. *Nat Cell Biol* (2015) 17:816–26. doi:10.1038/ncb3169
57. Croucher PI, McDonald MM, Martin TJ. Bone metastasis: the importance of the neighbourhood. *Nat Rev Cancer* (2016) 16:373–86. doi:10.1038/nrc.2016.44
58. Powell GJ, Southby J, Danks JA, Stillwell RG, Hayman JA, Henderson MA, et al. Localization of parathyroid hormone-related protein in breast cancer metastases: increased incidence in bone compared with other sites. *Cancer Res* (1991) 51:3059–61.
59. Martin TJ. Manipulating the environment of cancer cells in bone: a novel therapeutic approach. *J Clin Invest* (2002) 110:1399–401. doi:10.1172/JCI0217124
60. Li J, Karaplis AC, Huang DC, Siegel PM, Camirand A, Yang XF, et al. PTHrP drives breast tumor initiation, progression, and metastasis in mice and is a potential therapy target. *J Clin Invest* (2011) 121:4655–69. doi:10.1172/JCI46134
61. Lewis BP, Burge CB, Bartel DP. Conserved seed pairing, often flanked by adenosines, indicates that thousands of human genes are microRNA targets. *Cell* (2005) 120:15–20. doi:10.1016/j.cell.2004.12.035
62. Lim LP, Lau NC, Garrett-Engele P, Grimson A, Schelter JM, Castle J, et al. Microarray analysis shows that some microRNAs downregulate large numbers of target mRNAs. *Nature* (2005) 433:769–73. doi:10.1038/nature03315
63. Kozomara A, Griffiths-Jones S. miRBase: annotating high confidence microRNAs using deep sequencing data. *Nucleic Acids Res* (2014) 42:D68–73. doi:10.1093/nar/gkt1181
64. Valadi H, Ekström K, Bossios A, Sjöstrand M, Lee JJ, Lötvall JO. Exosome-mediated transfer of mRNAs and microRNAs is a novel mechanism of genetic exchange between cells. *Nat Cell Biol* (2007) 9:654–9. doi:10.1038/ncb1596
65. Vickers KC, Palmisano BT, Shoucri BM, Shamburek RD, Remaley AT. MicroRNAs are transported in plasma and delivered to recipient cells by high-density lipoproteins. *Nat Cell Biol* (2011) 13:423–33. doi:10.1038/ncb2210
66. Wang K, Zhang S, Weber J, Baxter D, Galas DJ. Export of microRNAs and microRNA-protective protein by mammalian cells. *Nucleic Acids Res* (2010) 38:7248–59. doi:10.1093/nar/gkq601
67. Weber JA, Baxter DH, Zhang S, Huang DY, Huang KH, Lee MJ, et al. The microRNA spectrum in 12 body fluids. *Clin Chem* (2010) 56:1733–41. doi:10.1373/clinchem.2010.147405
68. Hackl M, Heilmeier U, Weilner S, Grillari J. Circulating microRNAs as novel biomarkers for bone diseases – complex signatures for multifactorial diseases? *Mol Cell Endocrinol* (2016) 432:83–95. doi:10.1016/j.mce.2015.10.015
69. Sethi N, Kang Y. Dysregulation of developmental pathways in bone metastasis. *Bone* (2011) 48:16–22. doi:10.1016/j.bone.2010.07.005
70. Matsuda Y, Schlange T, Oakeley EJ, Boulay A, Hynes NE. WNT signaling enhances breast cancer cell motility and blockade of the WNT pathway by sFRP1 suppresses MDA-MB-231 xenograft growth. *Breast Cancer Res* (2009) 11:R32. doi:10.1186/bcr2317
71. Pratap J, Lian JB, Stein GS. Metastatic bone disease: role of transcription factors and future targets. *Bone* (2011) 48:30–6. doi:10.1016/j.bone.2010.05.035
72. Taipaleenmäki H, Browne G, Akech J, Zustin J, van Wijnen AJ, Stein JL, et al. Targeting of Runx2 by miR-135 and miR-203 impairs progression of breast cancer and metastatic bone disease. *Cancer Res* (2015) 75:1433–44. doi:10.1158/0008-5472.CAN-14-1026
73. Pratap J, Lian JB, Javed A, Barnes GL, van Wijnen AJ, Stein JL, et al. Regulatory roles of Runx2 in metastatic tumor and cancer cell interactions with bone. *Cancer Metastasis Rev* (2006) 25:589–600. doi:10.1007/s10555-006-9032-0
74. Blagodatski A, Poteryaev D, Katanaev VL. Targeting the Wnt pathways for therapies. *Mol Cell Ther* (2014) 2:28. doi:10.1186/2052-8426-2-28
75. Johnson RW, Merkel AR, Page JM, Ruppender NS, Guelcher SA, Sterling JA. Wnt signaling induces gene expression of factors associated with bone destruction in lung and breast cancer. *Clin Exp Metastasis* (2014) 31:945–59. doi:10.1007/s10585-014-9682-1
76. Hassan MQ, Maeda Y, Taipaleenmaki H, Zhang W, Jafferji M, Gordon JAR, et al. miR-218 directs a Wnt signaling circuit to promote differentiation of osteoblasts and osteomimicry of metastatic cancer cells. *J Biol Chem* (2012) 287:42084–92. doi:10.1074/jbc.M112.377515
77. Taipaleenmäki H, Farina NH, van Wijnen AJ, Stein JL, Hesse E, Stein GS, et al. Antagonizing miR-218-5p attenuates Wnt signaling and reduces metastatic bone disease of triple negative breast cancer cells. *Oncotarget* (2016) 7:79032–46. doi:10.18632/oncotarget.12593
78. Pollari S, Leivonen S-K, Perälä M, Fey V, Käkönen S-M, Kallioniemi O. Identification of microRNAs inhibiting TGF-β-induced IL-11 production in bone metastatic breast cancer cells. *PLoS One* (2012) 7:e37361. doi:10.1371/journal.pone.0037361
79. Png KJ, Halberg N, Yoshida M, Tavazoie SF. A microRNA regulon that mediates endothelial recruitment and metastasis by cancer cells. *Nature* (2012) 481:190–4. doi:10.1038/nature10661
80. Valencia K, Luis-Ravelo D, Bovy N, Antón I, Martínez-Canarias S, Zandueta C, et al. miRNA cargo within exosome-like vesicle transfer influences metastatic bone colonization. *Mol Oncol* (2014) 8:689–703. doi:10.1016/j.molonc.2014.01.012
81. Kagiya T. MicroRNAs and osteolytic bone metastasis: the roles of microRNAs in tumor-induced osteoclast differentiation. *J Clin Med* (2015) 4:1741–52. doi:10.3390/jcm4091741
82. Ell B, Kang Y. MicroRNAs as regulators of tumor-associated stromal cells. *Oncotarget* (2013) 4:2166–7. doi:10.18632/oncotarget.1625
83. Krzeszinski JY, Wei W, Huynh H, Jin Z, Wang X, Chang T-C, et al. miR-34a blocks osteoporosis and bone metastasis by inhibiting osteoclastogenesis and Tgif2. *Nature* (2014) 512:431–5. doi:10.1038/nature13375
84. Ell B, Mercatali L, Ibrahim T, Campbell N, Schwarzenbach H, Pantel K, et al. Tumor-induced osteoclast miRNA changes as regulators and biomarkers of osteolytic bone metastasis. *Cancer Cell* (2013) 24:542–56. doi:10.1016/j.ccr.2013.09.008
85. Lee DY, Deng Z, Wang C-H, Yang BB. MicroRNA-378 promotes cell survival, tumor growth, and angiogenesis by targeting SuFu and Fus-1 expression. *Proc Natl Acad Sci U S A* (2007) 104:20350–5. doi:10.1073/pnas.0706901104
86. Liu J, Li D, Dang L, Liang C, Guo B, Lu C, et al. Osteoclastic miR-214 targets TRAF3 to contribute to osteolytic bone metastasis of breast cancer. *Sci Rep* (2017) 7:40487. doi:10.1038/srep40487
87. Wang X, Guo B, Li Q, Peng J, Yang Z, Wang A, et al. miR-214 targets ATF4 to inhibit bone formation. *Nat Med* (2012) 19:93–100. doi:10.1038/nm.3026
88. Li D, Liu J, Guo B, Liang C, Dang L, Lu C, et al. Osteoclast-derived exosomal miR-214-3p inhibits osteoblastic bone formation. *Nat Commun* (2016) 7:10872. doi:10.1038/ncomms10872
89. Zhao C, Sun W, Zhang P, Ling S, Li Y, Zhao D, et al. miR-214 promotes osteoclastogenesis by targeting Pten/PI3k/Akt pathway. *RNA Biol* (2015) 12:343–53. doi:10.1080/15476286.2015.1017205

Conflict of Interest Statement: The authors declare that the research was conducted in the absence of any commercial or financial relationships that could be construed as a potential conflict of interest.

frontiers in Endocrinology

MINI REVIEW
published: 01 May 2018
doi: 10.3389/fendo.2018.00218

Soluble and Cell–Cell-Mediated Drivers of Proteasome Inhibitor Resistance in Multiple Myeloma

Mariah L. Farrell[1,2,3,4] *and Michaela R. Reagan*[1,2,3,4]*

[1] Reagan Laboratory, Maine Medical Center Research Institute, Scarborough, ME, United States, [2] Graduate School of Biomedical Sciences and Engineering, University of Maine, Orono, ME, United States, [3] School of Medicine, Tufts University, Boston, MA, United States, [4] Sackler School of Graduate Biomedical Sciences, Tufts University, Boston, MA, United States

It is becoming clear that myeloma cell-induced disruption of the highly organized bone marrow components (both cellular and extracellular) results in destruction of the marrow and support for multiple myeloma (MM) cell proliferation, survival, migration, and drug resistance. Since the first phase I clinical trial on bortezomib was published 15 years ago, proteasome inhibitors (PIs) have become increasingly common for treatment of MM and are currently an essential part of any anti-myeloma combination therapy. PIs, either the first generation (bortezomib), second generation (carfilzomib) or oral agent (ixazomib), all take advantage of the heavy reliance of myeloma cells on the 26S proteasome for their degradation of excessive or misfolded proteins. Inhibiting the proteasome can create a crisis specifically for myeloma cells due to their rapid production of immunoglobulins. PIs have relatively few side effects and can be very effective, especially in combination therapy. If PI resistance can be overcome, these drugs may prove even more useful to a greater range of patients. Both soluble and insoluble (contact mediated) signals drive PI-resistance *via* activation of various intracellular signaling pathways. This review discusses the currently known mechanisms of non-autonomous (microenvironment dependent) mechanisms of PI resistance in myeloma cells. We also introduce briefly cell-autonomous and stress-mediated mechanisms of PI resistance. Our goal is to help researchers design better ways to study and overcome PI resistance, to ultimately design better combination therapies.

Keywords: multiple myeloma, drug resistance, bone marrow MSCs, bortezomib, carfilzomib, ixazomib

OPEN ACCESS

Edited by:
Julie A. Sterling,
Vanderbilt University, United States

Reviewed by:
Han Qiao,
Shanghai Jiao-Tong University School of Medicine, China
Jawed Akhtar Siddiqui,
University of Nebraska Medical Center, United States

***Correspondence:**
Michaela R. Reagan
mreagan@mmc.org

Specialty section:
This article was submitted to Bone Research, a section of the journal Frontiers in Endocrinology

Received: *23 January 2018*
Accepted: *17 April 2018*
Published: *01 May 2018*

Citation:
Farrell ML and Reagan MR (2018) Soluble and Cell–Cell-Mediated Drivers of Proteasome Inhibitor Resistance in Multiple Myeloma. Front. Endocrinol. 9:218. doi: 10.3389/fendo.2018.00218

MYELOMA AND PROTEASOME INHIBITORS (PIs)

In 2017, there were an estimated 30,280 new cases of multiple myeloma (MM) diagnosed and ~12,590 deaths due to MM, which comprised ~2% of all cancer deaths (1). Although myeloma is typically considered an incurable cancer of the plasma cell, the overall survival for myeloma patients has improved from a prior median of 2.75 years around 1998 (1), to 6 years in 2010 (2), and up to 7.7 years for patients under 65 years old diagnosed between 2008 and 2015 (3). Current advances in the field aim to develop novel therapies using new targets in myeloma, determine better biomarkers for response or progression from the precursor disease monoclonal gammopathy of undefined significance, develop better combination treatments, and understand how to overcome drug resistance that occurs due to mutations or effects of the microenvironment on myeloma cells.

The proteasome is a multi-enzyme complex of the ubiquitin–proteasome system, which governs destruction of unwanted intracellular proteins and is needed to retain cellular health and homeostasis (3). Inhibition of proteasomal degradation results in cell apoptosis and death. Clinically, PIs are very useful in myeloma and other cancers. Bortezomib, a peptide boronic acid, is a slowly reversible

inhibitor of the β5 catalytic subunit within the 20S catalytic core complex. Carfilzomib irreversibly inhibits the same β5 site. Ixazomib is similar to bortezomib, and oprozomib is similar to carfilzomib, but both are, conveniently, orally administered. The investigational agent marizomib has a β-lactone unit that results in irreversible inhibition of both β2 and β5 catalytic sites (1). Off-target effects of PIs are typically minimal and can potentially be overcome with oral versions or tumor- or bone-targeted nanomedicine delivery systems (4). Gastrointestinal and cardiovascular toxicities, and other toxicities such as rash, have been observed with PIs (1).

Proteasome inhibitors inhibit key autocrine and paracrine signaling intracellular pathways associated with myeloma cell growth and survival, often signaled by extracellular matrix and cells of the bone marrow (BM), such as mesenchymal stromal cells (MSCs). PIs suppress the production of cytokines including interleukin-6 (IL-6), insulin-like growth factor 1 (IGF-1), and tumor necrosis factor α (TNFα), which can affect MSC and myeloma cell interactions (5). Interestingly, PIs can also suppress angiogenesis by decreasing VEGF secretion (5). PIs allow for the accumulation of misfolded and unfolded proteins, resulting in endoplasmic reticulum (ER) stress, reactive oxygen species (ROS)-induced oxidative stress, and the unfolded protein response in myeloma cells. PIs also inhibit NF-κB signaling (3), a major growth and survival signaling pathway in MM, which was the original reason for pursuing PIs in MM. However, NF-κB inhibition alone cannot account for the overall anti-MM activity of bortezomib, as demonstrated by studies comparing bortezomib to the IKK-B-specific inhibitor PS1145 (3). PIs also upregulate p53, a tumor suppressor that upregulates $p21^{Waf1}$ to induce cell cycle arrest (5). PIs can induce apoptosis through extrinsic caspase-8 cascade *via* activation of JNK, and *via* caspase-9 cleavage, associated with the upregulation of Noxa and inhibition of antiapoptotic Bcl-2 and XIAP family proteins (5, 6). PIs also suppress adhesion molecule and growth factor receptor expression (e.g., IL-6R) and inhibit cellular mechanisms for repairing double-strand DNA breaks (7). Unfortunately, many patients develop PI-refractory MM; the mechanisms of this resistance is discussed here (**Figure 1**).

STRESS-MEDIATED RESPONSES

Bortezomib can inhibit chymotrypsin-like proteasome activity in both bortezomib-sensitive and bortezomib-resistant cell lines, demonstrating that certain forms of bortezomib resistance are not dependent on the type or extent of proteasome inhibition (8). This suggests that certain pathways, such as stress-related pathways, are altered in PI-resistant cells, which may change their dependency on proteasome activity. Hypoxia, a state of low oxygen tension, can result from rapid tumor growth or be induced by chemotherapy. Muz and colleagues found that hypoxia drives PI resistance in MM1S, OPM1, and H929 myeloma

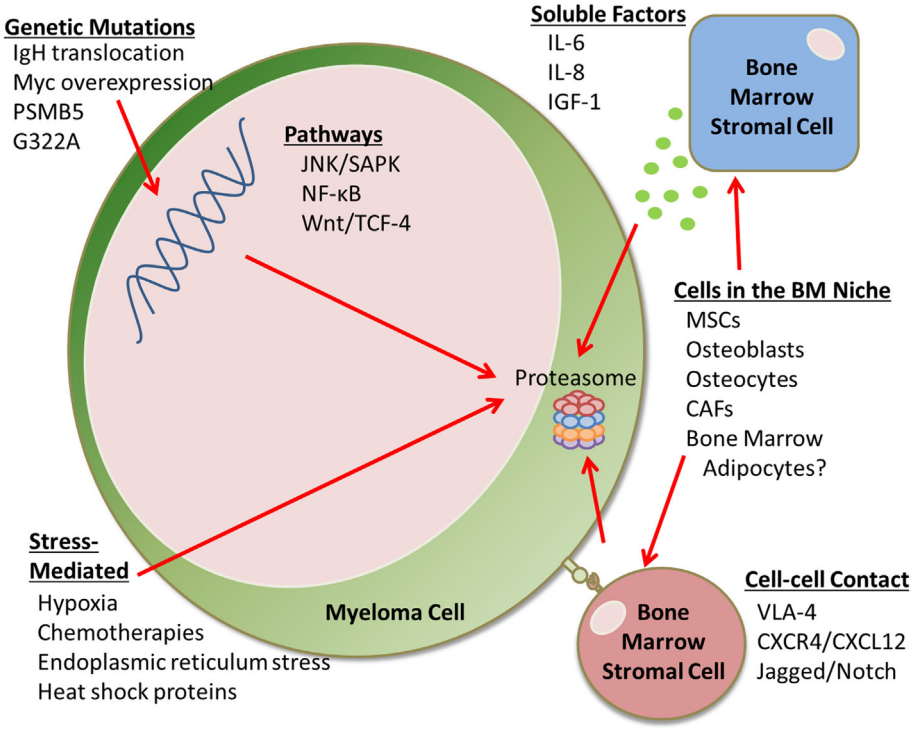

FIGURE 1 | Proteasome inhibition resistance mechanisms. This mini-review discusses the many factors that contribute to proteasome inhibitor (PI) resistance in the bone marrow (BM). For example, there are genetic mutations that can lead to drug resistance, as well as soluble factors and cell–cell contact-mediated signals from an array of BM stromal cells that can cause PI resistance. Cells that can cause drug resistance include mesenchymal stem cells (MSCs), osteoblasts, osteocytes, cancer-associated fibroblasts (CAFs), and potentially BM adipocytes. Stress-mediated responses can also cause PI resistance.

cells (9). Raninga et al. also found that hypoxic conditions induced bortezomib resistance; this resistance was linked to a decrease in NF-κB regulated genes (10). Treatment with selinexor, the first drug in a new class of agents known as Selective Inhibitor of Nuclear Export (SINE™) compounds, overcame hypoxia-induced bortezomib resistance by targeting the nuclear export protein exportin 1 (XPO1) in MM cells (11). Selinexor combined with bortezomib decreased tumor burden and extended survival in mice inoculated with bortezomib-resistant MM1S (11). Thus, selinexor and other inhibitors of XPO1, a protein found in the nucleus of cancer cells, hold great promise for combination therapy with PIs; currently, the STORM, STOMP, and BOSTON clinical trials are exploring this avenue.

Heat shock proteins (HSPs) are chaperone proteins that play a significant role in stressful conditions, such as chemotherapy exposure, and especially upon ER stress, typically triggered by accumulation of unfolded proteins. Many HSP-related genes are overexpressed, including HSP70, in bortezomib-resistant cells (8). Hamouda et al. demonstrated that HSPB8 gain or loss of function was a key factor in bortezomib resistance in U266 myeloma cells (12). Hsp27 has also been linked to bortezomib resistance, and Yasui et al. were able to overcome this by co-treating with BIRB 796 (13). In the study, bortezomib triggered upregulation of p38/MAPK and phosphorylation of Hsp27; BIRB 796 blocked this from occurring and ultimately led to cell death (13). Similarly, inhibiting Hsp90 with KW-2478, and co-treating with bortezomib induced caspase activation *in vitro*, and synergistic antitumor activity *in vivo* (14). Furthermore, Shringarpure et al. demonstrated that HSPs (HSP27, HSP70, and HSP90) and other chaperone proteins were more highly expressed in bortezomib-resistant SUDHL-4 lymphoma cells than in bortezomib-sensitive cells (8). HSP27 expression was also elevated in bortezomib-resistant HT-29 adenocarcinoma cells (15). Overall, the upregulation stress response genes and proteins, which cause cell survival and induce antiapoptotic pathways, induce PI resistance in many tumor types. For more on ER stress roles in the development of MM and drug resistance, we refer the reader to the recent review from Nikesitch et al. (16).

Environmental stresses, inflammatory cytokines, growth factors, and GPCR agonists can all also activate the JNK/SAPK pathway in myeloma cells. However, the role of this pathway in bortezomib is controversial. Some groups have found that bortezomib increases the stress kinase JNK pathway to induce apoptosis in myeloma cells (17) or cell death by overproduction of mitochondrial ROS (18); others suggest that the JNK signaling in myeloma cells induces their proliferation and PI-resistance (19, 20). The complicated feedback and overlap between the intercellular cellular signaling pathways further complicates identifying the pathways through which MM cells overcome PIs.

Recently, bortezomib has been shown to interfere with general protein biosynthesis at the stage of nuclear ribosome biogenesis (21). Galimberti et al. found that bortezomib-induced changes in cytoplasm morphology and nucleolar ultrastructure. These changes were associated with the accumulation of transcription factor (TF) ATF4 at nucleolar sites in ovarian and cervical cancer cells (21). ATF4 is a stress-inducible TF and it accumulates at specific rRNA-processing nucleolar regions. Thus, increased expression of proteins in this family may allow cells to survive under conditions of high proteotoxic cell stress and these proteins may be used by PI-resistant cells to handle stress induced by bortezomib. In lymphoma cells, ATF3, ATF4, and ATF5 can be induced by bortezomib treatment, but confusingly, their overexpression is associated with bortezomib sensitivity (8). Inhibiting the AAA ATPase, p97 with CB-5083 has recently shown excellent potential for overcoming PI resistance induced by p97-dependent retro-translocation of the TF, Nrf1, which transcribes proteasome subunit genes following exposure to a PI (22). More research into these TFs and epigenetic modulators in myeloma PI resistance is warranted.

Metabolic changes in MM cells have recently been discovered to contribute to PI-resistance. Cellular bioenergetics is significantly different between PI-resistant cells and their sensitive counterparts. Recent work from Thompson et al. demonstrated that targeting glutamine-induced respiration in PI resistant cells, using the glutaminase-1 inhibitor CB-839, synergized with PIs to induce cytotoxicity in MM cells (22). Targeting cellular metabolic pathways, and understanding how BM components change MM cell metabolic pathways, is likely an untapped resource in the fight against drug resistance in MM.

GENETIC MUTATION-MEDIATED DRUG RESISTANCE

In myeloma (23) and mesothelioma (24), high basal levels of proteasome activity or upregulation of proteasome subunits can overcome PI treatments. This finding suggests that an unfavorable load-versus-capacity balance represents a critical determinant of primary apoptotic sensitivity to bortezomib; understanding what modulates proteasomal activity thus may help in overcoming resistance. Genetic mutations, including mutations in the proteasome subunit 5 (PSMB5), mutations causing overexpression of MYC, and translocations of IgH gene locus, can induce very high basal levels of proteasome activity that overwhelm effects of proteasome inhibition. Oerlemans and colleagues observed that PI-resistant THP1 cells had a 60-fold increase in protein levels for PSMB5 and a G322A point mutation in the PSMB5 β-subunit of the bortezomib-binding pocket (25). A similar discovery was made by Balsas et al. in RPMI8226 myeloma cells, where overexpression of PSMB5 at the mRNA and protein level (although without a G322A mutation) was linked to their bortezomib resistance. Co-treatment with the histone deacetylase (HDAC) inhibitor trichostatin A induced synergistic effects with bortezomib to induce apoptosis (26). Indeed, HDAC inhibitors show efficacy in many combinatorial therapies to kill PI-resistant cells (27). Others have confirmed upregulation of PSMB5 gene and G332A mutations in other PI-resistant MM cells, which have a mutation cluster region in the binding pocket, particularly the S1 specificity pocket (28, 29). PSMB5 mutations had not been identified in humans until recently when Barrio et al. found certain subclones, resulting from branching evolution, that had mutations within PSMB5 resulting in PI resistance (30).

SOLUBLE FACTOR-MEDIATED DRUG RESISTANCE

Many soluble factors, including IL-6, IL-8, and IGF-1, in the BM microenvironment can also contribute to PI resistance. Voorhees and colleagues specifically found that CNTO 328, a monoclonal antibody against IL-6, enhanced cytotoxicity of bortezomib, activated caspase-3, -8, and -9, and induced HSP70 (31). Similarly, BM cancer-associated fibroblasts (CAFs) have recently been shown to protect against PI-induced apoptosis in myeloma cells, and produce high levels of IL-6, IL-8, and TGFβ (23). Bortezomib was found to induce ROS and autophagy in bortezomib-resistant CAFs by inhibiting mTOR and p62 and increasing light chain 3 protein-II (32). TGFβ was found to mediate bortezomib-induced autophagy, and a combination of bortezomib plus LY2109761, a selective TGFβRI/II inhibitor, induced apoptosis of RPMI8226 myeloma cells co-cultured with bortezomib-resistant CAFs (32). This study demonstrates how targeting stroma cells and stroma-derived factors can be useful in overcoming drug resistance and exemplifies how myeloma cells hijack their microenvironment to make it more tumor-supportive.

Similarly, primary MM cells have been found to be resistant to bortezomib partially from BM-MSC-derived cytokines. Interestingly, bortezomib and IL-8 may be involved in a positive feedback loop: in a study in which BM-MSCs were extracted from myeloma patients, bortezomib-resistant tumor cells had increased activity in the NF-κB pathway due to release of IL-8 from the MSCs (33). Myeloma patient MSCs secreted more IL-8 than healthy MSCs, and this was mimicked with cell co-cultures *in vitro*. Bortezomib further increased IL-8 expression from osteoclasts, stromal cells, and myeloma cell lines (23). Bortezomib may increase the expression of IL-8 through the p38 MAPK pathway (34). Kuhn et al. found that blocking IGF-1 or IGF-1R increased myeloma cell death synergistically when co-treating with bortezomib in cell lines and patient samples (35). Zheng et al. also found that mTOR and ERK1/2 signaling, *via* thioredoxin, can induce PI-resistance (36). The Azab lab also found that PI3K signaling in myeloma cells, and the PI3K-α isoform specifically, was induced by co-culturing myeloma cells with BM-MSCs and induced bortezomib resistance (37). The Ghobrial lab similarly found that a pan-class I PI3K inhibitor, buparlisib, could reduce MSC-induced survival in myeloma cells (38). These data suggest that PI3K and mTOR pathways contributed to PI resistance.

In addition to PI3K, NF-κB, activated *via* a range of stimuli, including ROS, TNFα, and IL-1β, is another pathway through which MSCs induce bortezomib resistance (33). MSC-derived exosomes induced PI-resistance in myeloma cells and contained contents that modulated JNK, p38, p53, and Akt pathways in myeloma cells (39). The HS-5 cell line has also been shown to induce bortezomib resistance in myeloma cells through CK2, a pivotal pro-survival kinase that activates NF-κB and STAT3 (40). The NF-κB signaling pathway has been shown to play a role in PI-resistance through numerous downstream signals including the upregulation of antiapoptotic BCL-XL (41). Moreover, hyaluronan and proteoglycan link protein 1 is produced in BM stromal cells from MM patients, is detected in patients' BM plasma, and has been shown to activate an atypical bortezomib-resistant NF-κB pathway in MM cells (16). Extensive new research has confirmed NF-κB signaling as critical in bortezomib resistance in MM cells (16). B-cell activating factor (BAFF), a cytokine in the TNF ligand family, is another important molecule shown to induce PI-resistance in MM cells (42). BAFF can drive macrophage-mediated PI-resistance and suppress caspase activation in MM cells through activation of Src, Erk1/2, Akt, and NF-κB signaling (42). Recent work from Qin et al. has shown that anti-BAFF-R antibody therapies had remarkable single-agent antitumor effects and induced potent antibody-dependent cellular cytotoxicity (ADCC) against multiple subtypes of human lymphoma and leukemia (16); we propose these may be useful in MM as well.

Macrophage inflammatory protein-1α is another macrophage (and myeloma) cell-derived cytokine that is able to induce bortezomib resistance. It functions through activation of ERK1/2, Akt, and mTOR pathways (43). Que et al. showed that the receptor tyrosine kinase c-Met is overexpressed in human myeloma cell lines and also causes PI-resistance *via* increased Akt/mTOR signaling (44). Akt can be activated by numerous agents (cytokines, integrins, RTKs, BCR signaling, and GPCR ligands) and can be downstream of the Jak1 and PI3K pathways. Recent studies in myeloma cells with N- and K-Ras mutations suggest that aspirin can increase the efficacy of bortezomib treatment *via* suppression of Akt phosphorylation, upregulation of survivin, and in part through suppressing Bcl-2 levels (45). The allosteric AKT inhibitor MK2206 was also found in myeloma cells to overcome bortezomib resistance induced by IL-6 or MSCs (46). Akt signaling has also been tied to autophagy, which is another mechanism of bortezomib resistance. Autophagy can result from signaling through CLCN5 (a member of the chloride channel family), which functions through the AKT/mTOR pathway (47). Blocking the mTOR/PI3K and Rad (Ras associated with diabetes) pathways have also been shown to overcome PI-resistance in lymphoma and hold potential in myeloma (48).

Soluble factors can also activate the Wnt signaling pathway, and the Wnt/TCF-4 signaling pathway may also be involved in PI resistance. In a bortezomib-resistant lymphoma cell line, increased TCF4 expression and increased transcription by the TCF-4/β-catenin complex was observed, accompanied by upregulation of their downstream target genes (c-myc and cyclin D1) (8). In myeloma, the β-catenin inhibitors BC2059 (46) and polyphyllin I (49) have been shown to be efficacious in combination with bortezomib.

CELL–CELL CONTACT-MEDIATED DRUG RESISTANCE

The BM niche contains many cells that directly interact with and alter myeloma cells in a bidirectional manner, leading to changes in both that support tumor progression, osteolysis, and disrupted hematopoiesis (50–53). Cell–cell contact-mediated drug resistance has become a widely recognized mechanism of drug resistance in the BM. Specific adhesion molecules of interest for MM PI-resistance include very late antigen-4 (VLA-4), CXC chemokine 12 (CXCL12) and its receptor CXC chemokine receptor 4 (CXCR4), and Jagged/Notch. VLA-4 has been linked to cell adhesion-mediated drug resistance (CAM-DR), and Noborio-Hatano et al. identified the α4-integrin (a subunit of VLA-4) as responsible for multiple drug

resistance in myeloma (54). BM-MSCs cause CAM-DR in part through the CXCR4/CXCL12 axis. Waldschmidt et al. showed that inhibiting CXCR4 with plerixafor or CXCL12 with NOX-A12 resensitized MM to PIs (55).

Jagged-1/Notch signaling has also been associated with PI resistance in MM, and this has been shown to be overcome with the use of PKC inhibitors (56). When notch ligand Dll1 on BM stromal cells binds to Notch2 receptor on myeloma cells, a cascade results that upregulates a cytochrome P450 enzyme involved in drug metabolism (CYP1A1), which ultimately leads to PI resistance. Treatment of cells with α-Naphthoflavone or CYP1A1 siRNA reintroduced PI sensitivity in myeloma cells (57). In sum, Jagged-1/Notch signaling has been a major pathway of focus for drug resistance in MM cells.

DTX3L is an ubiquitin ligase that plays an essential role in cell cycle and promotes adhesion to BM stromal cells or fibronectin. In work by Liu et al., inhibiting DTX3L induced an apoptotic response to bortezomib in myeloma cells (58). DTX3L was found to be regulated by focal adhesion kinase and represents another pathway through which CAM-DR is induced in myeloma cells. Bustany et al. compared myeloma cells that continually express cyclin D1 versus parental controls. Similarly with DTX3L, cyclin D1 expression increased myeloma adhesion to stromal cells and fibronectin. These cells also had stabilized F-actin fibers, enhanced chemotaxis, and inflammatory chemokine secretion. Both parental and cyclin D1-expressing cells were resistant to acute carfilzomib treatment when cultured on stromal cells, but this could be overcome in cyclin D1-expressing cells after pretreatment with lenalidomide. The team found changes in myeloma cell metabolism (specifically, increases in ROS) in cyclin-D expressing cells, and resulting increases in oxidative stress-induced ERK1/2 signaling (59).

FUTURE DIRECTIONS

There remains a great need to overcome bortezomib resistance in myeloma. As described here, AKT/PI3K and NF-κB pathways are heavily involved drug resistance in MM. Interestingly, there may be crosstalk between these two major pathways that has yet to be explored. Kloo et al. found that inhibiting PI3K in activated B cell like diffuse large B cell lymphoma (ABC DLBCL) cells decreased NF-κB target genes, which led to decreased survival of the ABC DLBCL cells (60). Similarly, findings in a study using an iMYC^{Eμ} B lymphoma line created by Han et al. suggested that constitutive activation of NF-κB and STAT3 was dependent on signaling through the PI3K pathway and was essential for survival and proliferation (61). While these studies did not look specifically at PI drug resistance, the crosstalk could be implicated in the drug resistance in myeloma. As this is becoming a growing focus in the lymphoma cancer field and because many labs have shown the importance of these two pathways in the progression of MM, this crosstalk should be investigated.

The future of PI-resistance, and drug resistance in general, will be greatly aided by advances in high-throughput "-omics" techniques that create an unprecedented opportunity for understanding PI-resistance at the genomic, transcriptomic, and proteomic level. Novel PIs are also being developed that can likely overcome resistance by targeting two or more proteasome subunits, such as the syringolin analog, syringolog-1, which inhibits the activity of both the β5 and β2 subunits (22).

As stemness, dedifferentiation, and drug resistance often correlate, a better characterization of the myeloma stem cell will likely provide even more information about drug resistance and emergence of a drug-resistant clone from a parental population (23, 62). Interestingly, Gu et al. demonstrated that inducing differentiation of MM cells made these more sensitive to bortezomib (23). For example, the blockade of PAX5 (also known as B cell-specific activator protein) (63) and changes in X-box-binding protein (62) TF splicing induce differentiation and targeting these proteins has been shown to reduce bortezomib resistance in MM (64). Finally, one of the areas that hold great potential for overcoming drug resistance is through therapeutically targeting BM stromal cells that have not previously been targeted, such as the BM adipocytes. As Falank et al. have recently shown, BM adipocytes may induce drug resistance in MM cells through both soluble and cell–cell contact-mediated mechanisms (65). More research into the roles of BM adipocytes in MM drug resistance is warranted.

CONCLUSION

Proteasome inhibitor resistance occurs through a variety of mechanisms, which evade different functions of PIs. PIs can also synergize or have additive activity with other chemotherapies or myeloma-targeted agents, and PI-based combination regimens are ubiquitous in myeloma treatment algorithms for clinicians, which often comprise immunomodulatory drugs, monoclonal antibodies, and HDAC inhibitors. However, myeloma patients may be resistance to PIs, based on a certain mutation, epigenetic change, or microenvironmental influence on their tumor cells, and patients often become refractory to PIs due to emergence of a PI-resistant clone. It is likely that more mechanisms of PI-resistance exist and these should be further explored. Combination therapies have proven essential for overcoming PI resistance in myeloma and other cancers, and further research in this arena, especially with consideration as to how to target the stroma or overcome stroma-induced PI-resistance, will likely further improve treatment options for myeloma patients. For more reading on the 26S PI resistance in myeloma beyond this mini-review, we refer the reader to the reviews by Gandolfi et al. (1), Larocca et al. (66), and Ziogas et al. (67).

AUTHOR CONTRIBUTIONS

MF and MR co-wrote and co-edited this review.

FUNDING

The authors' work is supported by the NIH/NIGMS U54GM115516, P30GM106391, P20GM121301, and P30GM103392; the NIH/NIDDK (R24 DK092759-01); the NIH/NIAMS P30AR066261; the American Cancer Society (Research Grant #IRG-16-191-33); and start-up funds from the Maine Medical Center Research Institute. The content is solely the responsibility of the authors and does not necessarily represent the official views of the NIH.

REFERENCES

1. Gandolfi S, Laubach JP, Hideshima T, Chauhan D, Anderson KC, Richardson PG. The proteasome and proteasome inhibitors in multiple myeloma. *Cancer Metastasis Rev* (2017) 36:561–84. doi:10.1007/s10555-017-9707-8
2. Kyle RA, Gertz MA, Witzig TE, Lust JA, Lacy MQ, Dispenzieri A, et al. Review of 1027 patients with newly diagnosed multiple myeloma. *Mayo Clin Proc* (2003) 78:21–33. doi:10.4065/78.1.21
3. Blimark CH, Turesson I, Genell A, Ahlberg L, Björkstrand B, Carlson K, et al. Outcome and survival of myeloma patients diagnosed 2008-2015. Real world data on 4904 patients from the Swedish Myeloma Registry (SMR). *Haematologica* (2018) 103(3):506–13. doi:10.3324/haematol.2017.178103
4. Swami A, Reagan MR, Basto P, Mishima Y, Kamaly N, Glavey S, et al. Engineered nanomedicine for myeloma and bone microenvironment targeting. *Proc Natl Acad Sci U S A* (2014) 111:10287–92. doi:10.1073/pnas.1401337111
5. Pei X-Y, Dai Y, Grant S. The proteasome inhibitor bortezomib promotes mitochondrial injury and apoptosis induced by the small molecule Bcl-2 inhibitor HA14-1 in multiple myeloma cells. *Leukemia* (2003) 17:2036–45. doi:10.1038/sj.leu.2403109
6. Adams J. The proteasome: a suitable antineoplastic target. *Nat Rev Cancer* (2004) 4:349–60. doi:10.1038/nrc1361
7. Cottini F, Guidetti A, Paba Prada C, Hideshima T, Maglio M, Varga C, et al. *Resistance to Proteasome Inhibitors in Multiple Myeloma*. Cham: Springer. p. 47–80. doi:10.1007/978-3-319-06752-0_2
8. Shringarpure R, Catley L, Bhole D, Burger R, Podar K, Tai Y-T, et al. Gene expression analysis of B-lymphoma cells resistant and sensitive to bortezomib. *Br J Haematol* (2006) 134:145–56. doi:10.1111/j.1365-2141.2006.06132.x
9. Muz B, de la Puente P, Azab F, Luderer M, Azab AK. Hypoxia promotes stem cell-like phenotype in multiple myeloma cells. *Blood Cancer J* (2014) 4:e262. doi:10.1038/bcj.2014.82
10. Raninga PV, Di Trapani G, Vuckovic S, Tonissen KF. TrxR1 inhibition overcomes both hypoxia-induced and acquired bortezomib resistance in multiple myeloma through NF-κβ inhibition. *Cell Cycle* (2016) 15:559–72. doi:10.1080/15384101.2015.1136038
11. Muz B, Azab F, de la Puente P, Landesman Y, Azab AK. Selinexor overcomes hypoxia-induced drug resistance in multiple myeloma. *Transl Oncol* (2017) 10:632–40. doi:10.1016/j.tranon.2017.04.010
12. Hamouda M-A, Belhacene N, Puissant A, Colosetti P, Robert G, Jacquel A, et al. The small heat shock protein B8 (HSPB8) confers resistance to bortezomib by promoting autophagic removal of misfolded proteins in multiple myeloma cells. *Oncotarget* (2014) 5:6252–66. doi:10.18632/oncotarget.2193
13. Yasui H, Hideshima T, Ikeda H, Jin J, Ocio EM, Kiziltepe T, et al. BIRB 796 enhances cytotoxicity triggered by bortezomib, heat shock protein (Hsp) 90 inhibitor, and dexamethasone via inhibition of p38 mitogen-activated protein kinase/Hsp27 pathway in multiple myeloma cell lines and inhibits paracrine tumour growth. *Br J Haematol* (2007) 136:414–23. doi:10.1111/j.1365-2141.2006.06443.x
14. Ishii T, Seike T, Nakashima T, Juliger S, Maharaj L, Soga S, et al. Anti-tumor activity against multiple myeloma by combination of KW-2478, an Hsp90 inhibitor, with bortezomib. *Blood Cancer J* (2012) 2:e68. doi:10.1038/bcj.2012.13
15. Suzuki E, Demo S, Deu E, Keats J, Arastu-Kapur S, Bergsagel PL, et al. Molecular mechanisms of bortezomib resistant adenocarcinoma cells. *PLoS One* (2011) 6:e27996. doi:10.1371/journal.pone.0027996
16. Nikesitch N, Lee JM, Ling S, Roberts TL. Endoplasmic reticulum stress in the development of multiple myeloma and drug resistance. *Clin Transl Immunology* (2018) 7(1):e1007. doi:10.1002/cti2.1007
17. Hoang B, Shi Y, Frost PJ, Mysore V, Bardeleben C, Lichtenstein A. SGK kinase activity in multiple myeloma cells protects against ER stress apoptosis via a SEK-dependent mechanism. *Mol Cancer Res* (2016) 14:397–407. doi:10.1158/1541-7786.MCR-15-0422
18. Song I-S, Jeong YJ, Jeong SH, Heo HJ, Kim HK, Lee SR, et al. Combination treatment with 2-methoxyestradiol overcomes bortezomib resistance of multiple myeloma cells. *Exp Mol Med* (2013) 45:e50. doi:10.1038/emm.2013.104
19. Xu G, Shen XJ, Pu J, Chu SP, Wang XD, Wu XH, et al. BLyS expression and JNK activation may form a feedback loop to promote survival and proliferation of multiple myeloma cells. *Cytokine* (2012) 60:505–13. doi:10.1016/j.cyto.2012.06.317
20. Shen X, Guo Y, Qi J, Shi W, Wu X, Ni H, et al. Study on the association between miRNA-202 expression and drug sensitivity in multiple myeloma cells. *Pathol Oncol Res* (2016) 22:531–9. doi:10.1007/s12253-015-0035-4
21. Galimberti V, Kinor N, Shav-Tal Y, Biggiogera M, Brüning A. The stress-inducible transcription factor ATF4 accumulates at specific rRNA-processing nucleolar regions after proteasome inhibition. *Eur J Cell Biol* (2016) 95:389–400. doi:10.1016/j.ejcb.2016.08.002
22. Thompson RM, Dytfeld D, Reyes L, Robinson RM, Smith B, Manevich Y, et al. Glutaminase inhibitor CB-839 synergizes with carfilzomib in resistant multiple myeloma cells. *Oncotarget* (2017) 8(22):35863–76. doi:10.18632/oncotarget.16262
23. Gu J, Li J, Zhou Z, Liu J, Huang B, Zheng D, et al. Differentiation induction enhances bortezomib efficacy and overcomes drug resistance in multiple myeloma. *Biochem Biophys Res Commun* (2012) 420:644–50. doi:10.1016/j.bbrc.2012.03.056
24. Cerruti F, Jocollè G, Salio C, Oliva L, Paglietti L, Alessandria B, et al. Proteasome stress sensitizes malignant pleural mesothelioma cells to bortezomib-induced apoptosis. *Sci Rep* (2017) 7:17626. doi:10.1038/s41598-017-17977-9
25. Oerlemans R, Franke NE, Assaraf YG, Cloos J, van Zantwijk I, Berkers CR, et al. Molecular basis of bortezomib resistance: proteasome subunit beta5 (PSMB5) gene mutation and overexpression of PSMB5 protein. *Blood* (2008) 112:2489–99. doi:10.1182/blood-2007-08-104950
26. Balsas P, Galán-Malo P, Marzo I, Naval J. Bortezomib resistance in a myeloma cell line is associated to PSMβ5 overexpression and polyploidy. *Leuk Res* (2011) 36:212–8. doi:10.1016/j.leukres.2011.09.011
27. Yao R, Han D, Sun X, Fu C, Wu Q, Yao Y, et al. Histone deacetylase inhibitor NaBut suppresses cell proliferation and induces apoptosis by targeting p21 in multiple myeloma. *Am J Transl Res* (2017) 9:4994–5002.
28. Franke N, Niewerth D, Assaraf Y, Van Meerloo J, Vojtekova K, Van Zantwijk C, et al. Impaired bortezomib binding to mutant β5 subunit of the proteasome is the underlying basis for bortezomib resistance in leukemia cells. *Leukemia* (2011) 26:757–68. doi:10.1038/leu.2011.256
29. Ri M, Iida S, Nakashima T, Miyazaki H, Mori F, Ito A, et al. Bortezomib-resistant myeloma cell lines: a role for mutated PSMB5 in preventing the accumulation of unfolded proteins and fatal ER stress. *Leukemia* (2010) 24:1506–12. doi:10.1038/leu.2010.137
30. Barrio S, Stühmer T, Teufel E, Barrio-Garcia C, Chatterjee M, Schreder M, et al. Parallel evolution of multiple PSMB5 mutations in a myeloma patient treated with bortezomib. *Blood* (2016) 128:3282.
31. Voorhees PM, Chen Q, Kuhn DJ, Small GW, Hunsucker SA, Strader JS, et al. Inhibition of interleukin-6 signaling with CNTO 328 enhances the activity of bortezomib in preclinical models of multiple myeloma. *Clin Cancer Res* (2007) 13(21):6469–78. doi:10.1158/1078-0432.CCR-07-1293
32. Frassanito MA, De Veirman K, Desantis V, Di Marzo L, Vergara D, Ruggieri S, et al. Halting pro-survival autophagy by TGFβ inhibition in bone marrow fibroblasts overcomes bortezomib resistance in multiple myeloma patients. *Leukemia* (2016) 30:640–8. doi:10.1038/leu.2015.289
33. Markovina S, Callander NS, O'Connor SL, Xu G, Shi Y, Leith CP, et al. Bone marrow stromal cells from multiple myeloma patients uniquely induce bortezomib resistant NF-kappaB activity in myeloma cells. *Mol Cancer* (2010) 9:176. doi:10.1186/1476-4598-9-176
34. Sanacora S, Urdinez J, Chang T-P, Vancurova I. Anticancer drug bortezomib increases interleukin-8 expression in human monocytes. *Biochem Biophys Res Commun* (2015) 460:375–9. doi:10.1016/j.bbrc.2015.03.041
35. Kuhn DJ, Berkova Z, Jones RJ, Woessner R, Bjorklund CC, Ma W, et al. Targeting the insulin-like growth factor-1 receptor to overcome bortezomib resistance in preclinical models of multiple myeloma. *Nat Rev Cancer* (2012) 12:252–64. doi:10.1182/blood-2011-10-386789
36. Zheng Z, Fan S, Zheng J, Huang W, Gasparetto C, Chao NJ, et al. Inhibition of thioredoxin activates mitophagy and overcomes adaptive bortezomib resistance in multiple myeloma. *J Hematol Oncol* (2018) 11(1):29. doi:10.1186/s13045-018-0575-7
37. Azab F, Vali S, Abraham J, Potter N, Muz B, de la Puente P, et al. PI3KCA plays a major role in multiple myeloma and its inhibition with BYL719 decreases proliferation, synergizes with other therapies and overcomes stroma-induced resistance. *Br J Haematol* (2014) 165:89–101. doi:10.1111/bjh.12734
38. Sahin I, Azab F, Mishima Y, Moschetta M, Tsang B, Glavey SV, et al. Targeting survival and cell trafficking in multiple myeloma and Waldenstrom

macroglobulinemia using pan-class I PI3K inhibitor, buparlisib. *Am J Hematol* (2014) 89:1030–6. doi:10.1002/ajh.23814
39. Wang J, Hendrix A, Hernot S, Lemaire M, De Bruyne E, Van Valckenborgh E, et al. Bone marrow stromal cell-derived exosomes as communicators in drug resistance in multiple myeloma cells. *Blood* (2014) 124:555–66. doi:10.1182/blood-2014-03-562439
40. Manni S, Brancalion A, Mandato E, Tubi LQ, Colpo A, Pizzi M, et al. Protein kinase CK2 inhibition down modulates the NF-κB and STAT3 survival pathways, enhances the cellular proteotoxic stress and synergistically boosts the cytotoxic effect of bortezomib on multiple myeloma and mantle cell lymphoma cells. *PLoS One* (2013) 8:e75280. doi:10.1371/journal.pone.0075280
41. Xiang Y, Remily-Wood ER, Oliveira V, Yarde D, He L, Cheng JQ, et al. Monitoring a nuclear factor-κB signature of drug resistance in multiple myeloma. *Mol Cell Proteomics* (2011) 10:M110.005520. doi:10.1074/mcp.M110.005520
42. Chen J, He D, Chen Q, Guo X, Yang L, Lin X, et al. BAFF is involved in macrophage-induced bortezomib resistance in myeloma. *Cell Death Dis* (2017) 8:e3161. doi:10.1038/cddis.2017.533
43. Tsubaki M, Takeda T, Tomonari Y, Mashimo K, Koumoto Y, Hoshida S, et al. The MIP-1α autocrine loop contributes to decreased sensitivity to anticancer drugs. *J Cell Physiol* (2018) 233(5):4258–71. doi:10.1002/jcp.26245
44. Que W, Chen J, Chuang M, Jiang D. Knockdown of c-Met enhances sensitivity to bortezomib in human multiple myeloma U266 cells via inhibiting Akt/mTOR activity. *APMIS* (2012) 120:195–203. doi:10.1111/j.1600-0463.2011.02836.x
45. Ding J-H, Yuan L-Y, Chen G-A. Aspirin enhances the cytotoxic activity of bortezomib against myeloma cells via suppression of Bcl-2, survivin and phosphorylation of AKT. *Oncol Lett* (2017) 13:647–54. doi:10.3892/ol.2016.5472
46. Xiang R-F, Wang Y, Zhang N, Xu W-B, Cao Y, Tong J, et al. MK2206 enhances the cytocidal effects of bufalin in multiple myeloma by inhibiting the AKT/mTOR pathway. *Cell Death Dis* (2017) 8:e2776. doi:10.1038/cddis.2017.188
47. Zhang H, Pang Y, Ma C, Li J, Wang H, Shao Z. ClC5 decreases the sensitivity of multiple myeloma cells to bortezomib via promoting pro-survival autophagy. *Oncol Res* (2017). doi:10.3727/096504017X15049221237147
48. Kim A, Park S, Lee J-E, Jang W-S, Lee S-J, Kang HJ, et al. The dual PI3K and mTOR inhibitor NVP-BEZ235 exhibits anti-proliferative activity and overcomes bortezomib resistance in mantle cell lymphoma cells. *Leuk Res* (2012) 36:912–20. doi:10.1016/j.leukres.2012.02.010
49. Liang Y, Li X, He X, Qiu X, Jin X, Zhao X, et al. Polyphyllin I induces cell cycle arrest and apoptosis in human myeloma cells via modulating *β*-catenin signaling pathway. *Eur J Haematol* (2016) 97:371–8. doi:10.1111/ejh.12741
50. Roccaro AMAM, Sacco A, Maiso P, Azab AKAK, Tai Y-T, Reagan M, et al. BM mesenchymal stromal cell-derived exosomes facilitate multiple myeloma progression. *J Clin Invest* (2013) 123:1542–55. doi:10.1172/JCI66517
51. McDonald MM, Reagan MR, Youlten SE, Mohanty ST, Seckinger A, Terry RL, et al. Inhibiting the osteocyte-specific protein sclerostin increases bone mass and fracture resistance in multiple myeloma. *Blood* (2017) 129:3452–64. doi:10.1182/blood-2017-03-773341
52. Fairfield H, Falank C, Avery L, Reagan MR. Multiple myeloma in the marrow: pathogenesis and treatments. *Ann N Y Acad Sci* (2016) 1364:32–51. doi:10.1111/nyas.13038
53. Reagan MR, Ghobrial IM. Multiple myeloma-mesenchymal stem cells: characterization, origin, and tumor-promoting effects. *Clin Cancer Res* (2012) 18:342–9. doi:10.1158/1078-0432.CCR-11-2212
54. Noborio-Hatano K, Kikuchi J, Takatoku M, Shimizu R, Wada T, Ueda M, et al. Bortezomib overcomes cell-adhesion-mediated drug resistance through downregulation of VLA-4 expression in multiple myeloma. *Oncogene* (2009) 28:231–42. doi:10.1038/onc.2008.385
55. Waldschmidt JM, Simon A, Wider D, Müller SJ, Follo M, Ihorst G, et al. CXCL12 and CXCR7 are relevant targets to reverse cell adhesion-mediated drug resistance in multiple myeloma. *Br J Haematol* (2017) 179:36–49. doi:10.1111/bjh.14807
56. Muguruma Y, Yahata T, Warita T, Hozumi K, Nakamura Y, Suzuki R, et al. Jagged1-induced Notch activation contributes to the acquisition of bortezomib resistance in myeloma cells. *Blood Cancer J* (2017) 7:650. doi:10.1038/s41408-017-0001-3
57. Xu D, Hu J, De Bruyne E, Menu E, Schots R, Vanderkerken K, et al. Dll1/Notch activation contributes to bortezomib resistance by upregulating CYP1A1 in multiple myeloma. *Biochem Biophys Res Commun* (2012) 428:518–24. doi:10.1016/j.bbrc.2012.10.071
58. Shen Y, Sun Y, Zhang L, Liu H. Effects of DTX3L on the cell proliferation, adhesion, and drug resistance of multiple myeloma cells. *Tumour Biol* (2017) 39:1–10. doi:10.1177/1010428317703941
59. Bustany S, Bourgeais J, Tchakarska G, Body S, Hérault O, Gouilleux F, et al. Cyclin D1 unbalances the redox status controlling cell adhesion, migration, and drug resistance in myeloma cells. *Oncotarget* (2016) 7:1–11. doi:10.18632/oncotarget.9901
60. Kloo B, Nagel D, Pfeifer M, Grau M, Düwel M, Vincendeau M, et al. Critical role of PI3K signaling for NF-kappaB-dependent survival in a subset of activated B-cell-like diffuse large B-cell lymphoma cells. *Proc Natl Acad Sci U S A* (2011) 108:272–7. doi:10.1073/pnas.1008969108
61. Han S-S, Yun H, Son D-J, Tompkins VS, Peng L, Chung S-T, et al. NF-κB/STAT3/PI3K signaling crosstalk in iMyc Eμ B lymphoma. *Mol Cancer* (2010) 9:97. doi:10.1186/1476-4598-9-97
62. Kawano Y, Fujiwara S, Wada N, Izaki M, Yuki H, Okuno Y, et al. Multiple myeloma cells expressing low levels of CD138 have an immature phenotype and reduced sensitivity to lenalidomide. *Int J Oncol* (2012) 41:876–84. doi:10.3892/ijo.2012.1545
63. Nera K-P, Kohonen P, Narvi E, Peippo A, Mustonen L, Terho P, et al. Loss of Pax5 promotes plasma cell differentiation. *Immunity* (2006) 24:283–93. doi:10.1016/j.immuni.2006.02.003
64. Wang D, Chen J, Li R, Wu G, Sun Z, Wang Z, et al. PAX5 interacts with RIP2 to promote NF-κB activation and drug-resistance in B-lymphoproliferative disorders. *J Cell Sci* (2016) 129:2261–72. doi:10.1242/jcs.183889
65. Falank C, Fairfield H, Farrell M, Reagan MR. New bone cell type identified as driver of drug resistance in multiple myeloma: the bone marrow adipocyte. *Blood* (2017) 130:122.
66. Larocca A, Mina R, Gay F, Bringhen S, Boccadoro M. Emerging drugs and combinations to treat multiple myeloma. *Oncotarget* (2017) 8:60656–72. doi:10.18632/oncotarget.19269
67. Ziogas DC, Terpos E, Kastritis E, Dimopoulos MA. An overview of the role of carfilzomib in the treatment of multiple myeloma. *Expert Opin Pharmacother* (2017) 18:1883–97. doi:10.1080/14656566.2017.1404575

Conflict of Interest Statement: The authors declare that the research was conducted in the absence of any commercial or financial relationships that could be construed as a potential conflict of interest.

The handling Editor declared a past co-authorship with the author MR.

frontiers in Endocrinology

ORIGINAL RESEARCH
published: 16 May 2018
doi: 10.3389/fendo.2018.00241

Parathyroid Hormone-Related Protein Negatively Regulates Tumor Cell Dormancy Genes in a PTHR1/Cyclic AMP-Independent Manner

Rachelle W. Johnson[1], Yao Sun[2,3], Patricia W. M. Ho[2], Audrey S. M. Chan[4], Jasmine A. Johnson[1], Nathan J. Pavlos[4], Natalie A. Sims[2,3] and T. John Martin[2,3]*

[1] Department of Medicine, Division of Clinical Pharmacology, Vanderbilt Center for Bone Biology, Vanderbilt University Medical Center, Nashville, TN, United States, [2] Bone Biology and Disease Unit, St. Vincent's Institute of Medical Research, Fitzroy, VIC, Australia, [3] Department of Medicine at St. Vincent's Hospital, University of Melbourne, Melbourne, VIC, Australia, [4] Cellular Orthopaedic Laboratory, School of Biomedical Sciences, The University of Western Australia, Crawley, WA, Australia

OPEN ACCESS

Edited by:
Chandi C. Mandal, Central University of Rajasthan, India

Reviewed by:
Han Qiao, Shanghai Jiao-Tong University School of Medicine, China
Petra Simic, Massachusetts Institute of Technology, United States

***Correspondence:**
Rachelle W. Johnson
rachelle.johnson@vanderbilt.edu

Specialty section:
This article was submitted to Bone Research, a section of the journal Frontiers in Endocrinology

Received: *27 January 2018*
Accepted: *26 April 2018*
Published: *16 May 2018*

Citation:
Johnson RW, Sun Y, Ho PWM, Chan ASM, Johnson JA, Pavlos NJ, Sims NA and Martin TJ (2018) Parathyroid Hormone-Related Protein Negatively Regulates Tumor Cell Dormancy Genes in a PTHR1/Cyclic AMP-Independent Manner. Front. Endocrinol. 9:241. doi: 10.3389/fendo.2018.00241

Parathyroid hormone-related protein (PTHrP) expression in breast cancer is enriched in bone metastases compared to primary tumors. Human MCF7 breast cancer cells "home" to the bones of immune deficient mice following intracardiac inoculation, but do not grow well and stain negatively for Ki67, thus serving as a model of breast cancer dormancy *in vivo*. We have previously shown that PTHrP overexpression in MCF7 cells overcomes this dormant phenotype, causing them to grow as osteolytic deposits, and that PTHrP-overexpressing MCF7 cells showed significantly lower expression of genes associated with dormancy compared to vector controls. Since early work showed a lack of cyclic AMP (cAMP) response to parathyroid hormone (PTH) in MCF7 cells, and cAMP is activated by PTH/PTHrP receptor (PTHR1) signaling, we hypothesized that the effects of PTHrP on dormancy in MCF7 cells occur through non-canonical (i.e., PTHR1/cAMP-independent) signaling. The data presented here demonstrate the lack of cAMP response in MCF7 cells to full length PTHrP(1–141) and PTH(1–34) in a wide range of doses, while maintaining a response to three known activators of adenylyl cyclase: calcitonin, prostaglandin E_2 (PGE_2), and forskolin. PTHR1 mRNA was detectable in MCF7 cells and was found in eight other human breast and murine mammary carcinoma cell lines. Although PTHrP overexpression in MCF7 cells changed expression levels of many genes, RNAseq analysis revealed that PTHR1 was unaltered, and only 2/32 previous PTHR1/cAMP responsive genes were significantly upregulated. Instead, PTHrP overexpression in MCF7 cells resulted in significant enrichment of the calcium signaling pathway. We conclude that PTHR1 in MCF7 breast cancer cells is not functionally linked to activation of the cAMP pathway. Gene expression responses to PTHrP overexpression must, therefore, result from autocrine or intracrine actions of PTHrP independent of PTHR1, through signals emanating from other domains within the PTHrP molecule.

Keywords: parathyroid hormone-related protein, cyclic AMP, MCF7, breast cancer, calcium signaling

INTRODUCTION

Parathyroid hormone-related protein (PTHrP, gene name *PTHLH/Pthlh*) is a cytokine with functions in both pathology and physiology (1, 2). Although it was identified as the circulating factor responsible for humoral hypercalcemia of malignancy (3), it more commonly acts in a paracrine manner: in breast cancer cells it promotes their metastasis (4, 5), in bone (osteoblasts and osteocytes) it stimulates bone formation (6, 7), and in cartilage cells (chondrocytes) it controls proliferation and hypertrophy (8).

In breast cancer cells that lay dormant in bone (9) we have previously shown that overexpression of PTHrP enables otherwise dormant human MCF7 breast cancer cells to aggressively colonize the bone marrow and induce osteolysis (5). Consistent with enhanced bone colonization, we recently reported that such overexpression of PTHrP in MCF7 cells results in the downregulation of several pro-dormancy genes (9).

The best understood actions of PTHrP are those that are mediated by its binding to the G protein-coupled receptor that it shares with parathyroid hormone (PTH) (PTHR1). Upon ligand binding to the receptor, cyclic AMP (cAMP) is activated, followed by protein kinase A (PKA) activation, cAMP responsive element binding protein (CREB) phosphorylation, and transcription of CREB target genes (10–13). This PTHR1-dependent signaling pathway is shared between PTH and PTHrP due to high sequence homology in their amino-terminal domains; the portion of the molecule that interacts with the receptor (14). Early work showed that MCF7 cells failed to respond to PTH treatment with any increase in cAMP or activation of cAMP-dependent protein kinase, suggesting that PTHR1 in those cells is not functionally linked to adenylyl cyclase (15). In contrast, MCF7 cells possess specific, high affinity receptors for calcitonin linked to adenylyl cyclase activation, and activate cAMP in response to prostaglandin E_2 (15, 16). These data suggest that the effect of PTHrP overexpression on tumor dormancy in MCF7 cells may occur through PTHR1-independent actions of the PTHrP molecule.

Using multiple assays, we report here that MCF7 cells, and many other breast cancer cell lines, express PTHR1 mRNA but do not bind PTH, nor do they activate cAMP formation or subsequent cAMP signaling events in response to PTH or PTHrP. Our RNAseq analyses identify many genes induced by PTHrP overexpression in MCF7 cells, and several potential alternative pathways, notably those related to calcium signaling.

MATERIALS AND METHODS

Cell Culture

Human MCF7 cells were obtained from ATCC and grown in DMEM supplemented with 10% FBS and penicillin/streptomycin (P/S). MCF7pcDNA and MCF7 PTHrP-overexpressing cells were generated as described previously (5) and grown in the same conditions as MCF7 cells; we utilized strains grown and maintained at two separate institutions to validate findings. All breast cancer and mouse mammary carcinoma cell lines were obtained and grown as previously described (9). The rat osteosarcoma (UMR106-01) cell line was maintained in DMEM supplemented with 10% FBS and P/S as described in Ref. (17). MC3T3-E1 cells were maintained in α-MEM supplemented with 10% FBS as described in Ref. (18).

cAMP Response Assay

Briefly, MCF7 cells were cultured in 12-well plate in cell culture media containing 1 mM isobutylmethylxanthine. Cells were then treated for 12 min with either PTH (100 nM) (sourced from Bachem, Bubendorf, Switzerland), PTHrP(1–141) (100 nM) [expressed in *Escherichia coli* and purified in house (7)], or the known agonists forskolin (10 μM) (sourced from Sigma), prostaglandin E_2 (1 μM) (sourced from Sigma), or salmon calcitonin (sCT) (1 μM) (kindly gifted by the late Dr. M Azria, Novartis AG, Basel, Switzerland). The cells were washed, acidified ethanol was added, and after air drying was reconstituted in assay buffer and cAMP formation assayed as previously (19).

CRE-Luciferase Assay

MCF7 cells were transiently transfected with cAMP response element (pCRE)-luciferase (Clontech), a vector containing multiple copies of CRE binding sequences. Fugene (Promega) was used to transfect cells. Four hours after agonist stimulation, cells were lysed, substrate (Promega) was added, and signal was measured using a Polarstar Optima.

Real-Time Quantitative PCR

Cell lines were harvested in TRIzol (Life Technologies) or TriSure (Bioline) for phenol/chloroform extraction of RNA, DNAse digested (TURBO DNA-free kit, Life Technologies), and cDNA was synthesized from 200 ng–1 μg RNA (iScript cDNA synthesis kit, Bio-Rad or Tetro cDNA synthesis kit, Bioline) per the manufacturer's instructions as previously described (9). Real-time PCR was performed on either a Quantstudio5 384-well plate format (Thermo Fisher) or Stratagene MX3000P (Agilent) with the following cycling conditions: 2 min at 50°C, 10 min at 95°C, (15 s at 95°C, 1 min at 60°C) × 40 cycles, and dissociation curve (15 s at 95°C, 1 min at 60°C, 15 s at 95°C) or 10 min at 95°C, (30 s at 95°C, 1 min at 60°C) × 40 cycles, and dissociation curve (1 min at 95°C, 30 s at 55°C, 30 s at 95°C). Primers for mouse *PTHR1* were previously published (20) and human *PTHR1* primer sequences were sourced from MGH Primerbank (F: CTGGGCATGATTTACACCGTG, R: CAGTG CAGCCGCCTAAAGTA). Human *PTHLH* primers were previously published (21) and human *HPRT1*, *RGS2*, *CREB*, *PRKAR1*, *AREG*, and *NR4A1* primers were previously published (22). Primer sequences for human *BDKRB1* and *CALML3* were designed using PrimerBLAST (*BDKRB1* F: AATGCTACGGCCTGTGACAA, R: TCCCTAGGAGGCCGAAGAAA; *CALML3* F: TGGTTGAT TCAGCCCACCTC, R: TCCGTGTCATTCAGACGAGC). Gene expression between samples was normalized to *B2M* expression or *B2M*: *HPRT1* geometric mean. Relative expression was quantified using the comparative CT method [$2^{-(\text{Gene Ct}-\text{Normalizer Ct})}$].

Confocal Microscopy

Antibodies and Reagents

Tetramethylrhodamine (TMR)-labeled PTH(1–34) (PTH^{-TMR}) was synthesized as previously described (23). Anti-VPS35 mouse

monoclonal was purchased from Santa Cruz Biotechnology Inc., USA. Alexa Fluor 488 anti-mouse secondary antibody was purchased from Molecular Probes®, Invitrogen, USA.

Imaging

MCF7 and UMR106-01 cells were cultured as described above, and seeded on poly-L-lysine-coated glass coverslips at 1×10^4 cells/well (96-well plate) for 24–48 h prior to agonist stimulation. Cells were then serum starved for 1 h prior to the addition of PTH^{-TMR} (100 nM) for 15 min at 37°C. Cells were then washed in ice-cold 1× PBS and fixed in 4% PFA at room temperature, permeabilized with 0.1% Triton X-100 for 5 min, washed in 0.2% BSA-PBS, and blocked in 3% BSA-PBS for 30 min. Cells were then incubated with anti-VPS35 antibody (Santa Cruz Biotechnology Inc.) for 1 h at room temperature, and washed in 0.2% BSA-PBS and 1× PBS prior to incubation with Alexa Fluor 488 anti-mouse secondary antibody (Molecular Probes®, Invitrogen), for 45 min at room temperature. Cells were then stained with DAPI stain and mounted in ProLong® Diamond Antifade (Molecular Probes®, Invitrogen). Detection of immunofluorescence was performed using a Nikon A1Si confocal microscope running NIS-C Elements Software (Nikon Corp., Japan). A 40× oil immersion objective lens (Nikon, Japan) was used, where serial optical sections (z-stack) of 0.5–1 μm were used to reconstruct 2D projections in FIJI (NIH, USA).

RNA Sequencing and Bioinformatics

RNA samples of MCF7pcDNA control and MCF7 PTHrP-overexpressing cells ($n = 3$ independent replicates/group) were submitted to the Stanford Functional Genomics Facility and analyzed for RNA integrity using a Bioanalyzer (Eukaryote Total RNA Nano, Agilent) and all samples had a RNA integrity number of 9.50–10 (10 is highest quality possible). RNA samples were sequenced on an Illumina NextSeq with coverage of approximately 40 million reads per sample. Sequence alignment and RNAseq bioinformatics analysis was performed by the Vanderbilt Technologies for Advanced Genomics Analysis and Research Design (VANGARD) core at Vanderbilt University Medical Center. RNAseq files are available in the GEO repository (GEO accession number GSE110713).

Statistics

All data are presented as the mean of $n = 3$ biological replicates obtained from three independent experiments (one biological replicate, with three technical replicates per experiment). For all graphs error bars indicate the SEM. Statistical tests used are indicated in the figure legends, and p-values were considered significant at $p < 0.05$.

RESULTS

PTHR1 mRNA Is Detected in Breast Cancer Cells

PTHR1 mRNA levels varied but were detectable across all human breast cancer and mouse mammary carcinoma cell lines tested (**Figure 1**). The panel included cell lines termed "high metastatic potential" [that aggressively colonize the bone after intracardiac inoculation or lung after tail vein inoculation (9)], and cell lines termed "Low metastatic potential" (9) [that do not colonize, or proliferate very slowly after inoculation (9)]. PTHR1 mRNA levels did not correspond to the metastatic potential of the cell lines. 4T1 and D2A1 cells had the lowest expression of PTHR1, which was nearly undetectable (4T1: Ct values = 33–39; D2A1: Ct values = 33–34). All breast cancer cell lines had at least 10-fold lower *PTHR1* mRNA levels than MC3T3-E1 cells, which have a robust cAMP response to exogenous PTH and PTHrP treatment (24).

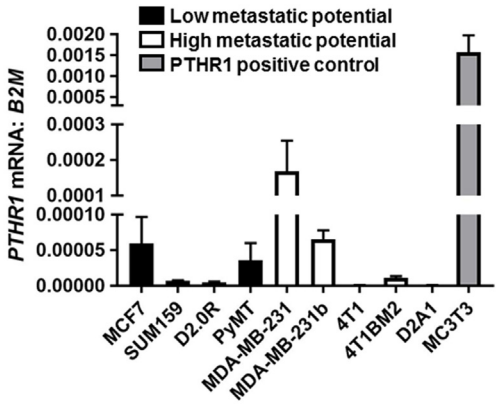

FIGURE 1 | PTHR1 is expressed by breast cancer cells. *PTHR1* mRNA levels in human breast cancer cell lines {MCF7, SUM159, MDA-MB-231, MDA-MB-231b [bone metastatic clone (25, 26)]}, mouse mammary carcinoma cell lines {D2.0R, PyMT, 4T1, 4T1BM2 [bone metastatic clone (27)], D2A1}, classified according to metastatic potential, and PTHR1/cyclic AMP responsive MC3T3-E1 cells. mRNA levels were normalized to β-2-microglobulin (*B2M*) housekeeping gene. Graphs = mean + SE. $n = 3$ replicates from independent experiments.

Neither PTH nor PTHrP Stimulates cAMP in Breast Cancer Cells

MCF7 cells robustly induced cAMP formation in response to forskolin, PGE_2, and sCT, but treatment with high dose PTH(1–34) or PTHrP(1–141) elicited no cAMP response (**Figure 2A**). This confirmed the lack of a cAMP response to PTH in MCF7 cells as reported at the time of discovery of the functional calcitonin receptor (15). In order to investigate later cellular responses, MCF7 cells were transiently transfected with a cAMP response element (CRE)-luciferase construct (CRE-Luc). Treatment with either sCT or PGE_2 resulted in substantial activation of the CRE-Luc reporter, with no detectable effect of PTH(1–34). All were used at multiple doses in repeated experiments, with no measureable effects detected (**Figure 2B**).

Tetramethylrhodamine-labeled PTH (PTH^{-TMR}) has proven useful for monitoring the surface binding and internalization of amino-terminal PTH upon its target cells through the PTHR1 (23). Vacuolar protein sorting 35 (VPS35) is an essential subunit of the mammalian retromer trafficking complex, where retromer coordinates both retrograde (endosome-to-Golgi) and recycling (endosome-to-plasma membrane) of many cell surface receptors

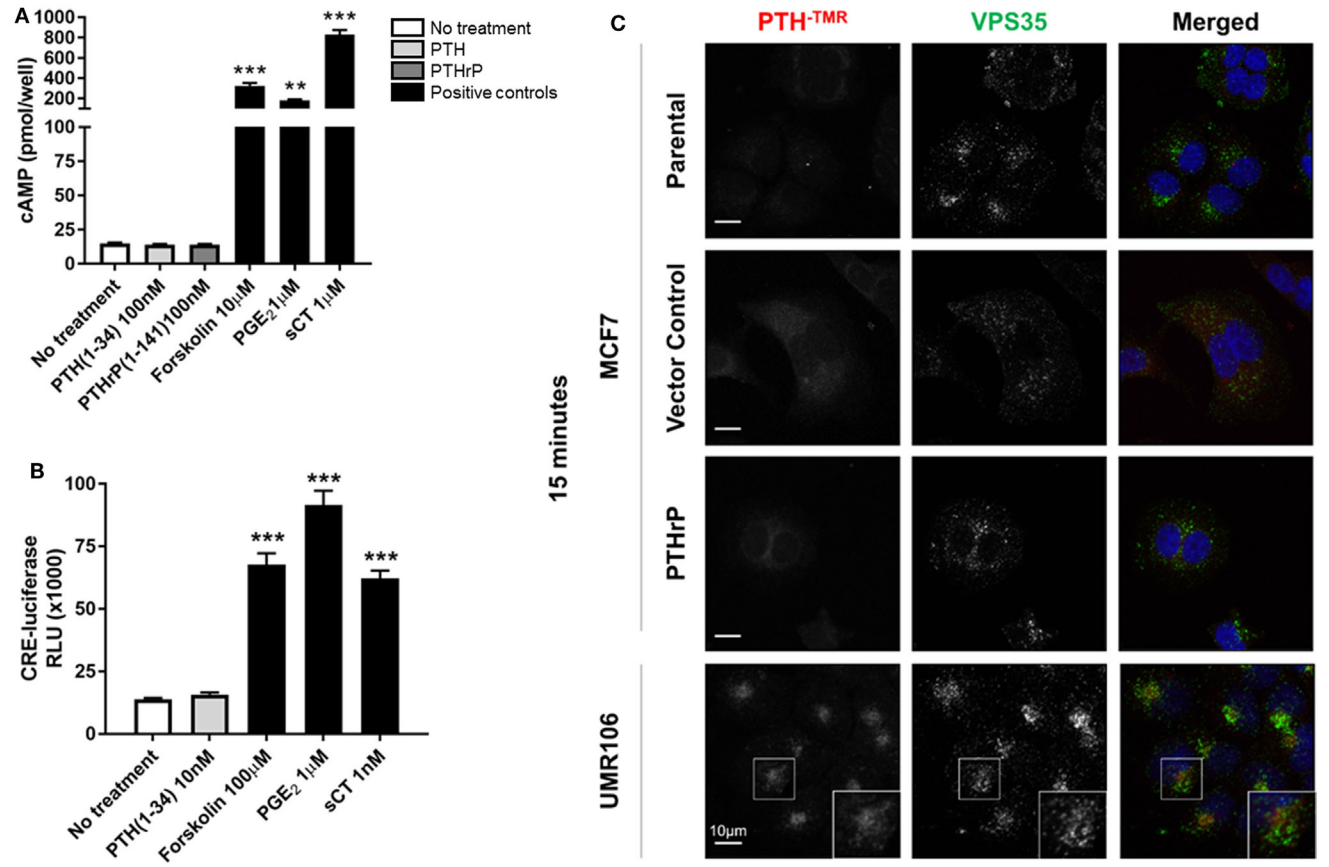

FIGURE 2 | Neither parathyroid hormone (PTH) nor parathyroid hormone-related protein (PTHrP) bind to/activate cyclic AMP (cAMP) in MCF7 cells. **(A)** cAMP production in MCF7 cells following 12 min stimulation with PTH(1–34) or PTHrP(1–141), or positive controls forskolin, prostaglandin E_2 (PGE_2), or salmon calcitonin (sCT). Graphs = mean + SE. $n = 3$ replicates from independent experiments. $^{**}p < 0.01$, $^{***}p < 0.001$ vs no treatment by one-way ANOVA with multiple comparisons. **(B)** cAMP response element (CRE)-luciferase signal following 4 h stimulation with PTH or positive controls forskolin, prostaglandin E_2 (PGE_2), or sCT. Graphs = mean + SE. $n = 3$ replicates from independent experiments. $^{***}p < 0.001$ vs no treatment by one-way ANOVA with multiple comparisons. **(C)** Confocal images of stable MCF7 and UMR106-01 cells cultured on poly-L-lysine-coated glass coverslips and serum starved for 1 h prior to the addition of tetramethylrhodamine-labeled PTH(1–34) (PTH^{-TMR}, 100 nM) for 15 min at 37°C. Cells were fixed in 4% PFA and immunostained for the endogenous retromer subunit, vacuolar protein sorting 35 (VPS35). Scale bar, 10 μm. Representative of $n = 3$ independent experiments.

(28), including PTHR1 (23, 29) along the endocytic pathway. VPS35, therefore, serves as a marker of internalized PTH^{-TMR}–PTHR1 ligand-receptor complexes following their sequestration into early endosomes (23). Accordingly, the addition of PTH^{-TMR} at saturating conditions (100 nM) for 15 min to UMR106-01 cells, was sufficient to visualize encapsulated ligand–receptor complexes in early endosomes, as determined by its co-localization with VPS35 (**Figure 2C**). This event coincides with the generation of cAMP following stimulation with either PTH and PTHrP peptides with identical dose responses (19). In contrast, neither PTH^{-TMR} internalization nor co-localization with VPS35 was detected in MCF7 parental, vector-transfected, or PTHrP-transfected cells (**Figure 2C**).

Lack of cAMP Gene Response in MCF7 Cells

In order to identify novel dormancy genes regulated by PTHrP, we used RNAseq to analyze which pathways are activated in response to PTHrP overexpression in MCF7 cells. We identified >2,500 genes differentially regulated with a $\log_2$ fold change >1 and $p < 0.05$ in MCF7 PTHrP-overexpressing vs MCF7 control cells (**Figure 3A**). Consistent with our finding that neither PTH nor PTHrP induce cAMP formation or early post-receptor activation events in MCF7 cells, RNAseq analysis confirmed that only 2 of a previously described panel of 32 CREB-responsive genes (22) were significantly upregulated in MCF7 PTHrP-overexpressing cells (**Table 1**). Three CREB-responsive genes were significantly downregulated, and the remaining 27 were not altered by PTHrP over-expression, confirming that even long term overexpression of PTHrP does not induce genes that result from cAMP signaling in MCF7 cells.

Validation of several candidate CREB-responsive genes in MCF7 PTHrP-overexpressing cell lines maintained at a separate institution was consistent with our RNAseq findings (**Figures 3B–E**). The one exception was *NR4A1*, which was found to be unaltered by RNAseq, but was significantly upregulated in

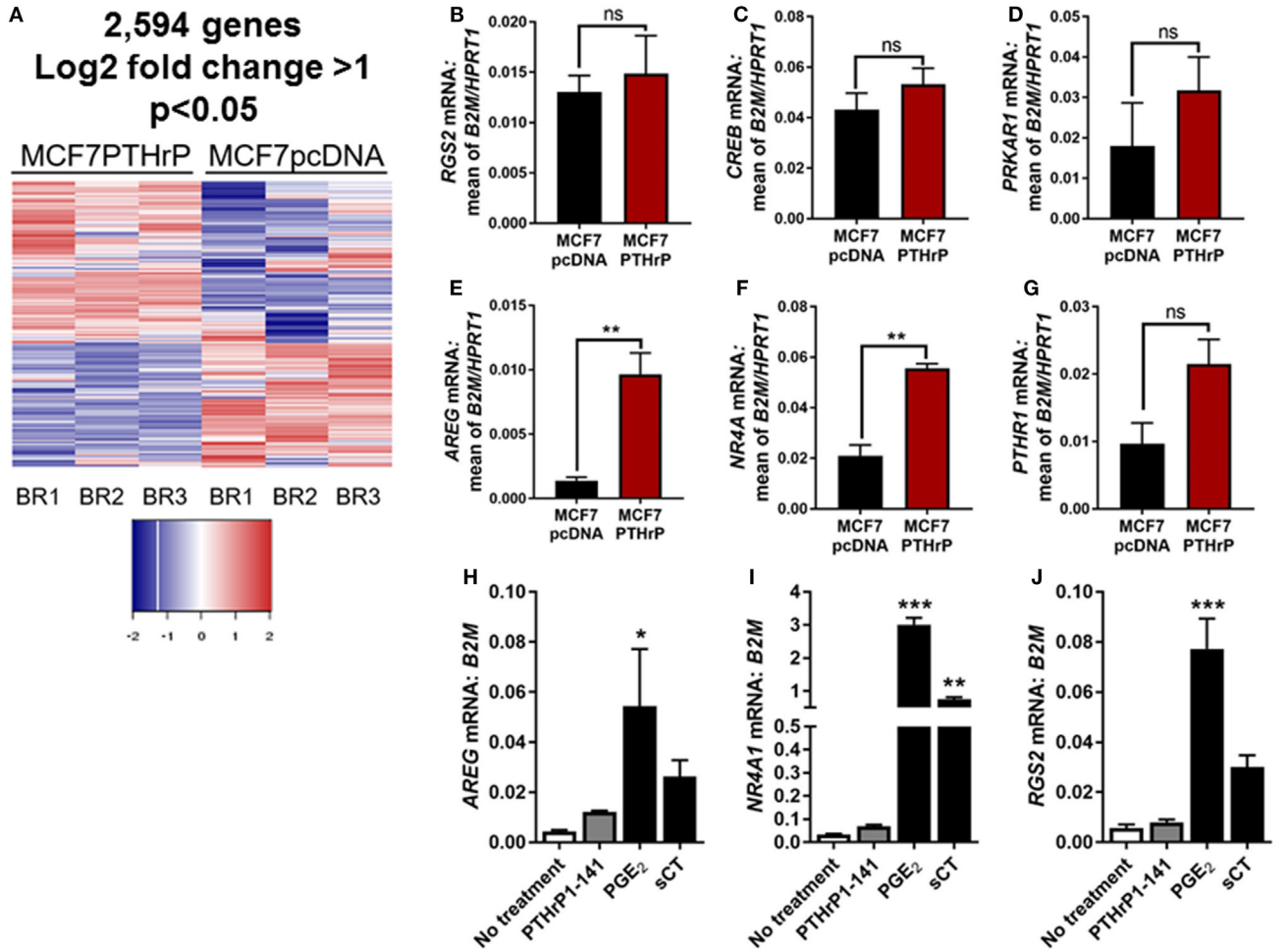

FIGURE 3 | Parathyroid hormone-related protein (PTHrP) overexpression does not induce cyclic AMP (cAMP) target genes. **(A)** Heat map of gene expression with 95% confidence intervals in MCF7pcDNA (empty vector control) or MCF7 PTHrP-overexpressing cells. BR1 = biological replicate 1, BR2 = biological replicate 2, BR3 = biological replicate 3. **(B–G)** qPCR for cAMP target genes in MCF7pcDNA or MCF7 PTHrP-overexpressing cells. mRNA levels were normalized to the geometric mean of *B2M* and *HPRT1* housekeeping genes. Graphs = mean + SE. $^{**}p < 0.01$ by unpaired Student's *T*-test. **(H–J)** qPCR for cAMP target genes in MCF7 cells following stimulation with PTHrP(1–141) or positive controls prostaglandin E_2 (PGE_2) or salmon calcitonin (sCT). Graphs = mean + SE. $n = 3$ replicates from independent experiments. $^{*}p < 0.05$, $^{**}p < 0.01$, $^{***}p < 0.001$ vs no treatment by one-way ANOVA with multiple comparisons.

PTHrP-overexpressing cells by real-time PCR (**Figure 3F**). We also confirmed that *PTHR1* is not downregulated with PTHrP overexpression (**Figure 3G**). In addition, treatment with positive controls PGE_2 and sCT induced significantly greater mRNA levels of CREB-responsive genes *AREG*, *NR4A1*, or *RGS2*, but exogenous treatment with PTHrP(1–141) had no significant effect (**Figures 3H–J**).

RNAseq Confirms PTHrP Overexpression Reduces Pro-Dormancy Genes

We previously reported that PTHrP overexpression in MCF7 cells significantly reduced the pro-dormancy genes *LIFR*, *SOCS3*, *TPM1*, *AMOT*, *P4HA1*, *HIST1H2BK*, *SELENBP1*, and *QSOX1* (9). RNAseq analysis confirmed that 6/8 of these genes were downregulated in MCF7 PTHrP-overexpressing cells (**Table 2**).

Calcium-Related Pathways Are Activated in Response to PTHrP Overexpression in MCF7 Cells

We next performed STRING analysis on the RNAseq data to identify significantly enriched pathways. We separately analyzed the 250 upregulated and downregulated genes (all $p < 0.05$) with the largest $\log_2$ fold change, a total of 500 genes analyzed (**Figures 4A,B**). STRING pathway analysis of this RNAseq data revealed that the most significantly enriched pathways (false discovery rate = 0.0081–0.0324) in MCF7 cells overexpressing PTHrP in comparison to parental MCF7 cells and across all 500 genes, were the calcium signaling pathway, cytokine–cytokine receptor interaction, chemokine signaling pathway, and inflammatory mediator regulation of transient receptor potential (TRP) channels (**Figure 4C**).

TABLE 1 | Cyclic AMP (cAMP) signaling is not induced by parathyroid hormone-related protein (PTHrP) in MCF7 cells.

Gene name	Log_2 fold change	*p*-Value	Direction
AREG	3.58	1.25E-07	Up
NRP1	0.75	5.12E-04	Up
FOS	−0.74	0.03	Down
AQP3	−1.07	1.14E-03	Down
CEBPD	−0.83	0.03	Down
SOX9	−0.41	0.41	–
NR4A3	−0.07	0.93	–
BTG2	−0.29	0.53	–
UGDH	0.06	0.87	–
DUSP1	−0.12	0.75	–
NR4A2	0.14	0.69	–
GEM	−0.47	0.66	–
RGS2	−0.12	0.93	–
TCF7	0.19	0.56	–
VEGFA	−0.03	0.96	–
NR4A1	0.52	0.53	–
TEX2	0.04	0.88	–
IFNGR1	0.07	0.88	–
EFNB2	0.53	0.10	–
SIK2	−0.16	0.49	–
PLAUR	0.39	0.34	–
BMP8A	0.14	0.82	–
JUNB	0.15	0.72	–
IER3	0.83	0.17	–
USP2	−0.38	0.40	–
NFIL3	0.02	0.95	–
NFKB2	0.08	0.75	–
DLEC1	0.25	0.65	–
FOXC2	0.67	0.65	–
LST1	−0.05	0.97	–
KCNE4	0.25	0.56	–
IL6	0.60	0.81	–
PTHR1	0.01	0.99	–

RNAseq values for 32 known cAMP target genes (22) and PTHR1 (bottom of table) in MCF7 PTHrP-overexpressing cells compared to MCF7 vector controls.
Red = significantly up-regulated, green = significantly down-regulated, gray = no significant change.

TABLE 2 | Dormancy genes are downregulated by parathyroid hormone-related protein (PTHrP) in MCF7 cells.

Gene name	Log_2 fold change	*p*-Value
LIFR	−0.57	$p = 0.09$
SOCS3	−1.18	$p = 0.01$*
AMOT	−0.45	$p = 0.04$*
P4HA1	−0.54	$p = 0.02$*
HIST1H2BK	−0.61	$p = 0.003$**
SELENBP1	−0.65	$p = 2.92 \times 10^{-5}$****
TPM1	0.02	$p = 0.945$
QSOX1	−0.35	$p = 0.13$

RNAseq values for eight pro-dormancy genes (9) in MCF7 PTHrP-overexpressing cells compared to MCF7 vector controls.
Green = significantly down-regulated, gray = no significant change.
*$p < 0.05$, **$p < 0.01$, ****$p < 0.0001$.*

The calcium signaling pathway and TRP channels are ion channels with high selectivity for Ca^{2+} (30), indicating calcium signaling is dramatically altered with PTHrP overexpression. There was overlap of 5/6 regulated genes in the "calcium signaling pathway" and "regulation of TRP channel pathway" from STRING analysis (*P2RX6* was specific for the calcium signaling pathway) (**Figure 5A**); there were no unique TRP channel pathway genes that were regulated. mRNA levels for *PTHLH* (control), *BDKRB1*, and *CALML3* (**Figures 5B–D**) confirmed the RNAseq findings in MCF7 PTHrP-overexpressing cells.

DISCUSSION

This work provides extensive evidence that PTHrP, although it is capable of inducing substantial changes in gene expression and behavior in MCF7 cells, does not signal through the PTHR1 to activate the cAMP pathway in these cells. Although PTHR1 is detected by qPCR, no cAMP response was detected, and no activity was observed in a CREB reporter assay. Furthermore, out of all the known cAMP responsive genes, only 2 of 32 were regulated in a positive direction by RNAseq analysis. In contrast, PTHrP overexpression in these cells upregulated genes associated with the calcium signaling pathway.

When human breast cancer cells were found to express functional receptors for calcitonin and PGE_2 linked to adenylyl cyclase activation, no such activation could be detected in response to PTH(1–34) (15). We confirm this observation in the present experiments and show that PTHrP(1–141) also lacks this activity. In addition, we report that PTH(1–34) has no effect on activation of a CREB reporter construct that is readily activated by either sCT or PGE_2. The latter two agonists, unlike PTH and PTHrP, also promoted expression of genes known to be regulated by the PKA–CREB pathway. There were only two cAMP responsive genes that were significantly upregulated with PTHrP overexpression by RNAseq: *AREG* and *NRP1*. Both of these genes have been implicated in cancer. *AREG* is essential for estrogen receptor-targeted therapeutic response (31). *NRP1* has been previously shown to promote tumorigenesis by enhancing angiogenesis (32) and NRP1-positive cells have been reported to have tumor-initiating properties (33). Thus the upregulation of these genes may result from indirect effects independent of cAMP, a possibility we will investigate. It is also worth noting that the PTHrP induction of *AREG* mRNA, and the CREB-responsive gene *NR4A1*, in MCF7s is much lower than its induction with the positive controls prostaglandin E_2 (PGE_2) and sCT. In a separate study, we have tested the same secreted form of PTHrP, and the same preparation of recombinant PTHrP(1–141) in Ocy454 cells, an osteocyte cell line that expresses the PTHR1 (7). Overexpression and exogenous treatment both induced a significant increase in cAMP in these cells, and overexpression increased the CREB responsive genes, *Nr4a1* and *Rgs2* (7) confirming that these forms of PTHrP are capable of inducing a CREB response, but not in MCF7 cells.

Our data also indicate that PTH, which shares with PTHrP the same ability to bind to the PTHR1, does not bind to MCF7 cells in any detectable manner. This is illustrated by use of the PTH^{-TMR} reagent, which requires functional PTHR1 for CREB activation and internalization into early endosomes. This suggests that the action of overexpressed PTHrP that suppresses dormancy and results in major changes in gene expression and osteolytic destruction of bone, is not only not cAMP-mediated, but is also not elicited through the PTHR1. However, we have not excluded the possibility that PTHrP binds to PTHR1 at levels below our detection limits, and initiates cAMP-independent signaling.

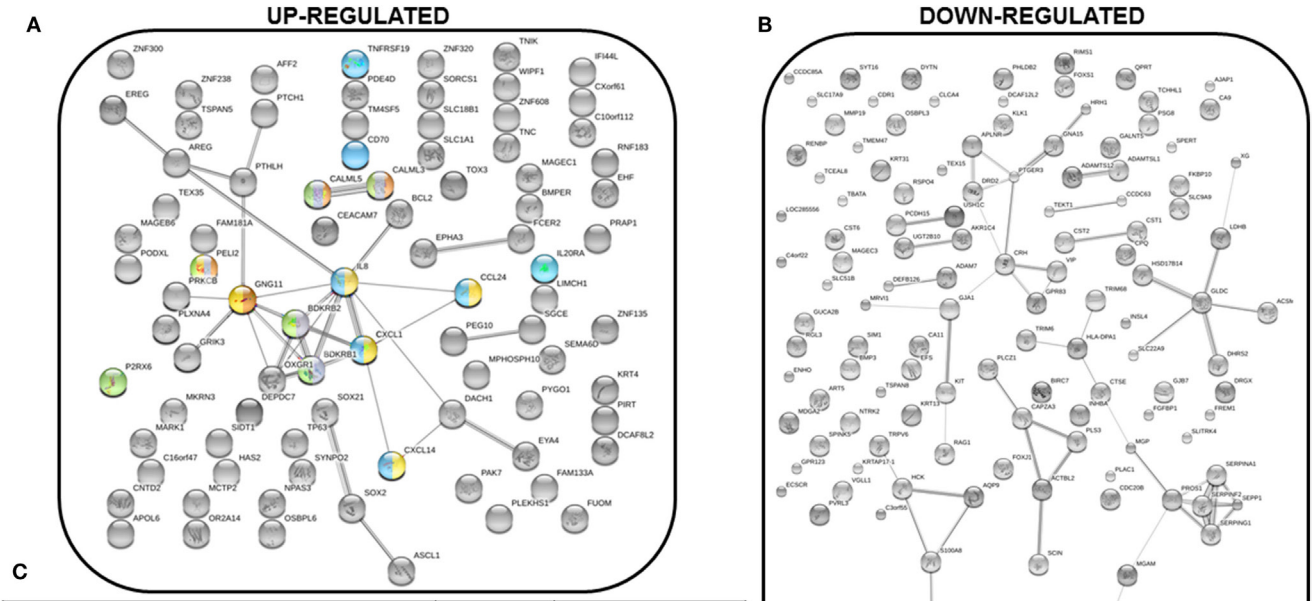

KEGG BIOLOGICAL PATHWAY (UP-REGULATED)	Gene count	False discovery rate
Calcium signaling pathway	6	0.0081
Cytokine-cytokine receptor interaction	7	0.0081
Chemokine signaling pathway	6	0.0081
Inflammatory mediator regulation of TRP channels	5	0.0081
Circadian entrainment	4	0.0324

FIGURE 4 | Multiple signaling pathways are upregulated in MCF7 parathyroid hormone-related protein-overexpressing cells. **(A)** STRING network analysis of the top 250 upregulated genes (with $\log_2$ fold change >1 and $p < 0.05$). Colors of each node correspond to the KEGG pathway indicated in **(C)**. **(B)** STRING network analysis of the top 250 downregulated genes (with $\log_2$ fold change <−1 and $p < 0.05$). **(C)** KEGG biological pathways significantly enriched for in the STRING analysis of the top 250 upregulated genes. There were no significantly enriched KEGG biological pathways for the top 250 downregulated genes. Colors correspond to the nodes in **(A)**.

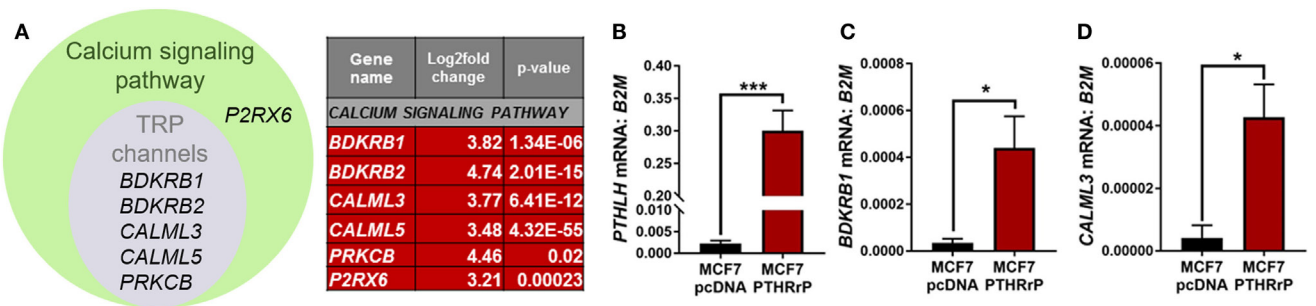

Gene name	Log2fold change	p-value
CALCIUM SIGNALING PATHWAY		
BDKRB1	3.82	1.34E-06
BDKRB2	4.74	2.01E-15
CALML3	3.77	6.41E-12
CALML5	3.48	4.32E-55
PRKCB	4.46	0.02
P2RX6	3.21	0.00023

FIGURE 5 | The calcium signaling pathway is significantly enriched downstream of parathyroid hormone-related protein (PTHrP) in MCF7 cells. **(A)** Venn diagram indicating the calcium signaling pathway and transient receptor potential (TRP) channel genes that were significantly upregulated in PTHrP-overexpressing cells (gray circle). There was also one significantly enriched gene that was unique to the calcium signaling pathway, P2RX6 (green circle). **(B)** *PTHLH* mRNA levels, shown as a control for PTHrP overexpression, in MCF7pcDNA control or MCF7 PTHrP-overexpressing cells **(C,D)**. qPCR for mRNA levels of calcium signaling pathway genes in MCF7pcDNA or MCF7 PTHrP-overexpressing cells. Graphs = mean + SE. $n = 3$ replicates from independent experiments. $^*p < 0.05$, $^{***}p < 0.001$ by Unpaired Student's *T*-test.

Parathyroid hormone and PTHrP have identical amino acids in 8 of their first 13 residues, but other similarities within the sequences are no more than would be expected by chance (1, 3). In PTHR1-bearing target cells, recombinant PTHrP(1–141) and synthetic shorter amino-terminal forms were equipotent on a molar basis with each other and with PTH(1–34) in their ability to promote cAMP activity (19). In exerting this function, PTHrP and PTH were shown to share actions upon a common receptor, PTHR1 (14). These functions are absent in MCF7 cells. Instead, our findings suggest that the major changes in gene expression

in MCF7 cells in response to PTHrP must occur through PTHrP actions mediated by domains of PTHrP distinct from the (1–34) region known to act on the cAMP–PKA pathway through PTHR1.

A number of biological activities have been ascribed to domains of PTHrP beyond the amino-terminal region, but although these domains have been defined on the basis of the primary amino acid sequence, no receptors for these responses have yet been identified. For example, (i) the mid-molecule portion, between residues 35 and 84, is responsible for placental calcium transport, (ii) many pharmacologic studies have shown biological effects of the C-terminal domain, beginning at residue 107, and (iii) a nuclear localizing sequence mediates transport of PTHrP to the nucleus in many cell types [reviewed in Ref. (1)]. These many biological activities within the PTHrP molecule led to it being regarded as a multifunctional cytokine (34, 35) but the specific intracellular pathways that mediate these non-PTHR1-mediated actions remain unknown. These possibilities have been raised recently with respect to the role of PTHrP in bone remodeling (7), since mice lacking PTHrP in osteocytes exhibit a bone phenotype that is markedly different from mice lacking the PTHR1 (36).

Thus in this work, where substantial effects of PTHrP overexpression on gene expression in MCF7 cells seem to be unrelated to PTHR1-mediated actions though cAMP/PKA/CREB activation, these other domains of PTHrP need to be considered. This question begins to be addressed with the findings from the RNAseq data, which identified the calcium signaling pathway as significantly upregulated by PTHrP overexpression. In cancer, upregulation of Ca^{2+} channels and pumps promotes tumor proliferation and drives tumorigenesis. Several of these signaling pathway components have been reported as overexpressed in breast, prostate, colon, pancreas, and lung tumors (37–39). It has also been shown that PTHrP nuclear action downstream of the calcium-sensing receptor (CaSR) promotes proliferation and reduces $p27^{Kip1}$ levels in breast cancer cells, ultimately preventing nuclear accumulation of apoptosis-inducing factor and the cell death that normally occurs when Ca^{2+} levels are in excess (40). While these actions have never been directly linked to PTHrP-induced bone destruction, our findings are consistent with the known roles for the calcium signaling pathway in cancer. These data suggest that CaSR acts upstream of PTHrP, and our data raise the possibility that PTHrP further promotes calcium signaling, possibly in a feed-forward loop.

We previously reported that PTHrP overexpression in MCF7 cells downregulates eight pro-dormancy genes (9) and our RNAseq analysis now provides a potential pathway through which PTHrP may function to downregulate these genes. Experiments to determine the functional significance of the calcium signaling pathway in tumor dormancy *in vivo* will be necessary to determine whether this is the pathway through which PTHrP enables dormant tumor cells to aggressively colonize the bone.

AUTHOR CONTRIBUTIONS

RJ, YS, PH, AC, and JJ performed experiments and analyzed data. RJ, NP, NS, and TM interpreted the data. RJ, NS, and TM wrote the manuscript. YS, PH, AC, JJ, and NP edited the manuscript.

ACKNOWLEDGMENTS

A portion of these data were previously published as a conference paper supplement (41). The authors wish to acknowledge the expert technical support of the VANGARD core facilities. RJ is supported in part by NIH award R00CA194198 (RJ). Experiments performed at Vanderbilt were supported in part by scholarship funds from NIH award P30CA068485 Vanderbilt-Ingram Cancer Center Support Grant. Experiments performed at SVI were supported in part by NHMRC grant 1081242 to NS and TM, and SVI receives support from the Victorian Government OIS Program. AC was supported in part by an Australian and New Zealand Bone and Mineral Society Christine & T. Jack Martin Research Travel Grant and NHMRC grant 1078280 to NP.

REFERENCES

1. Martin TJ. Parathyroid hormone-related protein, its regulation of cartilage and bone development, and role in treating bone diseases. *Physiol Rev* (2016) 96(3):831–71. doi:10.1152/physrev.00031.2015
2. McCauley LK, Martin TJ. Twenty-five years of PTHrP progress: from cancer hormone to multifunctional cytokine. *J Bone Miner Res* (2012) 27(6):1231–9. doi:10.1002/jbmr.1617
3. Suva LJ, Winslow GA, Wettenhall RE, Hammonds RG, Moseley JM, Diefenbach-Jagger H, et al. A parathyroid hormone-related protein implicated in malignant hypercalcemia: cloning and expression. *Science* (1987) 237(4817):893–6. doi:10.1126/science.3616618
4. Powell GJ, Southby J, Danks JA, Stillwell RG, Hayman JA, Henderson MA, et al. Localization of parathyroid hormone-related protein in breast cancer metastases: increased incidence in bone compared with other sites. *Cancer Res* (1991) 51(11):3059–61.
5. Thomas RJ, Guise TA, Yin JJ, Elliott J, Horwood NJ, Martin TJ, et al. Breast cancer cells interact with osteoblasts to support osteoclast formation. *Endocrinology* (1999) 140(10):4451–8. doi:10.1210/endo.140.10.7037
6. Martin TJ. Osteoblast-derived PTHrP is a physiological regulator of bone formation. *J Clin Invest* (2005) 115(9):2322–4. doi:10.1172/JCI26239
7. Ansari N, Ho PW, Crimeen-Irwin B, Poulton IJ, Brunt AR, Forwood MR, et al. Autocrine and paracrine regulation of the murine skeleton by osteocyte-derived parathyroid hormone-related protein. *J Bone Miner Res* (2018) 33(1):137–53. doi:10.1002/jbmr.3291
8. Kobayashi T, Chung UI, Schipani E, Starbuck M, Karsenty G, Katagiri T, et al. PTHrP and Indian hedgehog control differentiation of growth plate chondrocytes at multiple steps. *Development* (2002) 129(12):2977–86.
9. Johnson RW, Finger EC, Olcina MM, Vilalta M, Aguilera T, Miao Y, et al. Induction of LIFR confers a dormancy phenotype in breast cancer cells disseminated to the bone marrow. *Nat Cell Biol* (2016) 18(10):1078–89. doi:10.1038/ncb3408
10. Kemp BE, Moseley JM, Rodda CP, Ebeling PR, Wettenhall RE, Stapleton D, et al. Parathyroid hormone-related protein of malignancy: active synthetic fragments. *Science* (1987) 238(4833):1568–70. doi:10.1126/science.3685995
11. Pizurki L, Rizzoli R, Moseley J, Martin TJ, Caverzasio J, Bonjour JP. Effect of synthetic tumoral PTH-related peptide on cAMP production and Na-dependent Pi transport. *Am J Physiol* (1988) 255(5 Pt 2):F957–61. doi:10.1152/ajprenal.1988.255.5.F957
12. Fukayama S, Bosma TJ, Goad DL, Voelkel EF, Tashjian AH Jr. Human parathyroid hormone (PTH)-related protein and human PTH: comparative biological activities on human bone cells and bone resorption. *Endocrinology* (1988) 123(6):2841–8. doi:10.1210/endo-123-6-2841
13. Ebeling PR, Adam WR, Moseley JM, Martin TJ. Actions of synthetic parathyroid hormone-related protein(1-34) on the isolated rat kidney. *J Endocrinol* (1989) 120(1):45–50. doi:10.1677/joe.0.1200045

14. Juppner H, Abou-Samra AB, Freeman M, Kong XF, Schipani E, Richards J, et al. A G protein-linked receptor for parathyroid hormone and parathyroid hormone-related peptide. *Science* (1991) 254(5034):1024–6. doi:10.1126/science.1658941
15. Martin TJ, Findlay DM, MacIntyre I, Eisman JA, Michelangeli VP, Moseley JM, et al. Calcitonin receptors in a cloned human breast cancer cell line (MCF 7). *Biochem Biophys Res Commun* (1980) 96(1):150–6. doi:10.1016/0006-291X(80)91193-6
16. Findlay DM, deLuise M, Michelangeli VP, Ellison M, Martin TJ. Properties of a calcitonin receptor and adenylate cyclase in BEN cells, a human cancer cell line. *Cancer Res* (1980) 40(4):1311–7.
17. Martin TJ, Ng KW, Partridge NC, Livesey SA. Hormonal influences on bone cells. *Methods Enzymol* (1987) 145:324–36. doi:10.1016/0076-6879(87)45019-2
18. Mulcrone PL, Campbell JP, Clement-Demange L, Anbinder AL, Merkel AR, Brekken RA, et al. Skeletal colonization by breast cancer cells is stimulated by an osteoblast and beta2AR-dependent neo-angiogenic switch. *J Bone Miner Res* (2017) 32(7):1442–54. doi:10.1002/jbmr.3133
19. Hammonds RG Jr, McKay P, Winslow GA, Diefenbach-Jagger H, Grill V, Glatz J, et al. Purification and characterization of recombinant human parathyroid hormone-related protein. *J Biol Chem* (1989) 264(25):14806–11.
20. Allan EH, Hausler KD, Wei T, Gooi JH, Quinn JM, Crimeen-Irwin B, et al. EphrinB2 regulation by PTH and PTHrP revealed by molecular profiling in differentiating osteoblasts. *J Bone Miner Res* (2008) 23(8):1170–81. doi:10.1359/jbmr.080324
21. Richard V, Luchin A, Brena RM, Plass C, Rosol TJ. Quantitative evaluation of alternative promoter usage and 3' splice variants for parathyroid hormone-related protein by real-time reverse transcription-PCR. *Clin Chem* (2003) 49(8):1398–402. doi:10.1373/49.8.1398
22. Walia MK, Ho PM, Taylor S, Ng AJ, Gupte A, Chalk AM, et al. Activation of PTHrP-cAMP-CREB1 signaling following p53 loss is essential for osteosarcoma initiation and maintenance. *Elife* (2016) 5:e13446. doi:10.7554/eLife.13446
23. Chan AS, Clairfeuille T, Landao-Bassonga E, Kinna G, Ng PY, Loo LS, et al. Sorting nexin 27 couples PTHR trafficking to retromer for signal regulation in osteoblasts during bone growth. *Mol Biol Cell* (2016) 27(8):1367–82. doi:10.1091/mbc.E15-12-0851
24. Yamada H, Tsutsumi M, Fukase M, Fujimori A, Yamamoto Y, Miyauchi A, et al. Effects of human PTH-related peptide and human PTH on cyclic AMP production and cytosolic free calcium in an osteoblastic cell clone. *Bone Miner* (1989) 6(1):45–54. doi:10.1016/0169-6009(89)90022-6
25. Guise TA, Yin JJ, Taylor SD, Kumagai Y, Dallas M, Boyce BF, et al. Evidence for a causal role of parathyroid hormone-related protein in the pathogenesis of human breast cancer-mediated osteolysis. *J Clin Invest* (1996) 98(7):1544–9. doi:10.1172/JCI118947
26. Johnson RW, Nguyen MP, Padalecki SS, Grubbs BG, Merkel AR, Oyajobi BO, et al. TGF-beta promotion of Gli2-induced expression of parathyroid hormone-related protein, an important osteolytic factor in bone metastasis, is independent of canonical Hedgehog signaling. *Cancer Res* (2011) 71(3):822–31. doi:10.1158/0008-5472.CAN-10-2993
27. Kusuma N, Denoyer D, Eble JA, Redvers RP, Parker BS, Pelzer R, et al. Integrin-dependent response to laminin-511 regulates breast tumor cell invasion and metastasis. *Int J Cancer* (2012) 130(3):555–66. doi:10.1002/ijc.26018
28. Gallon M, Cullen PJ. Retromer and sorting nexins in endosomal sorting. *Biochem Soc Trans* (2015) 43(1):33–47. doi:10.1042/BST20140290
29. Feinstein TN, Wehbi VL, Ardura JA, Wheeler DS, Ferrandon S, Gardella TJ, et al. Retromer terminates the generation of cAMP by internalized PTH receptors. *Nat Chem Biol* (2011) 7(5):278–84. doi:10.1038/nchembio.545
30. Ramsey IS, Delling M, Clapham DE. An introduction to TRP channels. *Annu Rev Physiol* (2006) 68:619–47. doi:10.1146/annurev.physiol.68.040204.100431
31. Peterson EA, Jenkins EC, Lofgren KA, Chandiramani N, Liu H, Aranda E, et al. Amphiregulin is a critical downstream effector of estrogen signaling in ERalpha-positive breast cancer. *Cancer Res* (2015) 75(22):4830–8. doi:10.1158/0008-5472.CAN-15-0709
32. Miao HQ, Lee P, Lin H, Soker S, Klagsbrun M. Neuropilin-1 expression by tumor cells promotes tumor angiogenesis and progression. *FASEB J* (2000) 14(15):2532–9. doi:10.1096/fj.00-0250com
33. Jimenez-Hernandez LE, Vazquez-Santillan K, Castro-Oropeza R, Martinez-Ruiz G, Munoz-Galindo L, Gonzalez-Torres C, et al. NRP1-positive lung cancer cells possess tumor-initiating properties. *Oncol Rep* (2018) 39(1):349–57. doi:10.3892/or.2017.6089
34. Philbrick WM, Wysolmerski JJ, Galbraith S, Holt E, Orloff JJ, Yang KH, et al. Defining the roles of parathyroid hormone-related protein in normal physiology. *Physiol Rev* (1996) 76(1):127–73. doi:10.1152/physrev.1996.76.1.127
35. Martin TJ, Moseley JM, Williams ED. Parathyroid hormone-related protein: hormone and cytokine. *J Endocrinol* (1997) 154(Suppl):S23–37.
36. Saini V, Marengi DA, Barry KJ, Fulzele KS, Heiden E, Liu X, et al. Parathyroid hormone (PTH)/PTH-related peptide type 1 receptor (PPR) signaling in osteocytes regulates anabolic and catabolic skeletal responses to PTH. *J Biol Chem* (2013) 288(28):20122–34. doi:10.1074/jbc.M112.441360
37. El Hiani Y, Lehen'kyi V, Ouadid-Ahidouch H, Ahidouch A. Activation of the calcium-sensing receptor by high calcium induced breast cancer cell proliferation and TRPC1 cation channel over-expression potentially through EGFR pathways. *Arch Biochem Biophys* (2009) 486(1):58–63. doi:10.1016/j.abb.2009.03.010
38. Tsavaler L, Shapero MH, Morkowski S, Laus R. Trp-p8, a novel prostate-specific gene, is up-regulated in prostate cancer and other malignancies and shares high homology with transient receptor potential calcium channel proteins. *Cancer Res* (2001) 61(9):3760–9.
39. Dhennin-Duthille I, Gautier M, Faouzi M, Guilbert A, Brevet M, Vaudry D, et al. High expression of transient receptor potential channels in human breast cancer epithelial cells and tissues: correlation with pathological parameters. *Cell Physiol Biochem* (2011) 28(5):813–22. doi:10.1159/000335795
40. Kim W, Takyar FM, Swan K, Jeong J, VanHouten J, Sullivan C, et al. Calcium-sensing receptor promotes breast cancer by stimulating intracrine actions of parathyroid hormone-related protein. *Cancer Res* (2016) 76(18):5348–60. doi:10.1158/0008-5472.CAN-15-2614
41. Johnson RW, Sun Y, Ho PWM, Sims N, Martin TJ. 2017 Annual Meeting of the American Society for Bone and Mineral Research, Colorado Convention Center, Denver, CO, USA – September 8–11, 2017. *J Bone Miner Res* (2017) 32:S1–432. doi:10.1002/jbmr.3363

Conflict of Interest Statement: The authors declare that the research was conducted in the absence of any commercial or financial relationships that could be construed as a potential conflict of interest.

frontiers in Endocrinology

REVIEW
published: 18 May 2018
doi: 10.3389/fendo.2018.00247

Multifaceted Roles for Macrophages in Prostate Cancer Skeletal Metastasis

Chen Hao Lo[1,2] *and Conor C. Lynch*[2]*

[1] Cancer Biology Program, University of South Florida, Tampa, FL, United States, [2] Tumor Biology Department, H. Lee Moffitt Cancer Center and Research Institute, Tampa, FL, United States

Bone-metastatic prostate cancer is common in men with recurrent castrate-resistant disease. To date, therapeutic focus has largely revolved around androgen deprivation therapy (ADT) and chemotherapy. While second-generation ADTs and combination ADT/chemotherapy approaches have been successful in extending overall survival, the disease remains incurable. It is clear that molecular and cellular components of the cancer-bone microenvironment contribute to the disease progression and potentially to the emergence of therapy resistance. In bone, metastatic prostate cancer cells manipulate bone-forming osteoblasts and bone-resorbing osteoclasts to produce growth and survival factors. While osteoclast-targeted therapies such as bisphosphonates have improved quality of life, emerging data have defined important roles for additional cells of the bone microenvironment, including macrophages and T cells. Disappointingly, early clinical trials with checkpoint blockade inhibitors geared at promoting cytotoxic T cell response have not proved as promising for prostate cancer compared to other solid malignancies. Macrophages, including bone-resident osteomacs, are a major component of the bone marrow and play key roles in coordinating normal bone remodeling and injury repair. The role for anti-inflammatory macrophages in the progression of primary prostate cancer is well established yet relatively little is known about macrophages in the context of bone-metastatic prostate cancer. The focus of the current review is to summarize our knowledge of macrophage contribution to normal bone remodeling and prostate-to-bone metastasis, while also considering the impact of standard of care and targeted therapies on macrophage behavior in the tumor-bone microenvironment.

Keywords: bone, prostate cancer, metastasis, macrophage, polarization, therapy

OPEN ACCESS

Edited by:
Julie A. Sterling,
Vanderbilt University, United States

Reviewed by:
Jawed Akhtar Siddiqui,
University of Nebraska Medical Center, United States
Robin Mark Howard Rumney,
University of Portsmouth, United Kingdom

***Correspondence:**
Conor C. Lynch
conor.lynch@moffitt.org

Specialty section:
This article was submitted to Bone Research, a section of the journal Frontiers in Endocrinology

Received: *26 February 2018*
Accepted: *02 May 2018*
Published: *18 May 2018*

Citation:
Lo CH and Lynch CC (2018) Multifaceted Roles for Macrophages in Prostate Cancer Skeletal Metastasis. Front. Endocrinol. 9:247. doi: 10.3389/fendo.2018.00247

INTRODUCTION

In 2018 alone, approximately 28,000 deaths from prostate cancer are predicted (1). While early stage disease is often treated successfully with surgery, radiation, and/or androgen deprivation therapy (ADT), advanced prostate cancer remains a moving target. Advanced disease typically manifests in the skeleton where metastases are often sensitive to first- and second-generation ADT. However, in a short period, the cancer becomes castrate resistant. In bone, prostate cancer causes extensive bone remodeling and formation that result in intense pain and heightened risk of pathologic fracture (2). These symptoms drastically reduce the patients' quality of life and contribute substantially to disease morbidity and mortality. Bone-metastatic castrate-resistant prostate cancer (mCRPC) is currently incurable and appears to be refractory to recent advances in immunotherapy, such as checkpoint inhibitors (3–5). However, immune-based therapies such as Sipuleucel-T have been beneficial for some patients indicating that there may be room for alternative strategies in targeting the immune

microenvironment of bone mCRPC. Despite macrophages constituting 8–15% of healthy adult male bone marrow, their role in the context of the bone-metastatic CRPC remains relatively underexplored.

MACROPHAGE FUNCTION IN TISSUE HOMEOSTASIS

Macrophages are phagocytic cells of the innate immune system responsible for maintenance of tissue homeostasis. Myeloid in nature and originating from hematopoietic stem cells that mature and differentiate into myeloblasts and monocytes, macrophages are noted for their diverse morphology and function across various tissues (6–8). For example, microglia are residential macrophages of the brain and play an important role in regulating synapse behavior (9). These cells have further demonstrated roles in immune modulation of inflammatory response to brain trauma at the blood–brain barrier (10). Other organ-specific macrophages include kupffer cells which turnover heme molecules through phagocytosis and degradation of hemoglobin in the liver (11, 12), and alveolar macrophages which engulf and eliminate dust particulates and microbes from the air on the luminal side of the mucosal epithelium lining in the lung (13, 14). Precursor and mature macrophages derived from the bone marrow also circulate the body, surveying and infiltrating sites of injury and infection to regulate local responses. Macrophages are known for their plasticity, and depending on signaling cues, can polarize into pro- or anti-inflammatory phenotypes. Traditionally, these phenotypes have been referred to as M1 and M2, but more recently it has been recognized that there are a spectrum of phenotypes across the M1/M2 continuum. Inflammatory stimuli released by necrotic or damaged tissue, such as interferon-gamma (IFNγ), interleukin-12 (IL-12), and reactive oxygen species (ROS) promote polarization into a pro-inflammatory phenotype (15–19), leading to the secretion of pro-apoptotic cytokines such as tumor necrosis factor (TNF) to induce apoptosis of neighboring cells. Pro-inflammatory macrophages can remove apoptotic neutrophils and cellular debris through phagocytosis and efferocytosis (20–24) and participate in the adaptive immune response by presenting disease-associated antigens to T and B cells that specifically target infectious agents or diseased cells (25–27). Following injury/infection resolution, secretion of factors including interleukin-10 (IL-10) and transforming growth factor beta (TGFβ) by fibroblasts and platelets promote the polarization of anti-inflammatory macrophages (28). Anti-inflammatory macrophages suppress further inflammation by secreting TGFβ, vascular endothelial growth factor (VEGF), and ROS that will deactivate T cells and promote T_H2 response (29–32). These factors will also stimulate expansion of fibroblasts, endothelial cells, and other cell types for tissue repair (33, 34).

MACROPHAGE ROLES IN BONE REMODELING AND INJURY REPAIR

In the bone marrow, osteoclasts and osteoblasts are bone-specific cell populations that serve to resorb and mineralize the bone, respectively. The activities of these two populations are tightly coupled to ensure balanced bone turnover as well as returning the bone to homeostasis subsequent to injury. Osteoclasts are found residing on osteal surfaces and are histologically characterized as tartrate-resistant acid phosphatase (TRAP) positive and multi-nucleated (35, 36). Osteoclasts migrate to sites of active bone remodeling by chemotaxis, where they are involved in demineralization and resorption of the bone matrix (37–39). Upon apoptosis of the osteoclast, mesenchymal stem cell-derived osteoblasts rebuild the bone matrix *via* the deposition of type I collagen and hydroxyapatite (40). Traditionally, due to their myeloid origins and bone-specific functions, osteoclasts are considered the bone-resident macrophage population. However, roles for pro- and anti-inflammatory macrophages in controlling and coordinating osteoclast and osteoblast bone remodeling have been described. For example, IFNγ- and IL-12-stimulated NOS2 and TNF positive pro-inflammatory macrophages can promote osteoclast formation and bone resorption (41, 42). Conversely, anti-inflammatory macrophages are thought to contribute to bone formation (43).

A distinct population of bone-resident macrophages, osteomacs, has been described, and recent studies have shown important roles for these cells in modulating osteoblast activity in both bone homeostasis and injury repair (44). Osteomacs are morphologically characterized as mononuclear cells that form canopy-like structures around osteoblasts and can occupy as much as 75% of both murine and human endosteal and trabecular bone surfaces that are under active remodeling (45–48). Histologically, osteomacs are distinct from osteoclasts and are F4/80 positive but TRAP negative. Additionally, other groups have shown osteomacs to express common macrophage markers such as CD68, and also more specific markers, such as Mac-3 and CD169 (45, 46, 49). While osteomacs can be stimulated by receptor activator of nuclear kappa B ligand (RANKL) and colony stimulating factor-1 (CSF-1/M-CSF) to become osteoclasts *in vitro*, monocytes and other myeloid precursors were found to be more efficient osteoclast precursors (45). These data indicate that osteomacs are a plastic, yet distinct cell type, with specific functions in the bone marrow microenvironment. Indeed, further studies have revealed that osteomacs have diverse roles in regulating osteogenesis and osteolysis. Osteoblasts become inefficient as they age and need to be replenished to ensure proper homeostatic bone turnover (46). During normal bone turnover, osteomacs engulf apoptotic osteoblasts in a process called efferocytosis, which induces the secretion of TGFβ, TNF, and oncostatin M that facilitate osteoblastogenesis and bone formation (45, 46, 48). This mechanism has been confirmed in various *in vitro* and *in vivo* contexts. For example, removal of osteomacs from bone marrow-derived osteogenic co-cultures reduced osteoblast number and osteoblastic mineralization (47). The MAcrophage Fas-Induced Apoptosis (MAFIA) murine model is one in which administration of ligand AP20187 can systemically suppresses macrophage differentiation. Reduced osteoblast occupancy of the endosteal bone surfaces was observed in maturing MAFIA mice following AP20187 administration (47, 50). Congruently, parathyroid hormone-induced bone anabolism in the MAFIA model was suppressed upon macrophage ablation (51). Interestingly, when murine macrophages

were depleted by clodronate liposome-induced apoptosis, osteoblast numbers remained stable (47, 50). Further comparison between two methods of macrophage depletion showed that transient macrophage apoptosis induced osteomac expansion and efferocytosis, which further enhanced osteoblast activity (46, 51, 52). Additionally, C57BL/6 mice bone marrow treated with trabectedin, a chemotherapy antagonist of macrophages, showed diminished phagocytic genetic signature, efferocytotic osteomac-induced RUNX2 positive osteoblastogenesis, and associated BV/TV status (53). During bone fracture repair, osteomacs can also sense apoptotic damaged cells and in response, initiate inflammation and immune recruitment through secretion of immune attractant factors, such as chemokine (C–C motif) ligand 2 (CCL2) and M-CSF (48). Additionally, LPS-stimulated osteomacs express TNF and NOS2, and suppress osteoblast activity *in vitro* (45). *In vivo*, bone fracture induced pro-inflammatory polarization of immune macrophages and osteomacs to secrete TNF and IFNβ, driving osteoclastogenesis and osteolysis (45). In fact, osteomacs have been shown to associate with osteoclasts at catabolic sites, substantiating their distinction from osteoclasts, and supporting their additional roles in regulating osteolysis (48). These studies indicate that osteomacs can direct the transition between osteolysis and osteogenesis by directly modulating the expansion and activity of osteoclasts and osteoblasts for repair in the event of bone injury (46). Taken together, these studies demonstrate the complex roles of bone-resident macrophages in bone remodeling (54, 55). How they contribute to the progression of bone-metastatic prostate cancer and respond to applied therapies has not been fully elucidated at this juncture.

MACROPHAGES PROMOTE PRIMARY PROSTATE CANCER PROGRESSION

Just as in other cancers, chronic inflammation in prostate cancer is thought to serve as a prelude to tumorigenesis (56). In fact, in cases of premalignant prostatic inflammatory atrophy, macrophages were observed coalescing at sites where inflammation-driven neoplasia caused disruptions in the epithelial lining of the prostate (57). In primary prostate cancer, pro- and anti-inflammatory tumor-associated macrophages (TAMs) have been found to comprise a significant portion of the immune cells infiltrating the tumor microenvironment with studies beginning to dissect roles for each population with regards to progression of the disease (58, 59). The exact pro- and anti-inflammatory constitution of TAMs vary across cancer types, but protective roles for TAMs have been described in prostate cancer. For example, macrophages located in the tumor-peripheral stroma correlated with increased recurrence-free survival (60), while macrophages expressing CD204, a marker associated with activation of antigen presentation in dendritic cells, correlate with better overall survival and prognosis (60–62). However, for the most part, macrophages have been found to contribute to, or directly promote, primary prostate cancer progression with individual patient cohort and meta-analysis studies identifying that macrophage infiltration correlates with disease aggressiveness and poor prognosis in prostate cancer (63–67). With respect to therapy, the density of anti-inflammatory macrophages in the primary disease correlates with extracapsular and biochemical recurrence following radical prostatectomy and/or ADT (63, 65, 66, 68).

The tumor-promoting roles of anti-inflammatory macrophages are thought to revolve around their immune-suppressive and angiogenic effects, both of which are important hallmarks of prostate cancer progression (68–71). Prostate cancer cells have been shown to secrete factors such as CSF-1 and CCL2 that lead to the recruitment of monocytes and macrophages that facilitate these processes (68, 72–78). Once recruited to the microenvironment, macrophages are exposed to a milieu of environmental cues that can drive their polarization into pro- or anti-inflammatory states (58). For example, exposure to tumor-derived IL-10 and -13 promotes macrophage polarization into an anti-inflammatory state. Subsequently, macrophages secrete factors, such as epidermal growth factor (EGF), platelet derived growth factors, and VEGF that promote cancer cell proliferation and angiogenesis of the tumor microenvironment (69, 79–83). Furthermore, ARG1 and TGFβ positive anti-inflammatory macrophages, along with myeloid-derived suppressor cells and regulatory T cells, collectively suppress inflammation and immune response within the tumor microenvironment (84–88). Both pro- and anti-inflammatory macrophages can also modulate T cell expansion and cytotoxicity by regulating the bioavailability of L-arginine, an important amino acid for T cell activity and survival (89). In addition, NOS2 positive pro-inflammatory macrophages synthesize nitric oxide that can promote T cell T_H1 expansion (90, 91). Conversely, anti-inflammatory macrophages expand during T_H2 response and additionally suppress T cell proliferation through expression of co-inhibitory molecule PD-L2 (30). Importantly, macrophages can also contribute to the activity of non-immune cells in the tumor microenvironment, such as cancer-associated fibroblasts (CAFs). Macrophage-secreted factors such as TGFβ are known potent regulators of CAFs that also promote tumor growth and invasion into the peripheral tissue to facilitate metastasis (68, 71, 92, 93).

MACROPHAGE ROLES IN ESTABLISHING THE PRE-METASTATIC BONE MARROW NICHE?

While much is known about the role of macrophages in primary prostate cancer progression, less is known about how their polarization states in the bone marrow contribute to, or protect against prostate cancer metastasis to the bone and subsequent establishment. TNF, TGFβ, and VEGFA can be secreted by primary prostate cancer cells into circulation (94), which can activate marrow cell populations including bone-resident macrophages and hematopoietic progenitor cells. Furthermore, these tumor-derived factors have been shown to induce the recruitment of immunosuppressive myeloid populations into the bone that support immune evasion and ease the establishment of circulating tumor cells (95).

Emerging evidence has also defined important roles for prostate cancer-derived exosomes in the genesis of receptive pre-metastatic niches (96, 97). Exosomes are nanometer-sized

vesicles that can be shed in large numbers by cancer cells. The cargo contents of cancer cell-derived exosomes vary greatly, but can contain cell-adhesion molecules, receptor tyrosine kinases, proteases, miRNAs and miRNA processing machinery, mRNA, and DNA (98, 99). Injection of mice with exosomes derived from human prostate cancer peripheral blood or murine prostate cancer cells lines (TRAMPc1) demonstrated impaired murine osteoclast formation and enhanced osteoblast differentiation suggesting that prostate cancer-derived exosomes play a role in tipping the balance toward bone formation, a common hallmark of bone-metastatic prostate cancer (100, 101). Milk fat globule-EGF factor 8 protein (MFG-E8) was found in human prostate cancer patient exosomes, and tissue biopsies. MFG-E8 has been shown to mediate macrophage efferocytosis of apoptotic osteoblasts and cancer cells; these macrophages then exhibit an anti-inflammatory phenotype and in turn promote immune suppression through expression of TGFβ and ARG1 (102, 103). Characterization of prostate cancer-derived exosomes has identified various proteins and miRNA that can promote metastasis. Among the miRNA identified, miRNA-21 is particularly interesting given that it is upregulated in bone-metastatic prostate cancer and has known roles in regulating osteoclasto- and osteoblastogenesis (23, 97, 104, 105). Additionally, miRNA-21 is known to regulate macrophage phagocytosis of necrotic or diseased tissue in the context of wounding (23). Other miRNA identified in prostate cancer-derived exosomes that can influence osteoclast and osteoblast differentiation include miRNA-128 and -183 (95, 97).

Collectively, these studies show that bone marrow macrophages contribute to bone-metastatic outgrowth of disseminated prostate cancers, whereby cancer-derived signals or exosomes significantly influence macrophage activity in the pre-metastatic niche. In turn, these changes appear to be permissive for prostate cancer cell colonization of bone.

TAMs IN METASTATIC CASCADE OF PROSTATE CANCER

The role of TAM in the metastatic dissemination of primary prostate cancer has been extensively studied and reviewed. Here, we reference seminal review articles that outline the molecular and cellular communication between TAMs and primary prostate cancers resulting in tumor vascularization, epithelial-to-mesenchymal transition, intravasation, and eventual colonization of distal sites, including, specifically, the skeletal bone marrow (58, 83, 106–109).

MACROPHAGES IN THE PROGRESSION OF ESTABLISHED PROSTATE TO BONE METASTASES

Once actively growing in the skeleton, prostate cancer cells manipulate the cells of the bone microenvironment to promote areas of extensive osteolysis and osteogenesis. Osteoclasts have traditionally been regarded as a specialized bone-resident macrophage population due to their myeloid lineage and phagocytic nature in bone resorption, which leads to the release of bone matrix-sequestered factors that feed the metastatic prostate cancer cells (110–112). While macrophages can fuse and form into osteoclasts in response to RANKL (113, 114), the role of individual macrophage populations in controlling prostate cancer bone interaction remains relatively underexplored. Recent observations in patient biopsies have implicated the role of osteal macrophages in established bone-metastatic prostate cancer (115). CD68 positive macrophages were detectable at high density within the tumor, whereas osteoclasts and osteomacs were found at the tumor-bone interface, suggesting potentially differential functions for each population in the growing lesions (115). Studies have also defined causal roles for macrophage populations in the growth of prostate cancer in bone. For example, intratibial inoculation of RM1 prostate cancer cells into macrophage-depleted bone marrow of MAFIA mice resulted in decreased pathologic osteolysis (107, 116). Additionally, depleting macrophages using clodronate liposome prior to tumor inoculation significantly limited cancer growth in bone (116). Further evidence supporting contributory roles for macrophages in the progression of bone-metastatic prostate cancer lesions has been provided using similar total macrophage depletion approaches (107, 115). Additionally, roles for osteomacs in the cancer-bone microenvironment have also been described, where CD169 positive tumor-associated osteomacs were found to facilitate tumor-induced pathologic osteogenesis. Interestingly, CD169 negative macrophages have been shown to promote tumor growth (115) and phenotypically resemble CD206 positive anti-inflammatory macrophages found in primary prostate cancer (109, 117). Taken together, these studies suggest that macrophages contribute to prostate cancer metastasis and growth in the bone microenvironment (**Figure 1**). However, deeper investigations into the precise roles of pro- and anti-inflammatory macrophages and osteomacs in the process are warranted.

MACROPHAGE RESPONSE TO STANDARD OF CARE TREATMENTS/ THERAPIES

As discussed, macrophage polarization can have protective or contributory roles; however, the impact of standard of care approaches on macrophage behavior has not been explored in depth thus far. For men with bone-metastatic CRPC, treatment options largely focus on radiation therapy to alleviate pain and reduce tumor burden, or therapeutics that target the cancer cells, such as chemotherapy and ADT. Although castrate-resistant, CRPC prostate cancer cells remain dependent on androgen signaling *via* the expression of constitutively active androgen receptor splice variants, and/or autocrine expression of their own androgen (118–120). Underscoring this dependency on androgens or the AR receptor for survival, second-generation ADTs (enzalutamide and abiraterone) have been shown to significantly improve overall survival. In murine xenograft models, enzalutamide treatment of C4-2B and TRAMPc1 prostate tumors induced STAT3-mediated CCL2 expression and recruitment of CCR2 positive macrophages, enhancing angiogenesis and tumor invasion (121–123). Other second-generation ADTs, such as

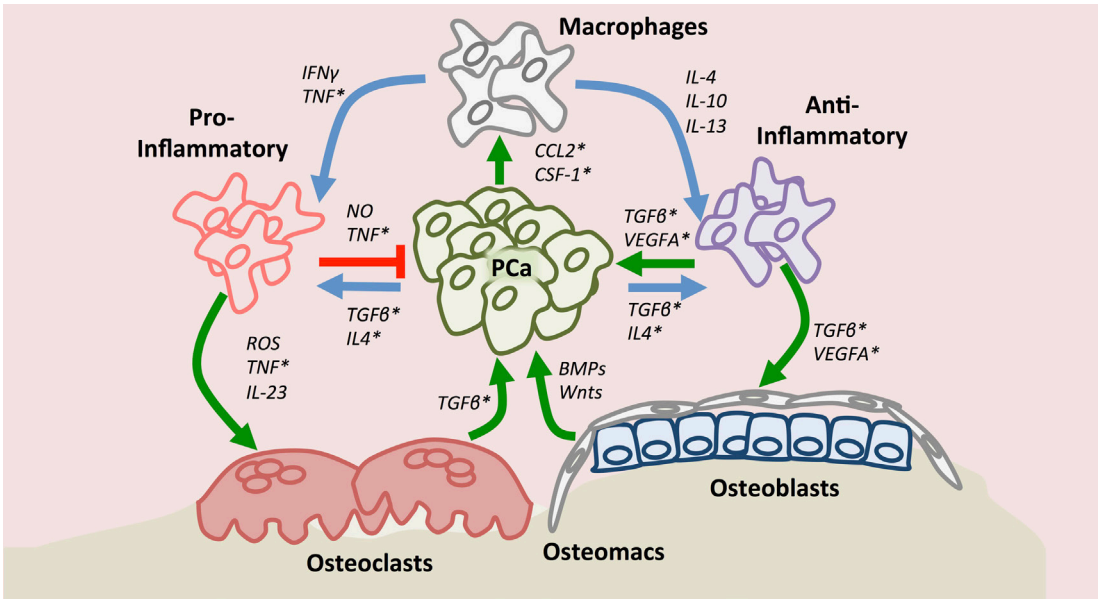

FIGURE 1 | Macrophage roles in the context of the bone-metastatic prostate cancer. Upon recruitment to the site of metastasis by chemokine (C–C motif) ligand 2 and or colony stimulating factor-1, macrophages may polarize (blue arrows) into pro- or anti-inflammatory states depending on environmental cues. Tumor-associated macrophages have protective (red arrow) or contributory effects (green arrow) directly on prostate cancer. Importantly, macrophages, including bone-resident osteomacs, impact osteoclast and osteoblast function (green arrows) thereby also indirectly regulating prostate cancer progression in bone. Asterisks denote factors to which small molecule or biological inhibitors have been developed.

abiraterone, have also been shown to upregulate cancer cell CSF1 expression to promote macrophage infiltration, wound healing and, subsequently, tumor proliferation (75). Additionally, ADT drives tumor secretion of IL-10 and -13 that contribute to the polarization of macrophages into an anti-inflammatory phenotype (75). While in-depth studies have not examined the precise effects of second-generation ADT on macrophage behavior in bone-metastatic disease, it is plausible that the drugs may have actions similar to those noted at the primary site by promoting an anti-inflammatory phenotype. Critically, little work has been done to explore the role of ADT on bone-resident macrophages. As discussed, osteomacs appear to be key regulators of bone formation, and androgen depletion may impact the ability of osteomacs and osteoblasts to generate bone. This would be beneficial in reducing the aberrant osteogenesis associated with bone-metastatic prostate cancer, although it could promote systemic osteoporosis, a phenomenon noted in men undergoing chronic ADT treatment (124).

Taxane chemotherapies such as docetaxel and cabazitaxel are also used for the treatment of advanced prostate cancer patients. These drugs inhibit microtubule disassembly during mitotic chromosome segregation and induce apoptosis in neoplastic cells, and they are commonly given to patients with mCRPC who have failed ADT (125–128). Interestingly, for chemotherapy-sensitive CRPC, docetaxel has immune-stimulatory effects and can inhibit myeloid-derived suppressor cells, while promoting a switch in macrophages from an anti- to pro-inflammatory phenotype (129, 130). However, bone-metastatic CRPCs eventually become resistant to docetaxel, at which point they progress. In the case of chemotherapy-resistant cancer, the cancer cells can now secrete inflammatory cytokines such as IL-6 and -8, to recruit and differentiate monocytes and endothelial cells, for immune suppression and angiogenesis, respectively (131–134). Specifically, IL-6-induced mature macrophages are subsequently driven by other secreted cytokines such as IL-4 to anti-inflammatory states to induce immune suppression (131). IL-6 also induces prostate cancer survival by inducing Bcl/Stat-mediated survival signaling (131). Docetaxel can also induce CCL2 expression in cancer cells, a potent factor that not only induces prostate cancer growth and is correlated with disease progression but also recruits anti-inflammatory macrophages that drive tumor progression (74, 131, 135–139). Anti-inflammatory macrophages may also promote bone formation, but studies have shown that docetaxel impacts bone remodeling by suppressing osteoclast formation and osteoblast expansion, therefore, potentially off-setting the contribution of anti-inflammatory macrophages to cancer-induced bone disease (140).

Newer therapies being employed in the clinic may also have important effects on macrophage behavior in bone. For example, radium-223 is an alpha-emitting radionuclide that binds to calcium and promotes prostate cancer cell death in the neighboring vicinity. The treatment has been successful in extending the overall survival of men with bone-metastatic CRPC. The apoptosis induced by radium-223 may increase the bioavailability of tumor antigen in a cytotoxic microenvironment. Since macrophages are strong antigen presenting cells that mediate T cell antigenicity, it will be interesting to explore whether peripheral macrophages become pro-inflammatory and immune-stimulatory (141).

However, the effects of radiation therapy can be double edged. In humans, myelosuppression, leucopenia, and lymphopenia, were noted in radium-223 patients (142, 143). Further, in multiple cancer models, radiotherapy has been demonstrated to enhance macrophage infiltration, and over time, the polarization of macrophages into an anti-inflammatory phenotype may promote angiogenesis and cancer cell survival/recurrence (144–146). Taken together, these studies indicate that while applied therapies are initially successful in limiting disease progression, the emergence of resistant disease is often coupled/correlated with changes in macrophage polarization. Whether chronic exposure to standard of care therapies alters the microenvironment which in turn facilitates the emergence of resistant cancer cells remains to be determined. Conversely, little is known as to whether the evolution of resistant cancer cells in response to therapy impacts the behavior of the surrounding microenvironment.

CAN MACROPHAGE-BASED THERAPIES BE IMPACTFUL FOR THE TREATMENT OF BONE-METASTATIC PROSTATE CANCER?

The addition of therapies geared at blocking macrophage function, in particular anti-inflammatory function, in combination with standard of care treatments may yield more effective and durable responses in addition to preventing the recurrence of resistant disease. The role of macrophages in promoting the progression of numerous solid malignancies has been described, and as a consequence, translational studies have been geared toward the development of targeted therapies that can either deplete myeloid populations and/or alter the polarization status of macrophages. Numerous factors control macrophage infiltration and polarization but can have dual tumor-promoting and -protective effects. For example, correlative and causal roles for TNF in the progression and metastasis of prostate cancer have been described (147–153). Given the roles of TNF in inflammatory diseases, such as arthritis, it is unsurprising that biologicals targeting either the ligand or the receptor have been an active area of research. In the cancer setting, TNF can promote tumor growth and angiogenesis with preclinical trials demonstrating efficacy for TNF blocking reagents (154). Conversely, however, tumor-protective roles have been described in addition to potential risks for the development of cancers such as soft tissue sarcoma. This, combined with the potential for adverse toxicity associated with TNF inhibition, has diminished enthusiasm for the application of TNF inhibitors in the cancer setting. However, more encouraging results for other targets that impact macrophage behavior have been noted including, CCL-2/CCR-2, IL-4, and CSF1 receptor (CSF1R).

CCL-2

Chemokine (C–C motif) ligand 2 is expressed by prostate cancer cells, and while it can promote cell growth and invasion in an autocrine manner, it has also been shown to be a key driver of CCR2-expressing (CCL2 receptor) macrophages and monocyte recruitment (73, 155, 156). Moreover, the role of CCL2 seems particularly relevant in the context of bone-metastatic disease, where CCL2-expressing prostate cancers recruit endothelial cells and osteoblasts to drive angiogenesis and osteogenesis, respectively, both of which enhance the progression of the disease (73, 157). Underscoring the importance of CCL2 in the tumor-bone microenvironment, studies demonstrated that neutralization of CCL2 with a monoclonal antibody (C1142) was successful in both attenuating tumor growth as well as bone pathology in various preclinical models (156, 158). As a result, the humanized version, CNTO 888 (Carlumab), was developed to neutralize CCL2 signaling function in advanced prostate cancer. While the drug was well-tolerated in clinical trials, no anti-tumor activity was noted as a single agent for the treatment of metastatic CRPC (158–161). Given that targeting CCL2, or the receptor CCR2, in other diseases has been shown to be impactful in reducing inflammatory responses, it is possible that combination with standard of care treatments may result in more profound effects. Interestingly, heightened levels of CCL2 were noted in patients that developed resistance to docetaxel, and pre-clinical studies in which docetaxel and C1142 were combined demonstrated significant inhibition of bone-metastatic cancer growth and associated bone disease (139, 162, 163). Surprisingly, a phase I clinical trial combining docetaxel with CNTO 888 demonstrated tolerability but not a suppression of serum CCL2 levels or tumor response. This may indicate that higher dosing is required to block the CCL2–CCR2 axis or a combination of CNTO 888 with CCR2-specific antibodies such as MLN1202 is needed to achieve effective responses in humans (164). In addition to potentially depleting macrophages from the bone-tumor microenvironment, CCL2/CCR2 therapies can also reduce osteoclast recruitment and formation thereby protecting the patient from skeletal-related events such as pathologic fracture (157, 165).

Interleukin 4 (IL-4)/IL-4R

Interleukin 4 is an anti-inflammatory cytokine found upregulated in various solid malignancies that can promote tumor growth by driving anti-inflammatory macrophage polarization which in turn facilitates tumor proliferation, angiogenesis, and metastasis (166–168). This effect may be concentration dependent as high levels of IL-4 have an anti-tumor effect (169–171). In prostate cancer, IL-4 trends with PSA expression and can stimulate IL-4 receptor (IL-4R) positive prostate cancer cells to grow and metastasize *via* downstream activation of JAK/STAT6 pathway (172). IL-4 can also promote anti-tumor immunity. While IL-4 supports proliferation of T cells, it converts mature CD8 T cells from T_H1 to T_H2 response; this transition suppresses their cytolytic potential and leads to immune evasion and tolerance (168). IL-4 expression is especially heightened in hormone-refractory versus hormone-sensitive prostate cancer (169, 172). In the context of ADT, studies have shown that IL-4 can induce AR signaling reactivation, independent of androgen, suggesting IL-4 over expression as a resistance mechanism to restore cancer growth in androgen-depleted prostate cancer (172, 173). Combination of anti-IL-4 agents with ADT may, therefore, extend tumor ADT sensitivity. To this end, IL-4-targeted therapies are in development for the treatment of asthma and allergic responses. However, the anti-cancer effects of the therapy could be lessened due to the potential impact of IL-4 blockade on the activity of cytotoxic

immune cells. Adverse systemic effects may also be an issue, but strategies that focus on cancer cell- or TAM-specific delivery may be of use. Furthermore, IL-4 has been shown to limit osteoblast proliferation and induce the expression of IL-6 while inhibiting osteoclastogenesis (174, 175). Therefore, while inhibiting IL-4 may exacerbate the cancer-associated bone disease, it would also inhibit IL-6 expression by osteoblasts which in turn may prevent macrophage-mediated resistance to chemotherapy (176).

CSF1/CSF1R

Prostate cancer-derived colony stimulatory factor 1 (CSF1) can lead to the recruitment of CSF1R positive macrophages. In the tumor, CSF1 signaling promotes macrophage survival and polarization into an ARG1, CD206, and IL-10 positive anti-inflammatory phenotype, while simultaneously inhibiting a NOS2 and IL-12 positive pro-inflammatory phenotype (75–77). Additionally, tumor-derived CSF1 recruits MDSC, and these immunosuppressive myeloid infiltrates are particularly important in tumor survival and progression (76). Interestingly, standard of care therapies such as radiation and ADT promote CSF1 expression by prostate cancer cells leading to increased infiltration of macrophages (75, 77). The CSF1/CSF1R axis is known to play a role in macrophage infiltration and anti-inflammatory polarization in other cancers and several anti-CSF1R agents have been developed, including GW2580 and PLX3397. These agents have demonstrated significant success in abrogating therapy-induced CSF1R positive macrophage infiltration using animal models of cancer progression, including prostate cancer (75, 77, 177–179). Further, treatment with ADT and PLX3397 or GW2580 reduced macrophage infiltration compared to either therapy as a single agent (75). This indicates that combination of ADT and anti-CSF1R therapy would be clinically beneficial. Currently, several clinical trials are ongoing that will test the efficacy and impact of CSF/CSF1R inhibitors. For prostate cancer, recent studies have shown that PLX3397 delays the emergence of CRPC by reducing the number of infiltrating TAM, and a phase II clinical trial was performed in a small cohort of bone-metastatic CRPC patients with results pending (NCT 01499043). Various other combination therapy studies for prostate cancer using ADT with PLX3397 and other anti-CSF1R agents are underway and it will be interesting to see how well they perform relative to when used as single agents (78). Of note, blockade of CSF1R signaling in mice significantly reduced osteoclast number, leading to increased bone mass that may be useful in offsetting ADT-associated osteoporosis (180).

CONCLUSION

Bone-metastatic CRPC is currently incurable and will be present in over 90% of the men who succumb to the disease. While ADTs and chemotherapy have improved overall survival rates, more work is required to help in controlling and/or eradicating the disease. This can be achieved by understanding the cellular and molecular mechanisms involved. To this end, clear roles for the stromal and immune components of the tumor microenvironment have been described. Macrophages represent a large component of the immune infiltrate, and depending on their polarization state, can contribute to the progression of the disease. Many standard of care therapies focus on elimination of the cancer cell but indirectly, these therapies also impact the behavior of the surrounding macrophage population and lessen therapeutic efficacy. The factors controlling macrophage infiltration and polarization are the focus of translational efforts with several reagents in clinical trials. Combination therapies such as ADT with anti-CCL2/CCR2 or anti-CSF1R inhibitors may prove to significantly extend the overall survival of men with bone-metastatic CRPC. Further, given the role of macrophages in controlling bone remodeling, dampening macrophage activity may reduce prostate cancer-induced osteogenesis, thereby directly improving patient quality of life.

AUTHOR CONTRIBUTIONS

CHL and CCL wrote and edited the review.

ACKNOWLEDGMENTS

This research was supported in part by NIH grant U01CA202958 (CCL and CHL). We would also like to thank Dr. Jeremy Frieling for his review of the manuscript and thoughtful contributions.

REFERENCES

1. American Cancer Society. *Cancer Facts and Figures*. (2018). Available from: https://www.cancer.org/research/cancer-facts-statistics.html (Accessed: March 1, 2018).
2. Roudier MP, True LD, Higano CS, Vesselle H, Ellis W, Lange P, et al. Phenotypic heterogeneity of end-stage prostate carcinoma metastatic to bone. *Hum Pathol* (2003) 34:646–53. doi:10.1016/S0046-8177(03)00190-4
3. Modena A, Ciccarese C, Iacovelli R, Brunelli M, Montironi R, Fiorentino M, et al. Immune checkpoint inhibitors and prostate cancer: a new frontier? *Oncol Rev* (2016) 10:293. doi:10.4081/oncol.2016.293
4. Goswami S, Aparicio A, Subudhi SK. Immune checkpoint therapies in prostate cancer. *Cancer J* (2016) 22:117–20. doi:10.1097/PPO.0000000000000176
5. Reinstein ZZ, Pamarthy S, Sagar V, Costa R, Abdulkadir SA, Giles FJ, et al. Overcoming immunosuppression in bone metastases. *Crit Rev Oncol Hematol* (2017) 117:114–27. doi:10.1016/j.critrevonc.2017.05.004
6. Alliot F, Godin I, Pessac B. Microglia derive from progenitors, originating from the yolk sac, and which proliferate in the brain. *Brain Res Dev Brain Res* (1999) 117:145–52. doi:10.1016/S0165-3806(99)00113-3
7. Gomez Perdiguero E, Klapproth K, Schulz C, Busch K, Azzoni E, Crozet L, et al. Tissue-resident macrophages originate from yolk-sac-derived erythro-myeloid progenitors. *Nature* (2015) 518:547–51. doi:10.1038/nature13989
8. van de Laar L, Saelens W, De Prijck S, Martens L, Scott CL, Van Isterdael G, et al. Yolk Sac macrophages, fetal liver, and adult monocytes can colonize an empty niche and develop into functional tissue-resident macrophages. *Immunity* (2016) 44:755–68. doi:10.1016/j.immuni.2016.02.017
9. Thomas WE. Brain macrophages: evaluation of microglia and their functions. *Brain Res Brain Res Rev* (1992) 17:61–74. doi:10.1016/0165-0173(92)90007-9
10. Gehrmann J, Matsumoto Y, Kreutzberg GW. Microglia: intrinsic immuneffector cell of the brain. *Brain Res Brain Res Rev* (1995) 20:269–87. doi:10.1016/0165-0173(94)00015-H

11. Haubrich WS. Kupffer of Kupffer cells. *Gastroenterology* (2004) 127:16. doi:10.1053/j.gastro.2004.05.041
12. Naito M, Hasegawa G, Takahashi K. Development, differentiation, and maturation of Kupffer cells. *Microsc Res Tech* (1997) 39:350–64. doi:10.1002/(SICI)1097-0029(19971115)39:4<350::AID-JEMT5>3.0.CO;2-L
13. Hussell T, Bell TJ. Alveolar macrophages: plasticity in a tissue-specific context. *Nat Rev Immunol* (2014) 14:81–93. doi:10.1038/nri3600
14. Joshi N, Walter JM, Misharin AV. Alveolar macrophages. *Cell Immunol* (2018) pii: S0008-8749(18)30005–4. doi:10.1016/j.cellimm.2018.01.005
15. Tan HY, Wang N, Li S, Hong M, Wang X, Feng Y. The reactive oxygen species in macrophage polarization: reflecting its dual role in progression and treatment of human diseases. *Oxid Med Cell Longev* (2016) 2016:2795090. doi:10.1155/2016/2795090
16. Liu YC, Zou XB, Chai YF, Yao YM. Macrophage polarization in inflammatory diseases. *Int J Biol Sci* (2014) 10:520–9. doi:10.7150/ijbs.8879
17. Zhou D, Huang C, Lin Z, Zhan S, Kong L, Fang C, et al. Macrophage polarization and function with emphasis on the evolving roles of coordinated regulation of cellular signaling pathways. *Cell Signal* (2014) 26:192–7. doi:10.1016/j.cellsig.2013.11.004
18. Sica A, Mantovani A. Macrophage plasticity and polarization: in vivo veritas. *J Clin Invest* (2012) 122:787–95. doi:10.1172/JCI59643
19. Wang N, Liang H, Zen K. Molecular mechanisms that influence the macrophage M1–M2 polarization balance. *Front Immunol* (2014) 5:614. doi:10.3389/fimmu.2014.00614
20. Allen JE, Ruckerl D. The silent undertakers: macrophages programmed for efferocytosis. *Immunity* (2017) 47:810–2. doi:10.1016/j.immuni.2017.10.010
21. Chang CF, Goods BA, Askenase MH, Hammond MD, Renfroe SC, Steinschneider AF, et al. Erythrocyte efferocytosis modulates macrophages towards recovery after intracerebral hemorrhage. *J Clin Invest* (2018) 128:607–24. doi:10.1172/JCI95612
22. Campana L, Starkey Lewis PJ, Pellicoro A, Aucott RL, Man J, O'Duibhir E, et al. The STAT3-IL-10-IL-6 pathway is a novel regulator of macrophage efferocytosis and phenotypic conversion in sterile liver injury. *J Immunol* (2018) 200:1169–87. doi:10.4049/jimmunol.1701247
23. Das A, Ganesh K, Khanna S, Sen CK, Roy S. Engulfment of apoptotic cells by macrophages: a role of microRNA-21 in the resolution of wound inflammation. *J Immunol* (2014) 192:1120–9. doi:10.4049/jimmunol.1300613
24. Michlewska S, Dransfield I, Megson IL, Rossi AG. Macrophage phagocytosis of apoptotic neutrophils is critically regulated by the opposing actions of pro-inflammatory and anti-inflammatory agents: key role for TNF-alpha. *FASEB J* (2009) 23:844–54. doi:10.1096/fj.08-121228
25. Roberts CA, Dickinson AK, Taams LS. The interplay between monocytes/macrophages and CD4(+) T cell subsets in rheumatoid arthritis. *Front Immunol* (2015) 6:571. doi:10.3389/fimmu.2015.00571
26. Pozzi LA, Maciaszek JW, Rock KL. Both dendritic cells and macrophages can stimulate naive CD8 T cells in vivo to proliferate, develop effector function, and differentiate into memory cells. *J Immunol* (2005) 175:2071–81. doi:10.4049/jimmunol.175.4.2071
27. Arango Duque G, Descoteaux A. Macrophage cytokines: involvement in immunity and infectious diseases. *Front Immunol* (2014) 5:491. doi:10.3389/fimmu.2014.00491
28. Pakyari M, Farrokhi A, Maharlooei MK, Ghahary A. Critical role of transforming growth factor beta in different phases of wound healing. *Adv Wound Care (New Rochelle)* (2013) 2:215–24. doi:10.1089/wound.2012.0406
29. Kraaij MD, Savage ND, van der Kooij SW, Koekkoek K, Wang J, van den Berg JM, et al. Induction of regulatory T cells by macrophages is dependent on production of reactive oxygen species. *Proc Natl Acad Sci U S A* (2010) 107:17686–91. doi:10.1073/pnas.1012016107
30. Huber S, Hoffmann R, Muskens F, Voehringer D. Alternatively activated macrophages inhibit T-cell proliferation by Stat6-dependent expression of PD-L2. *Blood* (2010) 116:3311–20. doi:10.1182/blood-2010-02-271981
31. Schebesch C, Kodelja V, Muller C, Hakij N, Bisson S, Orfanos CE, et al. Alternatively activated macrophages actively inhibit proliferation of peripheral blood lymphocytes and CD4+ T cells in vitro. *Immunology* (1997) 92:478–86. doi:10.1046/j.1365-2567.1997.00371.x
32. Gelderman KA, Hultqvist M, Pizzolla A, Zhao M, Nandakumar KS, Mattsson R, et al. Macrophages suppress T cell responses and arthritis development in mice by producing reactive oxygen species. *J Clin Invest* (2007) 117:3020–8. doi:10.1172/JCI31935
33. Minutti CM, Knipper JA, Allen JE, Zaiss DM. Tissue-specific contribution of macrophages to wound healing. *Semin Cell Dev Biol* (2017) 61:3–11. doi:10.1016/j.semcdb.2016.08.006
34. Mantovani A, Biswas SK, Galdiero MR, Sica A, Locati M. Macrophage plasticity and polarization in tissue repair and remodelling. *J Pathol* (2013) 229:176–85. doi:10.1002/path.4133
35. Yavropoulou MP, Yovos JG. Osteoclastogenesis – current knowledge and future perspectives. *J Musculoskelet Neuronal Interact* (2008) 8:204–16.
36. Asagiri M, Takayanagi H. The molecular understanding of osteoclast differentiation. *Bone* (2007) 40:251–64. doi:10.1016/j.bone.2006.09.023
37. Teitelbaum SL. Bone resorption by osteoclasts. *Science* (2000) 289:1504–8. doi:10.1126/science.289.5484.1504
38. Nijweide PJ, Burger EH, Feyen JH. Cells of bone: proliferation, differentiation, and hormonal regulation. *Physiol Rev* (1986) 66:855–86. doi:10.1152/physrev.1986.66.4.855
39. Schindeler A, McDonald MM, Bokko P, Little DG. Bone remodeling during fracture repair: the cellular picture. *Semin Cell Dev Biol* (2008) 19:459–66. doi:10.1016/j.semcdb.2008.08.008
40. McArdle A, Marecic O, Tevlin R, Walmsley GG, Chan CK, Longaker MT, et al. The role and regulation of osteoclasts in normal bone homeostasis and in response to injury. *Plast Reconstr Surg* (2015) 135:808–16. doi:10.1097/PRS.0000000000000963
41. Yamaguchi T, Movila A, Kataoka S, Wisitrasameewong W, Ruiz Torruella M, Murakoshi M, et al. Proinflammatory M1 macrophages inhibit RANKL-induced osteoclastogenesis. *Infect Immun* (2016) 84:2802–12. doi:10.1128/IAI.00461-16
42. Huang R, Wang X, Zhou Y, Xiao Y. RANKL-induced M1 macrophages are involved in bone formation. *Bone Res* (2017) 5:17019. doi:10.1038/boneres.2017.19
43. Sesia SB, Duhr R, Medeiros da Cunha C, Todorov A, Schaeren S, Padovan E, et al. Anti-inflammatory/tissue repair macrophages enhance the cartilage-forming capacity of human bone marrow-derived mesenchymal stromal cells. *J Cell Physiol* (2015) 230:1258–69. doi:10.1002/jcp.24861
44. Hume DA, Loutit JF, Gordon S. The mononuclear phagocyte system of the mouse defined by immunohistochemical localization of antigen F4/80: macrophages of bone and associated connective tissue. *J Cell Sci* (1984) 66:189–94.
45. Pettit AR, Chang MK, Hume DA, Raggatt L-J. Osteal macrophages: a new twist on coupling during bone dynamics. *Bone* (2008) 43:976–82. doi:10.1016/j.bone.2008.08.128
46. Sinder BP, Pettit AR, McCauley LK. Macrophages: their emerging roles in bone. *J Bone Miner Res* (2015) 30:2140–9. doi:10.1002/jbmr.2735
47. Chang MK, Raggatt LJ, Alexander KA, Kuliwaba JS, Fazzalari NL, Schroder K, et al. Osteal tissue macrophages are intercalated throughout human and mouse bone lining tissues and regulate osteoblast function in vitro and in vivo. *J Immunol* (2008) 181:1232–44. doi:10.4049/jimmunol.181.2.1232
48. Batoon L, Millard SM, Raggatt LJ, Pettit AR. Osteomacs and bone regeneration. *Curr Osteoporos Rep* (2017) 15:385–95. doi:10.1007/s11914-017-0384-x
49. Batoon L, Millard SM, Wullschleger ME, Preda C, Wu AC, Kaur S, et al. CD169(+) macrophages are critical for osteoblast maintenance and promote intramembranous and endochondral ossification during bone repair. *Biomaterials* (2017). doi:10.1016/j.biomaterials.2017.10.033
50. Alexander KA, Raggatt L-J, Millard S, Batoon L, Chiu-Ku Wu A, Chang M-K, et al. Resting and injury-induced inflamed periosteum contain multiple macrophage subsets that are located at sites of bone growth and regeneration. *Immunol Cell Biol* (2016) 95:7–16. doi:10.1038/icb.2016.74
51. Cho SW, Soki FN, Koh AJ, Eber MR, Entezami P, Park SI, et al. Osteal macrophages support physiologic skeletal remodeling and anabolic actions of parathyroid hormone in bone. *Proc Natl Acad Sci U S A* (2014) 111:1545–50. doi:10.1073/pnas.1315153111
52. Shi M, Wang C, Wang Y, Tang C, Miron RJ, Zhang Y. Deproteinized bovine bone matrix induces osteoblast differentiation via macrophage polarization. *J Biomed Mater Res A* (2017) 106:1236–46. doi:10.1002/jbm.a.36321
53. Sinder BP, Zweifler L, Koh AJ, Michalski MN, Hofbauer LC, Aguirre JI, et al. Bone mass is compromised by the chemotherapeutic trabectedin in

association with effects on osteoblasts and macrophage efferocytosis. *J Bone Miner Res* (2017) 32:2116–27. doi:10.1002/jbmr.3196
54. Bozec A, Soulat D. Latest perspectives on macrophages in bone homeostasis. *Pflügers Arch* (2017) 469:517–25. doi:10.1007/s00424-017-1952-8
55. Kaur S, Raggatt LJ, Batoon L, Hume DA, Levesque JP, Pettit AR. Role of bone marrow macrophages in controlling homeostasis and repair in bone and bone marrow niches. *Semin Cell Dev Biol* (2017) 61:12–21. doi:10.1016/j.semcdb.2016.08.009
56. Sfanos KS, De Marzo AM. Prostate cancer and inflammation: the evidence. *Histopathology* (2012) 60:199–215. doi:10.1111/j.1365-2559.2011.04033.x
57. De Marzo AM, Marchi VL, Epstein JI, Nelson WG. Proliferative inflammatory atrophy of the prostate: implications for prostatic carcinogenesis. *Am J Pathol* (1999) 155:1985–92. doi:10.1016/S0002-9440(10)65517-4
58. Pollard JW. Tumour-educated macrophages promote tumour progression and metastasis. *Nat Rev Cancer* (2004) 4:71–8. doi:10.1038/nrc1256
59. Comito G, Giannoni E, Segura CP, Barcellos-de-Souza P, Raspollini MR, Baroni G, et al. Cancer-associated fibroblasts and M2-polarized macrophages synergize during prostate carcinoma progression. *Oncogene* (2014) 33:2423–31. doi:10.1038/onc.2013.191
60. Takayama H, Nonomura N, Nishimura K, Oka D, Shiba M, Nakai Y, et al. Decreased immunostaining for macrophage scavenger receptor is associated with poor prognosis of prostate cancer. *BJU Int* (2009) 103:470–4. doi:10.1111/j.1464-410X.2008.08013.x
61. Shimura S, Yang G, Ebara S, Wheeler TM, Frolov A, Thompson TC. Reduced infiltration of tumor-associated macrophages in human prostate cancer: association with cancer progression. *Cancer Res* (2000) 60:5857–61.
62. Cao J, Liu J, Xu R, Zhu X, Zhao X, Qian BZ. Prognostic role of tumour-associated macrophages and macrophage scavenger receptor 1 in prostate cancer: a systematic review and meta-analysis. *Oncotarget* (2017) 8:83261–9. doi:10.18632/oncotarget.18743
63. Lissbrant IF, Stattin P, Wikstrom P, Damber JE, Egevad L, Bergh A. Tumor associated macrophages in human prostate cancer: relation to clinicopathological variables and survival. *Int J Oncol* (2000) 17:445–51. doi:10.3892/ijo.17.3.445
64. Bingle L, Brown NJ, Lewis CE. The role of tumour-associated macrophages in tumour progression: implications for new anticancer therapies. *J Pathol* (2002) 196:254–65. doi:10.1002/path.1027
65. Nonomura N, Takayama H, Nakayama M, Nakai Y, Kawashima A, Mukai M, et al. Infiltration of tumour-associated macrophages in prostate biopsy specimens is predictive of disease progression after hormonal therapy for prostate cancer. *BJU Int* (2011) 107:1918–22. doi:10.1111/j.1464-410X.2010.09804.x
66. Gollapudi K, Galet C, Grogan T, Zhang H, Said JW, Huang J, et al. Association between tumor-associated macrophage infiltration, high grade prostate cancer, and biochemical recurrence after radical prostatectomy. *Am J Cancer Res* (2013) 3:523–9.
67. Lin D, Wang X, Choi SYC, Ci X, Dong X, Wang Y. Immune phenotypes of prostate cancer cells: evidence of epithelial immune cell-like transition? *Asian J Urol* (2016) 3:195–202. doi:10.1016/j.ajur.2016.08.002
68. Lanciotti M, Masieri L, Raspollini MR, Minervini A, Mari A, Comito G, et al. The role of M1 and M2 macrophages in prostate cancer in relation to extracapsular tumor extension and biochemical recurrence after radical prostatectomy. *Biomed Res Int* (2014) 2014:6. doi:10.1155/2014/486798
69. Hillen F, Griffioen AW. Tumour vascularization: sprouting angiogenesis and beyond. *Cancer Metastasis Rev* (2007) 26:489–502. doi:10.1007/s10555-007-9094-7
70. Strasner A, Karin M. Immune infiltration and prostate cancer. *Front Oncol* (2015) 5:128. doi:10.3389/fonc.2015.00128
71. Yang KQ, Liu Y, Huang QH, Mo N, Zhang QY, Meng QG, et al. Bone marrow-derived mesenchymal stem cells induced by inflammatory cytokines produce angiogenetic factors and promote prostate cancer growth. *BMC Cancer* (2017) 17:878. doi:10.1186/s12885-017-3879-z
72. Zhang J, Lu Y, Pienta KJ. Multiple roles of chemokine (C-C motif) ligand 2 in promoting prostate cancer growth. *J Natl Cancer Inst* (2010) 102:522–8. doi:10.1093/jnci/djq044
73. Mizutani K, Sud S, McGregor NA, Martinovski G, Rice BT, Craig MJ, et al. The chemokine CCL2 increases prostate tumor growth and bone metastasis through macrophage and osteoclast recruitment. *Neoplasia* (2009) 11:1235–42. doi:10.1593/neo.09988
74. Loberg RD, Ying C, Craig M, Yan L, Snyder LA, Pienta KJ. CCL2 as an important mediator of prostate cancer growth in vivo through the regulation of macrophage infiltration. *Neoplasia* (2007) 9:556–62. doi:10.1593/neo.07307
75. Escamilla J, Schokrpur S, Liu C, Priceman SJ, Moughon D, Jiang Z, et al. CSF1 receptor targeting in prostate cancer reverses macrophage-mediated resistance to androgen blockade therapy. *Cancer Res* (2015) 75:950–62. doi:10.1158/0008-5472.CAN-14-0992
76. Priceman SJ, Sung JL, Shaposhnik Z, Burton JB, Torres-Collado AX, Moughon DL, et al. Targeting distinct tumor-infiltrating myeloid cells by inhibiting CSF-1 receptor: combating tumor evasion of antiangiogenic therapy. *Blood* (2010) 115:1461–71. doi:10.1182/blood-2009-08-237412
77. Xu J, Escamilla J, Mok S, David J, Priceman S, West B, et al. CSF1R signaling blockade stanches tumor-infiltrating myeloid cells and improves the efficacy of radiotherapy in prostate cancer. *Cancer Res* (2013) 73:2782–94. doi:10.1158/0008-5472.CAN-12-3981
78. Cannarile MA, Weisser M, Jacob W, Jegg AM, Ries CH, Ruttinger D. Colony-stimulating factor 1 receptor (CSF1R) inhibitors in cancer therapy. *J Immunother Cancer* (2017) 5:53. doi:10.1186/s40425-017-0257-y
79. Redente EF, Dwyer-Nield LD, Merrick DT, Raina K, Agarwal R, Pao W, et al. Tumor progression stage and anatomical site regulate tumor-associated macrophage and bone marrow-derived monocyte polarization. *Am J Pathol* (2010) 176:2972–85. doi:10.2353/ajpath.2010.090879
80. Lin EY, Nguyen AV, Russell RG, Pollard JW. Colony-stimulating factor 1 promotes progression of mammary tumors to malignancy. *J Exp Med* (2001) 193:727–40. doi:10.1084/jem.193.6.727
81. Qian BZ, Li J, Zhang H, Kitamura T, Zhang J, Campion LR, et al. CCL2 recruits inflammatory monocytes to facilitate breast-tumour metastasis. *Nature* (2011) 475:222–5. doi:10.1038/nature10138
82. Allavena P, Sica A, Solinas G, Porta C, Mantovani A. The inflammatory micro-environment in tumor progression: the role of tumor-associated macrophages. *Crit Rev Oncol Hematol* (2008) 66:1–9. doi:10.1016/j.critrevonc.2007.07.004
83. Condeelis J, Pollard JW. Macrophages: obligate partners for tumor cell migration, invasion, and metastasis. *Cell* (2006) 124:263–6. doi:10.1016/j.cell.2006.01.007
84. Wan YY, Flavell RA. TGF-beta and regulatory T cell in immunity and autoimmunity. *J Clin Immunol* (2008) 28:647–59. doi:10.1007/s10875-008-9251-y
85. Zhang L, Yi H, Xia XP, Zhao Y. Transforming growth factor-beta: an important role in CD4+CD25+ regulatory T cells and immune tolerance. *Autoimmunity* (2006) 39:269–76. doi:10.1080/08916930600753903
86. Wang X, Lee SO, Xia S, Jiang Q, Luo J, Li L, et al. Endothelial cells enhance prostate cancer metastasis via IL-6–>androgen receptor–>TGF-beta–>MMP-9 signals. *Mol Cancer Ther* (2013) 12:1026–37. doi:10.1158/1535-7163.MCT-12-0895
87. Fiorio Pla A, Brossa A, Bernardini M, Genova T, Grolez G, Villers A, et al. Differential sensitivity of prostate tumor derived endothelial cells to sorafenib and sunitinib. *BMC Cancer* (2014) 14:939. doi:10.1186/1471-2407-14-939
88. Shangguan L, Ti X, Krause U, Hai B, Zhao Y, Yang Z, et al. Inhibition of TGF-beta/Smad signaling by BAMBI blocks differentiation of human mesenchymal stem cells to carcinoma-associated fibroblasts and abolishes their protumor effects. *Stem Cells* (2012) 30:2810–9. doi:10.1002/stem.1251
89. Geiger R, Rieckmann JC, Wolf T, Basso C, Feng Y, Fuhrer T, et al. L-arginine modulates T cell metabolism and enhances survival and anti-tumor activity. *Cell* (2016) 167:829–842.e13. doi:10.1016/j.cell.2016.09.031
90. Niedbala W, Cai B, Liew FY. Role of nitric oxide in the regulation of T cell functions. *Ann Rheum Dis* (2006) 65(Suppl 3):iii37–iii40. doi:10.1136/ard.2006.058446
91. Niedbala W, Wei XQ, Campbell C, Thomson D, Komai-Koma M, Liew FY. Nitric oxide preferentially induces type 1 T cell differentiation by selectively up-regulating IL-12 receptor beta 2 expression via cGMP. *Proc Natl Acad Sci U S A* (2002) 99:16186–91. doi:10.1073/pnas.252464599
92. Shiga K, Hara M, Nagasaki T, Sato T, Takahashi H, Takeyama H. Cancer-associated fibroblasts: their characteristics and their roles in tumor growth. *Cancers (Basel)* (2015) 7:2443–58. doi:10.3390/cancers7040902
93. Jung Y, Kim JK, Shiozawa Y, Wang J, Mishra A, Joseph J, et al. Recruitment of mesenchymal stem cells into prostate tumours promotes metastasis. *Nat Commun* (2013) 4:1795. doi:10.1038/ncomms2766

94. Kaplan RN, Psaila B, Lyden D. Bone marrow cells in the "pre-metastatic niche": within bone and beyond. *Cancer Metastasis Rev* (2006) 25:521–9. doi:10.1007/s10555-006-9036-9
95. Zoni E, van der Pluijm G. The role of microRNAs in bone metastasis. *J Bone Oncol* (2016) 5:104–8. doi:10.1016/j.jbo.2016.04.002
96. Weidle HU, Birzele F, Kollmorgen G, RÜGer R. The multiple roles of exosomes in metastasis. *Cancer Genomics Proteomics* (2017) 14:1–16. doi:10.21873/cgp.20015
97. Sanchez CA, Andahur EI, Valenzuela R, Castellon EA, Fulla JA, Ramos CG, et al. Exosomes from bulk and stem cells from human prostate cancer have a differential microRNA content that contributes cooperatively over local and pre-metastatic niche. *Oncotarget* (2016) 7:3993–4008. doi:10.18632/oncotarget.6540
98. Rauschenberger L, Staar D, Thom K, Scharf C, Venz S, Homuth G, et al. Exosomal particles secreted by prostate cancer cells are potent mRNA and protein vehicles for the interference of tumor and tumor environment. *Prostate* (2016) 76:409–24. doi:10.1002/pros.23132
99. Mathivanan S, Fahner CJ, Reid GE, Simpson RJ. ExoCarta 2012: database of exosomal proteins, RNA and lipids. *Nucleic Acids Res* (2012) 40:D1241–4. doi:10.1093/nar/gkr828
100. Pan J, Ding M, Xu K, Yang C, Mao LJ. Exosomes in diagnosis and therapy of prostate cancer. *Oncotarget* (2017) 8:97693–700. doi:10.18632/oncotarget.18532
101. Karlsson T, Lundholm M, Widmark A, Persson E. Tumor cell-derived exosomes from the prostate cancer cell line TRAMP-C1 impair osteoclast formation and differentiation. *PLoS One* (2016) 11:e0166284. doi:10.1371/journal.pone.0166284
102. Soki FN, Koh AJ, Jones JD, Kim YW, Dai J, Keller ET, et al. Polarization of prostate cancer-associated macrophages is induced by milk fat globule-EGF factor 8 (MFG-E8)-mediated efferocytosis. *J Biol Chem* (2014) 289:24560–72. doi:10.1074/jbc.M114.571620
103. Aziz M, Jacob A, Matsuda A, Wu R, Zhou M, Dong W, et al. Pre-treatment of recombinant mouse MFG-E8 downregulates LPS-induced TNF-alpha production in macrophages via STAT3-mediated SOCS3 activation. *PLoS One* (2011) 6:e27685. doi:10.1371/journal.pone.0027685
104. Bonci D, Coppola V, Patrizii M, Addario A, Cannistraci A, Francescangeli F, et al. A microRNA code for prostate cancer metastasis. *Oncogene* (2016) 35:1180–92. doi:10.1038/onc.2015.176
105. Sugatani T, Vacher J, Hruska KA. A microRNA expression signature of osteoclastogenesis. *Blood* (2011) 117:3648–57. doi:10.1182/blood-2010-10-311415
106. Shiozawa Y, Eber MR, Berry JE, Taichman RS. Bone marrow as a metastatic niche for disseminated tumor cells from solid tumors. *Bonekey Rep* (2015) 4:689. doi:10.1038/bonekey.2015.57
107. Sousa S, Määttä J. The role of tumour-associated macrophages in bone metastasis. *J Bone Oncol* (2016) 5:135–8. doi:10.1016/j.jbo.2016.03.004
108. Qian B-Z, Pollard JW. Macrophage diversity enhances tumor progression and metastasis. *Cell* (2010) 141:39–51. doi:10.1016/j.cell.2010.03.014
109. Zarif JC, Taichman RS, Pienta KJ. TAM macrophages promote growth and metastasis within the cancer ecosystem. *Oncoimmunology* (2014) 3:e941734. doi:10.4161/21624011.2014.941734
110. Teti A. Mechanisms of osteoclast-dependent bone formation. *Bonekey Rep* (2013) 2:449. doi:10.1038/bonekey.2013.183
111. Mundy GR. The effects of TGF-beta on bone. *Ciba Found Symp* (1991) 157:137–43; discussion 143–51.
112. Keller ET, Brown J. Prostate cancer bone metastases promote both osteolytic and osteoblastic activity. *J Cell Biochem* (2004) 91:718–29. doi:10.1002/jcb.10662
113. Zhang Z, Jimi E, Bothwell AL. Receptor activator of NF-kappa B ligand stimulates recruitment of SHP-1 to the complex containing TNFR-associated factor 6 that regulates osteoclastogenesis. *J Immunol* (2003) 171:3620–6. doi:10.4049/jimmunol.171.7.3620
114. Takeshita S, Kaji K, Kudo A. Identification and characterization of the new osteoclast progenitor with macrophage phenotypes being able to differentiate into mature osteoclasts. *J Bone Miner Res* (2000) 15:1477–88. doi:10.1359/jbmr.2000.15.8.1477
115. Wu AC, He Y, Broomfield A, Paatan NJ, Harrington BS, Tseng H-W, et al. CD169+ macrophages mediate pathological formation of woven bone in skeletal lesions of prostate cancer. *J Pathol* (2016) 239:218–30. doi:10.1002/path.4718
116. Soki FN, Cho SW, Kim YW, Jones JD, Park SI, Koh AJ, et al. Bone marrow macrophages support prostate cancer growth in bone. *Oncotarget* (2015) 6:35782–96. doi:10.18632/oncotarget.6042
117. Yang L, Zhang Y. Tumor-associated macrophages: from basic research to clinical application. *J Hematol Oncol* (2017) 10:58. doi:10.1186/s13045-017-0430-2
118. Antonarakis ES, Lu C, Wang H, Luber B, Nakazawa M, Roeser JC, et al. AR-V7 and resistance to enzalutamide and abiraterone in prostate cancer. *N Engl J Med* (2014) 371:1028–38. doi:10.1056/NEJMoa1315815
119. Hoefer J, Akbor M, Handle F, Ofer P, Puhr M, Parson W, et al. Critical role of androgen receptor level in prostate cancer cell resistance to new generation antiandrogen enzalutamide. *Oncotarget* (2016) 7:59781–94. doi:10.18632/oncotarget.10926
120. Seitz AK, Thoene S, Bietenbeck A, Nawroth R, Tauber R, Thalgott M, et al. AR-V7 in peripheral whole blood of patients with castration-resistant prostate cancer: association with treatment-specific outcome under abiraterone and enzalutamide. *Eur Urol* (2017) 72:828–34. doi:10.1016/j.eururo.2017.07.024
121. Lin TH, Izumi K, Lee SO, Lin WJ, Yeh S, Chang C. Anti-androgen receptor ASC-J9 versus anti-androgens MDV3100 (enzalutamide) or casodex (bicalutamide) leads to opposite effects on prostate cancer metastasis via differential modulation of macrophage infiltration and STAT3-CCL2 signaling. *Cell Death Dis* (2013) 4:e764. doi:10.1038/cddis.2013.270
122. Lin TH, Lee SO, Niu Y, Xu D, Liang L, Li L, et al. Differential androgen deprivation therapies with anti-androgens casodex/bicalutamide or MDV3100/enzalutamide versus anti-androgen receptor ASC-J9(R) lead to promotion versus suppression of prostate cancer metastasis. *J Biol Chem* (2013) 288:19359–69. doi:10.1074/jbc.M113.477216
123. Wang XJ, Zhuo J, Luo GH, Zhu YP, Yu DJ, Zhao RZ, et al. Androgen deprivation accelerates the prostatic urethra wound healing after thulium laser resection of the prostate by promoting re-epithelialization and regulating the macrophage polarization. *Prostate* (2017) 77:708–17. doi:10.1002/pros.23301
124. Wang A, Karunasinghe N, Plank L, Zhu S, Osborne S, Bishop K, et al. Effect of androgen deprivation therapy on bone mineral density in a prostate cancer cohort in New Zealand: a pilot study. *Clin Med Insights Oncol* (2017) 11:1179554917733449. doi:10.1177/1179554917733449
125. Crawford ED, Higano CS, Shore ND, Hussain M, Petrylak DP. Treating patients with metastatic castration resistant prostate cancer: a comprehensive review of available therapies. *J Urol* (2015) 194:1537–47. doi:10.1016/j.juro.2015.06.106
126. Paller CJ, Antonarakis ES. Cabazitaxel: a novel second-line treatment for metastatic castration-resistant prostate cancer. *Drug Des Devel Ther* (2011) 5:117–24. doi:10.2147/DDDT.S13029
127. Colloca G, Venturino A, Checcaglini F. Second-line chemotherapy in metastatic docetaxel-resistant prostate cancer: a review. *Med Oncol* (2012) 29:776–85. doi:10.1007/s12032-011-9855-6
128. Petrylak DP. Practical guide to the use of chemotherapy in castration resistant prostate cancer. *Can J Urol* (2014) 21:77–83.
129. Yin Y, Huang X, Lynn KD, Thorpe PE. Phosphatidylserine-targeting antibody induces M1 macrophage polarization and promotes myeloid-derived suppressor cell differentiation. *Cancer Immunol Res* (2013) 1:256–68. doi:10.1158/2326-6066.CIR-13-0073
130. Kodumudi KN, Woan K, Gilvary DL, Sahakian E, Wei S, Djeu JY. A novel chemoimmunomodulating property of docetaxel: suppression of myeloid-derived suppressor cells in tumor bearers. *Clin Cancer Res* (2010) 16:4583–94. doi:10.1158/1078-0432.CCR-10-0733
131. Mahon KL, Lin HM, Castillo L, Lee BY, Lee-Ng M, Chatfield MD, et al. Cytokine profiling of docetaxel-resistant castration-resistant prostate cancer. *Br J Cancer* (2015) 112:1340–8. doi:10.1038/bjc.2015.74
132. Wolff B, Burns AR, Middleton J, Rot A. Endothelial cell "memory" of inflammatory stimulation: human venular endothelial cells store interleukin 8 in Weibel-Palade bodies. *J Exp Med* (1998) 188:1757–62. doi:10.1084/jem.188.9.1757
133. Utgaard JO, Jahnsen FL, Bakka A, Brandtzaeg P, Haraldsen G. Rapid secretion of prestored interleukin 8 from Weibel-Palade bodies of microvascular endothelial cells. *J Exp Med* (1998) 188:1751–6. doi:10.1084/jem.188.9.1751
134. Brat DJ, Bellail AC, Van Meir EG. The role of interleukin-8 and its receptors in gliomagenesis and tumoral angiogenesis. *Neuro Oncol* (2005) 7:122–33. doi:10.1215/S1152851704001061

135. Magadoux L, Isambert N, Plenchette S, Jeannin JF, Laurens V. Emerging targets to monitor and overcome docetaxel resistance in castration resistant prostate cancer (review). *Int J Oncol* (2014) 45:919–28. doi:10.3892/ijo.2014.2517
136. Lu Y, Cai Z, Galson DL, Xiao G, Liu Y, George DE, et al. Monocyte chemotactic protein-1 (MCP-1) acts as a paracrine and autocrine factor for prostate cancer growth and invasion. *Prostate* (2006) 66:1311–8. doi:10.1002/pros.20464
137. Roca H, Varsos ZS, Pienta KJ. CCL2 is a negative regulator of AMP-activated protein kinase to sustain mTOR complex-1 activation, survivin expression, and cell survival in human prostate cancer PC3 cells. *Neoplasia* (2009) 11:1309–17. doi:10.1593/neo.09936
138. Loberg RD, Day LL, Harwood J, Ying C, St John LN, Giles R, et al. CCL2 is a potent regulator of prostate cancer cell migration and proliferation. *Neoplasia* (2006) 8:578–86. doi:10.1593/neo.06280
139. Qian DZ, Rademacher BL, Pittsenbarger J, Huang CY, Myrthue A, Higano CS, et al. CCL2 is induced by chemotherapy and protects prostate cancer cells from docetaxel-induced cytotoxicity. *Prostate* (2010) 70:433–42. doi:10.1002/pros.21077
140. Takahashi M, Mizoguchi T, Uehara S, Nakamichi Y, Yang S, Naramoto H, et al. Docetaxel inhibits bone resorption through suppression of osteoclast formation and function in different manners. *J Bone Miner Metab* (2009) 27:24–35. doi:10.1007/s00774-008-0013-y
141. Yeku O, Slovin SF. Radium-223 and concomitant therapies: prospects and prudence. *Transl Androl Urol* (2016) 5:968–70. doi:10.21037/tau.2016.11.04
142. Wenter V, Herlemann A, Fendler WP, Ilhan H, Tirichter N, Bartenstein P, et al. Radium-223 for primary bone metastases in patients with hormone-sensitive prostate cancer after radical prostatectomy. *Oncotarget* (2017) 8:44131–40. doi:10.18632/oncotarget.17311
143. Parker CC, Coleman RE, Sartor O, Vogelzang NJ, Bottomley D, Heinrich D, et al. Three-year safety of radium-223 dichloride in patients with castration-resistant prostate cancer and symptomatic bone metastases from phase 3 randomized alpharadin in Symptomatic Prostate Cancer Trial. *Eur Urol* (2018) 73:427–35. doi:10.1016/j.eururo.2017.06.021
144. Armstrong CW, Maxwell PJ, Ong CW, Redmond KM, McCann C, Neisen J, et al. PTEN deficiency promotes macrophage infiltration and hypersensitivity of prostate cancer to IAP antagonist/radiation combination therapy. *Oncotarget* (2016) 7:7885–98. doi:10.18632/oncotarget.6955
145. Teresa Pinto A, Laranjeiro Pinto M, Patricia Cardoso A, Monteiro C, Teixeira Pinto M, Filipe Maia A, et al. Ionizing radiation modulates human macrophages towards a pro-inflammatory phenotype preserving their pro-invasive and pro-angiogenic capacities. *Sci Rep* (2016) 6:18765. doi:10.1038/srep18765
146. Vanpouille-Box C, Diamond JM, Pilones KA, Zavadil J, Babb JS, Formenti SC, et al. TGFbeta is a master regulator of radiation therapy-induced antitumor immunity. *Cancer Res* (2015) 75:2232–42. doi:10.1158/0008-5472.CAN-14-3511
147. Mizokami A, Gotoh A, Yamada H, Keller ET, Matsumoto T. Tumor necrosis factor-alpha represses androgen sensitivity in the LNCaP prostate cancer cell line. *J Urol* (2000) 164:800–5. doi:10.1016/S0022-5347(05)67318-1
148. Michalaki V, Syrigos K, Charles P, Waxman J. Serum levels of IL-6 and TNF-alpha correlate with clinicopathological features and patient survival in patients with prostate cancer. *Br J Cancer* (2004) 90:2312–6. doi:10.1038/sj.bjc.6601814
149. Sethi G, Sung B, Aggarwal BB. TNF: a master switch for inflammation to cancer. *Front Biosci* (2008) 13:5094–107. doi:10.2741/3066
150. Lam J, Takeshita S, Barker JE, Kanagawa O, Ross FP, Teitelbaum SL. TNF-alpha induces osteoclastogenesis by direct stimulation of macrophages exposed to permissive levels of RANK ligand. *J Clin Invest* (2000) 106:1481–8. doi:10.1172/JCI11176
151. Kobayashi K, Takahashi N, Jimi E, Udagawa N, Takami M, Kotake S, et al. Tumor necrosis factor alpha stimulates osteoclast differentiation by a mechanism independent of the ODF/RANKL-RANK interaction. *J Exp Med* (2000) 191:275–86. doi:10.1084/jem.191.2.275
152. Zhang YH, Heulsmann A, Tondravi MM, Mukherjee A, Abu-Amer Y. Tumor necrosis factor-alpha (TNF) stimulates RANKL-induced osteoclastogenesis via coupling of TNF type 1 receptor and RANK signaling pathways. *J Biol Chem* (2001) 276:563–8. doi:10.1074/jbc.M008198200
153. Osta B, Benedetti G, Miossec P. Classical and paradoxical effects of TNF-alpha on bone homeostasis. *Front Immunol* (2014) 5:48. doi:10.3389/fimmu.2014.00048
154. Joseph IB, Isaacs JT. Macrophage role in the anti-prostate cancer response to one class of antiangiogenic agents. *J Natl Cancer Inst* (1998) 90:1648–53. doi:10.1093/jnci/90.21.1648
155. Zhang J, Patel L, Pienta KJ. CC chemokine ligand 2 (CCL2) promotes prostate cancer tumorigenesis and metastasis. *Cytokine Growth Factor Rev* (2010) 21:41–8. doi:10.1016/j.cytogfr.2009.11.009
156. Craig MJ, Loberg RD. CCL2 (monocyte chemoattractant protein-1) in cancer bone metastases. *Cancer Metastasis Rev* (2006) 25:611–9. doi:10.1007/s10555-006-9027-x
157. Li X, Loberg R, Liao J, Ying C, Snyder LA, Pienta KJ, et al. A destructive cascade mediated by CCL2 facilitates prostate cancer growth in bone. *Cancer Res* (2009) 69:1685–92. doi:10.1158/0008-5472.CAN-08-2164
158. Loberg RD, Ying C, Craig M, Day LL, Sargent E, Neeley C, et al. Targeting CCL2 with systemic delivery of neutralizing antibodies induces prostate cancer tumor regression in vivo. *Cancer Res* (2007) 67:9417–24. doi:10.1158/0008-5472.CAN-07-1286
159. Sandhu SK, Papadopoulos K, Fong PC, Patnaik A, Messiou C, Olmos D, et al. A first-in-human, first-in-class, phase I study of carlumab (CNTO 888), a human monoclonal antibody against CC-chemokine ligand 2 in patients with solid tumors. *Cancer Chemother Pharmacol* (2013) 71:1041–50. doi:10.1007/s00280-013-2099-8
160. Zhang J, Patel L, Pienta KJ. Targeting chemokine (C-C motif) ligand 2 (CCL2) as an example of translation of cancer molecular biology to the clinic. *Prog Mol Biol Transl Sci* (2010) 95:31–53. doi:10.1016/B978-0-12-385071-3.00003-4
161. Pienta KJ, Machiels JP, Schrijvers D, Alekseev B, Shkolnik M, Crabb SJ, et al. Phase 2 study of carlumab (CNTO 888), a human monoclonal antibody against CC-chemokine ligand 2 (CCL2), in metastatic castration-resistant prostate cancer. *Invest New Drugs* (2013) 31:760–8. doi:10.1007/s10637-012-9869-8
162. Kirk PS, Koreckij T, Nguyen HM, Brown LG, Snyder LA, Vessella RL, et al. Inhibition of CCL2 signaling in combination with docetaxel treatment has profound inhibitory effects on prostate cancer growth in bone. *Int J Mol Sci* (2013) 14:10483–96. doi:10.3390/ijms140510483
163. Rozel S, Galban CJ, Nicolay K, Lee KC, Sud S, Neeley C, et al. Synergy between anti-CCL2 and docetaxel as determined by DW-MRI in a metastatic bone cancer model. *J Cell Biochem* (2009) 107:58–64. doi:10.1002/jcb.22056
164. Brana I, Calles A, LoRusso PM, Yee LK, Puchalski TA, Seetharam S, et al. Carlumab, an anti-C-C chemokine ligand 2 monoclonal antibody, in combination with four chemotherapy regimens for the treatment of patients with solid tumors: an open-label, multicenter phase 1b study. *Target Oncol* (2015) 10:111–23. doi:10.1007/s11523-014-0320-2
165. Li X, Qin L, Bergenstock M, Bevelock LM, Novack DV, Partridge NC. Parathyroid hormone stimulates osteoblastic expression of MCP-1 to recruit and increase the fusion of pre/osteoclasts. *J Biol Chem* (2007) 282:33098–106. doi:10.1074/jbc.M611781200
166. Craig M, Ying C, Loberg RD. Co-inoculation of prostate cancer cells with U937 enhances tumor growth and angiogenesis in vivo. *J Cell Biochem* (2008) 103:1–8. doi:10.1002/jcb.21379
167. DeNardo DG, Barreto JB, Andreu P, Vasquez L, Tawfik D, Kolhatkar N, et al. CD4(+) T cells regulate pulmonary metastasis of mammary carcinomas by enhancing protumor properties of macrophages. *Cancer Cell* (2009) 16:91–102. doi:10.1016/j.ccr.2009.06.018
168. Apte SH, Groves P, Olver S, Baz A, Doolan DL, Kelso A, et al. IFN-gamma inhibits IL-4-induced type 2 cytokine expression by CD8 T cells in vivo and modulates the anti-tumor response. *J Immunol* (2010) 185:998–1004. doi:10.4049/jimmunol.0903372
169. Goldstein R, Hanley C, Morris J, Cahill D, Chandra A, Harper P, et al. Clinical investigation of the role of interleukin-4 and interleukin-13 in the evolution of prostate cancer. *Cancers (Basel)* (2011) 3:4281–93. doi:10.3390/cancers3044281
170. Toi M, Bicknell R, Harris AL. Inhibition of colon and breast carcinoma cell growth by interleukin-4. *Cancer Res* (1992) 52:275–9.

171. Atkins MB, Vachino G, Tilg HJ, Karp DD, Robert NJ, Kappler K, et al. Phase I evaluation of thrice-daily intravenous bolus interleukin-4 in patients with refractory malignancy. *J Clin Oncol* (1992) 10:1802–9. doi:10.1200/JCO.1992.10.11.1802
172. Takeshi U, Sadar MD, Suzuki H, Akakura K, Sakamoto S, Shimbo M, et al. Interleukin-4 in patients with prostate cancer. *Anticancer Res* (2005) 25:4595–8.
173. Lee SO, Pinder E, Chun JY, Lou W, Sun M, Gao AC. Interleukin-4 stimulates androgen-independent growth in LNCaP human prostate cancer cells. *Prostate* (2008) 68:85–91. doi:10.1002/pros.20691
174. Frost A, Jonsson KB, Brandstrom H, Ljunghall S, Nilsson O, Ljunggren O. Interleukin (IL)-13 and IL-4 inhibit proliferation and stimulate IL-6 formation in human osteoblasts: evidence for involvement of receptor subunits IL-13R, IL-13Ralpha, and IL-4Ralpha. *Bone* (2001) 28:268–74. doi:10.1016/S8756-3282(00)00449-X
175. Yamada A, Takami M, Kawawa T, Yasuhara R, Zhao B, Mochizuki A, et al. Interleukin-4 inhibition of osteoclast differentiation is stronger than that of interleukin-13 and they are equivalent for induction of osteoprotegerin production from osteoblasts. *Immunology* (2007) 120:573–9. doi:10.1111/j.1365-2567.2006.02538.x
176. Shree T, Olson OC, Elie BT, Kester JC, Garfall AL, Simpson K, et al. Macrophages and cathepsin proteases blunt chemotherapeutic response in breast cancer. *Genes Dev* (2011) 25:2465–79. doi:10.1101/gad.180331.111
177. DeNardo DG, Brennan DJ, Rexhepaj E, Ruffell B, Shiao SL, Madden SF, et al. Leukocyte complexity predicts breast cancer survival and functionally regulates response to chemotherapy. *Cancer Discov* (2011) 1:54–67. doi:10.1158/2159-8274.CD-10-0028
178. Brahmi M, Vinceneux A, Cassier PA. Current systemic treatment options for tenosynovial giant cell tumor/pigmented villonodular synovitis: targeting the CSF1/CSF1R axis. *Curr Treat Options Oncol* (2016) 17:10. doi:10.1007/s11864-015-0385-x
179. Tap WD, Wainberg ZA, Anthony SP, Ibrahim PN, Zhang C, Healey JH, et al. Structure-guided blockade of CSF1R kinase in tenosynovial giant-cell tumor. *N Engl J Med* (2015) 373:428–37. doi:10.1056/NEJMoa1411366
180. Sauter KA, Pridans C, Sehgal A, Tsai YT, Bradford BM, Raza S, et al. Pleiotropic effects of extended blockade of CSF1R signaling in adult mice. *J Leukoc Biol* (2014) 96:265–74. doi:10.1189/jlb.2A0114-006R

Conflict of Interest Statement: The authors declare that the research was conducted in the absence of any commercial or financial relationships that could be construed as a potential conflict of interest.

frontiers in Endocrinology

REVIEW
published: 18 June 2018
doi: 10.3389/fendo.2018.00335

Androgen Receptor-CaMKK2 Axis in Prostate Cancer and Bone Microenvironment

*Ushashi C. Dadwal, Eric S. Chang and Uma Sankar**

Department of Anatomy and Cell Biology, Indiana University School of Medicine, Indianapolis, IN, United States

The skeletal system is of paramount importance in advanced stage prostate cancer (PCa) as it is the preferred site of metastasis. Complex mechanisms are employed sequentially by PCa cells to home to and colonize the bone. Bone-resident PCa cells then recruit osteoblasts (OBs), osteoclasts (OCs), and macrophages within the niche into entities that promote cancer cell growth and survival. Since PCa is heavily reliant on androgens for growth and survival, androgen-deprivation therapy (ADT) is the standard of care for advanced disease. Although it significantly improves survival rates, ADT detrimentally affects bone health and significantly increases the risk of fractures. Moreover, whereas the majority patients with advanced PCa respond favorably to androgen deprivation, most experience a relapse of the disease to a hormone-refractory form within 1–2 years of ADT. The tumor adapts to surviving under low testosterone conditions by selecting for mutations in the androgen receptor (AR) that constitutively activate it. Thus, AR signaling remains active in PCa cells and aids in its survival under low levels of circulating androgens and additionally allows the cancer cells to manipulate the bone microenvironment to fuel its growth. Hence, AR and its downstream effectors are attractive targets for therapeutic interventions against PCa. Ca^{2+}/calmodulin-dependent protein kinase kinase 2 (CaMKK2), was recently identified as a key downstream target of AR in coordinating PCa cell growth, survival, and migration. Additionally, this multifunctional serine/threonine protein kinase is a critical mediator of bone remodeling and macrophage function, thus emerging as an attractive therapeutic target downstream of AR in controlling metastatic PCa and preventing ADT-induced bone loss. Here, we discuss the role played by AR-CaMKK2 signaling axis in PCa survival, metabolism, cell growth, and migration as well as the cell-intrinsic roles of CaMKK2 in OBs, OCs, and macrophages within the bone microenvironment.

Keywords: castrate-resistant prostate cancer, androgen-deprivation therapy, CAMKK2, bone–tumor microenvironment, treatment induced bone loss

OPEN ACCESS

Edited by:
Chandi C. Mandal,
Central University of Rajasthan, India

Reviewed by:
Michael Koutsilieris,
National and Kapodistrian University of Athens, Greece
Jawed Akhtar Siddiqui,
University of Nebraska Medical Center, United States

***Correspondence:**
Uma Sankar
usankar@iupui.edu

Specialty section:
This article was submitted to Bone Research, a section of the journal Frontiers in Endocrinology

Received: *17 February 2018*
Accepted: *31 May 2018*
Published: *18 June 2018*

Citation:
Dadwal UC, Chang ES and Sankar U (2018) Androgen Receptor-CaMKK2 Axis in Prostate Cancer and Bone Microenvironment. Front. Endocrinol. 9:335. doi: 10.3389/fendo.2018.00335

INTRODUCTION

Prostate cancer (PCa) is the second leading cause of cancer-related deaths in American men and accounts for 15% of all cancers diagnosed in men worldwide (1, 2). The American Cancer Society estimates that in 2018 alone, 164,690 men will be newly diagnosed with PCa and 29,430 men will die from it in the United States. Routine testing of prostate serum antigen (PSA) levels has resulted in early diagnosis and treatment of PCa. Consequently, men with early-stage PCa have a high, near 100%, 10-year rate of survival. Among patients with non-localized disease, however, about 40%

develop metastases to distant sites such as bone, lymph nodes, lung, and brain and their 5-year survival rate drops dramatically to 30% (3). PCa displays a preferential tropism toward bone which is the primary site of metastasis in 80% of patients with advanced disease (4). Metastatic PCa becomes lodged in the bone marrow (BM)-rich axial skeleton, which provides the perfect "soil" for the disease to develop to an advanced form often termed "castrate-resistant PCa (CRPC)" as it is resistant to hormone-ablation.

Bone is an organ of utmost importance in PCa. Bone metastasis is often a leading cause of patient mortality in PCa (4). Once they "home" and colonize the bone, PCa cells disrupt the homeostatic balance between bone-forming osteoblasts (OBs) and bone-resorbing osteoclasts (OCs). Similar to breast cancer, PCa stimulates osteolysis. However, a unique feature of bone-lodged PCa cells is that they stimulate the OBs to produce weak woven bone instead of the strong lamellar bone that is normally synthesized. Such skeletal-related events (SREs) triggered by PCa in the bone culminate in pathological fractures, spinal cord compression, and sclerosis, detrimentally affecting the overall quality of life and survival rate among patients (5–8).

Prostate cancer cells express the androgen receptor (AR) and are heavily reliant on androgens for growth and survival. Hence, most patients with locally advanced or metastatic PCa receive androgen-deprivation therapy (ADT) as a gold standard treatment (9). Although it significantly improves survival rates, ADT detrimentally affects skeletal health, causing tremendous bone loss and rendering the patients at risk for fragility fractures (10). Therapies that inhibit bone resorption such as bisphosphonates prevent ADT-induced bone loss and may additionally delay bone colonization by the tumor by interfering with its ability to manipulate the bone microenvironment (11). PCa patients initially respond positively to ADT, though most experience a relapse of the cancer to a hormone-refractory form called CRPC, which occur when cancer cells adapt to growth under low androgen conditions by constitutively upregulating AR (12). Consequently, AR and its downstream effectors are attractive therapeutic targets to combat tumor growth in androgen-resistant PCa. Indeed, clinical studies indicate that AR inhibitors such as enzalutamide delay SREs and improve survival rates in patients (13–15). Still, novel therapies that preserve musculoskeletal heath while significantly inhibiting tumor growth are acutely needed in the clinic.

In this review, we will briefly discuss the steps involved in bone metastasis of PCa, the role of AR activation in the development of CRPC and skeletal complications associated with ADT. We will additionally discuss recent findings that identify Ca^{2+}/calmodulin (CaM)-dependent protein kinase kinase 2 (CaMKK2), an AR-regulated gene with additional roles in bone remodeling and inflammation, as a novel therapeutic target to inhibit PCa growth and prevention of ADT-associated bone loss.

BONE METASTASIS OF PCa

Prostate cancer cells show an almost exclusive tropism for bone. Although the exact mechanisms that drive bone metastasis are unknown, it has been proposed that the BM microenvironment may provide the ideal condition for the PCa cells to thrive. The "seed and soil" hypothesis proposed by Steven Paget in 1889, wherein the "seeds" or tumor cells develop a tropism and metastasize to the "soil" or target organ that is well suited or "fertile ground" for its growth (16) still remains a guiding principle in understanding the role BM microenvironment plays in bone metastasis of PCa.

Metastasis of PCa to bone involves several steps including decreased cell adhesion, epithelial to mesenchymal transition (EMT), local migration, invasion, intravasation into the circulation, homing, and colonization of bone (17, 18). Cell–cell adhesion in normal prostate epithelium is maintained by integrins and tight junctions composed of cell adhesion molecules, such as selectins and cadherins. There are two main types of cadherins, E-cadherin and N-cadherin, expressed by epithelial cells and mesenchymal cells, respectively. During early transformation, prostate epithelial cells exhibit alterations in cell adhesion factors, including a downregulation of E-cadherin and an upregulation of N-cadherin, a process termed cadherin switching and a main feature in EMT. Decreased expression of integrins and Wnt-target protein β-catenin also play important roles in EMT (17–19). The next step is migration and it involves an upregulation of focal adhesion. During normal cell migration, focal adhesions formed on the leading edges of the cells are used as anchors by the cells to pull themselves forward over the extracellular matrix (ECM). Disassembly of focal adhesions on the rear edge of the cell enables the cell to move forward (20). This process involves the binding of focal adhesion kinases (FAKs) to integrins and their subsequent activation by the Src family of kinases, initiating signaling events including those involving Rho that regulate focal adhesion turnover and migration. Expression of FAK and Src as well as Rho activities are elevated in bone metastases and CRPC, indicating increased focal adhesion turnover and cell mobility.

Once the transformed prostate epithelial cells gain the ability to migrate, they need to dissociate from the ECM, which is composed of the basement membrane and connective tissue. Prostate epithelial cells that have undergone mesenchymal transition have the ability to secrete proteases such as matrix metalloproteases and serine proteinases, such as urokinase-type plasminogen activator and PSA, which partially degrade the ECM, allowing the cells to disseminate, invade the surrounding tissue and intravasate into blood vessels (17, 20, 21). Homing to the target organ is only possible if the PCa cells survive in the circulation, and they achieve this by attaching to the vascular endothelium. PCa cells have been shown to interact with BM endothelial cells (BMECs) with high affinity through a mechanism involving E-selectin receptor on PCa cells and E-selectin on BMECs and integrins such as αVβ3, αVβ1, and α3β1 (18). Additionally, CD44 on PCa cells binds to vascular cell adhesion molecule 1 on BMECs in a process that is enhanced by IL-17 and IGF1 in circulation. The subsequent homing of PCa cells to bone is facilitated by multiple chemokine-mediated mechanisms. For instance, BM stromal cells and OBs in the bone secrete C–X–C motif chemokine ligand 12 (CXCL12) or stromal derived factor-1 (SDF1) whereas PCa cells express its receptor CXCR4. CXCL12/SDF–CXCR4 interaction allows PCa cells to home to the bone, adapting a similar mechanism as the one utilized by hematopoietic stem cells (22). Additionally, CXCL12/SDF1 from OBs activates the expression of the adhesion molecule αVβ3 integrin on PCa cells that further contribute to their homing to the BM. Further, the expression of yet another

chemokine ligand CXCL16 allows PCa cells to recruit and convert CXCR6-expressing mesenchymal stem cells into cancer-associated fibroblasts that also secrete high levels of CXCL12/SDF1. Finally, recent reports provide evidence for microRNA (miR)-containing exosomes from PCa cells arriving early in the BM to enable the modification of the bone microenvironment to favor cancer cell homing to the bone (23–25).

Colonization of the bone by PCa is aided by their ability to (a) attach to the bone matrix and (b) manipulate the BM microenvironment into favoring their growth and survival. PCa express two key integrins αVβ3 and α2β1, which allow the cells to attach to the bone matrix and migrate along the surface to identify suitable "niches" for their outgrowth. PCa cells preferentially home to OB-rich niches within the bone, allowing physical contact between these two cell types, facilitated in part by adhesion molecules such as cadherin-11 expressed on both OBs and malignant PCa cells (26, 27). Interestingly, physical contact between PCa and OBs appear to disrupt the normal order of matters within the bone. Kimura et al. noted that in the presence of PCa cells, the bone-resident OBs which usually line neatly along the collagen matrix become disorganized and that this anisotropy requires cell–cell contact (28). Unlike other solid tumor malignancies which are mostly osteolytic, bone-metastatic PCa is primarily an osteoblastic disease driven in part by the ability of PCa cells to perform "osteomimicry" wherein they adopt the genetic and phenotypic characteristics of OBs (29). OB growth and differentiation are governed by complex signaling pathways, such as Wnts, bone morphogenic proteins (BMPs), insulin growth factor (IGF), and transforming growth factor β (TGF-β) (30, 31). In contrast, OC differentiation is regulated by receptor activator of NF-κB ligand (RANKL), osteoprotegerin, parathyroid hormone, and TGF-β. Differentiated OBs secrete these factors, but many are also released from the bone matrix by OCs themselves during bone resorption. Interestingly, bone-lodged PCa cells produce many of the same factors that stimulate the proliferation and differentiation of OBs and OCs (17, 30). In addition to producing factors that favor bone cell differentiation, PCa cells also induce other cell types to transdifferentiate into OBs (32). Recently, Lin et al. reported an endothelial cell-to-OB conversion as one of the mechanisms underlying osteoblastic bone disease in PCa (33). These authors showed that PCa induces the overexpression of BMP4 in BMECs driving their transdifferentiation to OBs (33). Recent studies from multiple myeloma highlight the importance of osteocytes, the most abundant bone cells, in tumor-bone interactions (34). Although studies have indicated a role for osteocytes in PCa (35), more research is needed to fully comprehend the contribution of these cells to bone metastasis by PCa. Taken together, these studies suggest that cancer cells disrupt the homeostatic mechanisms within the BM and hijack the normal paracrine and autocrine mechanisms regulating normal bone remodeling to create a "vicious cycle" that ultimately favors PCa colonization and growth within the bone (**Table 1**).

TABLE 1 | Growth factors involved in aiding skeletal metastasis of prostate cancer.

Factor	Role	Function	Source cells
CXCL12/SDF1	Homing	Binding partner to CXCR4	Osteoblasts (OBs) (36)
CXCR4	Homing	Binding partner to CXCL12	Tumor Cells (36)
E-selectin ligands	Colonizing	Critical for initial tethering and rolling on E-selectin	Tumor Cells (37)
CXCR6	Progression	Recruits and converts mesenchymal stem cells (MSCs) into Cancer-associated fibroblasts	MSCs (38)
BMP4	Progression	Drives endothelial cell conversion into OBs	Tumor cells (33)
IGF1	Progression	Stimulates proliferation of human prostate epithelial cells	Tumor cells (39)
Endothelin 1	Progression	Suppresses Dickkoph 1, increases OB mitogensis and osteoclast apoptosis	Tumor cells (40)
B7-H ligand	Progression	Evading immune cell surveillance	Tumor cells (41)
Androgens	Proliferation	Stimulate androgen receptor signaling mediated bone formation in OBs	Tumor cells (42)

ANDROGENS, AR, BONE, AND ADT

Since the original description by Charles Huggins in 1942 of the heavy dependence of PCa on androgens and the benefits of orchiectomy in PCa patients, androgens, and AR have remained the main therapeutic targets in PCa treatment (43–46). In men, Leydig cells of the testis produce about 90% of the circulating androgens or testosterone and the adrenal cortex produces the remaining 10% (47). Testosterone diffuses into the prostate epithelial cells where it is converted into dihydrotestosterone (DHT) by the enzyme 5α-reductase (47, 48). DHT binds to AR, a member of the nuclear hormone receptor family of transcription factors. Upon ligand binding, AR translocates to the nucleus, undergoes homodimerization and binds to androgen response elements (ARE) within the promoters of AR-target genes such as PSA. AR then recruits cofactors and initiates the transcription of target genes that regulate proliferation, metabolism, and survival of PCa cells (45, 49, 50).

The goal of ADT is to starve the tumor cells of androgens by drastically diminishing their circulating amount (<5% of normal range). This is achieved by blocking testosterone production surgically *via* castration or chemically by treating patients with luteinizing hormone releasing hormone agonists or first generation antiandrogen drugs, such as flutamide, nilutamide, and bicalutamide, that competitively block DHT binding to AR (51). Testosterone is converted into estradiol, the primary male estrogen *via* aromatization and it binds to the estrogen receptor α (ERα) present on both OBs and OCs. OBs express both AR and ERα, whereas OCs express only ERα. These receptors promote OB survival, numbers, and activity, while ERα inhibits OC differentiation. Moreover, the combined action of these two nuclear receptors stimulate periosteal apposition and lengthening of the epiphyseal growth plate in men while maintaining their cortical and trabecular bone. The continued periosteal growth during adult life in men partially offsets age-related increase in endosteal bone loss (7, 10). All these processes are

affected by ADT as it suppresses not only androgens but also estradiol, resulting in the abrogation of the stimulatory effect of androgens on OBs and the inhibitory effect of estradiol on OCs. This triggers increased bone turnover in patients on ADT, resulting in a significantly high rate of bone loss at 4.6% per year, which exceeds the annual bone loss in aging men and postmenopausal women (10). The maximum bone loss occurs during the first year of therapy, ranging from 1.5 to 4%, depending on the skeletal location examined (10). Thus, ADT renders these men, who are often older and possess lower bone mass to begin with, four times more likely to develop osteoporosis. This enhances their risk of fragility fractures and in turn, their mortality risk (7).

Nitrogen-containing bisphosphonates, such as alendronate, risedronate, and zoledronic acid, as well as denosumab, a monoclonal antibody to RANKL are all FDA-approved to treat osteoporosis in PCa patients on ADT. Selective ER modulators such as raloxifene and Toremifene have also been shown to preserve bone in clinical trials with PCa patients undergoing ADT (7, 15, 52–56). Moreover, second-generation antiandrogens, such as abiraterone and enzalutamide, as well as radiotherapies such as Radium-223 have shown to suppress tumor growth and delay SREs (13, 14, 57–60). Teriparatide, though FDA-approved, is not recommended for PCa patients at risk for bone metastasis. A list of current therapies and novel compounds in clinical trials in the treatment of bone-metastatic PCa are detailed in **Tables 2** and **3**.

AR ACTIVATION IN CRPC

Androgen-deprivation therapy results in diminished tumor burden in about 90% of patients with advanced PCa. However, over time, the cancer cells adapt undergo selection to proliferate and survive under low levels of circulating androgens by upregulating AR and becoming unresponsive to ADT. The disease at this stage is termed CRPC (17, 71). AR is the main driver of CPRC development, while a minority of metastatic PCa are associated with the loss of *p53*, *PTEN*, or *Rb* (13, 72). The main mechanisms for AR reactivation in CRPC include amplification leading to overexpression, activating mutations, structural gene alterations, expression of constitutively active variants, mutations in the AR that confer broader ligand specificity to the receptor, upregulation of co-regulators, increased expression of steroidogenic enzymes, as well as upregulation of cross-talk signal transduction pathways such as interleukin 6, STAT3, Src, and IGF that can activate AR in a ligand-independent manner (71). These mechanisms have been extensively reviewed elsewhere (21, 72–74). Gain-of-function AR splicing variants (AR-Vs) often lack portions of the ligand-binding domain (LBD) but possess constitutive transcriptional activity even in the absence of androgens. The most well-characterized among these is AR-V7 whose expression has been shown to increase in response to ADT and has been shown to confer resistance to drugs, such as abiraterone and enzalutamide that either block androgen synthesis or antagonize AR (75). AR-V7 was identified as the most frequently occurring variant in patients

TABLE 2 | Androgen receptor (AR) targeted therapies—FDA-approved drugs in clinic.

Drug	Target	Mechanism of action	Clinical use	Reference
Abiraterone acetate	Cytochrome P450 c17 (CYP17)	Inhibits androgen biosynthesis	Castration-resistant and high-risk castration sensitive prostate cancer (PCa)	(57)
Enzalutamide (Xtandi)	AR	Inhibits nuclear translocation of the AR	Metastasized castrate-resistant prostate cancer	(14)
Leuprolide acetate	Luteinizing hormone releasing hormone	Inhibits secretion of luteinizing hormone, androgen, and estradiol	Approved for palliative treatment of advanced PCa	(61)
R-Bicalutamide (CASODEX)	Cytosolic AR	Inhibits androgen activity by binding cytosolic ARs and stimulating AR nuclear translocation	Approved for metastasized PCa	(62)

TABLE 3 | Novel therapies against castrate-resistant prostate cancer (CRPC) currently in trials.

Drug	Target	Mechanism of action	Trial Status	Reference
Novel androgen receptor (AR) therapeutics currently in clinical trial				
ARN-509 (apalutamide)	Androgen receptor (AR)	Competitively inhibits transcription	Phase II	(57, 63, 64)
EPI-506	AR	Inhibits transcription	Phase II	(53)
AZD3514	AR	Inhibition of AR nuclear translocation and AR-regulating gene transcription	Phase I	(65)
Ketoconazole	Cytochrome P450 c17 (CYP17)	Inhibits adrenal testosterone synthesis	Phase II	(66)
MDV3100	AR	Inhibits AR binding and nuclear translocation of the AR	Phase I	(35)
Other novel drug targets				
Radium-223 (Xofigo)	Bone mineral hydroxyapatite	Induces double-strand DNA breaks	FDA approved for CRPC, bone metastasis	(67)
LGK974	Porcupine [PORCN] (WNT-specific acyltransferase)	Inhibits Wnt signaling	Phase I	(68)
Cytarabine (Cytosine Arabinoside)	DNA polymerase	Inhibits DNA synthesis	Phase II	(69)
Ipatasertib	AKT (protein Kinase B)	Inhibits three isoforms of AKT	Phase II	(55, 70)

with CRPC and its expression correlates with increased disease recurrence (76–78). AR-V7 expression is associated with the upregulation of some AR-target genes relevant for proliferation and survival, such as *UBE2C*, *CCNA2*, *C-MYC*, *AKT1*, *EDN2*, and *ETS2* (71, 78).

Mechanisms that enable CRPCs to activate AR and continually acquire resistance to therapies underscore the importance of gaining a comprehensive understanding of the downstream effectors of AR signaling that play crucial roles in cancer progression, as they could serve as druggable targets in the treatment of CRPC. Several studies have attempted to identify AR-regulated genes by focusing on genome-wide AR-binding sites on cell lines and clinical samples, or by examining temporal regulation of androgen stimulation in one or more PCa cell lines such as LNCaP (harbors an LBD mutation of AR), VCaP (contains AR gene amplification) or C4-2B (a CRPC cell line) (66, 79–85). These studies have identified several AR-target genes with functions in gene transcription (*NKX3.1*, *FOX* family), growth stimulation (IGF1R), cell cycle regulation (*CDK6*, *UBE2C*), signaling (*MEK5*, *FKBP5*), autophagy (*ATG4B*, *ULK1*, *TFEB*), non-coding RNA (*miR-21*, *miR141*), glycolysis (*GLUT1*), and central metabolism [*MTOR*, Ca^{2+}/CaM-dependent protein kinase kinase 2 (*CaMKK2*)]. Among these, *CaMKK2* has emerged as an attractive therapeutic candidate in PCa as it is a direct target of AR, containing AREs on its promoter and is consistently overexpressed in clinical CRPC samples as well as AR-positive PCa cell lines (86, 87).

CaMKK2: A MOLECULAR HUB DIRECTED BY AR IN PCa CELLS

Intracellular Ca^{2+} is a universal second messenger that regulates diverse cellular processes. Transient variations in intracellular Ca^{2+} are immediately sensed by the ubiquitous high-affinity intracellular Ca^{2+} receptor, CaM. This initiates a cascade of Ca^{2+}/CaM-mediated signaling events that culminate in changes to key cellular events such as proliferation, differentiation, survival, and metabolism (88). In particular, Ca^{2+}/CaM complexes bind to and activate CaM kinases (CaMKs), which are a family of multifunctional Ser/Thr protein kinases that includes CaMKK1, CaMKK2, CaMKI, CaMKII, and CaMKIV. The upstream kinases, CaMKKs 1 and 2, are activated through Ca^{2+}/CaM binding and intramolecular phosphorylation. Binding of Ca^{2+}/CaM allows the activation loop in CaMKs to unravel and expose a critical threonine residue that becomes phosphorylated by the two upstream CaMKKs, resulting in their full activation, triggering the formation of a CaMK signaling cascade that is regulated by Ca^{2+}/CaM at multiple levels (89–91). Interestingly, unlike CaMKK1, which is solely dependent on Ca^{2+}/CaM for activity, CaMKK2 possesses considerable autonomous activity in the absence of Ca^{2+}/CaM. This autonomous activity is regulated by phosphorylation by Ca^{2+}/CaM-independent kinases such as glycogen synthase kinase 3β (GSK3β) and cyclin-dependent kinase 5 (CDK5) (92, 93). As it is not dependent on rapid fluxes in intracellular Ca^{2+} for basal activity, CaMKK2 is capable of responding to other stimuli of longer duration and phosphorylating novel substrates outside of the CaMK cascade. Indeed, CaMKK2 (not CaMKK1) directly phosphorylates and activates adenosine monophosphate activated protein kinase (AMPK), a heterotrimeric kinase that co-ordinates cellular energy balance, autophagy, cell proliferation, and cytoskeletal organization (94, 95). The CaMKK2–AMPK pathway plays key roles in the regulation of hypothalamic feeding behavior, hepatic gluconeogenesis, adipocyte differentiation, and macroautophagy (94, 96–98). Recent studies indicate roles for CaMKK2 in hepatic cancer, macrophage-mediated inflammation, and bone remodeling through non-AMPK-mediated mechanisms (99–103).

CaMKK2 is increasingly being considered a hub of signaling mechanisms that regulate PCa cell metabolism, proliferation and migration downstream of AR (104). Frigo et al. identified the presence of an AR-binding region located 2.3-kb upstream of the *CaMKK2* transcriptional start site and reported the recruitment of AR to this region in an androgen-dependent manner (87). These authors also found that the knockdown of *CaMKK2* or its pharmacological inhibition using a selective inhibitor STO-609 or inhibition of the CaMKK2-target protein AMPK abrogates PCa cell migration and invasion (68, 87, 105). Overexpression of CaMKK2 alone was sufficient to induce AMPK phosphorylation and facilitate PCa cell migration, implying that androgens promote PCa cell migration through an AR-CaMKK2-AMPK signaling axis (87). Massie et al. integrated genome-wide AR-binding transcript profiling with an analysis of androgen-stimulated recruitment of the transcriptional machinery to a core set of AR-binding sites and identified *CaMKK2* to be consistently enriched in PCa clinical cohorts, in a pattern similar to that of the established PCa marker AMACR (86). Similar to previous reports (87), these authors also observed AR recruitment to *CaMKK2* promoter in both androgen-dependent and CRPC cell lines and an early upregulation of the CaMKK2 transcripts and protein within 4 and 12 h of androgen stimulation, respectively, indicating direct AR regulation (86). Subsequent functional studies identified CaMKK2 as a key effector of AR in stimulating glycolysis through its activation of AMPK and phosphofructokinase (PFK), which in turn drives anabolism and PCa cell proliferation (86). Of note, the AR-CaMKK2–AMPK–PFK axis does not affect cellular biosynthesis through mTOR in PCa, indicating its primary role in regulating glucose uptake and lactate production. *In vivo* inhibition of CaMKK2 using STO-609 resulted in a significant reduction in the growth of C4-2B xenografts in nude mice, and this treatment was additive with AR inhibition achieved *via* castration (86). It should be noted that CaMKK2 inhibition by itself did not affect the size of the normal prostate or its epithelium in nude mice, and the *CaMKK2*$^{-/-}$ mice do not possess any prostate anomalies or fertility deficits (86, 87). Thus, the inhibition of CaMKK2, rather than AR itself, may offer greater selective advantage over PCa at all stages.

Karacosta et al. examined PCa in clinical samples and found strong CaMKK2 immunoreactivity in the epithelium of malignant glands, compared to extremely low expression in the adjacent normal epithelium (106). Moreover, CaMKK2 staining intensity increased with the Gleason score of the tumors, and the staining pattern shifted from predominantly cytoplasmic to perinuclear and nuclear (106). CaMKK2 intensity increased with tumor progression in a transgenic adenocarcinoma of the mouse

prostate (TRAMP) mouse model of PCa, and its expression was higher in castration-resistant tumor xenografts than androgen-responsive ones. These authors also observed upregulation of CaMKK2 as well as its nuclear translocation in LNCaP following DHT treatment and a reversal with androgen withdrawal. Further, silencing of *CaMKK2* using small interfering RNA elicited G1 arrest of LNCaP cells, reducing their proliferation, along with lowering the levels of PSA as well as AR-regulated cell cycle proteins such as cyclin D1 and hyperphosphorylated Rb (106). Karacosta et al. proposed a novel positive feedback loop in the PCa in which CaMKK2 is induced by AR, and it in turn stabilizes AR to promote its transcriptional activity and cell cycle progression (106). In a recent follow-up study, these authors confirmed the higher nuclear expression of CaMKK2 in CRPC C4-2 cells, and showed that this occurs due to the association of CaMKK2 with nuclear pore complexes through its direct interaction with nucleoporin 62 (NUP62) (107). These authors showed that silencing NUP62 reduces the growth and viability of C4-2 cells, and provided evidence for the recruitment of NUP62, CaMKK2, and AR complexes to the AR-binding regions in the promoters of target genes such as *PSA*, suggesting a novel CaMKK2-NUP62 mechanism of AR transcriptional regulation in advanced PCa (107).

Similar to the aforementioned studies, Shima et al. performed genome-wide analysis of a small set of clinical samples and found a sixfold higher *CaMKK2* expression in PCa compared to normal prostate (108). However, in contrast to previous studies (82, 87, 106, 107), these authors provide evidence for an inhibitory role for CaMKK2 to AR signaling and hypothesize that while CaMKK2 supports growth of tumors in early PCa, it inhibits excessive proliferation in CRPC (108). Whereas additional studies are warranted to validate these intriguing findings and hypotheses, the consensus emerging from all of these studies is that CaMKK2 is a key effector of AR signaling in PCa cells, regulating cell cycle by stabilizing AR, cell migration through AMPK signaling, and glycolysis by activating the AMPK–PFK pathway. AR is essential for PCa cell viability, proliferation, invasion, and bone metastasis, and the tumor cells are under constant selective pressure to maintain AR signaling, especially under the conditions of low testosterone such as ADT (86). Therefore, targeting downstream effectors such as CaMKK2 would be an effective approach to abrogate AR signaling in metastatic PCa.

CaMKK2 IN BONE MICROENVIRONMENT

CaMKK2 and Bone Cells

Prostate cancer recruits OBs and OCs within the bone microenvironment and transforms them into entities that support tumor growth (30). Studies discussed above show that CaMKK2 is expressed in PCa cells where it acts as a molecular hub downstream of AR in regulating tumor cell growth. CaMKK2 is expressed by OBs and OCs and plays important cell-intrinsic roles in these cells (99). During homeostatic conditions, CaMKK2 stimulates OC differentiation by activating phosphorylated form of cyclic adenosine monophosphate (cAMP) response element binding protein (pCREB) and its transcriptional target, nuclear factor of activated T cells c1 in a CaMKIV-dependent manner. Hence, inhibition or deletion of CaMKK2 inhibits OCs. On the other hand, CaMKK2 inhibits OB differentiation by inhibiting cAMP-protein kinase A (PKA) signaling under normal conditions. Therefore, the inhibition or absence of CaMKK2 relieves this inhibition and results in the stimulation of OB differentiation (99). Mice null for *CaMKK2* possess higher bone mass along with significantly more OBs and fewer multinuclear OCs. Inhibition of CaMKK2 promotes bone fracture healing, and confers protection from ovariectomy and age-related osteoporosis (99, 100, 102). Taken together, these studies reveal profound roles for CaMKK2 in the two main bone cell types that interact with PCa in the bone microenvironment.

CaMKK2 and Macrophages

Immune cells, such as macrophages and lymphocytes, are also part of the bone–tumor microenvironment and play important roles in tumor growth and bone metastasis (109). For example, chronic inflammation sustained by macrophage activation plays a pivotal role in the regulation of tumor microenvironment in many solid tumors (104). Chronic inflammatory conditions existing within the tumor recruit myeloid cells and induce their differentiation into tumor-associated macrophages, the infiltration of which negatively correlates with prognosis in advanced PCa. Recently, Roca et al. reported that macrophage-driven efferocytosis accelerates CXCL5-mediated inflammation and PCa growth within the bone (110). Among immune cells, CaMKK2 is selectively expressed in macrophages and its ablation impairs their ability to spread, phagocytose, and produce inflammatory cytokines and chemokines in response to lipopolysaccharides (101). CaMKK2 regulates metabolic responses and cytokine release in response toll-like receptor/integrin stimulation in macrophages. Indeed, *Camkk2*$^{-/-}$ mice are resistant to irritants that lead to systemic inflammation (101). Thus, CaMKK2 plays roles in multiple cell types, including OBs, OCs, and macrophages, that form the PCa microenvironment in the bone. AR is expressed in OBs and macrophages, and it plays an indirect role in OCs through ERα. However, whether CaMKK2 plays a role downstream of AR in OBs and macrophages is unknown. Nevertheless, we hypothesize that AR signaling in PCa cells uses CaMKK2 as a downstream hub regulating several molecular mechanisms in OBs, OCs, and macrophages to manipulate the BM niche to the benefit of the cancer cells (**Figure 1**).

PERSPECTIVES AND CONCLUDING REMARKS

Complex mechanisms employed by PCa cells allow it to home and thrive in bone, their preferred site of metastasis. Once lodged in the bone, the cancer cells recruit OBs, OCs, and macrophages within the skeletal niche to become entities that secrete growth factors and chemokines that allow the PCa cells to proliferate and survive even under low circulating testosterone conditions such as following ADT. AR signaling remains critical for PCa cell survival even under ADT and this creates selective pressure for

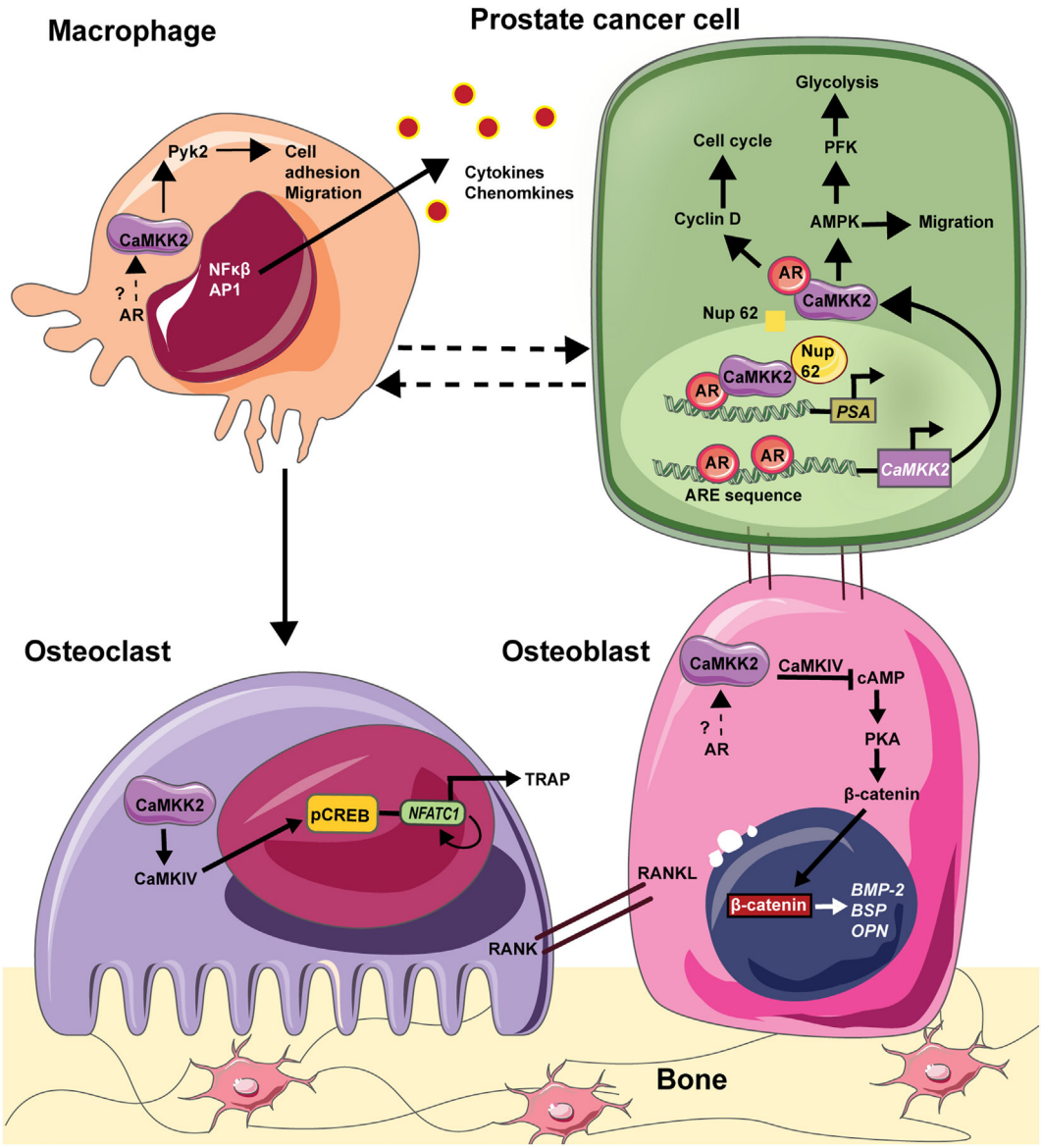

FIGURE 1 | CAMKK2 as a molecular hub downstream in the bone–prostate cancer (PCa) microenvironment. In PCa cells, the androgen receptor (AR) binds to androgen response element (ARE) on *CaMKK2* promoter which is situated upstream of the transcriptional start site. Thus, CaMKK2 is a direct transcriptional target of AR and its expression is highly elevated in metastatic PCa. Once transcribed and translated, CaMKK2 binds to AR initiating a positive feedback loop to stimulate AR transcriptional activity in the activation of AR-dependent genes that regulate cell cycle progression such as cyclin D. Additionally, CaMKK2 through its activation of AMPK regulates PCa cell migration. CaMKK2-AMPK signaling pathway also regulates cellular glycolysis *via* the activation of phosphofructokinase (PFK). This drives PCa cell anabolism and in turn promotes cell proliferation and tumor growth. Furthermore, in CRPCs, CaMKK2 binds to nucleoporin 62 (NUP62) to enter the nucleus, where it along with AR and NUP62 are recruited to the ARE in the promoters of downstream targets such as prostate serum antigen (PSA). PCa cells that metastasize to the bone physically interacts with OBs to alter their organization and function. Although both AR and CaMKK2 are expressed in OBs, whether CaMKK2 operates downstream of AR in these cells is not known. In OBs, CaMKK2 signaling inhibits cyclic adenosine monophosphate (cAMP) production and protein kinase A (PKA) activation. PKA is an important regulator of OB differentiation. Thus, the inhibition of CaMKK2 would relieve this inhibition of PKA signaling and OB differentiation. In osteoclasts (OCs), CaMKK2 signaling through CaMKIV-pCREB activates nuclear factor of activated T cells c1 (NFATc1), which is the master regulator of OC differentiation. In macrophages, CaMKK2 regulates cytoskeletal rearrangement *via* its regulation of Pyk2. Moreover, CaMKK2-CaMK1 signaling regulates cytokine/chemokine production by macrophages. Thus, CaMKK2 is a key component of AR signaling in PCa cells and additionally regulates multiple cell types that constitute the tumor microenvironment within the bone.

the generation of *AR* gene mutations that facilitate the constitutive activation of the AR signaling cascade. Thus, AR and its downstream effectors are attractive therapeutic targets against bone-metastatic PCa.

The CaMKK2-AMPK signaling pathway operates downstream of AR to mediate PCa cell cycle, metabolism, migration, and invasion. CaMKK2 inhibition interferes with the growth and survival of bone-lodged PCa, and will presumably interfere with its ability

to secrete factors that modify OBs into cancer-promoting entities. Similar to PCa, AR signaling plays an active pro-survival role in OBs. However, whether it operates upstream of CaMKK2 in OBs is unclear. Various signaling pathways, including cAMP-PKA, CDK5, and GSK3, have been implicated as upstream regulators of CaMKK2 in other cell types. In addition to AR-binding elements, *CaMKK2* promoter also contains consensus-binding sites for several transcription factors including runt-related transcription factor 2 (RUNX2), the master regulator of OB differentiation. In macrophages, CaMKK2 is activated by toll-like receptors, G_q-coupled receptors, and voltage-gated Ca^{2+} channels on the plasma membrane (101). Although monocytes express AR, its role in the regulation of CaMKK2 in these cells is unclear. Nevertheless, we can conclude from the studies discussed above that the AR-CaMKK2 signaling axis acts as a molecular hub promoting PCa survival and in turn its ability to manipulate the bone microenvironment. Cell-intrinsic roles of CaMKK2 in OBs, OCs, and macrophages may aid in this process, ultimately enhancing the malignancy, SREs, and bone fragility.

In addition to the studies reviewed herein, CaMKK2 inhibition or genetic ablation has been shown to protect against diet-induced glucose intolerance, insulin resistance, diabetes, hepatocellular carcinoma, and non-alcoholic high fat liver disease [reviewed in Ref. (111)]. In case of PCa, CaMKK2 emerges as an attractive and druggable target downstream of AR that when inhibited, abrogates tumor growth, inhibits macrophage-mediated inflammation, and improves bone health. Future studies will provide a comprehensive understanding of the precise molecular mechanisms by which CaMKK2 regulates PCa cells as well as how AR-CaMKK2 signaling in these cells affects CaMKK2 function in bone cells and macrophages that constitute the bone microenvironment. Nonetheless, highly selective small molecule inhibitors of CaMKK2 should be developed as potent "dual-hit" therapeutic interventions to abrogate bone-metastatic PCa growth while preventing ADT-associated bone loss. Together with improving bone mass and strength in PCa patients, who are often elderly, CaMKK2 inhibition would offer the best odds for long-term disease-free survival.

AUTHOR CONTRIBUTIONS

UD and US contributed to conception, design, and writing of the manuscript. EC contributed to the literature search and drafted tables for manuscript. US critically reviewed the drafts of the manuscript and wrote the final version. UD and US read and approved the final manuscript.

ACKNOWLEDGMENTS

The authors would like to thank Servier Medical art for the use of their image bank. This work was supported by grants from the American Cancer Society (RSG-13-301-01) and National Institutes of Arthritis and Musculoskeletal and Skin Diseases (NIAMS) R01 AR068332 to US.

REFERENCES

1. Ferlay J, Shin HR, Bray F, Forman D, Mathers C, Parkin DM. Estimates of worldwide burden of cancer in 2008: GLOBOCAN 2008. *Int J Cancer* (2010) 127(12):2893–917. doi:10.1002/ijc.25516
2. Pernar CH, Ebot EM, Wilson KM, Mucci LA. The epidemiology of prostate cancer. *Cold Spring Harb Perspect Med* (2018). doi:10.1101/cshperspect.a030361
3. Noone AM, Howlader N, Krapcho M, Miller D, Brest A, Yu M, et al., editors. *SEER Cancer Statistics Review, 1975–2015*. Bethesda, MD: National Cancer Institute (2017). Available from: https://seer.cancer.gov/csr/1975_2015/ (Accessed: April, 2018).
4. Bubendorf L, Schöpfer A, Wagner U, Sauter G, Moch H, Willi N, et al. Metastatic patterns of prostate cancer: an autopsy study of 1,589 patients. *Hum Pathol* (2000) 31(5):578–83. doi:10.1053/hp.2000.6698
5. Saad F, Gleason DM, Murray R, Tchekmedyian S, Venner P, Lacombe L, et al. Long-term efficacy of zoledronic acid for the prevention of skeletal complications in patients with metastatic hormone-refractory prostate cancer. *J Natl Cancer Inst* (2004) 96(11):879–82. doi:10.1093/jnci/djh235
6. Saad F, Ivanescu C, Phung D, Loriot Y, Abhyankar S, Beer TM, et al. Skeletal-related events significantly impact health-related quality of life in metastatic castration-resistant prostate cancer: data from PREVAIL and AFFIRM trials. *Prostate Cancer Prostatic Dis* (2017) 20(1):110–6. doi:10.1038/pcan.2016.62
7. Bienz M, Saad F. Androgen-deprivation therapy and bone loss in prostate cancer patients: a clinical review. *Bonekey Rep* (2015) 4:716. doi:10.1038/bonekey.2015.85
8. Oefelein MG, Ricchiuti V, Conrad W, Resnick MI. Skeletal fractures negatively correlate with overall survival in men with prostate cancer. *J Urol* (2002) 168(3):1005–7. doi:10.1097/00005392-200209000-00024
9. Cooperberg MR, Grossfeld GD, Lubeck DP, Carroll PR. National practice patterns and time trends in androgen ablation for localized prostate cancer. *J Natl Cancer Inst* (2003) 95(13):981–9. doi:10.1093/jnci/95.13.981
10. Cianferotti L, Bertoldo F, Carini M, Kanis JA, Lapini A, Longo N, et al. The prevention of fragility fractures in patients with non-metastatic prostate cancer: a position statement by the international osteoporosis foundation. *Oncotarget* (2017) 8(43):75646–63. doi:10.18632/oncotarget.17980
11. Nagao K, Matsuyama H, Nozawa M, Hara I, Nishioka T, Komura T, et al. Zoledronic acid combined with androgen-deprivation therapy may prolong time to castration-resistant prostate cancer in hormone-naïve metastatic prostate cancer patients – a propensity scoring approach. *Asian J Urol* (2016) 3(1):33–8. doi:10.1016/j.ajur.2015.10.003
12. Holzbeierlein J, Lal P, LaTulippe E, Smith A, Satagopan J, Zhang L, et al. Gene expression analysis of human prostate carcinoma during hormonal therapy identifies androgen-responsive genes and mechanisms of therapy resistance. *Am J Pathol* (2004) 164(1):217–27. doi:10.1016/S0002-9440(10)63112-4
13. Logothetis C, Morris MJ, Den R, Coleman RE. Current perspectives on bone metastases in castrate-resistant prostate cancer. *Cancer Metastasis Rev* (2018) 37(1):189–96. doi:10.1007/s10555-017-9719-4
14. Scher HI, Fizazi K, Saad F, Taplin ME, Sternberg CN, Miller K, et al. Increased survival with enzalutamide in prostate cancer after chemotherapy. *N Engl J Med* (2012) 367(13):1187–97. doi:10.1056/NEJMoa1207506
15. Tombal B, Borre M, Rathenborg P, Werbrouck P, Van Poppel H, Heidenreich A, et al. Long-term antitumor activity and safety of enzalutamide monotherapy in hormone naive prostate cancer: 3-year open label followup results. *J Urol* (2018) 199(2):459–64. doi:10.1016/j.juro.2017.08.103
16. Paget S. The distribution of secondary growths in cancer of the breast. *Lancet* (1889) 1:571–3. doi:10.1016/S0140-6736(00)49915-0
17. Jin JK, Dayyani F, Gallick GE. Steps in prostate cancer progression that lead to bone metastasis. *Int J Cancer* (2011) 128(11):2545–61. doi:10.1002/ijc.26024
18. Park SH, Keller ET, Shiozawa Y. Bone marrow microenvironment as a regulator and therapeutic target for prostate cancer bone metastasis. *Calcif Tissue Int* (2018) 102(2):152–62. doi:10.1007/s00223-017-0350-8
19. Yokoyama NN, Shao S, Hoang BH, Mercola D, Zi X. Wnt signaling in castration-resistant prostate cancer: implications for therapy. *Am J Clin Exp Urol* (2014) 2(1):27–44.

20. Sulzmaier FJ, Jean C, Schlaepfer DD. FAK in cancer: mechanistic findings and clinical applications. *Nat Rev Cancer* (2014) 14:598. doi:10.1038/nrc3792
21. Karantanos T, Corn PG, Thompson TC. Prostate cancer progression after androgen deprivation therapy: mechanisms of castrate resistance and novel therapeutic approaches. *Oncogene* (2013) 32(49):5501–11. doi:10.1038/onc.2013.206
22. Taichman RS, Cooper C, Keller ET, Pienta KJ, Taichman NS, McCauley LK. Use of the stromal cell-derived factor-1/CXCR4 pathway in prostate cancer metastasis to bone. *Cancer Res* (2002) 62(6):1832–7.
23. Hannafon BN, Ding WQ. Intercellular communication by exosome-derived microRNAs in cancer. *Int J Mol Sci* (2013) 14(7):14240–69. doi:10.3390/ijms140714240
24. Ye Y, Li SL, Ma YY, Diao YJ, Yang L, Su MQ, et al. Exosomal miR-141-3p regulates osteoblast activity to promote the osteoblastic metastasis of prostate cancer. *Oncotarget* (2017) 8(55):94834–49. doi:10.18632/oncotarget.22014
25. Kumar S, Nag A, Mandal CC. A comprehensive review on miR-200c, a promising cancer biomarker with therapeutic potential. *Curr Drug Targets* (2015) 16(12):1381–403. doi:10.2174/1389450116666150325231419
26. Chu K, Cheng CJ, Ye X, Lee YC, Zurita AJ, Chen DT, et al. Cadherin-11 promotes the metastasis of prostate cancer cells to bone. *Mol Cancer Res* (2008) 6(8):1259–67. doi:10.1158/1541-7786.MCR-08-0077
27. Lee YC, Bilen MA, Yu G, Lin SC, Huang CF, Ortiz A, et al. Inhibition of cell adhesion by a cadherin-11 antibody thwarts bone metastasis. *Mol Cancer Res* (2013) 11(11):1401–11. doi:10.1158/1541-7786.MCR-13-0108
28. Kimura Y, Matsugaki A, Sekita A, Nakano T. Alteration of osteoblast arrangement via direct attack by cancer cells: new insights into bone metastasis. *Sci Rep* (2017) 7:44824. doi:10.1038/srep44824
29. Rucci N, Teti A. Osteomimicry: how the seed grows in the soil. *Calcif Tissue Int* (2018) 102(2):131–40. doi:10.1007/s00223-017-0365-1
30. Croucher PI, McDonald MM, Martin TJ. Bone metastasis: the importance of the neighbourhood. *Nat Rev Cancer* (2016) 16:373. doi:10.1038/nrc.2016.44
31. Lee Y, Schwarz E, Davies M, Jo M, Gates J, Wu J, et al. Differences in the cytokine profiles associated with prostate cancer cell induced osteoblastic and osteolytic lesions in bone. *J Orthop Res* (2003) 21(1):62–72. doi:10.1016/S0736-0266(02)00095-5
32. Peng J, Kang Y. The bony side of endothelial cells in prostate cancer. *Dev Cell* (2017) 41(5):451–2. doi:10.1016/j.devcel.2017.05.015
33. Lin SC, Lee YC, Yu G, Cheng CJ, Zhou X, Chu K, et al. Endothelial-to-osteoblast conversion generates osteoblastic metastasis of prostate cancer. *Dev Cell* (2017) 41(5):467–80.e3. doi:10.1016/j.devcel.2017.05.005
34. Delgado-Calle J, Anderson J, Cregor MD, Hiasa M, Chirgwin JM, Carlesso N, et al. Bidirectional notch signaling and osteocyte-derived factors in the bone marrow microenvironment promote tumor cell proliferation and bone destruction in multiple myeloma. *Cancer Res* (2016) 76(5):1089–100. doi:10.1158/0008-5472.CAN-15-1703
35. Sottnik JL, Dai J, Zhang H, Campbell B, Keller ET. Tumor-induced pressure in the bone microenvironment causes osteocytes to promote the growth of prostate cancer bone metastases. *Cancer Res* (2015) 75(11):2151–8. doi:10.1158/0008-5472.CAN-14-2493
36. Sun YX, Schneider A, Jung Y, Wang J, Dai J, Wang J, et al. Skeletal localization and neutralization of the SDF-1(CXCL12)/CXCR4 axis blocks prostate cancer metastasis and growth in osseous sites in vivo. *J Bone Miner Res* (2005) 20(2):318–29. doi:10.1359/JBMR.041109
37. Dimitroff CJ, Lechpammer M, Long-Woodward D, Kutok JL. Rolling of human bone-metastatic prostate tumor cells on human bone marrow endothelium under shear flow is mediated by E-selectin. *Cancer Res* (2004) 64(15):5261–9. doi:10.1158/0008-5472.CAN-04-0691
38. Jung Y, Kim JK, Shiozawa Y, Wang J, Mishra A, Joseph J, et al. Recruitment of mesenchymal stem cells into prostate tumours promotes metastasis. *Nat Commun* (2013) 4:1795. doi:10.1038/ncomms2766
39. Wolk A, Mantzoros CS, Andersson SO, Bergström R, Signorello LB, Lagiou P, et al. Insulin-like growth factor 1 and prostate cancer risk: a population-based, case-control study. *J Natl Cancer Inst* (1998) 90(12):911–5. doi:10.1093/jnci/90.12.911
40. Schmidt LJ, Tindall DJ. Steroid 5 α-reductase inhibitors targeting BPH and prostate cancer. *J Steroid Biochem Mol Biol* (2011) 125(1):32–8. doi:10.1016/j.jsbmb.2010.09.003
41. Chavin G, Sheinin Y, Crispen PL, Boorjian SA, Roth TJ, Rangel L, et al. Expression of immunosuppresive B7-H3 ligand by hormone-treated prostate cancer tumors and metastases. *Clin Cancer Res* (2009) 15(6):2174–80. doi:10.1158/1078-0432.CCR-08-2262
42. Chiang C, Chiu M, Moore AJ, Anderson PH, Ghasem-Zadeh A, McManus JF, et al. Mineralization and bone resorption are regulated by the androgen receptor in male mice. *J Bone Miner Res* (2009) 24(4):621–31. doi:10.1359/jbmr.081217
43. Huggins C. Effect of orchiectomy and irradiation on cancer of the prostate. *Ann Surg* (1942) 115(6):1192–200. doi:10.1097/00000658-194206000-00030
44. Benoist GE, van der Meulen E, van Oort IM, Beumer JH, Somford DM, Schalken JA, et al. Development and validation of a bioanalytical method to quantitate enzalutamide and its active metabolite N-desmethylenzalutamide in human plasma: application to clinical management of metastatic castration-resistant prostate cancer patients. *Ther Drug Monit* (2018) 40(2):222–9. doi:10.1097/FTD.0000000000000484
45. Schweizer MT, Yu EY. AR-signaling in human malignancies: prostate cancer and beyond. *Cancers (Basel)* (2017) 9(1):E7. doi:10.3390/cancers9010007
46. Smith MR, Saad F, Chowdhury S, Oudard S, Hadaschik BA, Graff JN, et al. Apalutamide treatment and metastasis-free survival in prostate cancer. *N Engl J Med* (2018) 378(15):1408–18. doi:10.1056/NEJMoa1715546
47. Allan CA, McLachlan RI. Chapter 139 – androgen deficiency disorders A2. 7th ed. In: Larry JJ, Groot LJD, de Kretser DM, Giudice LC, Grossman AB, Melmed S, et al., editors. *Endocrinology: Adult and Pediatric*. Philadelphia: W.B. Saunders (2016). p. 2394–420.e13.
48. Schmidt LJ, Tindall DJ. Steroid 5 α-reductase inhibitors targeting BPH and prostate cancer. *J Steroid Biochem Mol Biol* (2011) 125(1):32–8. doi:10.1016/j.jsbmb.2010.09.003
49. Robinson-Rechavi M, Escriva Garcia H, Laudet V. The nuclear receptor superfamily. *J Cell Sci* (2003) 116(Pt 4):585–6. doi:10.1242/jcs.00247
50. Takayama K-I, Inoue S. Transcriptional network of androgen receptor in prostate cancer progression. *Int J Urol* (2013) 20(8):756–68. doi:10.1111/iju.12146
51. Labrie F, Cusan L, Gomez J, Luu-The V, Candas B, Bélanger A, et al. Major impact of hormonal therapy in localized prostate cancer – death can already be an exception. *J Steroid Biochem Mol Biol* (2004) 92(5):327–44. doi:10.1016/j.jsbmb.2004.10.011
52. Smith MR, Fallon MA, Lee H, Finkelstein JS. Raloxifene to prevent gonadotropin-releasing hormone agonist-induced bone loss in men with prostate cancer: a randomized controlled trial. *J Clin Endocrinol Metab* (2004) 89(8):3841–6. doi:10.1210/jc.2003-032058
53. Smith MR, Morton RA, Barnette KG, Sieber PR, Malkowicz SB, Rodriguez D, et al. Toremifene to reduce fracture risk in men receiving androgen deprivation therapy for prostate cancer. *J Urol* (2013) 189(1 Suppl):S45–50. doi:10.1016/j.juro.2012.11.016
54. Smith MR, Morton RA, Barnette KG, Sieber PR, Malkowicz SB, Rodriguez D, et al. Toremifene to reduce fracture risk in men receiving androgen deprivation therapy for prostate cancer. *J Urol* (2010) 184(4):1316–21. doi:10.1016/j.juro.2010.06.022
55. Smith MR, Malkowicz SB, Brawer MK, Hancock ML, Morton RA, Steiner MS. Toremifene decreases vertebral fractures in men younger than 80 years receiving androgen deprivation therapy for prostate cancer. *J Urol* (2011) 186(6):2239–44. doi:10.1016/j.juro.2011.07.090
56. Smith MR, Coleman RE, Klotz L, Pittman K, Milecki P, Ng S, et al. Denosumab for the prevention of skeletal complications in metastatic castration-resistant prostate cancer: comparison of skeletal-related events and symptomatic skeletal events. *Ann Oncol* (2015) 26(2):368–74. doi:10.1093/annonc/mdu519
57. James ND, de Bono JS, Spears MR, Clarke NW, Mason MD, Dearnaley DP, et al. Abiraterone for prostate cancer not previously treated with hormone therapy. *N Engl J Med* (2017) 377(4):338–51. doi:10.1056/NEJMoa1702900
58. Suominen MI, Fagerlund KM, Rissanen JP, Konkol YM, Morko JP, Peng Z, et al. Radium-223 inhibits osseous prostate cancer growth by dual targeting of cancer cells and bone microenvironment in mouse models. *Clin Cancer Res* (2017) 23(15):4335–46. doi:10.1158/1078-0432.CCR-16-2955
59. Parimi S, Tsang E, Alexander A, Mckenzie M, Bachand F, Sunderland K, et al. A population-based study of the use of radium 223 in metastatic

castration-resistant prostate cancer: factors associated with treatment completion. *Can Urol Assoc J* (2017) 11(10):350–5. doi:10.5489/cuaj.4415
60. Sartor O, Vogelzang NJ, Sweeney C, Fernandez DC, Almeida F, Iagaru A, et al. Radium-223 safety, efficacy, and concurrent use with abiraterone or enzalutamide: first U.S. experience from an expanded access program. *Oncologist* (2018) 23(2):193–202. doi:10.1634/theoncologist.2017-0413
61. Huntjens KM, Kosar S, van Geel TACM, Geusens PP, Willems P, Kessels A, et al. Risk of subsequent fracture and mortality within 5 years after a non-vertebral fracture. *Osteoporos Int* (2010) 21(12):2075–82. doi:10.1007/s00198-010-1178-5
62. Masiello D, Cheng S, Bubley GJ, Lu ML, Balk SP. Bicalutamide functions as an androgen receptor antagonist by assembly of a transcriptionally inactive receptor. *J Biol Chem* (2002) 277(29):26321–6. doi:10.1074/jbc.M203310200
63. Clegg NJ, Wongvipat J, Joseph JD, Tran C, Ouk S, Dilhas A, et al. ARN-509: a novel antiandrogen for prostate cancer treatment. *Cancer Res* (2012) 72(6):1494–503. doi:10.1158/0008-5472.CAN-11-3948
64. Rathkopf DE, Morris MJ, Fox JJ, Danila DC, Slovin SF, Hager JH, et al. Phase I study of ARN-509, a novel antiandrogen, in the treatment of castration-resistant prostate cancer. *J Clin Oncol* (2013) 31(28):3525–30. doi:10.1200/JCO.2013.50.1684
65. James GD, Symeonides SN, Marshall J, Young J, Clack G. Continual reassessment method for dose escalation clinical trials in oncology: a comparison of prior skeleton approaches using AZD3514 data. *BMC Cancer* (2016) 16:703. doi:10.1186/s12885-016-2702-6
66. Blessing AM, Rajapakshe K, Reddy Bollu L, Shi Y, White MA, Pham AH, et al. Transcriptional regulation of core autophagy and lysosomal genes by the androgen receptor promotes prostate cancer progression. *Autophagy* (2017) 13(3):506–21. doi:10.1080/15548627.2016.1268300
67. Parker C, Nilsson S, Heinrich D, Helle SI, O'Sullivan JM, Fosså SD, et al. Alpha emitter radium-223 and survival in metastatic prostate cancer. *N Engl J Med* (2013) 369(3):213–23. doi:10.1056/NEJMoa1213755
68. Tokumitsu H, Inuzuka H, Ishikawa Y, Ikeda M, Saji I, Kobayashi R. STO-609, a specific inhibitor of the $Ca^{(2+)}$/calmodulin-dependent protein kinase kinase. *J Biol Chem* (2002) 277(18):15813–8. doi:10.1074/jbc.M201075200
69. Dhani NC, Emmenegger U, Adams L, Jongstra J, Tannock IF, Sridhar SS, et al. Phase II study of cytarabine in men with docetaxel-refractory, castration-resistant prostate cancer with evaluation of TMPRSS2-ERG and SPINK1 as serum biomarkers. *BJU Int* (2012) 110(6):840–5. doi:10.1111/j.1464-410X.2011.10922.x
70. Kim SB, Dent R, Im SA, Espié M, Blau S, Tan AR, et al. Ipatasertib plus paclitaxel versus placebo plus paclitaxel as first-line therapy for metastatic triple-negative breast cancer (LOTUS): a multicentre, randomised, double-blind, placebo-controlled, phase 2 trial. *Lancet Oncol* (2017) 18(10):1360–72. doi:10.1016/S1470-2045(17)30450-3
71. Jernberg E, Bergh A, Wikstrom P. Clinical relevance of androgen receptor alterations in prostate cancer. *Endocr Connect* (2017) 6(8):R146–61. doi:10.1530/EC-17-0118
72. Wadosky KM, Koochekpour S. Molecular mechanisms underlying resistance to androgen deprivation therapy in prostate cancer. *Oncotarget* (2016) 7(39):64447–70. doi:10.18632/oncotarget.10901
73. Attar RM, Takimoto CH, Gottardis MM. Castration-resistant prostate cancer: locking up the molecular escape routes. *Clin Cancer Res* (2009) 15(10):3251–5. doi:10.1158/1078-0432.CCR-08-1171
74. Antonarakis E. AR signaling in human malignancies: prostate cancer and beyond. *Cancers* (2018) 10(1):22. doi:10.3390/cancers10010022
75. Yu Z, Chen S, Sowalsky AG, Voznesensky OS, Mostaghel EA, Nelson PS, et al. Rapid induction of androgen receptor splice variants by androgen deprivation in prostate cancer. *Clin Cancer Res* (2014) 20(6):1590–600. doi:10.1158/1078-0432.CCR-13-1863
76. De Laere B, van Dam PJ, Whitington T, Mayrhofer M, Diaz EH, Van den Eynden G, et al. Comprehensive profiling of the androgen receptor in liquid biopsies from castration-resistant prostate cancer reveals novel intra-AR structural variation and splice variant expression patterns. *Eur Urol* (2017) 72(2):192–200. doi:10.1016/j.eururo.2017.01.011
77. Guo Z, Yang X, Sun F, Jiang R, Linn DE, Chen H, et al. A novel androgen receptor splice variant is up-regulated during prostate cancer progression and promotes androgen depletion-resistant growth. *Cancer Res* (2009) 69(6):2305–13. doi:10.1158/0008-5472.CAN-08-3795
78. Hörnberg E, Ylitalo EB, Crnalic S, Antti H, Stattin P, Widmark A, et al. Expression of androgen receptor splice variants in prostate cancer bone metastases is associated with castration-resistance and short survival. *PLoS One* (2011) 6(4):e19059. doi:10.1371/journal.pone.0019059
79. Wang Q, Li W, Zhang Y, Yuan X, Xu K, Yu J, et al. Androgen receptor regulates a distinct transcription program in androgen-independent prostate cancer. *Cell* (2009) 138(2):245–56. doi:10.1016/j.cell.2009.04.056
80. Velasco AM, Gillis KA, Li Y, Brown EL, Sadler TM, Achilleos M, et al. Identification and validation of novel androgen-regulated genes in prostate cancer. *Endocrinology* (2004) 145(8):3913–24. doi:10.1210/en.2004-0311
81. Varambally S, Yu J, Laxman B, Rhodes DR, Mehra R, Tomlins SA, et al. Integrative genomic and proteomic analysis of prostate cancer reveals signatures of metastatic progression. *Cancer Cell* (2005) 8(5):393–406. doi:10.1016/j.ccr.2005.10.001
82. Massie CE, Adryan B, Barbosa-Morais NL, Lynch AG, Tran MG, Neal DE, et al. New androgen receptor genomic targets show an interaction with the ETS1 transcription factor. *EMBO Rep* (2007) 8(9):871–8. doi:10.1038/sj.embor.7401046
83. Nelson PS, Clegg N, Arnold H, Ferguson C, Bonham M, White J, et al. The program of androgen-responsive genes in neoplastic prostate epithelium. *Proc Natl Acad Sci U S A* (2002) 99(18):11890–5. doi:10.1073/pnas.182376299
84. Sadeghi M, Ranjbar B, Ganjalikhany MR, Khan FM, Schmitz U, Wolkenhauer O, et al. MicroRNA and transcription factor gene regulatory network analysis reveals key regulatory elements associated with prostate cancer progression. *PLoS One* (2016) 11(12):e0168760. doi:10.1371/journal.pone.0168760
85. Rhodes DR, Yu J, Shanker K, Deshpande N, Varambally R, Ghosh D, et al. ONCOMINE: a cancer microarray database and integrated data-mining platform. *Neoplasia* (2004) 6(1):1–6. doi:10.1016/S1476-5586(04)80047-2
86. Massie CE, Lynch A, Ramos-Montoya A, Boren J, Stark R, Fazli L, et al. The androgen receptor fuels prostate cancer by regulating central metabolism and biosynthesis. *EMBO J* (2011) 30(13):2719–33. doi:10.1038/emboj.2011.158
87. Frigo DE, Howe MK, Wittmann BM, Brunner AM, Cushman I, Wang Q, et al. CaM kinase kinase beta-mediated activation of the growth regulatory kinase AMPK is required for androgen-dependent migration of prostate cancer cells. *Cancer Res* (2011) 71(2):528–37. doi:10.1158/0008-5472.CAN-10-2581
88. Lu KP, Means AR. Regulation of the cell cycle by calcium and calmodulin. *Endocr Rev* (1993) 14(1):40–58. doi:10.1210/edrv-14-1-40
89. Colomer J, Means AR. Physiological roles of the Ca^{2+}/CaM-dependent protein kinase cascade in health and disease. *Subcell Biochem* (2007) 45:169–214. doi:10.1007/978-1-4020-6191-2_7
90. Hook SS, Means AR. Ca^{2+}/CaM-dependent kinases: from activation to function. *Annu Rev Pharmacol Toxicol* (2001) 41(1):471–505. doi:10.1146/annurev.pharmtox.41.1.471
91. Racioppi L, Means AR. Calcium/calmodulin-dependent protein kinase kinase 2: roles in signaling and pathophysiology. *J Biol Chem* (2012) 287(38):31658–65. doi:10.1074/jbc.R112.356485
92. Green MF, Scott JW, Steel R, Oakhill JS, Kemp BE, Means AR. Ca^{2+}/calmodulin-dependent protein kinase kinase {beta} is regulated by multisite phosphorylation. *J Biol Chem* (2011) 286(32):28066–79. doi:10.1074/jbc.M111.251504
93. Tokumitsu H, Hatano N, Fujimoto T, Yurimoto S, Kobayashi R. Generation of autonomous activity of $Ca^{(2+)}$/calmodulin-dependent protein kinase kinase beta by autophosphorylation. *Biochemistry* (2011) 50(38):8193–201. doi:10.1021/bi201005g
94. Anderson KA, Ribar TJ, Lin F, Noeldner PK, Green MF, Muehlbauer MJ, et al. Hypothalamic CaMKK2 contributes to the regulation of energy balance. *Cell Metab* (2008) 7(5):377–88. doi:10.1016/j.cmet.2008.02.011
95. Hardie DG, Ross FA, Hawley SA. AMPK: a nutrient and energy sensor that maintains energy homeostasis. *Nat Rev Mol Cell Biol* (2012) 13(4):251–62. doi:10.1038/nrm3311
96. Høyer-Hansen M, Bastholm L, Szyniarowski P, Campanella M, Szabadkai G, Farkas T, et al. Control of macroautophagy by calcium, calmodulin-dependent kinase kinase-beta, and Bcl-2. *Mol Cell* (2007) 25(2):193–205. doi:10.1016/j.molcel.2006.12.009
97. Anderson KA, Lin F, Ribar TJ, Stevens RD, Muehlbauer MJ, Newgard CB, et al. Deletion of CaMKK2 from the liver lowers blood glucose and improves

whole-body glucose tolerance in the mouse. *Mol Endocrinol* (2012) 26(2):281–91. doi:10.1210/me.2011-1299

98. Lin F, Ribar TJ, Means AR. The Ca^{2+}/calmodulin-dependent protein kinase kinase, CaMKK2, inhibits preadipocyte differentiation. *Endocrinology* (2011) 152(10):3668–79. doi:10.1210/en.2011-1107
99. Cary RL, Waddell S, Racioppi L, Long F, Novack DV, Voor MJ, et al. Inhibition of $Ca^{(2)(+)}$/calmodulin-dependent protein kinase kinase 2 stimulates osteoblast formation and inhibits osteoclast differentiation. *J Bone Miner Res* (2013) 28(7):1599–610. doi:10.1002/jbmr.1890
100. Pritchard ZJ, Cary RL, Yang C, Novack DV, Voor MJ, Sankar U. Inhibition of CaMKK2 reverses age-associated decline in bone mass. *Bone* (2015) 75:120–7. doi:10.1016/j.bone.2015.01.021
101. Racioppi L, Noeldner PK, Lin F, Arvai S, Means AR. Calcium/calmodulin-dependent protein kinase kinase 2 regulates macrophage-mediated inflammatory responses. *J Biol Chem* (2012) 287(14):11579–91. doi:10.1074/jbc.M111.336032
102. Williams JN, Kambrath AV, Patel RB, Kang KS, Mével E, Li Y, et al. Inhibition of CaMKK2 enhances fracture healing by stimulating Indian hedgehog signaling and accelerating endochondral ossification. *J Bone Miner Res* (2018) 33(5):930–44. doi:10.1002/jbmr.3379
103. Lin F, Marcelo KL, Rajapakshe K, Coarfa C, Dean A, Wilganowski N, et al. The camKK2/camKIV relay is an essential regulator of hepatic cancer. *Hepatology* (2015) 62(2):505–20. doi:10.1002/hep.27832
104. Racioppi L. CaMKK2: a novel target for shaping the androgen-regulated tumor ecosystem. *Trends Mol Med* (2013) 19(2):83–8. doi:10.1016/j.molmed.2012.12.004
105. York B, Li F, Lin F, Marcelo KL, Mao J, Dean A, et al. Pharmacological inhibition of CaMKK2 with the selective antagonist STO-609 regresses NAFLD. *Sci Rep* (2017) 7(1):11793. doi:10.1038/s41598-017-12139-3
106. Karacosta LG, Foster BA, Azabdaftari G, Feliciano DM, Edelman AM. A regulatory feedback loop between Ca^{2+}/calmodulin-dependent protein kinase kinase 2 (CaMKK2) and the androgen receptor in prostate cancer progression. *J Biol Chem* (2012) 287(29):24832–43. doi:10.1074/jbc.M112.370783
107. Karacosta LG, Kuroski LA, Hofmann WA, Azabdaftari G, Mastri M, Gocher AM, et al. Nucleoporin 62 and $Ca^{(2+)}$/calmodulin dependent kinase kinase 2 regulate androgen receptor activity in castrate resistant prostate cancer cells. *Prostate* (2016) 76(3):294–306. doi:10.1002/pros.23121
108. Shima T, Mizokami A, Miyagi T, Kawai K, Izumi K, Kumaki M, et al. Down-regulation of calcium/calmodulin-dependent protein kinase kinase 2 by androgen deprivation induces castration-resistant prostate cancer. *Prostate* (2012) 72(16):1789–801. doi:10.1002/pros.22533
109. Owen KL, Parker BS. Beyond the vicious cycle: the role of innate osteoimmunity, automimicry and tumor-inherent changes in dictating bone metastasis. *Mol Immunol* (2017). doi:10.1016/j.molimm.2017.11.023
110. Roca H, Jones JD, Purica MC, Weidner S, Koh AJ, Kuo R, et al. Apoptosis-induced CXCL5 accelerates inflammation and growth of prostate tumor metastases in bone. *J Clin Invest* (2018) 128(1):248–66. doi:10.1172/JCI92466
111. Marcelo KL, Means AR, York B. The $Ca^{(2+)}$/calmodulin/CaMKK2 axis: nature's metabolic CaMshaft. *Trends Endocrinol Metab* (2016) 27(10):706–18. doi:10.1016/j.tem.2016.06.001

Conflict of Interest Statement: The authors declare that the research was conducted in the absence of any commercial or financial relationships that could be construed as a potential conflict of interest.

frontiers in Endocrinology

REVIEW
published: 19 June 2018
doi: 10.3389/fendo.2018.00322

The Role of Semaphorin 4D in Bone Remodeling and Cancer Metastasis

*Konstantinos Lontos[1], Juraj Adamik[1], Anastasia Tsagianni[2], Deborah L. Galson[1], John M. Chirgwin[3] and Attaya Suvannasankha[3]**

[1] Hematology-Oncology Division, Department of Medicine, UPMC Hillman Cancer Center, McGowan Institute for Regenerative Medicine, University of Pittsburgh, Pittsburgh, PA, United States, [2] Department of Medicine, University of Pittsburgh Medical Center, Pittsburgh, PA, United States, [3] Hematology and Oncology Division, Department of Medicine, Indiana University School of Medicine, Richard L. Roudebush VA Medical Center, Indianapolis, IN, United States

Semaphorin 4D (Sema4D; CD100) is a transmembrane homodimer 150-kDa glycoprotein member of the Semaphorin family. Semaphorins were first identified as chemorepellants that guide neural axon growth. Sema4D also possesses immune regulatory activity. Recent data suggest other Sema4D functions: inactivation of platelets, stimulation of angiogenesis, and regulation of bone formation. Sema4D is a coupling factor expressed on osteoclasts that inhibits osteoblast differentiation. Blocking Sema4D may, therefore, be anabolic for bone. Sema4D and its receptor Plexin-B1 are commonly dysregulated in cancers, suggesting roles in cancer progression, invasion, tumor angiogenesis, and skeletal metastasis. This review focuses on Sema4D in bone and cancer biology and the molecular pathways involved, particularly Sema4D–Plexin-B1 signaling crosstalk between cancer cells and the bone marrow microenvironment—pertinent areas since a humanized Sema4D-neutralizing antibody is now in early phase clinical trials in cancers and neurological disorders.

Keywords: semaphorin 4D, Sema4D, Plexin-B1, plexin, osteoclasts, osteoblasts, cancer

OPEN ACCESS

Edited by:
Julie A. Sterling, Vanderbilt University, United States

Reviewed by:
Jawed Akhtar Siddiqui, University of Nebraska Medical Center, United States
Christa Maes, KU Leuven, Belgium

****Correspondence:***
Attaya Suvannasankha
asuvanna@iu.edu

Specialty section:
This article was submitted to Bone Research, a section of the journal Frontiers in Endocrinology

Received: *15 February 2018*
Accepted: *28 May 2018*
Published: *19 June 2018*

Citation:
Lontos K, Adamik J, Tsagianni A, Galson DL, Chirgwin JM and Suvannasankha A (2018) The Role of Semaphorin 4D in Bone Remodeling and Cancer Metastasis. Front. Endocrinol. 9:322. doi: 10.3389/fendo.2018.00322

INTRODUCTION

Semaphorin 4D (Sema4D; also known as CD100), is a member of class IV of the Semaphorin protein family, with established functions as an immune regulator. This review focuses on additional, emerging roles of Sema4D in bone biology and cancer bone metastases. Recent pivotal findings support the pertinence of Sema4D in bone and cancers: (1) Negishi-Koga et al. (1) identified Sema4D as a major coupling factor expressed on osteoclasts that inhibits osteoblast differentiation. They found that mice with a global knockout of *Sema4d* had increased bone volume. (2) Terpos et al. (2) reported increased soluble Sema4D in serum and bone marrow plasma of patients with myeloma, a bone marrow cancer with uncoupled osteoclast activation and osteoblast suppression, compared to controls. (3) Sema4D and its primary receptor Plexin-B1 are commonly overexpressed in cancers. (4) Yang et al. (3) found that shRNA knockdown of Sema4D in MDA-MB-231 breast cancer cells decreased bone metastases in a standard xenograft model. (5) A humanized antibody that neutralizes Sema4D has shown antitumor activity in animal models and is under clinical testing in early phase clinical trials (4).

SEMA4D STRUCTURE AND ROLE IN HUMAN PHYSIOLOGY

Semaphorins form a highly conserved family of proteins that contain a signature amino-terminal sema domain. The semaphorin family contains more than 20 genes divided into seven classes, of

which classes III–VII are expressed in vertebrates. They have diverse roles in human biology including regulation of tumor growth and metastasis, angiogenesis, axonal guidance, bone formation, tissue regeneration, and autoimmunity (5).

Sema4D belongs to class IV of the Semaphorin family. In addition to the signature sema domain, the C-terminal region of Sema4D includes an IgG-like domain, a transmembrane domain, and a short cytoplasmic tail that contains one tyrosine phosphorylation site and multiple sites for serine–threonine phosphorylation. Membrane-bound Sema4D forms a stable homodimer *via* a disulfide bond between cysteines 679 within the sema domain. Proteolytic shedding of Sema4D by membrane-type 1-matrix metalloproteinase (MT1-MMP/MMP14) gives rise to soluble, dimeric Sema4D (sSema4D) (6). Both membrane-bound and soluble Sema4D can activate Plexin-B1 signaling.

Sema4D is expressed by many tissues including brain, kidney, and heart. However, Sema4D knockout mice have immune defects without other obvious organ dysfunctions, suggesting that its major role is in immune regulation. Sema4D is expressed strongly by resting T cells and weakly on B and antigen-presenting cells. Expression is increased upon cellular activation (7). Engagement of Sema4D enhances its association with the membrane protein tyrosine phosphatase CD45, which is expressed broadly in hematopoietic cells (8). The complex becomes active and recruits further proteins to sustain B and T cell activation and aggregation.

Most work on Sema4D function has focused on its role as a ligand in soluble form after proteolytic shedding. Several receptors for Sema4D have been identified, including C-type lectin protein CD72, and three members of the plexin family; Plexin-B1, Plexin-B2, and Plexin-C1 (9–12). Target cells express different receptors, leading to a broad variety of potential responses to Sema4D in different tissues. CD72 is the main Sema4D receptor on immune cells, although monocytes and immature dendritic cells require Plexin-C1 and Plexin-B1, respectively. Plexins-B1 and -B2 mediate the Sema4D responses on non-immune cells. CD72 (also known as Lyb-2) is a 45-kDa type II transmembrane protein of the C-type lectin family (13) which is expressed throughout B-cell differentiation (14). The CD72 cytoplasmic domain contains two immune-receptor tyrosine-based inhibition motifs that recruit the tyrosine phosphatase SHP-1, resulting in inhibition of src family kinases and JNK and B cell inhibition (15). Sema4D engagement of CD72 triggers tyrosine dephosphorylation of CD72, leading to SHP-1 dissociation (10), thereby relieving CD72-mediated B cell inhibition. Since Sema4D and CD72 are expressed preferentially on T and B cell, respectively, their interaction couples T and B cells to dial the immune reaction up or down. Dendritic cells, macrophages, and some subpopulations of T cells express CD72 (16). Sema4D may, therefore, play an additional role in T cell communication *via* these other immune cells.

Plexins are transmembrane proteins with a sema ligand-binding domain in their extracellular domain. Upon ligand binding, Plexin-B1 and Plexin-B2 extracellular domains undergo proteolysis by subtilisin-like proprotein convertases to further increase their affinity for Sema4D (17). The highly conserved cytoplasmic region of plexins is devoid of enzymatic activity, but it can interact, directly or indirectly, with small G proteins for various functions (18). Transduction cascades downstream of the Sema4D/Plexin-B1 complex vary, dependent on the different membrane proteins and G proteins recruited to the complex.

Figure 1 details downstream signaling of Sema4D/Plexin-B1. Without engagement with Sema4D, the cytoplasmic tail of Plexin-B1 is in an inactive conformation. R-Ras is in a GTP-bound state and activates membrane integrin to control cellular adhesion to the extracellular matrix. Rac is not bound to Plexin-B1 and promotes activation of p21-activated kinase (PAK) to activate LIMK1 and cofilin to increase actin polymerization and microtubule assembly (19). Binding of Sema4D to Plexin-B1 alters Plexin-B1 conformation allowing recruitment of Rac1, which sequesters it from the PAK-LIMK1-cofilin signaling cascade, causing disassembly of actin fibers (20). Initiation of PlexinB1-GAP activity inhibits R-Ras-mediated integrin activation, which blocks cell adhesion and increase cell motility and invasion (21). Deactivation of R-Ras further decreases the PI3K–Akt–GSK3β pathway, which leads to deactivation of CRMP-2 and subsequent microtubule disassembly (22).

Whether Sema4D/Plexin-B1 complexes activate or inhibit downstream GTPases also depends on their interactions with specific receptor tyrosine kinases: ErbB-2 or c-Met (23). In ErbB2 expressing cells, binding of Sema4D to Plexin-B1 activates the intrinsic tyrosine kinase activity of ErbB-2, resulting in the phosphorylation of both Plexin-B1 and ErbB-2 (24), generating docking sites on Plexin-B1 for the SH2 domains of 1-phosphatidylinositol-4,5-bisphosphate phosphodiesterase gamma-1/2 (PLCγ1/2) (25). The SH3 domain of the recruited PLCγ1/2 activates the guanine nucleotide-exchange factors (GEFs) LARG (leukemia-associated RhoGEF) and PRG (PDZ-RhoGEF) that constitutively bind to the PDZ binding site of the carboxyl-terminal sequence of Plexin-B1 (26). Activated RhoGEFs LARG and PRG mediate activation of the small GTPase RhoA, which cooperates with Ras to activate the serine/threonine kinases Raf and Rho-associated kinases (e.g., ROCK1/2) to stimulate various pathways, including mitogen-activated phosphokinases (MAPKs) ERK1/2 and p38, protein kinases (PI3/Akt—phosphatidylinositol 3′-kinase) (27). Downstream activation of MAPKs and PI3K control dendritic and axonal morphogenesis by differentially regulating branching and extension (27). On the other hand, Sema4D/Plexin-B1 can interact with Rnd1 to downregulate the GTPase activity of R-Ras, inducing growth cone collapse in hippocampal neurons (28). Plexin-B1 also binds and competes for activated Rho GTPase Rac, thus preventing Rac from activating its downstream effector PAK to initiate actin polymerization. In endothelial cells, Sema4D/Plexin-B1 signals stimulate PI3K-Akt to activate PYK2 and Src to control endothelial cell migration (29). c-Met (HGF receptor tyrosine kinase) and macrophage stimulating protein (MSP, encoded by the Ron gene) are members of the Scatter Factor Receptors family. They share structural homology with Plexin-B1 (30, 31). In cells with c-Met expression but absent ErbB2, Sema4D/Plexin-B1 recruits and activates c-Met or Ron kinases to regulate cell motility and invasiveness. In normal fibroblasts, phosphorylation of c-Met creates a docking site for growth factor receptor bound-2 (Grb2), which then interacts with p190 RhoGAP and inactivates RhoA, causing inhibition of fibroblast motility (32).

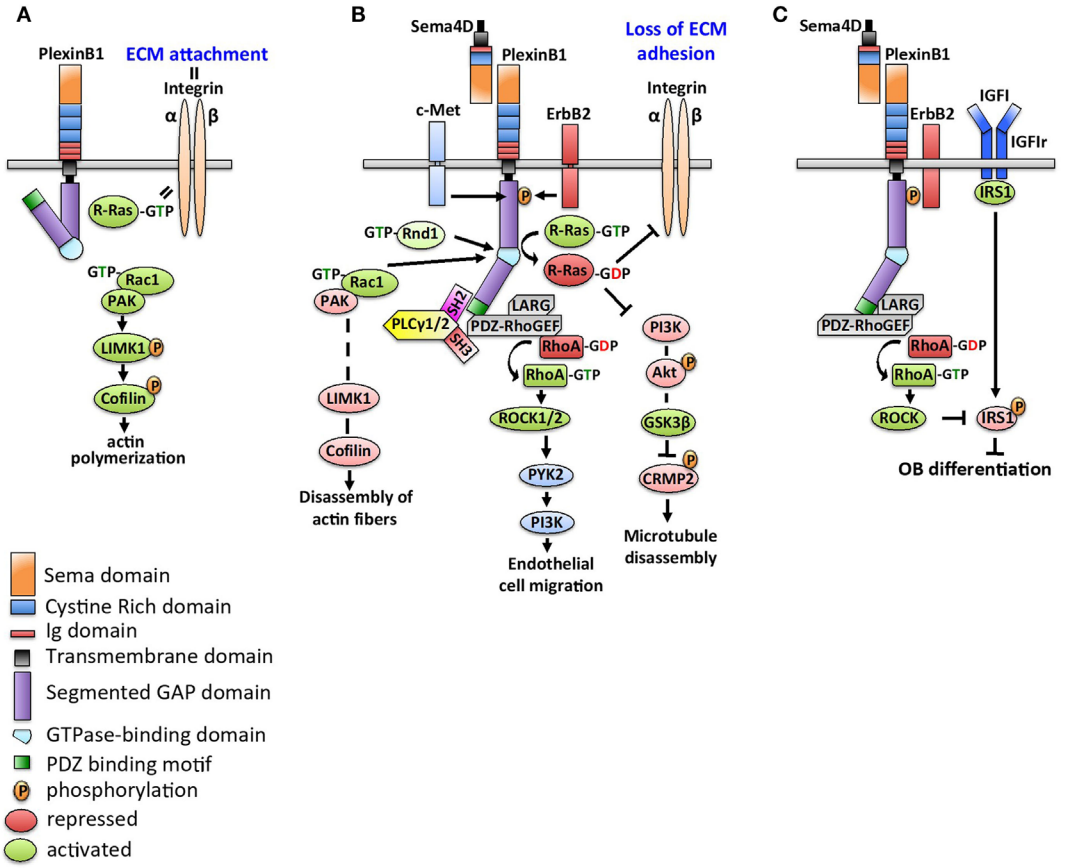

FIGURE 1 | Schematics of Sema4D/Plexin-B1 signaling. **(A)** In the absence of Sema4D, the cytoplasmic tail of Plexin-B1 is in an inactive conformation. R-Ras is in a GTP-bound state to collaborate with integrin and control cellular adhesion to the extracellular matrix (ECM). With Plexin-B1 in an inactive state, Rac activates p21-activated kinase (PAK) to trigger LIMK1 signaling and downstream phosphorylation of cofilin, which results in increased actin polymerization and microtubule assembly. **(B)** Sema4D binding to Plexin-B1 alters the Plexin-B1 conformation, recruits Rac1 to the complex, and inhibits activation of the PAK–LIMK1–cofilin signaling cascade. In addition, R-Ras recruitment to the Sema4D/Plexin-B1 complex inhibits its ability to regulate integrin-mediated activation, resulting in increased cell motility. Deactivation of R-Ras further decreases PI3K-Akt GSK3β pathway, which leads to deactivation of CRMP-2 and subsequent microtubule disassembly. In an ErbB2-dependent signaling step, PLCγ1/2 is recruited to Plexin-B1 *via* its SH2 domain. Structural interaction of the PLCγ1/2 SH3 domain triggers PDZ-RhoGEF/LARG complex, resulting in RhoA activation. Active GTP-RhoA acts on Raf and Rho-associated kinases (ROCK1/2), which in turn stimulate PYK2 to induce cell invasiveness and migration. **(C)** Sema4D-Plexin-B1 signaling inhibits osteoblast differentiation. Plexin-B1/ErbB2-dependent RhoA activation stimulates activation of downstream kinase ROCK, which phosphorylates the insulin receptor substrate 1 (IRS1). This causes suppression of insulin like growth factor (IGF1)-dependent signaling and blocks osteoblast differentiation.

SEMA4D IN BONE PHYSIOLOGY

Successful crystallization of Sema4D and solution of its structure led to a recognition of the homology between the Sema4D homodimer and the αVβ3 integrin heterodimer, the first clue to a role for Sema4D in bone biology (33). αVβ3 integrin is an osteoclast regulator, and β3 integrin knockout mice become progressively osteosclerotic with age due to dysfunctional osteoclasts that fail to polarize correctly and display abnormal ruffled membranes (34).

Two groups reported an increased bone mass in Sema4D knockout animals and the expression of Sema4D in osteoclasts but not osteoblasts (1, 35). Negishi-Koga and coworkers comprehensively surveyed osteoclasts and osteoblasts for expression of candidate molecules to couple bone formation to resorption, including the members of the ephrin, netrin, semaphorin, and slit gene families. They found that only Sema4D was highly expressed in RANKL-activated osteoclasts. Utilizing a soluble Fc receptor-Sema4D fusion protein, they evaluated directly the effects of the Sema4D extracellular domain on osteoblasts. Fc-Sema4D inhibited the osteoblast differentiation markers alkaline phosphatase and osteocalcin, as well as the formation of mineralized nodules in culture, without a change in osteoblast proliferation. Co-immunoprecipitation confirmed a complex of Fc-Sema4D with Plexin-B1, which is highly expressed in osteoblasts. This complex leads to ErbB2 phosphorylation and downstream activation of RhoA. *Plexin*$^{-/-}$ animals, as well as mice expressing an osteoblast-targeted dominant negative RhoA, had a high bone mass due to enhanced osteoblastic bone formation, recapitulating the bone phenotype of the *Sema4d*$^{-/-}$ mice. A recent study used optoPlexin (optogenetic activation of Plexin-B1) in osteoblasts to show that Plexin-B1 activation results in retraction of the leading

edge and induces distal membrane protrusions, causing the osteoblasts to migrate. Thus, osteoclast-produced Sema4D may cause repulsion of osteoblasts *via* activation of both the RhoA and ras-GTP pathways (36). Overall, these findings support the function of the Sema4D/Plexin-B1/RhoA axis in osteoblast inhibition by osteoclasts (1). However, Sema4D's regulation of bone mass may be more complicated. Dacquin et al (35) noted that the increased bone mass phenotype in *Sema4d*$^{-/-}$ mice primarily occurred in mature female mice. The increased bone mass phenotype in *Sema4d*$^{-/-}$ mice was not reversed after a transplantation of bone marrow cells from wild-type mice, as a source of new osteoclasts. *Sema4d*$^{-/-}$ mice have impaired ovarian function, small litter size, and decreased hypothalamic gonadotropin-hormone releasing hormone. The authors propose an indirect mechanism by which Sema4D regulates bone mass *via* the hypothalamic–pituitary–ovarian axis (35).

Serum Sema4D has been explored as a biomarker in osteoporosis, with conflicting results to date, likely reflecting different patient populations, the non-randomized nature of the trials and different time points for Sema4D analysis. In postmenopausal women, serum Sema4D was higher among those with osteoporosis (37). However, in an open label study of osteoporotic women receiving the osteoclast-targeting agents zoledronic acid or RANKL monoclonal antibody denosumab or the bone-anabolic agent teriparatide (PTH1-34), serum Sema4D decreased after 3 months of teriparatide treatment, while it increased with denosumab and zoledronic acid (38). There was no attempt to correlate the Sema4D levels with degree of osteoporosis, and serum Sema4D was assayed at only one time point, not allowing a determination of kinetics, which may differ among treatment groups.

Congenital defects due to mutation or loss of Sema4D have been little studied in humans. Segmental copy number loss in the region of the Sema4D gene was seen in one third of patients with acetabular dysplasia, which increases risk of osteoarthritis, but a causal relationship was not explored (39).

Sema4D has been implicated in bone and joint inflammation. In rheumatoid arthritis (RA), Sema4D was elevated in both serum and synovial fluid from RA patients, and disease activity markers were correlated with serum Sema4D levels. Sema4D-expressing cells also accumulated in RA synovium, and sSema4D-induced tumor necrosis factor α (TNFα) and interleukin-6 (IL-6) production from CD14+ monocytes (40). Movila and group explored treatment-related osteonecrosis of the jaw and showed increased Sema4D-expressing γδ-T cells in bone lesions, which were decreased by anti-Sema4D antibody (41). In osteoarthritis, bone tissue had low Plexin-B1 expression compared to age- and gender-matched cadaveric control bones, indicating that the loss of Sema4D/Plexin-B1 inhibition of osteoblast activity may lead to an increased bone volume fraction and decreased bone matrix mineralization, contributing to osteoarthritis (42).

Elevated Sema4D is observed in diseases unrelated to the musculoskeletal systems, including hemorrhagic fever with renal syndrome (43) and autoimmune diseases (44). Inflammation and increased shedding from peripheral blood mononuclear cells are possible sources. Serum Sema4D is also increased in non-inflammatory condition such as atrial fibrillation (45). The value of sSema4D as a biomarker in some of these diseases may warrant further investigation.

SEMA4D IN CANCER

While other semaphorins such as Sema3B and 3F are tumor suppressors, Sema4D promotes tumor growth (46, 47). Sema4D and Plexin-B1 are abnormally expressed in various cancers and have been associated with invasive phenotypes and poor prognosis. The mechanisms by which Sema4D confers these features are complex and involve both tumor cells and their microenvironment. While not directly linked to malignant transformation, Sema4D/Plexin-B1 signaling contributes to many critical aspects of cancer progression, including proliferation, invasion, angiogenesis, immune escape, and metastasis. We summarize the role of Sema4D/Plexin-B1 in cancers based on overexpression of Sema4D or Plexin-B1 by the cancer cells or by other cells in the tumor microenvironment including immune cells, and the role of Sema4D/Plexin-B1 in distant metastasis.

Because of its known role in lymphoid cells, Sema4D expression in cancer was first evaluated in lymphoma and lymphoblastic leukemia. T cell lymphomas universally express Sema4D, while only a minority of B cell lymphomas are Sema4D positive (48), paralleling the expression of Sema4D by normal T and B cells. In chronic lymphocytic leukemia (CLL), CD38 is a known negative predictor of survival. CD38 binds to (49) stromal cells expressing CD31, leading to relocalization of Sema4D, facilitating its binding to Plexin-B1 on bone marrow cells. The increased expression of Plexin-B1 in stromal cells, follicular dendritic cells, and activated T-cells, enhances the complex interplay of CD38/CD31 and Sema4D/Plexin-B1 to sustain CLL growth (50, 51).

Sema4D is highly expressed by many solid tumors including prostate, glioma, lung, ovarian, sarcoma, and cutaneous squamous cell carcinoma. Expression is correlated with tumor aggressiveness and poor prognosis, but controversial data exist for some tumors. In an array of 888 genes, Sema4D mRNA was highest in early stage breast cancer compared to normal tissue and downregulated in advanced disease (52). Jiang and coworkers confirmed high Sema4D protein in breast cancer cell lines compared to normal breast epithelial cells. In addition, knockdown of Sema4D by shRNA inhibit breast cancer proliferation and tumor growth in xenografts (49). Malik et al., however, showed an opposite result of decreased Sema4D, Plexin-B1 and -B2 protein in primary breast tumors of patients who subsequently developed local recurrence, compared to the patients who remained disease-free (53). These studies used whole tumor tissues and may be confounded by different cell types within the tissue, since other cells in the microenvironment, including endothelial cells and macrophages, also express Sema4D. In whole-blood RNA, Sema4D was identified as one of six RNAs strongly predicting shorter survival among patients with castrate-resistant prostate cancer (54). Most data on Sema4D and clinical outcomes are based on small sample sizes with subjects receiving different treatments and not controlled for other prognostic markers. Prognostic value of Sema4D requires further validation in larger cohorts of patients, controlled for treatment types and other variables.

Overexpression of Plexin-B1 has been reported in skin, prostate and pancreatic cancers, and sarcoma (55–57). It correlates with lymph node metastasis, distant metastasis, and poor prognosis in patients with pancreas cancer (56). Plexin-B1 activation increases phosphorylation and translocation into the nucleus of the androgen receptor (AR), leading to activation of AR-regulated genes, which could play a role in castration resistance in prostate cancer (58). However, Rody et al. showed a rather opposite finding in breast cancer, in which loss of Plexin-B1 identifies a subgroup of estrogen receptor expressing breast cancer with high proliferative rate and hormone resistance (59). Cancer cell lines that express higher levels of Plexin-B1 exhibit increased perineural invasion. The mechanism is proposed to be the attraction of the cells due to Sema4D production from the nerves. Interestingly, higher nerve density in tumors expressing Sema4D (60) suggests that these tumors may use nerve-secreted factors for growth, pointing to a possible role of Sema4D in cancer pain.

While no Sema4D mutation has been reported in human cancers, Plexin-B1 mutations and copy number changes are noted commonly in various cancers, including melanomas, pancreas, breast, and prostate cancers (58, 61, 62). Thirteen somatic missense mutations in the cytoplasmic domain of Plexin-B1 were found in 46% of prostate cancers. Mutational hotspots mapped to the Rho GTPase binding domain in the cytoplasmic region of the receptor, causing loss of Rac and R-Ras binding and R-RasGAP activity. This resulted in an increase in cell motility, invasion, and adhesion, and could explain the metastatic phenotype (61). In some cancers, however, Plexin-B1 acts as a tumor suppressor. For example, Plexin-B1 is lost in deep and metastatic melanomas. Introducing Plexin-B1 into melanoma cells suppresses c-Met and hence proliferative responses to HGF. Increased Plexin-B1 confers resistance to cisplatin (63). A similar finding was noted in clear cell carcinoma (64). Sema4D/Plexin-B1 responses may vary among different cell lines of the same tumor type. Sema4D/Plexin-B1 increased the proliferative and invasive potential of LNCaP prostate cancer cells through the activation of ErbB2 and Akt, but decreased the motility and proliferation of PC3 prostate cells (65).

Different phenotypes of Sema4D/Plexin-B1-expressing tumors may depend on the expression of its partner proteins ErbB2 and c-Met. Since c-Met is one of the most commonly deregulated oncogene in cancers, its collaboration with Sema4D/Plexin-B1 is an alternative pathway to promote tumor invasion (66). Constitutive activation of Met in tumor cells with high Plexin-B1 can occur in the absence of Sema4D (66). T lymphoma invasion and metastasis 1 (Tiam1) is another Rac-specific guanine nucleotide-exchange factor that is activated by Sema4D/Plexin-B1 to stimulate Rac and promote proliferation, invasion, and metastasis in oral squamous cell carcinoma (67). In cancer cells that express both Sema4D and Plexin-B1, the pair could function in an autocrine/paracrine manner, although this requires future study.

In addition to direct proliferative actions in cancer cells, Sema4D/Plexin-B1 abnormalities within the tumor niche support cancer progression by promoting angiogenesis. Sema4D/Plexin-B1 function in angiogenesis was first described by Basile and coworkers (68), who showed that recombinant Sema4D-induced chemotaxis of endothelial cells, *in vitro* tubulogenesis and enhanced blood vessel formation in an *in vivo* mouse model. Sema4D/Plexin-B1 phosphorylation of c-Met promotes angiogenesis in a non-redundant manner from HGF (69). Sema4D can also stimulate angiogenesis *via* a c-Met-independent pathway through recruitment of PDZ-RhoGEF and LARG to the Sema4D/Plexin-B1 complex leading to Rho pathway activation, followed by downstream AKT and NF-κB activation and increased expression of proangiogenic IL-8 (70). Hypoxia induces Sema4D in a HIF-1-dependent manner. Sema4D then cooperates with VEGF to promote tumor growth and vascularity (71, 72). In addition, tumor-secreted Sema4D increases endothelial expression of platelet-derived growth factor-B and angiopoietin-like protein 4, which promote endothelial proliferation and vascular permeability (73). Lentiviral overexpression of Sema4D in colorectal cancer cell lines caused a proangiogenic response regardless of VEGF status (74). Sema4D may also be a biomarker for tumor angiogenesis, since its expression in ovarian cancer correlates with HIF-1, VEGF, and poor prognosis. Sema4D inhibition causes dissociation of endothelial cells from pericytes, a crucial step for successful antiangiogenic therapy (75). Both VEGF and Sema4D may cooperate in a multi-step process to reorganize the vasculature within the malignant niche. Tumor cells increase their Sema4D expression as an escape mechanism from anti-VEGF treatment (75). Concurrent targeting of VEGF and Sema4D may have additive or synergistic antiangiogenic effects. Sema4D may also support lymphangiogenesis, since Sema4D targeting with neutralizing antibody or shRNA suppressed VEGF-C and VEGF-D, key factors for lymphangiogenesis (76).

The role of Sema4D in immune regulation supports the importance of dysregulated Sema4D in immune escape of cancer cells. In a head and neck cancer model, tumor-secreted Sema4D promoted the expansion of myeloid-derived suppressor cells, which inhibit T-cell functions (77). Sema4D affects both the activities of immune cells and their recruitment to the tumor microenvironment. Delaire and coworkers noted that Sema4D inhibited both spontaneous and chemokine-induced migration of human monocytes (78). Strong expression of Sema4D at the invasive margins of actively growing tumors changed the infiltration and distribution of leukocytes within the tumor microenvironment. Neutralization of Sema4D by blocking antibodies disrupted this gradient of expression and enhanced recruitment of activated monocytes and lymphocytes into the tumor. This shifted the balance of cells and cytokines in a pro-inflammatory and antitumorigenic direction and was associated with durable tumor rejection in murine Colon26 and ERBB2 $^{+}$ mammary carcinoma models (4). These functions are at odds with the known roles of Sema4D in T and B cell activation. The dual nature of Sema4D between pro and antitumor action may depend on subsets of immune cells in the tumor niche, which in turn may depend on the plasticity of macrophages and T cells within the tumor. Classical activation of macrophages with interferon γ (M1) promotes the differentiation of cytotoxic T cells, which can improve antigen phagocytosis. However, alternative pathway of macrophage activation by IL-4, IL-14, or LPS gives rise to M2 macrophages. Tumor-associated monocytes are M2 and communicate effectively with regulatory T cells (Treg) to suppress antigen recognition and promote an inflammatory tumor microenvironment, angiogenesis, and

tumor progression (79). In tumors with high M2 macrophages and Tregs, Sema4D may contribute to immune suppression, even though in normal physiology, Sema4D is required for T and B cell function.

Sema4D may promote metastasis at distant sites. Many cancer cells, including head and neck squamous cell carcinoma lines, express the membrane-tethered collagenase, MT1-MMP which cleaves Sema4D. sSema4D could thus promote angiogenesis and cell migration both locally and at distant sites, thereby promoting metastasis (80).

SEMA4D IN THE BONE MARROW METASTATIC NICHE

The involvement of Sema4D in bone biology and cancer progression suggests a role in bone metastasis. Bone is the most common site of distant metastases for prostate and breast cancers. Bone metastases are driven by complex interactions between cancer cells, bone marrow cells, and bone cells, often leading to increased osteoclast and suppressed osteoblast activities. Even in osteosclerotic metastasis, occurring in prostate and some breast cancers, the newly formed bone is poorly organized, and osteoclasts remain activated, leading to loss of bone quality. Osteolysis with osteoblast suppression is a hallmark of multiple myeloma, an incurable blood cancer that originates within bone (81, 82). Current treatments are limited to osteoclast-targeting agents, which provide palliative benefit with marginal effect on tumor control. Zoledronic acid modestly prevents bone metastases in breast and prostate cancer xenograft models, but its benefit as a bone metastasis prevention is limited to postmenopausal women (83). No survival advantage was seen in premenopausal women or men with prostate cancers. This evidence suggests that osteoclast targeting alone is inadequate for tumor control.

Sema4D is a coupling molecule of osteoclasts and osteoblasts (1). In the tumor niche, Sema4D from the tumor cells and activated osteoclasts inhibits osteoblast differentiation, while inducing IL-8 secretion to further promote osteoclast proliferation and activity (70). Because soluble Sema4D can reach distant bone sites, it could hypothetically prime the bone niche to support future metastasis. Since tumor cells with high Sema4D also have high motility and invasiveness and Sema4D promotes angiogenesis, Sema4D could contribute to metastasis at both at the primary tumor site and distant sites. This notion is supported by a decrease in skeletal metastasis when Sema4D was knocked down using shRNA in the MDA-MB-231 breast cancer model (3).

Terpos and coworkers (2) showed increased Sema4D in peripheral blood and bone marrow plasma from myeloma patients compared to controls. We have shown that myeloma cell lines and primary myeloma cells express Sema4D at higher levels than MDA-MB-131 cells. In addition, we found that coculture of myeloma cells with bone increased expression of Sema4D by both tumor cells and bone (84). Myeloma cells, as well as breast cancers, express MMP14 (MT1-MMP), which releases membrane-bound Sema4D by proteolytic cleavage (85). Sema4D can promote angiogenesis, which is required for myeloma progression. Sema4D is, therefore, a potential target in myeloma, as well as in cancers that metastasize to the skeleton.

STRATEGY FOR SEMA4D/PLEXIN-B1 TARGETING

VX15/2503 is the first and only currently available humanized Sema4D blocking antibody in clinical testing. The antibody was generated in *Sema4D*$^{-/-}$ mice by using a panel of SEMA4D-specific hybridomas that react with murine, primate, and human SEMA4D (86). VX15/2503 bound with high affinity (1–5 nmol/L) to Sema4D and achieved complete Sema4D blockade in animal models, and its activity was subsequently confirmed in humans. No dose-limiting toxicity or maximal tolerated dose was observed at the dose required for complete Sema4D blockade in phase I clinical trials of multiple sclerosis and refractory solid malignancies (87, 88).

In the phase I study of 42 patients with refractory cancers receiving dose escalation of VX15/2503, one patient (2.4%) achieved partial response and 27 patients (64.3%) achieved long duration stable disease. Subjects with elevated baseline B and T lymphocytes exhibited longer progression-free survival, suggesting involvement of immune-mediated antitumor activity. Bone parameters and development of metastases were not endpoints. Tumor response was based on reduction in tumor size; therefore, patients with isolated bone metastases without other measurable tumor masses were not included.

The large, planar binding interface of the Sema4D/Plexin-B1 interaction makes it challenging to target with small molecules. Matsunaga and coworkers discovered a macrocyclic peptide, PB1m6, which binds Plexin-B1 with high affinity and specifically inhibits binding of the physiological ligand Sema4D and completely suppressed Sema4D-induced cell collapse *in vitro* (89). No data for this peptide *in vivo* or in cancer models are currently available.

Because of the central role of Sema4D in osteoblast inhibition, Zhang and group developed bone-specific drug delivery of *Sema4D siRNA* using *N*-(2-hydroxypropyl) methacrylamide copolymers with D-aspartic acid octapeptide (90). They showed that in an osteoporotic animal model induced by ovariectomy, weekly intravenous injections of this compound decreased osteoclast Sema4D expression and increased osteoblast differentiation. Treated animals showed higher femoral bone volume both in prevention and treatment models. Similar reduction of bone loss was seen in alveolar bone of the mandibles (91). Clinical testing of this molecule in patients has not been reported, but the study provides a proof of benefit for Sema4D targeting in bone.

While blocking the Sema4D/Plexin-B1 complex is of potential benefit in cancers and neuroinflammatory diseases, some cancers are growth inhibited by Sema4D signaling. In an acute myeloid leukemia cell line Kasumi-1, Sema4D binding of CD72, its preferred receptor in immune cells, leads to inhibition of growth and cell death, as a result of phosphorylation of CD72, the formation of the CD72–SHP-1 complex and dephosphorylation of src family kinases and JNK (15). Future development of Sema4D targeting should take into account the cellular context where Sema4D exerts its function.

DISCUSSION

We highlight Sema4D as a novel regulator of bone homeostasis. Sema4D also supports crucial steps in tumor progression, ranging from invasion, migration, angiogenesis, and immune suppression, to the pathological alteration of the tumor niche to support metastasis. Targeting Sema4D in the clinic has become practical with the development of a specific neutralizing antibody, which has low toxicity and an impressive response rate in early clinical trials of patients with refractory cancers. Because of the potential role of Sema4D in bone metastasis, this molecule should be further explored in these specific disease groups, and bone metastases should be included in clinical endpoints. Our preliminary data also support the potential of Sema4D blockade in multiple myeloma. Baseline B and T cell profiles have been correlated to response in a preliminary cancer clinical trial and should be further developed as a screening tool to identify patients likely to respond, or as a biomarker of response. In addition, Sema4D targeting may have synergistic antitumor effects when combined with immunomodulatory agents, warranting further study.

A major open question is whether Sema4D from non-osteoclast sources plays a significant role to inhibit osteoblast activity in cancer/bone diseases. Sema4D is expressed on tumor cells that colonize bone, while cells of the microenvironment other than osteoclasts may also express Sema4D. Although the extracellular domain can be proteolytically shed, it seems unlikely that local sSema4D concentrations are sufficient to activate osteoblast Plexin-B1. Both Negishi-Koga et al. (1) and Yang et al. (3) showed osteoblast suppression with micrograms per milliliter amounts of sSema4D:Fc fusions, orders of magnitude higher than those found in bone marrow plasma from multiple myeloma by Terpos et al. (2). Non-osteoblast and tumor sources of Sema4D could still inhibit osteoblast activity by direct cell:cell contact. Direct evidence for such actions is lacking; they may occur only in the context of co-receptors specific to the osteoclast. Patient data from clinical trials with Sema4D-neutralizing antibody could provide answers to these questions. Patients receiving antibody treatment should have increased bone mineral density. If the osteoclast Sema4D axis is the only significant contributor to osteoblast suppression, then there may be little bone effect of treatment in patients also receiving anti-osteoclast drugs (bisphosphonates or denosumab), which are the standard of care for cancer bone diseases.

AUTHOR CONTRIBUTIONS

All authors contributed to the writing of the manuscript.

FUNDING

Work was supported by the VA merit award CX000977 and pilot research funding of the Indiana University Simon Cancer Center (AS and JC), NIH/NIAMS R01 AR059679 and Funding from the Hematology-Oncology Division, Department of Medicine, University of Pittsburgh (DG) and the American Society of Hematology HONORS award (KL).

REFERENCES

1. Negishi-Koga T, Shinohara M, Komatsu N, Bito H, Kodama T, Friedel RH, et al. Suppression of bone formation by osteoclastic expression of semaphorin 4D. *Nat Med* (2011) 17(11):1473–80. doi:10.1038/nm.2489
2. Terpos E, Kastritis E, Bagratuni T, Christoulas D, Papatheodorou A, Kanellias N, et al. Semaphorin-4D and plexin-B1 are elevated in multiple myeloma microenvironment and possibly contribute in the development of lytic bone disease. *Blood* (2012) 120:1819.
3. Yang YH, Buhamrah A, Schneider A, Lin YL, Zhou H, Bugshan A, et al. Semaphorin 4D promotes skeletal metastasis in breast cancer. *PLoS One* (2016) 11(2):e0150151. doi:10.1371/journal.pone.0150151
4. Evans EE, Jonason AS Jr, Bussler H, Torno S, Veeraraghavan J, Reilly C, et al. Antibody blockade of semaphorin 4D promotes immune infiltration into tumor and enhances response to other immunomodulatory therapies. *Cancer Immunol Res* (2015) 3(6):689–701. doi:10.1158/2326-6066.CIR-14-0171
5. Worzfeld T, Offermanns S. Semaphorins and plexins as therapeutic targets. *Nat Rev Drug Discov* (2014) 13(8):603–21. doi:10.1038/nrd4337
6. Elhabazi A, Delaire S, Bensussan A, Boumsell L, Bismuth G. Biological activity of soluble CD100. I. The extracellular region of CD100 is released from the surface of T lymphocytes by regulated proteolysis. *J Immunol* (2001) 166(7):4341–7. doi:10.4049/jimmunol.166.7.4341
7. Bougeret C, Mansur IG, Dastot H, Schmid M, Mahouy G, Bensussan A, et al. Increased surface expression of a newly identified 150-kDa dimer early after human T lymphocyte activation. *J Immunol* (1992) 148(2):318–23.
8. Delaire S, Elhabazi A, Bensussan A, Boumsell L. CD100 is a leukocyte semaphorin. *Cell Mol Life Sci* (1998) 54(11):1265–76. doi:10.1007/s000180050252
9. Tamagnone L, Artigiani S, Chen H, He Z, Ming GI, Song H, et al. Plexins are a large family of receptors for transmembrane, secreted, and GPI-anchored semaphorins in vertebrates. *Cell* (1999) 99(1):71–80. doi:10.1016/S0092-8674(00)80063-X
10. Kumanogoh A, Watanabe C, Lee I, Wang X, Shi W, Araki H, et al. Identification of CD72 as a lymphocyte receptor for the class IV semaphorin CD100: a novel mechanism for regulating B cell signaling. *Immunity* (2000) 13(5):621–31. doi:10.1016/S1074-7613(00)00062-5
11. Chabbert-de Ponnat I, Marie-Cardine A, Pasterkamp RJ, Schiavon V, Tamagnone L, Thomasset N, et al. Soluble CD100 functions on human monocytes and immature dendritic cells require plexin C1 and plexin B1, respectively. *Int Immunol* (2005) 17(4):439–47. doi:10.1093/intimm/dxh224
12. Luque MC, Gutierrez PS, Debbas V, Kalil J, Stolf BS. CD100 and plexins B2 and B1 mediate monocyte-endothelial cell adhesion and might take part in atherogenesis. *Mol Immunol* (2015) 67(2 Pt B):559–67. doi:10.1016/j.molimm.2015.07.028
13. Biancone L, Bowen MA, Lim A, Aruffo A, Andres G, Stamenkovic I. Identification of a novel inducible cell-surface ligand of CD5 on activated lymphocytes. *J Exp Med* (1996) 184(3):811–9. doi:10.1084/jem.184.3.811
14. Gordon J. B-cell signalling via the C-type lectins CD23 and CD72. *Immunol Today* (1994) 15(9):411–7. doi:10.1016/0167-5699(94)90270-4
15. Kataoka TR, Kumanogoh A, Hirata M, Moriyoshi K, Ueshima C, Kawahara M, et al. CD72 regulates the growth of KIT-mutated leukemia cell line Kasumi-1. *Sci Rep* (2013) 3:2861. doi:10.1038/srep02861
16. Kumanogoh A, Kikutani H. Biological functions and signaling of a transmembrane semaphorin, CD100/Sema4D. *Cell Mol Life Sci* (2004) 61(3):292–300. doi:10.1007/s00018-003-3257-7
17. Artigiani S, Barberis D, Fazzari P, Longati P, Angelini P, van de Loo JW, et al. Functional regulation of semaphorin receptors by proprotein convertases. *J Biol Chem* (2003) 278(12):10094–101. doi:10.1074/jbc.M210156200
18. Gherardi E, Love CA, Esnouf RM, Jones EY. The sema domain. *Curr Opin Struct Biol* (2004) 14(6):669–78. doi:10.1016/j.sbi.2004.10.010
19. Wells CM, Jones GE. The emerging importance of group II PAKs. *Biochem J* (2010) 425(3):465–73. doi:10.1042/BJ20091173
20. Vikis HG, Li W, Guan KL. The plexin-B1/Rac interaction inhibits PAK activation and enhances Sema4D ligand binding. *Genes Dev* (2002) 16(7):836–45. doi:10.1101/gad.966402
21. Oinuma I, Katoh H, Negishi M. Semaphorin 4D/Plexin-B1-mediated R-Ras GAP activity inhibits cell migration by regulating beta(1) integrin activity. *J Cell Biol* (2006) 173(4):601–13. doi:10.1083/jcb.200508204

22. Ito Y, Oinuma I, Katoh H, Kaibuchi K, Negishi M. Sema4D/plexin-B1 activates GSK-3beta through R-Ras GAP activity, inducing growth cone collapse. *EMBO Rep* (2006) 7(7):704–9. doi:10.1038/sj.embor.7400737
23. Swiercz JM, Worzfeld T, Offermanns S. ErbB-2 and met reciprocally regulate cellular signaling via plexin-B1. *J Biol Chem* (2008) 283(4):1893–901. doi:10.1074/jbc.M706822200
24. Swiercz JM, Kuner R, Offermanns S. Plexin-B1/RhoGEF-mediated RhoA activation involves the receptor tyrosine kinase ErbB-2. *J Cell Biol* (2004) 165(6):869–80. doi:10.1083/jcb.200312094
25. Swiercz JM, Worzfeld T, Offermanns S. Semaphorin 4D signaling requires the recruitment of phospholipase C gamma into the plexin-B1 receptor complex. *Mol Cell Biol* (2009) 29(23):6321–34. doi:10.1128/MCB.00103-09
26. Aurandt J, Vikis HG, Gutkind JS, Ahn N, Guan KL. The semaphorin receptor plexin-B1 signals through a direct interaction with the Rho-specific nucleotide exchange factor, LARG. *Proc Natl Acad Sci U S A* (2002) 99(19):12085–90. doi:10.1073/pnas.142433199
27. Aurandt J, Li W, Guan KL. Semaphorin 4D activates the MAPK pathway downstream of plexin-B1. *Biochem J* (2006) 394(Pt 2):459–64. doi:10.1042/BJ20051123
28. Oinuma I, Ishikawa Y, Katoh H, Negishi M. The semaphorin 4D receptor plexin-B1 is a GTPase activating protein for R-Ras. *Science* (2004) 305(5685):862–5. doi:10.1126/science.1097545
29. Basile JR, Afkhami T, Gutkind JS. Semaphorin 4D/plexin-B1 induces endothelial cell migration through the activation of PYK2, Src, and the phosphatidylinositol 3-kinase-Akt pathway. *Mol Cell Biol* (2005) 25(16):6889–98. doi:10.1128/MCB.25.16.6889-6898.2005
30. Bottaro DP, Rubin JS, Faletto DL, Chan AM, Kmiecik TE, Vande Woude GF, et al. Identification of the hepatocyte growth factor receptor as the c-met proto-oncogene product. *Science* (1991) 251(4995):802–4. doi:10.1126/science.1846706
31. Gaudino G, Follenzi A, Naldini L, Collesi C, Santoro M, Gallo KA, et al. RON is a heterodimeric tyrosine kinase receptor activated by the HGF homologue MSP. *EMBO J* (1994) 13(15):3524–32.
32. Sun T, Krishnan R, Swiercz JM. Grb2 mediates semaphorin-4D-dependent RhoA inactivation. *J Cell Sci* (2012) 125(Pt 15):3557–67. doi:10.1242/jcs.101063
33. Love CA, Harlos K, Mavaddat N, Davis SJ, Stuart DI, Jones EY, et al. The ligand-binding face of the semaphorins revealed by the high-resolution crystal structure of SEMA4D. *Nat Struct Biol* (2003) 10(10):843–8. doi:10.1038/nsb977
34. McHugh KP, Hodivala-Dilke K, Zheng MH, Namba N, Lam J, Novack D, et al. Mice lacking beta3 integrins are osteosclerotic because of dysfunctional osteoclasts. *J Clin Invest* (2000) 105(4):433–40. doi:10.1172/JCI8905
35. Dacquin R, Domenget C, Kumanogoh A, Kikutani H, Jurdic P, Machuca-Gayet I. Control of bone resorption by semaphorin 4D is dependent on ovarian function. *PLoS One* (2011) 6(10):e26627. doi:10.1371/journal.pone.0026627
36. Deb Roy A, Yin T, Choudhary S, Rodionov V, Pilbeam CC, Wu YI. Optogenetic activation of Plexin-B1 reveals contact repulsion between osteoclasts and osteoblasts. *Nat Commun* (2017) 8:15831. doi:10.1038/ncomms15831
37. Zhang Y, Feng E, Xu Y, Wang W, Zhang T, Xiao L, et al. Serum Sema4D levels are associated with lumbar spine bone mineral density and bone turnover markers in patients with postmenopausal osteoporosis. *Int J Clin Exp Med* (2015) 8(9):16352–7.
38. Anastasilakis AD, Polyzos SA, Makras P, Gkiomisi A, Sakellariou G, Savvidis M, et al. Circulating semaphorin-4D and plexin-B1 levels in postmenopausal women with low bone mass: the 3-month effect of zoledronic acid, denosumab or teriparatide treatment. *Expert Opin Ther Targets* (2015) 19(3):299–306. doi:10.1517/14728222.2014.983078
39. Sekimoto T, Ishii M, Emi M, Kurogi S, Funamoto T, Hamada H, et al. Segmental copy number loss in the region of semaphorin 4D gene in patients with acetabular dysplasia. *J Orthop Res* (2013) 31(6):957–61. doi:10.1002/jor.22310
40. Yoshida Y, Ogata A, Kang S, Ebina K, Shi K, Nojima S, et al. Semaphorin 4D contributes to rheumatoid arthritis by inducing inflammatory cytokine production: pathogenic and therapeutic implications. *Arthritis Rheumatol* (2015) 67(6):1481–90. doi:10.1002/art.39086
41. Movila A, Mawardi H, Nishimura K, Kiyama T, Egashira K, Kim JY, et al. Possible pathogenic engagement of soluble semaphorin 4D produced by gammadelta T cells in medication-related osteonecrosis of the jaw (MRONJ). *Biochem Biophys Res Commun* (2016) 480(1):42–7. doi:10.1016/j.bbrc.2016.10.012
42. Hopwood B, Gronthos S, Kuliwaba JS, Robey PG, Findlay DM, Fazzalari NL. Identification of differentially expressed genes between osteoarthritic and normal trabecular bone from the intertrochanteric region of the proximal femur using cDNA microarray analysis. *Bone* (2005) 36(4):635–44. doi:10.1016/j.bone.2005.02.003
43. Liu B, Ma Y, Yi J, Xu Z, Zhang YS, Zhang C, et al. Elevated plasma soluble Sema4D/CD100 levels are associated with disease severity in patients of hemorrhagic fever with renal syndrome. *PLoS One* (2013) 8(9):e73958. doi:10.1371/journal.pone.0073958
44. Wang X, Kumanogoh A, Watanabe C, Shi W, Yoshida K, Kikutani H. Functional soluble CD100/Sema4D released from activated lymphocytes: possible role in normal and pathologic immune responses. *Blood* (2001) 97(11):3498–504. doi:10.1182/blood.V97.11.3498
45. Xiang L, You T, Chen J, Xu W, Jiao Y. Serum soluble semaphorin 4D is associated with left atrial diameter in patients with atrial fibrillation. *Med Sci Monit* (2015) 21:2912–7. doi:10.12659/MSM.895441
46. Huang C, Wang Y, Huang JH, Liu W. Sema3A drastically suppresses tumor growth in oral cancer Xenograft model of mice. *BMC Pharmacol Toxicol* (2017) 18(1):55. doi:10.1186/s40360-017-0163-4
47. Liu MH, Fu WJ, Cui YH, Guo QN, Zhou Y. Downregulation of semaphorin-3F is associated with poor prognostic significance in osteosarcoma patients. *Am J Cancer Res* (2016) 6(10):2252–62.
48. Dorfman DM, Shahsafaei A, Nadler LM, Freeman GJ. The leukocyte semaphorin CD100 is expressed in most T-cell, but few B-cell, non-Hodgkin's lymphomas. *Am J Pathol* (1998) 153(1):255–62. doi:10.1016/S0002-9440(10)65566-6
49. Jiang H, Chen C, Sun Q, Wu J, Qiu L, Gao C, et al. The role of semaphorin 4D in tumor development and angiogenesis in human breast cancer. *Onco Targets Ther* (2016) 9:5737–50. doi:10.2147/OTT.S114708
50. Deaglio S, Vaisitti T, Bergui L, Bonello L, Horenstein AL, Tamagnone L, et al. CD38 and CD100 lead a network of surface receptors relaying positive signals for B-CLL growth and survival. *Blood* (2005) 105(8):3042–50. doi:10.1182/blood-2004-10-3873
51. Granziero L, Circosta P, Scielzo C, Frisaldi E, Stella S, Geuna M, et al. CD100/Plexin-B1 interactions sustain proliferation and survival of normal and leukemic CD5+ B lymphocytes. *Blood* (2003) 101(5):1962–9. doi:10.1182/blood-2002-05-1339
52. Gabrovska PN, Smith RA, Tiang T, Weinstein SR, Haupt LM, Griffiths LR. Semaphorin-plexin signalling genes associated with human breast tumourigenesis. *Gene* (2011) 489(2):63–9. doi:10.1016/j.gene.2011.08.024
53. Malik MF, Ye L, Jiang WG. Reduced expression of semaphorin 4D and plexin-B in breast cancer is associated with poorer prognosis and the potential linkage with oestrogen receptor. *Oncol Rep* (2015) 34(2):1049–57. doi:10.3892/or.2015.4015
54. Ross RW, Galsky MD, Scher HI, Magidson J, Wassmann K, Lee GS, et al. A whole-blood RNA transcript-based prognostic model in men with castration-resistant prostate cancer: a prospective study. *Lancet Oncol* (2012) 13(11):1105–13. doi:10.1016/S1470-2045(12)70263-2
55. Cao J, Zhang C, Chen T, Tian R, Sun S, Yu X, et al. Plexin-B1 and semaphorin 4D cooperate to promote cutaneous squamous cell carcinoma cell proliferation, migration and invasion. *J Dermatol Sci* (2015) 79(2):127–36. doi:10.1016/j.jdermsci.2015.05.002
56. Kato S, Kubota K, Shimamura T, Shinohara Y, Kobayashi N, Watanabe S, et al. Semaphorin 4D, a lymphocyte semaphorin, enhances tumor cell motility through binding its receptor, plexinB1, in pancreatic cancer. *Cancer Sci* (2011) 102(11):2029–37. doi:10.1111/j.1349-7006.2011.02053.x
57. Moriarity BS, Otto GM, Rahrmann EP, Rathe SK, Wolf NK, Weg MT, et al. A Sleeping Beauty forward genetic screen identifies new genes and pathways driving osteosarcoma development and metastasis. *Nat Genet* (2015) 47(6):615–24. doi:10.1038/ng.3293
58. Williamson M, de Winter P, Masters JR. Plexin-B1 signalling promotes androgen receptor translocation to the nucleus. *Oncogene* (2016) 35(8):1066–72. doi:10.1038/onc.2015.160
59. Rody A, Holtrich U, Gaetje R, Gehrmann M, Engels K, von Minckwitz G, et al. Poor outcome in estrogen receptor-positive breast cancers predicted by loss of plexin B1. *Clin Cancer Res* (2007) 13(4):1115–22. doi:10.1158/1078-0432.CCR-06-2433
60. Binmadi NO, Yang YH, Zhou H, Proia P, Lin YL, De Paula AM, et al. Plexin-B1 and semaphorin 4D cooperate to promote perineural invasion in a RhoA/

ROK-dependent manner. *Am J Pathol* (2012) 180(3):1232–42. doi:10.1016/j.ajpath.2011.12.009
61. Wong OG, Nitkunan T, Oinuma I, Zhou C, Blanc V, Brown RS, et al. Plexin-B1 mutations in prostate cancer. *Proc Natl Acad Sci U S A* (2007) 104(48):19040–5. doi:10.1073/pnas.0702544104
62. Balakrishnan A, Penachioni JY, Lamba S, Bleeker FE, Zanon C, Rodolfo M, et al. Molecular profiling of the "plexinome" in melanoma and pancreatic cancer. *Hum Mutat* (2009) 30(8):1167–74. doi:10.1002/humu.21017
63. Stevens L, McClelland L, Fricke A, Williamson M, Kuo I, Scott G. Plexin B1 suppresses c-Met in melanoma: a role for plexin B1 as a tumor-suppressor protein through regulation of c-Met. *J Invest Dermatol* (2010) 130(6):1636–45. doi:10.1038/jid.2010.13
64. Gomez Roman JJ, Garay GO, Saenz P, Escuredo K, Sanz Ibayondo C, Gutkind S, et al. Plexin B1 is downregulated in renal cell carcinomas and modulates cell growth. *Transl Res* (2008) 151(3):134–40. doi:10.1016/j.trsl.2007.12.003
65. Damola A, Legendre A, Ball S, Masters JR, Williamson M. Function of mutant and wild-type plexinb1 in prostate cancer cells. *Prostate* (2013) 73(12):1326–35. doi:10.1002/pros.22678
66. Conrotto P, Corso S, Gamberini S, Comoglio PM, Giordano S. Interplay between scatter factor receptors and B plexins controls invasive growth. *Oncogene* (2004) 23(30):5131–7. doi:10.1038/sj.onc.1207650
67. Zhou H, Kann MG, Mallory EK, Yang YH, Bugshan A, Binmadi NO, et al. Recruitment of Tiam1 to semaphorin 4D activates Rac and enhances proliferation, invasion, and metastasis in oral squamous cell carcinoma. *Neoplasia* (2017) 19(2):65–74. doi:10.1016/j.neo.2016.12.004
68. Basile JR, Barac A, Zhu T, Guan KL, Gutkind JS. Class IV semaphorins promote angiogenesis by stimulating Rho-initiated pathways through plexin-B. *Cancer Res* (2004) 64(15):5212–24. doi:10.1158/0008-5472.CAN-04-0126
69. Conrotto P, Valdembri D, Corso S, Serini G, Tamagnone L, Comoglio PM, et al. Sema4D induces angiogenesis through Met recruitment by Plexin B1. *Blood* (2005) 105(11):4321–9. doi:10.1182/blood-2004-07-2885
70. Yang YH, Zhou H, Binmadi NO, Proia P, Basile JR. Plexin-B1 activates NF-kappaB and IL-8 to promote a pro-angiogenic response in endothelial cells. *PLoS One* (2011) 6(10):e25826. doi:10.1371/journal.pone.0025826
71. Zhou H, Yang YH, Binmadi NO, Proia P, Basile JR. The hypoxia-inducible factor-responsive proteins semaphorin 4D and vascular endothelial growth factor promote tumor growth and angiogenesis in oral squamous cell carcinoma. *Exp Cell Res* (2012) 318(14):1685–98. doi:10.1016/j.yexcr.2012.04.019
72. Sun Q, Zhou H, Binmadi NO, Basile JR. Hypoxia-inducible factor-1-mediated regulation of semaphorin 4D affects tumor growth and vascularity. *J Biol Chem* (2009) 284(46):32066–74. doi:10.1074/jbc.M109.057166
73. Zhou H, Yang YH, Basile JR. The semaphorin 4D-plexin-B1-RhoA signaling axis recruits pericytes and regulates vascular permeability through endothelial production of PDGF-B and ANGPTL4. *Angiogenesis* (2014) 17(1):261–74. doi:10.1007/s10456-013-9395-0
74. Ding X, Qiu L, Zhang L, Xi J, Li D, Huang X, et al. The role of semaphorin 4D as a potential biomarker for antiangiogenic therapy in colorectal cancer. *Onco Targets Ther* (2016) 9:1189–204. doi:10.2147/OTT.S98906
75. Zhou H, Binmadi NO, Yang YH, Proia P, Basile JR. Semaphorin 4D cooperates with VEGF to promote angiogenesis and tumor progression. *Angiogenesis* (2012) 15(3):391–407. doi:10.1007/s10456-012-9268-y
76. Liu H, Yang Y, Xiao J, Yang S, Liu Y, Kang W, et al. Semaphorin 4D expression is associated with a poor clinical outcome in cervical cancer patients. *Microvasc Res* (2014) 93:1–8. doi:10.1016/j.mvr.2014.02.007
77. Younis RH, Han KL, Webb TJ. Human head and neck squamous cell carcinoma-associated semaphorin 4D induces expansion of myeloid-derived suppressor cells. *J Immunol* (2016) 196(3):1419–29. doi:10.4049/jimmunol.1501293
78. Delaire S, Billard C, Tordjman R, Chedotal A, Elhabazi A, Bensussan A, et al. Biological activity of soluble CD100. II. Soluble CD100, similarly to H-SemaIII, inhibits immune cell migration. *J Immunol* (2001) 166(7):4348–54. doi:10.4049/jimmunol.166.7.4348
79. Hao NB, Lu MH, Fan YH, Cao YL, Zhang ZR, Yang SM. Macrophages in tumor microenvironments and the progression of tumors. *Clin Dev Immunol* (2012) 2012:948098. doi:10.1155/2012/948098
80. Basile JR, Holmbeck K, Bugge TH, Gutkind JS. MT1-MMP controls tumor-induced angiogenesis through the release of semaphorin 4D. *J Biol Chem* (2007) 282(9):6899–905. doi:10.1074/jbc.M609570200
81. Silbermann R, Roodman GD. Current controversies in the management of myeloma bone disease. *J Cell Physiol* (2016) 231(11):2374–9. doi:10.1002/jcp.25351
82. Galson DL, Silbermann R, Roodman GD. Mechanisms of multiple myeloma bone disease. *Bonekey Rep* (2012) 1:135. doi:10.1038/bonekey.2012.135
83. Beuzeboc P, Scholl S. Prevention of bone metastases in breast cancer patients. Therapeutic perspectives. *J Clin Med* (2014) 3(2):521–36. doi:10.3390/jcm3020521
84. Suvannasankha A, Crean CD, Tompkins DR, Delgado-Calle J, Bellido TM, David Roodman G, et al. Regulation of osteoblast function in myeloma bone disease by semaphorin 4D. *Blood* (2016) 128:4439.
85. Parmo-Cabanas M, Molina-Ortiz I, Matias-Roman S, Garcia-Bernal D, Carvajal-Vergara X, Valle I, et al. Role of metalloproteinases MMP-9 and MT1-MMP in CXCL12-promoted myeloma cell invasion across basement membranes. *J Pathol* (2006) 208(1):108–18. doi:10.1002/path.1876
86. Fisher TL, Reilly CA, Winter LA, Pandina T, Jonason A, Scrivens M, et al. Generation and preclinical characterization of an antibody specific for SEMA4D. *MAbs* (2016) 8(1):150–62. doi:10.1080/19420862.2015.1102813
87. LaGanke C, Samkoff L, Edwards K, Jung Henson L, Repovic P, Lynch S, et al. Safety/tolerability of the anti-semaphorin 4D Antibody VX15/2503 in a randomized phase 1 trial. *Neurol Neuroimmunol Neuroinflamm* (2017) 4(4):e367. doi:10.1212/NXI.0000000000000367
88. Patnaik A, Weiss GJ, Leonard JE, Rasco DW, Sachdev JC, Fisher TL, et al. Safety, pharmacokinetics, and pharmacodynamics of a humanized anti-semaphorin 4D antibody, in a first-in-human study of patients with advanced solid tumors. *Clin Cancer Res* (2016) 22(4):827–36. doi:10.1158/1078-0432.CCR-15-0431
89. Matsunaga Y, Bashiruddin NK, Kitago Y, Takagi J, Suga H. Allosteric inhibition of a semaphorin 4D receptor plexin B1 by a high-affinity macrocyclic peptide. *Cell Chem Biol* (2016) 23(11):1341–50. doi:10.1016/j.chembiol.2016.09.015
90. Zhang Y, Wei L, Miron RJ, Shi B, Bian Z. Anabolic bone formation via a site-specific bone-targeting delivery system by interfering with semaphorin 4D expression. *J Bone Miner Res* (2015) 30(2):286–96. doi:10.1002/jbmr.2322
91. Zhang Y, Wei L, Miron RJ, Zhang Q, Bian Z. Prevention of alveolar bone loss in an osteoporotic animal model via interference of semaphorin 4D. *J Dent Res* (2014) 93(11):1095–100. doi:10.1177/0022034514552676

Conflict of Interest Statement: The authors declare that the research was conducted in the absence of any commercial or financial relationships that could be construed as a potential conflict of interest.

frontiers in Endocrinology

ORIGINAL RESEARCH
published: 29 June 2018
doi: 10.3389/fendo.2018.00344

XRK3F2 Inhibition of p62-ZZ Domain Signaling Rescues Myeloma-Induced GFI1-Driven Epigenetic Repression of the *Runx2* Gene in Pre-osteoblasts to Overcome Differentiation Suppression

Juraj Adamik[1†], Rebecca Silbermann[2,3†], Silvia Marino[2], Quanhong Sun[1], Judith L. Anderson[2], Dan Zhou[2], Xiang-Qun Xie[4], G. David Roodman[2,5] and Deborah L. Galson[1]*

[1] Division of Hematology/Oncology, Department of Medicine, UPMC Hillman Cancer Center, The McGowan Institute for Regenerative Medicine, University of Pittsburgh, Pittsburgh, PA, United States, [2] Division of Hematology-Oncology, Department of Medicine, Indiana University, Indianapolis, IN, United States, [3] Hematology and Medical Oncology, Knight Cancer Institute, Oregon Health & Science University, Portland, OR, United States, [4] Department of Pharmaceutical Sciences, School of Pharmacy, University of Pittsburgh, Pittsburgh, PA, United States, [5] Richard L. Roudebush VA Medical Center, Indianapolis, IN, United States

OPEN ACCESS

Edited by:
Julie A. Sterling, Vanderbilt University, United States

Reviewed by:
Sanja Štifter, Faculty of Medicine, University of Rijeka, Croatia
Michelle Anne Lawson, University of Sheffield, United Kingdom

***Correspondence:**
Deborah L. Galson
galson@pitt.edu;
dlgalson@gmail.com

[†]These authors have contributed equally to this work.

Specialty section:
This article was submitted to Bone Research, a section of the journal Frontiers in Endocrinology

Received: *09 March 2018*
Accepted: *07 June 2018*
Published: *29 June 2018*

Citation:
Adamik J, Silbermann R, Marino S, Sun Q, Anderson JL, Zhou D, Xie X-Q, Roodman GD and Galson DL (2018) XRK3F2 Inhibition of p62-ZZ Domain Signaling Rescues Myeloma-Induced GFI1-Driven Epigenetic Repression of the Runx2 Gene in Pre-osteoblasts to Overcome Differentiation Suppression. Front. Endocrinol. 9:344. doi: 10.3389/fendo.2018.00344

Multiple myeloma bone disease (MMBD) is characterized by non-healing lytic bone lesions that persist even after a patient has achieved a hematologic remission. We previously reported that p62 (sequestosome-1) in bone marrow stromal cells (BMSC) is critical for the formation of MM-induced signaling complexes that mediate OB suppression. Importantly, XRK3F2, an inhibitor of the p62-ZZ domain, blunted MM-induced *Runx2* suppression *in vitro*, and induced new bone formation and remodeling in the presence of tumor *in vivo*. Additionally, we reported that MM cells induce the formation of repressive chromatin on the *Runx2* gene in BMSC via direct binding of the transcriptional repressor GFI1, which recruits the histone modifiers, histone deacetylase 1 (HDAC1) and Enhancer of zeste homolog 2 (EZH2). In this study we investigated the mechanism by which blocking p62-ZZ domain-dependent signaling prevents MM-induced suppression of *Runx2* in BMSC. XRK3F2 prevented MM-induced upregulation of *Gfi1* and repression of the *Runx2* gene when present in MM-preOB co-cultures. We also show that p62-ZZ-domain blocking by XRK3F2 also prevented MM conditioned media and TNF plus IL7-mediated *Gfi1* mRNA upregulation and the concomitant *Runx2* repression, indicating that XRK3F2's prevention of p62-ZZ domain signaling within preOB is involved in the response. Chromatin immunoprecipitation (ChIP) analyses revealed that XRK3F2 decreased MM-induced GFI1 occupancy at the *Runx2-P1* promoter and prevented recruitment of HDAC1, thus preserving the transcriptionally permissive chromatin mark H3K9ac on *Runx2* and allowing osteogenic differentiation. Furthermore, treatment of MM-exposed preOB with XRK3F2 after MM removal decreased GFI1 enrichment at *Runx2*-P1 and rescued MM-induced suppression of *Runx2* mRNA and its

downstream osteogenic gene targets together with increased osteogenic differentiation. Further, primary BMSC (hBMSC) from MM patients (MM-hBMSC) had little ability to increase H3K9ac on the *Runx2* promoter in osteogenic conditions when compared to hBMSC from healthy donors (HD). XRK3F2 treatment enriched *Runx2* gene H3K9ac levels in MM-hBMSC to the level observed in HD-hBMSC, but did not alter HD-hBMSC H3K9ac. Importantly, XRK3F2 treatment of long-term MM-hBMSC cultures rescued osteogenic differentiation and mineralization. Our data show that blocking p62-ZZ domain-dependent signaling with XRK3F2 can reverse epigenetic-based mechanisms of MM-induced *Runx2* suppression and promote osteogenic differentiation.

Keywords: myeloma bone disease, p62-ZZ domain inhibitor, XRK3F2, GFI1, HDAC1, epigenetic, osteoblast suppression, chromatin immunoprecipitation

INTRODUCTION

Multiple myeloma (MM) is the second most common hematologic malignancy and the most frequent cancer to involve bone (1, 2). Over 80% of patients develop osteolytic bone lesions that can result in severe bone pain, frequent pathological fractures and hasten mortality (3–5). MM patients with fractures have a 20% increased risk of death as compared to MM patients without fractures (4). Therefore, the clinical and economic impact of bone disease in patients with MM can be catastrophic. MM cells in the bone marrow microenvironment increase osteoclast (OCL) differentiation, which generates the bone lesions (6). Unfortunately, MM bone lesions rarely heal due to MM-induced alteration of osteoblast precursors (preOB) within the bone marrow stromal cell (BMSC) population that prevents their differentiation into bone-forming osteoblasts (OB) (7). In addition, the MM altered bone microenvironment enhances support of MM growth, survival, and drug-resistance (8). Importantly, the MM-induced OB suppression persists after eradication of MM cells, suggesting that MM cells induce repressive, heritable, epigenetic changes at the *Runx2* gene, the key transcription factor required for OB differentiation (9). Thus, new bone formation at the site of MM lytic lesions is suppressed or absent, resulting in lesions that persist after MM cells are eradicated (7). Although new therapies for MM that target both MM cells and the bone compartment have greatly improved progression-free survival and overall survival, most patients eventually develop resistance to the available treatments and MM remains an incurable disease (10). Further, although proteasome inhibitors have been reported to transiently increase bone formation in MM patients (11), a lack of anabolic bone agents that can reliably repair bone lesions in MM patients remains a major clinical challenge. Thus, studies that address the underlying pathophysiology of MM effects on the bone environment are critical to develop new approaches to improve the quality of life and enhance the survival of MM patients.

Increasing evidence demonstrates that BMSCs from MM patients display distinctive tumor-promoting features and impaired osteogenic differentiation as compared to normal donors (12). Several deregulated signaling molecules and receptor pathways, including the Wnt signaling inhibitor DKK1 (13), sclerostin (14), the cytokines IL3, IL7, TNFα (15, 16), and the chemokine cytokine ligand 3 (CCL3) (17), are associated with anti-osteogenic, pro-osteolytic and growth-supporting properties of the myeloma tumor-microenvironment. However, the mechanisms responsible for the prolonged propagation of osteogenic-inhibition of MM-BMSCs in the absence of persistent myeloma signals are still largely unresolved.

The autophagic cargo receptor and signaling platform protein p62 (sequestosome-1) is an important modulator of bone turnover, and mutations associated with its impaired function result in skeletal disorders such as Paget's disease of bone (18). As a scaffold protein, p62 is a multi-domain adaptor protein modulates and integrates signaling by interacting directly with signaling proteins from multiple cell surface receptors (e.g., TNFα-TNFR signaling mediated via the RIP1 binding domain of p62 (ZZ domain) and RANKL-RANK, IL1β-ILIR, NGF-TrkA mediated via the TRAF6 binding domain of p62), connecting them to multiple downstream pathways (e.g., NFκB, p38 MAPK, PKCζ, JNK) [for a review see (19)]. This multifunctional protein also serves as a scaffold molecule connecting proteasomal and autophagic protein degradation (20). Its elevated expression is also associated with increased resistance to proteasome inhibitors in MM (21, 22).

TNFα induces RIP1 interaction with the ZZ domain of p62. A study by Hiruma et al. (23) demonstrated that p62 is required for stromal cell support of MM growth and OCL formation (23). Both MM cell and TNFα required the presence of p62 in BMSC (23) for their induction of the protein levels of vascular cell adhesion molecule-1 (VCAM1), which mediates BMSC-MM cell interactions (24), IL6, a pro-inflammatory and myeloma pro-survival factor (25), and RANKL, important for osteoclastogenesis (26, 27). Importantly, the p62-ZZ domain was found through deletion analyses to be specifically required for these activities (28). We recently reported the identification of a novel small molecule inhibitor the p62-ZZ domain of signaling, XRK3F2, that blocks TNFα and MM activation of downstream signaling from the p62-signaling hub (29). In addition, XRK3F2 also directly decreased OCL formation. Further, XRK3F2 directly inhibited cell growth of primary CD138+ MM cells and human MM cell lines *in vitro*, without negatively affecting the growth of BMSC. However, XRK3F2 did not reduce MM growth in a

5TGM1-MM mouse model. Surprisingly, a periosteal reaction was observed in the tibiae directly injected with MM and treated with XRK3F2, but not in the contralateral non-MM-injected limb or saline-injected controls, indicating that XRK3F2 induced new cortical bone formation in the 5TGM1-murine model of Multiple myeloma bone disease (MMBD) *in vivo* (29).

We reported that BMSC from MM patients expressed elevated levels of the transcriptional repressor GFI1 at both the RNA and protein level (30). Similarly, GFI1 was elevated in murine BMSC exposed to MM *in vitro* or *in vivo*. Knock-down of GFI1 was found to decrease the ability of MM to induce OB suppression and could reverse established Runx2 repression (30). GFI1 is a transcriptional repressor of *Runx2* in BMSC that directly binds and recruits the chromatin corepressor complex consisting of HDAC1 and EZH2 to the *Runx2-P1* promoter (31). Enrichment of these histone modifiers inhibits transcriptional activity of *Runx2* by reducing the active chromatin mark acetylated histone H3 at lysine 9 (H3K9ac) and enhancing the repressive chromatin mark trimethylated H3 at lysine 27 (H3K27me3) at the *Runx2* promoter (31). This epigenetic-based mechanism maintains inhibition of the *Runx2-P1* promoter even in the absence of MM exposure, which results in a prolonged suppression of BMSC differentiation into OB. In a study by Wang et al. (32), downregulation of GFI1 in response to AMPK activation in MC4 preOB upregulated gene expression of the osteogenic mediator *Osteopontin* (*Opn*), which promoted osteogenesis. The molecular function of GFI1 has been primarily investigated during the differentiation of lymphoid and myeloid cells (33, 34), and there are only a few reports of its activity in osteogenic cells and very little is known about its transcriptional and post-translational regulation (35, 36). We tested the hypothesis that XRK3F2 might be generating new bone growth in MM-bearing bone by blocking GFI1 epigenetic repression of *Runx2*.

MATERIALS AND METHODS

Reagents

Cell culture media, penicillin and streptomycin (pen/strep), DTT, and all DNA primers were from Invitrogen. FCS was from Atlanta Biologicals (S12450). Ascorbic acid (A4403) was from Sigma-Aldrich. Histone 3 (H3) (9715) Ab was from Cell Signaling. Chromatin immunoprecipitation (ChIP) Abs for H3K9ac (61251) and HDAC1 (40967) were from Active Motif. GFI1 (ab21061) Ab was from Abcam. GoTaq Flexi DNA polymerase was from Promega. TRIzol reagent (10296028) was from Life Technologies. Mouse recombinant TNFα (410-MT) was from R&D Systems.

Cell Lines, Primary Murine BMSC, and Co-cultures

All cultures described below contained 10% FCS-1% pen/strep. The pre-OB murine cell line MC3T3-E1 subclone-4 (MC4) was obtained from Dr. Guozhi Xiao (37, 38) in 2009 and subclone-14 (MC14) was obtained from ATCC (CRL-2594) in 2014. MC3T3-E1 subclone-4 (MC4) was used in experiment 1A and MC3T3-E1 subclone-14 (MC4) was used for the rest of the experiments. Both were maintained in ascorbic acid-free αMEM proliferation media. MM cell lines were generously provided by Dr. Steven Rosen (MM1.S) and Babtunde O Oyajobi (5TGM1) were maintained in RPMI1640. The stably transduced murine 5TGM1-GFP-TK (5TGM1) MM cells (30) and human MM1.S-GFP cells (23) were previously described. Cell lines were authenticated by morphology, gene expression profile, and tumorigenic capacity (MM cells). MC4 cells were grown to 90% confluency prior to co-culture. MM1.S Conditioned media was generated by growing MM1.S cells for 24 h at confluence of 1×10^6 cells/ml. Harvested media was filtered using a 0.22-μm filter prior to its use in experiments. Direct 5TGM1-MC4 (10:1) co-cultures and indirect co-cultures of MM1.S cells in transwells (10:1) with MC4(14) cells were carried out in 50:50 RPMI1640/αMEM proliferation media. MM1.S in transwells (Corning Inc., 3450) or 5TGM1 cells were carefully removed (FACS analysis demonstrated that ≤1% 5TGM1 cells remained). The MC4 (14) cells were isolated immediately or subjected to OB differentiation first. BM cells were isolated from C57BL/6 mice femurs and tibia. Animal studies were approved by the IACUC at the VA Pittsburgh Healthcare System. BM cells were harvested from tibiae and femurs as previously described (30). After overnight incubation, the non-adherent cells were removed and the remaining stromal cell population was washed with PBS and maintained in ascorbic acid-free αMEM-10% FCS, 1% pen/strep proliferation media. BMSC were expanded for 2.5 weeks to reach optimal confluence. Co-cultures with MM cells or cytokine treatments and RNA preparation analyses were conducted as described for MC4 cells.

Human Samples and Primary hBMSC Cultures

BM aspirates were collected in heparin from 5 healthy donors and 7 MM patients. This study was carried out in accordance with the recommendations and protocol approvals by the University of Pittsburgh and Indiana University Institutional Review Boards (IRBs). All subjects gave written informed consent in accordance with the Declaration of Helsinki. BM mononuclear cells were separated by Ficoll-Hypaque density sedimentation and the nonadherent cells removed after overnight incubation in Iscove's Modified Dulbecco's Medium (IMDM)-10%FCS. The adherent cultures were then continued for 21 d with media changes every 4 d to obtain BMSC. Subconfluent cells were detached with trypsin and replated (10^5 cells/10-cm dish) for use at passage 2 and 3.

OB Differentiation, and Alkaline Phosphatase and Alizarin Red Assays

OB differentiation media (αMEM supplemented with 50 μg/ml ascorbic acid and 10 mM β-glycerophosphate, and 10 nM Dex) was added to primary hBMSC; media was changed every 3 days. Alkaline phosphatase staining was performed using SIGMAFAST BCIP/NBT (Sigma, B5655-5TAB) protocol. Mineralization at 20 days was assessed using alizarin red staining (30). The staining

density quantitation was carried out using a ProteinSimple FluorChem™ M imaging system.

Real-Time Quantitative PCR (*q*PCR) RNA Expression Analyses

RNA was isolated using TRIzol reagent and converted to cDNA using First-Strand cDNA Synthesis System (Life Technologies, 11904-018). *q*PCR was carried out using 2x Maxima SYBR Green/ROX *q*PCR Master Mix (K0223, Thermo Fisher) in Fast 96-Well Reaction Plates (Applied Biosystems) using a StepOnePlus (Applied Biosystems). Relative mRNA levels were calculated using the ΔΔCt method using *18SrRNA* for normalization. The *q*PCR primers are listed in **Table 1.**

Chip Assays

Chromatin from MC4 cells, MM-BMSC, and HD-BMSC was analyzed using a modification of the ChIP Millipore/Upstate protocol (MCPROTO407) as described (31, 39) using Magna ChIP Protein A+G Beads (16-663, Millipore). In brief, a total of 2×10^7 cells were fixed in 1% formaldehyde (F79-500, Fisher) for 10 min at room temperature. Samples were sonicated (to generate DNA fragments of 250 base pairs (bp) average length) on ice using a Fisher Scientific Sonic Dismembrator (Model 100) and centrifuged at 12,000 RPM for 10 min. Chromatin from 4×10^6 cells was diluted 7-fold in ChIP Dilution Buffer (0.01% SDS, 1.1% Triton X-100, 1.2 mM EDTA, 16.7 mM Tris-HCl, pH8.1, 167 mM NaCl) and incubated at 4°C overnight with respective antibodies. Aliquots for input and non-specific IgG control samples were included with each experiment. IgG ChIP was run on untreated MC4 samples. ChIP-*q*PCR primers are listed in **Table 2**. Fold enrichment was calculated based on Ct as $2^{(\Delta Ct)}$, where $\Delta Ct = (Ct_{Input} - Ct_{IP})$. The IgG ΔCt was subtracted from the specific Ab ΔCt to generate $\Delta\Delta Ct = (\Delta Ct_{specificAb} - \Delta Ct_{IgG})$.

Statistical Analysis

All experiments were repeated at least two independent times. Most data is presented as biological triplicates and results reported as means±SD unless otherwise stated. Statistical significance was evaluated by either the Student's *t*-test using Graphpad Prism 6 as indicated. Degree of significance is represented using ρ values: $^*\rho \leq 0.05$, $^{**}\rho \leq 0.01$, $^{***}\rho \leq 0.001$, $^{****}\rho \leq 0.0001$ (Different symbols may be used to reflect multiple two-way comparisons).

RESULTS

XRK3F2 Prevents and Reverses MM-Induced *Gfi1* Upregulation and Rescues OB Gene Expression in MM Suppressed preOB

While little is known about how MM cells upregulate GFI1 in preOB, we have previously reported and demonstrate in this study that both TNFα and IL-7 can upregulate *Gfi1* mRNA and induce its nuclear translocation in MC4 preOB (30, 31). We investigated if p62 signaling plays a role in MM cell upregulation of GFI1 expression and induces GFI1-mediated epigenetic repression of *Runx2*. Direct co-culture (48 h) of murine 5TGM1 MM with murine preOB MC4 cells in proliferation media suppressed *Runx2* mRNA (**Figure 1A**, d0). The *Runx2* mRNA inhibition persisted for 4 days after removal of MM cells and addition of osteogenic media (**Figure 1A**, d4). The presence of XRK3F2 during MM-preOB co-cultures prevented *Runx2* suppression at both d0 and d4 (**Figure 1**). Furthermore, XRK3F2 blocked MM-induced upregulation of *Gfi1* (**Figure 1B**). To determine if XRK3F2 directly affects the preOB response to MM signals in MM-preOB co-cultures, we determined if XRK3F2 could block the ability of MM1.S conditioned media or a combination of TNFα plus IL7 to induce *Gfi1* expression in primary mouse BMSC. XRK3F2 blocked the induction of *Gfi1* mRNA in BMSC in both treatment conditions (**Figure 1C**). In contrast, XRK3F2 prevented both MM1.S CM and TNFα plus IL7-mediated *Runx2* suppression. Further, the pro-inflammatory and myeloma pro-survival factor *IL6* mRNA was also reduced by XRK3F2 treatment (**Figure 1C**). In addition, XRK3F2 also prevented TNFα-mediated upregulation of *Gfi1* and rescued inhibition of *Runx2* in MC4 preOB (**Figure 1D**). The prevention of TNFα-induced suppression of preOB by XRK3F2 was further confirmed by increased levels of alkaline phosphatase staining in preOB (**Figure 1E**). This suggests that a direct XRK3F2-mediated inhibition of p62 signaling within preOB prevents *Gfi1* induction

TABLE 1 | *q*PCR primers for Mouse (m) and Human (h) mRNA analysis.

Gene	Forward primer (5′->3′)	Reverse primer (5′->3′)
m*Runx2*	CCTCTGACTTCTGCCTCTGG	ATGAAATGCTTGGGAACTGC
m*Gfi1*	GGCTCCTACAAATGCATCAAATG	TGCCACAGATCTTACAGTCAAAG
m*18srRNA*	GAGCGACCAAAGGAACCATA	CGCTTCCTTACCTGGTTGAT
mOCN	TAGTGAACAGACTCCGGCGCTA	TGTAGGCGGTCTTCAAGCCAT
mBSP	AAGAAGAGGAAGAGGAAGAAAATGA	GCTTCTTCTCCGTTGTCTCC
mOsx (Sp7)	AGAGGTTCACTCGCTCTGACGA	TTGCTCAAGTGGTCGCTTCTG
mIL6	CAAAGCCAGAGTCCTTCAGA	GCCACTCCTTCTGTGACTCC
mVcam1	TGCCGAGCTAAATTACACATTG	CCTTGTGGAGGGATGTACAGA
hRUNX2	CATTTCAGATGATGACACTGCC	GTGAGGGATGAAATGCTTGG
hGFI1	GAGCCTGGAGCAGCACAAAG	GTGGATGACCTTTTGAAGCTCTTC

TABLE 2 | Murine and human ChIP-*q*PCR *Runx2-P1* primers.

ChIP amplicons*	Forward (5′->3′)	Reverse (5′->3′)
Murine −670	AAGGCAAACAGAAGGAAGCA	TGCTGCTTTGCAGTAATTCG
Murine −36 (3)	TGAGGTCACAAACCACATGA	TGAAGCATTCACACAATCCAA
Murine +150 (5)	CGTTTTGTTTTGTTTCCTTGC	CCCAGTCCCTGTTTTAGTTG
Murine +363 (6)	CAGGGACTGGGTATGGTTTG	ACGCCATAGTCCCTCCTTTT
Murine +33130	AGGTAGCCCAGCAAAAACCT	CCCCTCTGTGAGCCAAAATA
Human +185	CACCGAGACCAACAGAGTCA	TGGTAACATGTGAAAAGCAAAGA
Human +66065	AAGGCCCCACCTCTAACACT	AGACAACAGGCGAGGCTAAA

**Numbers represent midpoints of amplicons relative to the Runx2-P1 transcription start site. Numbers in parentheses were used to designate the amplicons in our previous publication (31).*

TABLE 3 | Multiple myeloma patient characterization.

ID	Age	Gender	Race	Newly diagnosed	ISS stage	Skeletal disease
MM1	60	M	White	Yes	I	No
MM2	55	M	Unknown	No	II	Yes
MM3	76	M	White	No	Unknown	Yes
MM4	80	M	White	No	I	No
MM5	58	F	White	No	II	Yes
MM6	50	M	White	No	II	Yes
MM7	44	F	White	No	I	Unknown

by MM signaling, which prevents GFI1 suppression of *Runx2* in BMSC.

XRK3F2 Prevents and Reverses Epigenetic Suppression of *Runx2* by Blocking the Recruitment of GFI1 and Its Co-repressor HDAC1 to the *Runx2-P1* Promoter

We previously reported that MM cells induce the transcriptional repressor Gfi1 to directly bind to the *Runx2-P1* promoter in preOB cells and recruit the chromatin corepressor HDAC1 to *Runx2*, reducing euchromatin marks such as H3K9ac (30, 31). Importantly, this reduction persists in the absence of MM cells, suggesting that these epigenetic changes result in long term OB suppression. Therefore, we tested if XRK3F2 prevents the GFI1-mediated epigenetic suppression of *Runx2* observed following MM exposure using ChIP-qPCR analysis of the murine *Runx2-P1* promoter using the amplicons depicted (**Figure 2A**). In MC4 preOB, XRK3F2 prevented MM-induced GFI1 occupancy at the *Runx2-P1* promoter (**Figure 2B**) and recruitment of the chromatin co-repressor HDAC1 (**Figure 2C**). Consistent with the lack of HDAC1 recruitment, histone acetylation levels of H3K9 at *Runx2-P1* were not reduced in XRK3F2-treated MM-exposed preOB (**Figure 2D**). As a control, we also evaluated the H3K9ac status at the center of the long intron between the two *Runx2* promoters where GFI1 does not bind, and observed that HDAC1 is not recruited there, and MM exposure did not modify the H3K9ac status. This data argues that XRK3F2 can prevent the MM induced recruitment of the GFI1-HDAC1 complex to the *Runx2-P1* promoter, thus blocking establishment of the repressive chromatin architecture at the *Runx2* gene and, thereby, protecting the capacity for OB differentiation.

XRK3F2 Rescues Transcriptional Suppression of *Runx2* by Reversing the Recruitment of the GFI1-HDAC1 Complex to the *Runx2-P1* promoter

We reported that maintenance of the MM-induced Runx2 suppression in the absence of MM cells requires the continued presence of GFI1 and HDAC1 activity (30, 31). Therefore, we performed a set of "rescue" experiments to test whether XRK3F2 can be used to reverse the epigenetic suppression of preOB following MM exposure. In this model, MC4 preOB were co-cultured in direct contact with 5TGM1 MM cells in proliferation media. After 48 h, the MM cells were removed and the MM-exposed MC4 cells were subjected to osteogenic differentiation in the presence or absence of 2 doses of XRK3F2 (**Figure 3A**). Addition of either dose of XRK3F2 to differentiating MM-exposed preOBs significantly elevated *Runx2* mRNA together with downstream RUNX2 target genes Osteocalcin (*Ocn)*, Bone sialoprotein (*Bsp)* and Osterix (*Osx)* (40), which are critical for osteogenic differentiation (**Figures 3B–E**). However, genes induced by MM, including *Gfi1*, *Il6,* and *Vcam1,* which we have shown are sensitive to XRK3F2 inhibition during preOB MM or TNFα exposure [**Figure 1C** and (23, 29)], did not respond to XRK3F2 after the MM cells were removed (**Figures 3F–H**). The MM-induced expression of *Gfi1* mRNA after 48 h (d0) was reduced after MM cell removal, but was persistently expressed at a low level in MM-exposed MC4 during 4 days of osteogenic differentiation as compared to preOB not exposed to MM. We did not observe a significant difference in *Gfi1* mRNA with XRK3F2 treatment in day 4 differentiated preOBs (**Figure 3F**). ChIP analyses demonstrated that enhanced binding of GFI1 at the *Runx2-P1* promoter persists 4 days following MM removal (**Figure 4A**). In the XRK3F2 "rescue treatment" paradigm, in which XRK3F2 was added to MC4 preOB osteogenic cultures after 5TGM1 MM cells (direct contact) were removed, the amount of GFI1 binding at the *Runx2-P1* promoter in MM-exposed MC4 preOB was significantly reduced while the levels of H3K9ac increased (**Figure 4B**). This XRK3F2 rescue

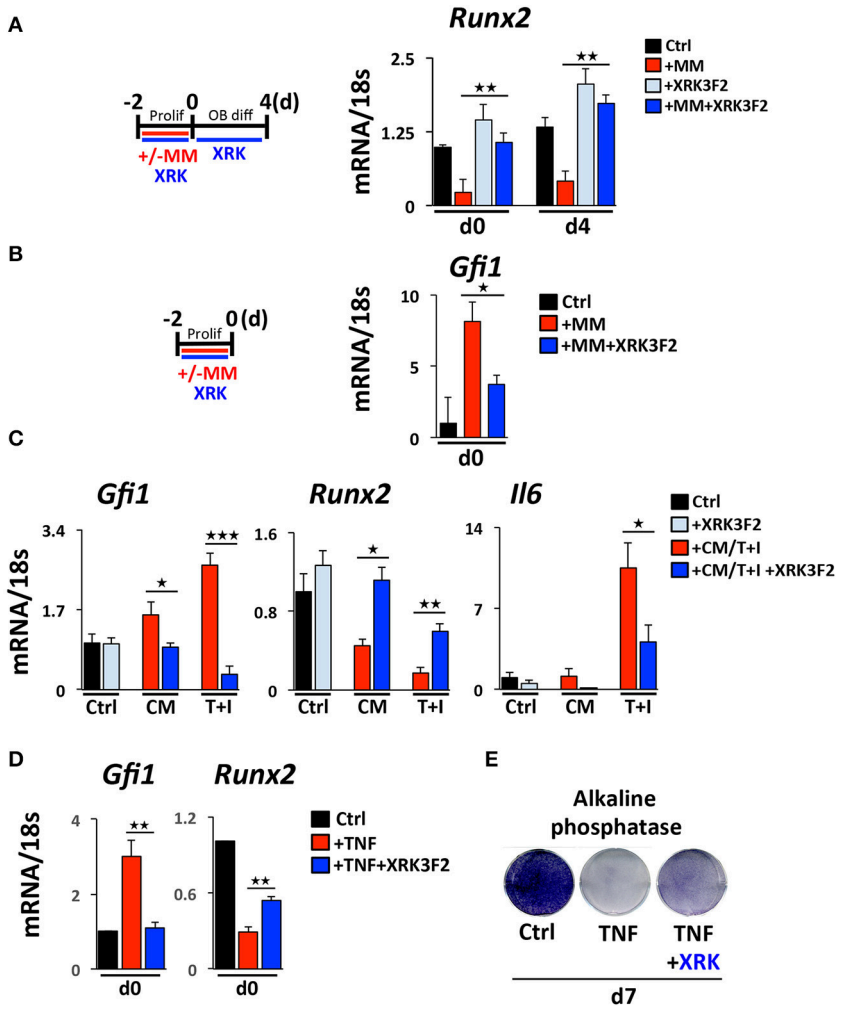

FIGURE 1 | Upregulation of GFI1 in myeloma pre-OB is blocked by XRK3F2. **(A)** As depicted in the schematic, MC4 cells were cultured in with or without 5TGM1 MM cells (in direct contact) for 48 h under proliferation conditions +/– XRK3F2 (5 μM). MM cells were then removed by washing and media was changed to osteogenic differentiation conditions +/– XRK3F2. MC4 cells were collected at the time of MM cell removal (day 0), and after 4 days of differentiation culture in the absence of MM cells (day 4). **(B)** MM cells were co-cultured with MC4 cells for 48 h under proliferation conditions +/– XRK3F2 (5 μM). **(C)** Primary murine BMSC were treated with MM1.S conditioned media (described in Materials and Methods) or TNF plus IL7 (5 ng each) for 48 h. **(A–C)** Expression levels of *Gfi1*, *Runx2* and *Il6* were measured using qPCR as indicated. SEM for 3 biological replicates is indicated. **(D)** MC4 cells were cultured with vehicle or TNFα (10 ng/ml) +/– XRK3F2 (3 μM) for 48 h under proliferation conditions. Expression levels of *Gfi1* and *Runx2* were measured using qPCR as indicated. SD for 3 biological replicates are indicated. **(E)** MC4 cells were cultured with or without TNFα (2.5 ng/ml) +/– XRK3F2 (3 μM) for 7 days under differentiation conditions. Results present alkaline phosphatase staining representative of 3 biological replicates. *$p \leq 0.05$; **$p \leq 0.01$; ***$p \leq 0.001$.

treatment also restored OB differentiation as reflected in alkaline phosphatase staining (**Figure 4C**). In a similar experiment, XRK3F2 was used in both prevention (present during co-cultures) and rescue (added after MM cell removal) models in a transwell experiment using MM1.S and MC4 preOB. Alkaline phosphatase activity was quantified after 5 days of differentiation in osteogenic media. Consistent with the previous results, alkaline phosphatase staining showed that XRK3F2 rescued osteogenesis of preOB exposed to MM cells indirectly in trans-wells (**Figure 4D**). These results are consistent with the observations that even after MM-exposure, XRK3F2 decreased GFI1 binding and rescued chromatin acetylation at the *Runx2-P1* promoter, resulting in elevated *Runx2* expression.

XRK3F2 Rescues Acetylation Levels at the *RUNX2* Promoter in MM Patient hBMSC

We tested the ability of XRK3F2 to reverse the MM-induced long-term repressive chromatin architecture on the *Runx2* gene after MM exposure *in vivo*. We compared the effects of XRK3F2 on the *Runx2* promoter acetylation levels during differentiation of healthy normal donor (HD-hBMSC) and MM patient hBMSC (MM-hBMSC). As **Figure 5A** demonstrates, the H3K9 acetylation levels at *Runx2* increased when the HD-hBMSC were cultured for 4 days in osteogenic media as a result of activation of osteoblast differentiation pathways (31, 41). XRK3F2 did not affect the increase in *Runx2* promoter H3K9ac levels during normal differentiation. In contrast, the H3K9ac

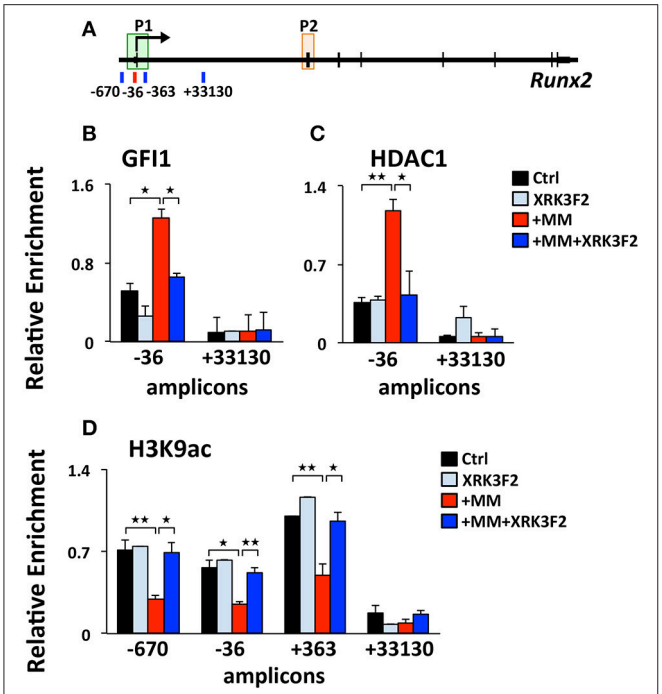

FIGURE 2 | XRK3F2 prevents MM-induced decrease of H3K9ac at the *Runx2* promoter by blocking the recruitment of GFI1 and histone deacetylase HDAC1. **(A)** Schematic representation of the murine *Runx2* gene and positions of amplicons used for ChIP-qPCR analysis. Shown are ChIP data for **(B)** GFI1, **(C)** HDAC1 binding and **(D)** H3K9ac levels at the *Runx2-P1* promoter in MC4 preOB after 48 h in proliferation media control (d0), control treated with 5 μM XRK3F2 (d0+XRK3F2), 5TGM1-MM-treated (d0+MM), and 5TGM1-MM-treated in the presence of XRK3F2 (d0+MM+XRK3F2). IgG non-specific control was subtracted in the H3K9ac data set. SEM represents 2 (for GFI1 and HDAC1) and 3 (for H3K9ac) biological replicates. $^{*}p \leq 0.05$; $^{**}p \leq 0.01$.

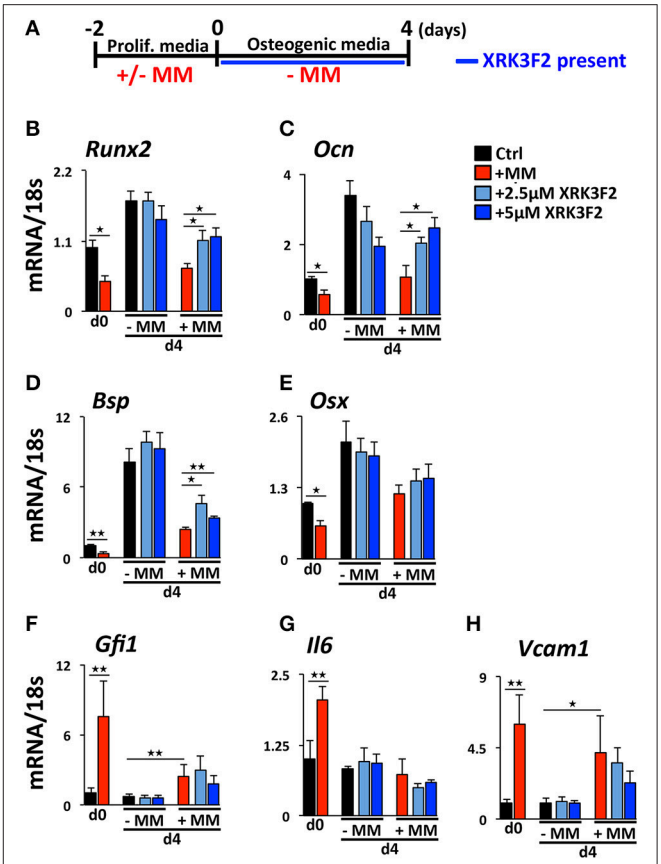

FIGURE 3 | XRK3F2 rescues expression of osteogenic genes in MM-exposed preOB. **(A)** As depicted in the experimental design schematic, MC4 cells were cultured with or without 5TGM1 MM cells (in a direct contact) for 48 h under proliferation conditions. MM cells were then removed by washing (d0) and media was changed to osteogenic conditions +/– XRK3F2 (2.5, 5 μM) for 4 days (d4). MC4 cells were harvested at both d0 and d4 for mRNA analyses. qPCR mRNA profiles for **(B)** *Runx2*, **(C)** *Ocn*, **(D)** *Bsp*, **(E)** *Osx*, **(F)** *Gfi1*, **(G)** *Il6*, and **(H)** *Vcam1* are shown. SEM for 3 experimental wells and a representative of 2 biological replicates are shown. $^{*}p \leq 0.05$; $^{**}p \leq 0.01$.

levels at *Runx2* remained unresponsive to osteogenic signals in MM patient hBMSC (**Figure 5B**). However, XRK3F2 treatment significantly rescued the H3K9ac levels at *Runx2* in MM patient hBMSC, which suggested that XRK3F2 would enhance their response to osteogenic differentiation. Therefore, we set up co-cultures of primary HD-hBMSC with the MM1.S MM cell line in hBMSC proliferation media (**Figures 5C,D**). After removal of the MM cells, we subjected the MM-exposed hBMSC cells to osteogenic differentiation for 5 days in the presence of vehicle or XRK3F2. As **Figure 5C** demonstrates, MM1.S cell exposure prevented the *Runx2* increase after osteogenic stimuli, which is consistent with chromatin repression of the *Runx2* promoter. Addition of XRK3F2 following MM1.S cell removal and addition of osteogenic media rescued the *Runx2* mRNA levels, consistent with the results obtained with mouse cells in **Figure 3B.** Further, MM cell co-culture increased *Gfi1* expression in the HD-hBMSC, which persisted for 5 days after MM cell removal (**Figure 5D**). XRK3F2 addition after MM removal decreased *Gfi1* mRNA, although the difference did not reach significance. These observations are consistent with the observation that the GFI1-HDAC1 complex is required to both establish repression and to persistently repress *Runx2* in BMSCs in the absence of MM cells. Further, these data reveal that signaling through the p62-ZZ domain is required in the absence of MM cells, suggesting the induction of feed-forward suppressive autocrine signaling.

XRK3F2 Rescues the OB Mineralization Potential of MM Patient hBMSC

Since BMSCs obtained from MM patients exhibit an impaired ability to differentiate into mineralizing OB, and XRK3F2 can rescue early steps in osteogenesis, we asked whether XRK3F2 could rescue the complete osteogenesis pathway as demonstrated by the ability to mineralize. We cultured MM-hBMSC for 20 days in the presence of vehicle or XRK3F2 (through day 14) in osteogenic media and assessed their mineral deposition using Alizarin Red staining. Addition of XRK3F2 significantly increased mineralization by the MM-hBMSC from 3 patient samples (**Figure 6A**) as compared to the vehicle control.

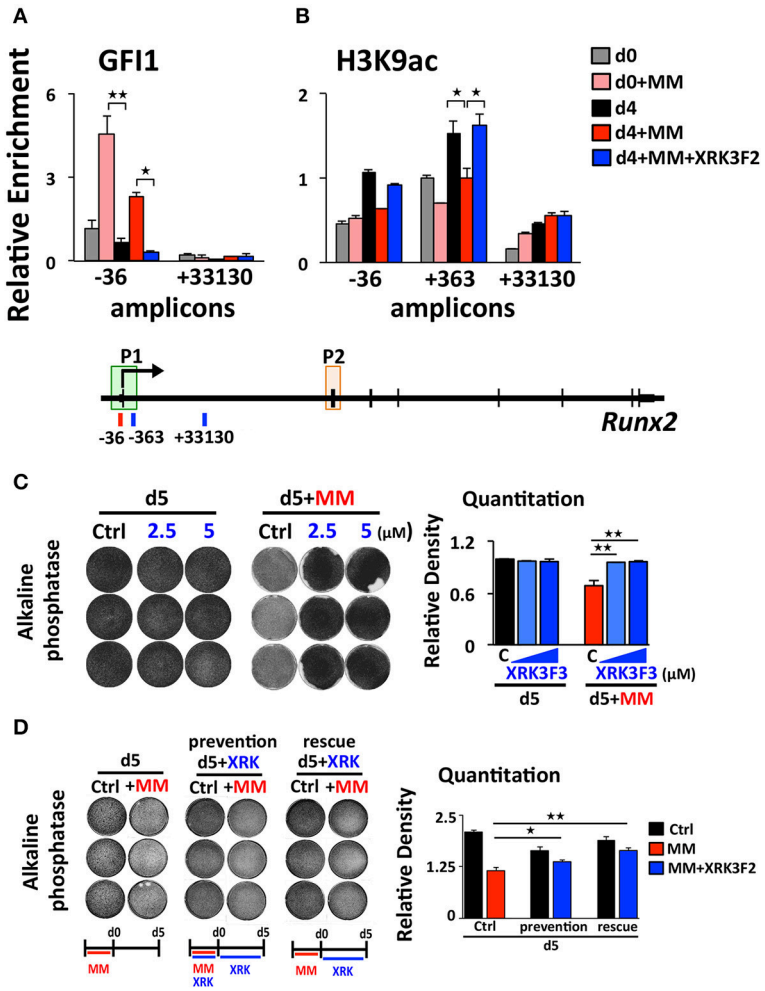

FIGURE 4 | XRK3F2 reverses GFI1 occupancy and reverses loss of H3K9ac at *Runx2* in MM-exposed preOB. **(A)** MC4 cells were cultured as depicted and described in 3A, with XRK3F2 added only after MM cells were removed. Shown are ChIP data for **(A)** GFI1 occupancy and **(B)** H3K9ac at the *Runx2-P1* promoter obtained from MC4 cells harvested after culture (48 h) in proliferation media in the absence or presence of 5TMG1 cells in direct co-culture (d0, d0+MM) or continued in the absence of MM cells in osteogenic media (d4, d4+MM) or continued in osteogenic media with 5 μM XRK3F2 (d4+MM+XRK3F2). **(C)** MC4 preOB were co-cultured with MM1.S (direct contact) for 72 h in proliferation media, MM cells were removed and remaining preOB were subjected to osteogenic differentiation for 5 days +/− XRK3F2 (2.5, 5 μM). **(D)** MC4 preOB were co-cultured with MM1.S (in transwells) for 72 h in proliferation media +/− 5 μM XRK3F2 (during), then the MM cells were removed and the preOB were subjected to osteogenic differentiation for 5 days +/− 5 μM XRK3F2 (after). MC4 were treated with XRK3F2 either during MM exposure or afterwards, but not both. **(C,D)** Alkaline phosphatase staining with quantitation measurements is shown as a representative of 2 independent experiments. SEM for 3 experimental wells and representative of 2 biological replicates is indicated. *$p \leq 0.05$; **$p \leq 0.01$.

Figure 6B shows that 5 μM XRK3F2 did not affect differentiation of HD-BMSC.

DISCUSSION

In this paper, we address the mechanisms associated with XRK3F2-mediated *Runx2* derepression in myeloma-exposed preOB. The involvement of MM-induced GFI1-mediated epigenetic suppression of *Runx2* expression in BMSC prompted us to examine whether p62 signaling is associated with the GFI1-*Runx2* inhibition axis (30, 31). First, we recapitulated our previous findings in which MM exposure upregulated *Gfi1* mRNA and protein expression in BMSC from MM patients and MM-injected mice (30). Blocking p62 signaling using XRK3F2, the p62-ZZ domain inhibitor, prevented GFI1 upregulation and subsequent binding of GFI1 to epigenetically repress *Runx2* in MM-exposed MC4 pre-OB following either direct contact (5TGM1) or indirect (trans-wells, MM1.S) co-culture. As neither of these allow separation of the effects of the inhibitor on each cell type, we showed that XRK3F2 prevents *Gfi1* upregulation in MC4 preOB and primary human BM-MSCs treated with MM1.S conditioned media, or TNFα alone and in combination with IL7. Using blocking antibodies, we previously reported that MM cell down-regulation of *Runx2* mRNA in MC4 preOB cells required both TNFα and IL7 (30). While p62 can transmit signaling from multiple receptor

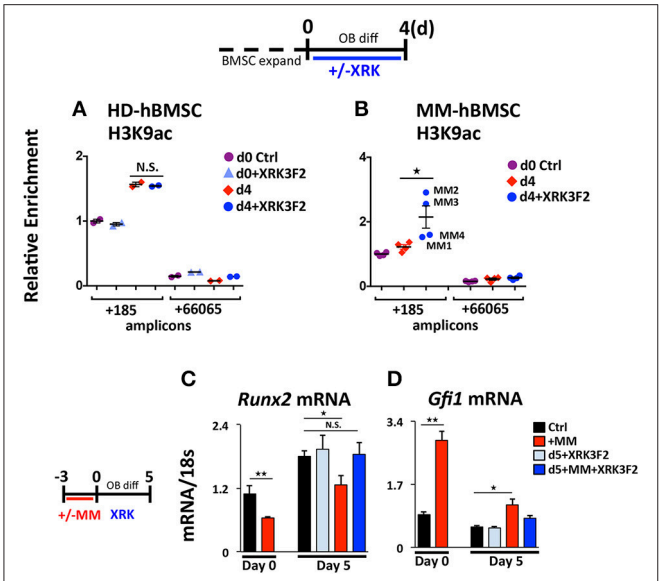

FIGURE 5 | XRK3F2 rescues H3K9ac levels and subsequent osteogenic differentiation of MM hBMSCs. Human BMSC samples were expanded in proliferation media and harvested for ChIP-*q*PCR at either: (Day 0) the day of the switch into osteogenic media +/– XRK3F4 (5 μM) or (Day 4) after four days of differentiation. In the control healthy donor (HD)-BMSC, the d0+XRK3F2 sample was kept in proliferation media from d0 through d4 in the presence of XRK3F2. Anti-H3K9Ac ChIP-*q*PCR analysis of **(A)** HD-hBMSC ($n = 2$) and **(B)** MM-hBMSC (MM) ($n = 4$, MM patient samples MM1-4, **Table 3**) using amplicons +185 and +66065 relative to the *hRunx2* P1 TSS. Day 0 (d0) anti-H3K9Ac ChIP amplicon +185 N sample result was used as the reference sample for other samples on graphs and ΔΔCt shown. **(C)** Healthy donor BMSC were co-cultured with MM1.S for 72 h in proliferation media, MM cells were removed and the remaining hBMSC were subjected to osteogenic differentiation for 5 days +/– XRK3F2 (5 μM). qPCR profiles for *Runx2* **(C)** and *Gfi1* **(D)** mRNA are shown. SEM for 3 experimental wells and representative of 2 biological replicates is indicated. $^{*}p \leq 0.05$; $^{**}p \leq 0.01$.

pathways, TNFα signals through the p62-ZZ domain via the TNFα signaling adaptor RIP1 (19). RIP1 binding with the p62-ZZ domain transduces downstream activation of NFκB via the atypical protein kinase Cζ (aPKCζ) (42), as well as transcription factor C/EBPβ via the p38 MAPK pathway (43), which each have binding sites on p62. PKCζ interacts with the N-terminal PB1 domain of p62 and p38 MAPK interacts with the p38 interaction domain, which overlaps the LIM-domain protein binding (LB) region (44, 45). We hypothesize that NFκB and/or C/EBPβ may be involved in transcriptional regulation of *Gfi1* downstream of TNFα receptor (**Figure 7**). Though *Gfi1* promoter regulation has not yet been well characterized in any cell type, a study by Lidonnici et al. (46) implicated C/EBPα in activation of *Gfi1* in BCR/ABL-expressing cells. Future experiments will delineate the p62-mediated transcription factor regulatory networks regulating *Gif1* activation downstream of cytokine receptor signaling and direct-MM contact in BMSCs.

Together with inhibition of MM-induced *Gfi1* expression, we observed that XRK3F2 increased *Runx2* mRNA in MM-exposed cells and restored osteogenic differentiation, as evidenced by rescued alkaline phosphatase activity and mineralization. This suggested that XRK3F2 treatment enhanced OB differentiation of MM-preOB. We found that XRK3F2 also prevented MM-induced recruitment of GFI1 to the *Runx2* gene, and alleviated its inhibitory chromatin effects (**Figure 7**). GFI1 interacts with various chromatin remodeling enzymes such as histone deacetylase HDAC1, and histone demethylases G9a and LSD1 to form repressive complexes and target gene promoters (47, 48). Further, we have reported that GFI1 also recruits the transmethylase EZH2, which catalyzes the repressive methylation of H3K27 (31). Our data indicate that XRK3F2 blocked MM-induced GFI1 binding and HDAC1 recruitment to the *Runx2-P1* promoter, thereby preventing MM-induced loss of the transcriptionally permissive chromatin acetylation, H3K9ac at the *Runx2* gene in preOB (**Figure 7**). It is interesting to note that in the ChIP experiments detecting acetylation levels at *Runx2* (**Figure 5B**), patients with pre-existing skeletal disease (MM2, 3) responded better to XRK2F2 treatment than the ones without a skeletal disease diagnosis (MM1, 4). Of the mineralization assays in **Figure 6A**, although they represent a wide variation in their intrinsic differentiation capacity, all three patient BMSC responded to XRK3F2 with increased mineralization; two samples were from MM patients with bone disease and the bone disease status of the third was unknown. Since we demonstrated the importance of targeting the p62-ZZ-GFI1 signaling axis within BMSCs to decrease (or rescue from) their response to MM cells, altogether our patient data suggests that patients with bone involvement may benefit more from XRK3F2 treatment than those without bone disease. Future experiments using additional samples from patients with variety of MM disease stages and skeletal involvement may provide valuable information about the importance of blocking the p62-ZZ-GFI1 signaling axis in MM-BMSC interactions in the clinical setting. Since GFI1 is also subjected to regulation at the level of cytoplasmic vs. nuclear localization (30), we speculate that in addition to transcriptional inhibition, XRK3F2 may also act at the level of post-translational modifications that regulate GFI1 nuclear translocation induced by MM-exposure, TNF, and IL7 signaling in MC4 preOB (**Figure 7**) (30). In addition, the cytoplasmic shuttling factor LIM domain-containing protein Ajuba has been reported to bind and function as a co-repressor for GFI1, in an Ajuba-GFI1-HDAC protein complex, on select target genes including *Runx2* (49, 50). Interestingly, Ajuba has also been implicated in aPKC/p62 activation of NFκB in response to either TNFα or IL1β in MEFs via binding to the LIM-binding (LB) domain between the ZZ domain and the TRAF6 binding domains (51). Therefore, we hypothesize that XRK3F2 selective blocking of the p62-ZZ domain-signaling module, may also influence cytoplasmic-nuclear shuttling and/or Ajuba-dependent binding of GFI1 to the *Runx2* promoter.

In rescue experiments, in which the myeloma-induced repressive chromatin structure was already established on the *Runx2* gene in preOB before addition of XRK3F2, we found that XRK3F2 can reverse the established epigenetic *Runx2* suppression and alleviate this block to osteogenic differentiation. This is consistent with the results found using XRK3F2 to

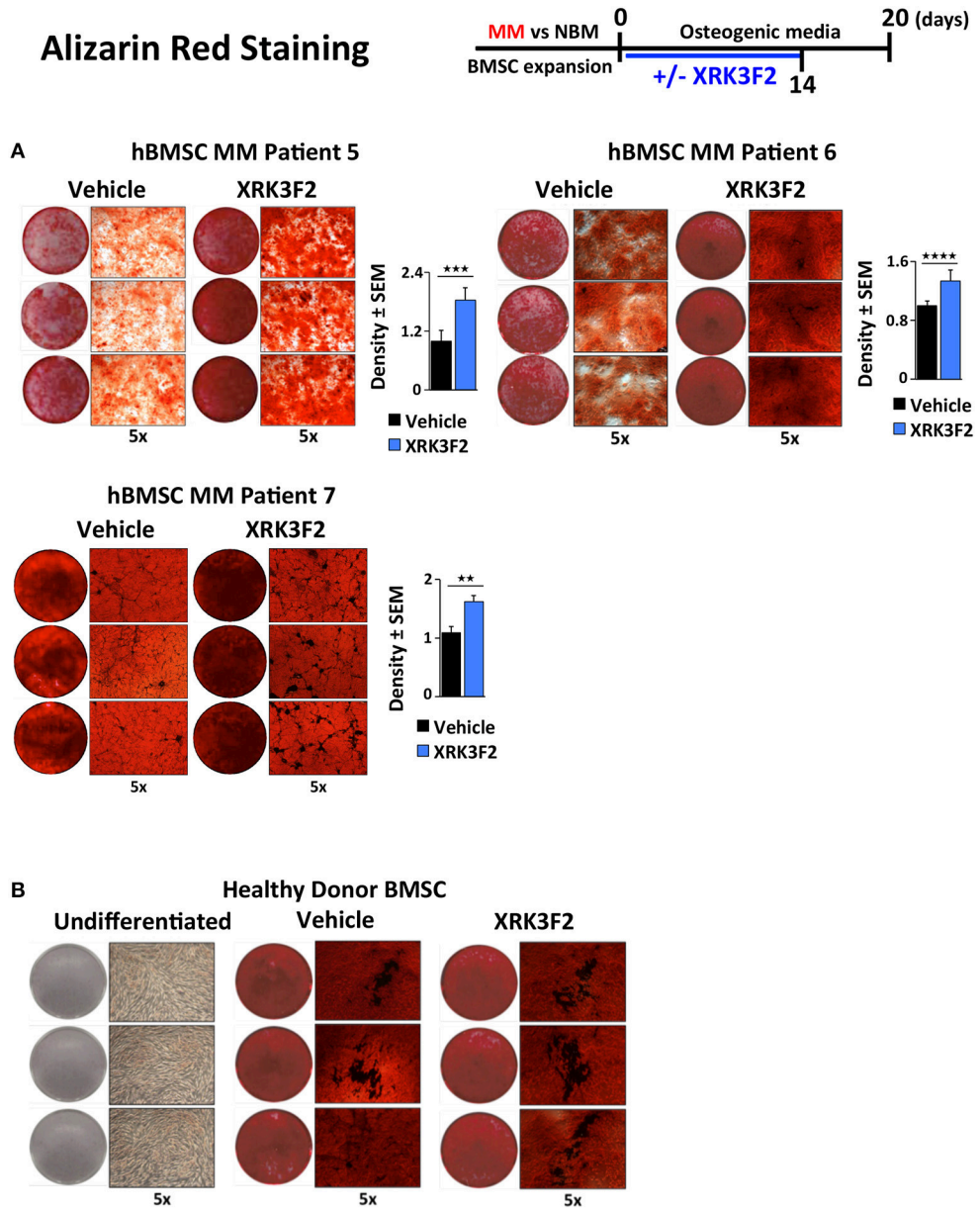

FIGURE 6 | XRK3F2 rescues MM-BM-MSC OB mineralization. **(A)** Myeloma (MM)-BMSC from three different patients (MM patient samples MM5-7, **Table 3**) were cultured for 20 days in osteogenic media. Vehicle control (DMSO) or XRK3F2 (5 μM) was supplemented only for the first 14 days of the differentiation experiment. The presence of calcium deposition/mineralization was assessed using Alizarin red staining. Three independent wells from each treatment group per patient are shown, with 5X magnification images next to entire wells. However, 6 wells from each patient sample group were used for quantitation of Alizarin red staining density using the ProteinSimple AlphaView software, with SEM indicated. **(B)** Alizarin red images of undifferentiated HD-BMSC (negative control) and HD-hBMSC treated with vehicle (DMSO) or XRK3F2 (5 μM) during incubation in osteogenic media for 20 days. $^{**}p \leq 0.01$; $^{***}p \leq 0.001$; $^{****}p \leq 0.0001$.

treat an *in vivo* MM-mouse model in which the tumor was first allowed to grow for 2 weeks before drug administration (29). The clinical implications of this finding are also intriguing as they suggest that MM-induced bone destruction could be reversed, which is particularly important since patients often present with myeloma-induced bone osteolysis at diagnosis (52). In addition to reversing epigenetic suppression of *Runx2* and transcription of several downstream osteogenic genes, XRK3F2 treatment of *ex vivo* expanded primary MM patient BMSCs rescued both epigenetic repression at *Runx2* and osteogenic differentiation reflected in mineralization potential. Since the goal of this study was to understand the mechanism underlying our previously reported work that revealed that XRK3F2 could rescue the bone underlying MM cells in a MM *in vivo* model using 5TGM1 MM cells, we have primarily focused on the use of 5TGM1 and MM1.S myeloma cells in our co-culture

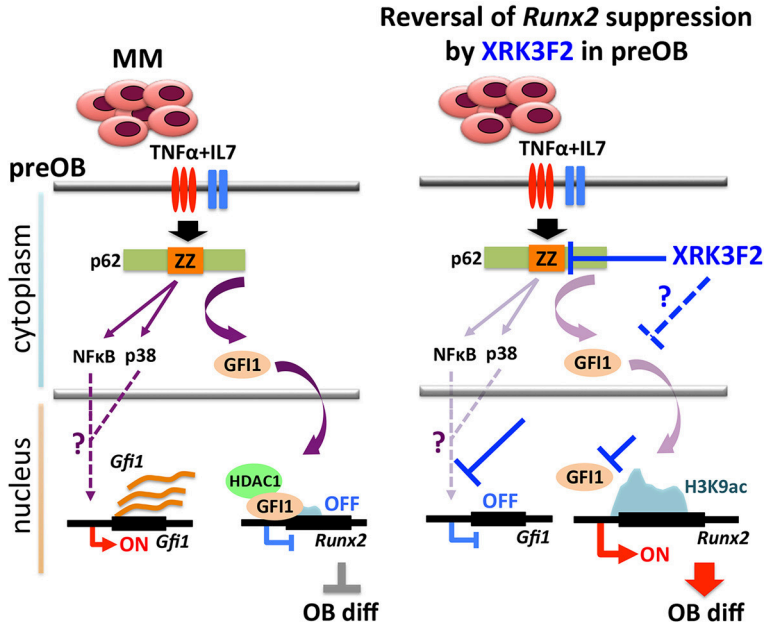

FIGURE 7 | Proposed mechanism of XRK3F2 drug action on p62 signaling in MMBD. MM cell co-culture or TNFα plus IL7 stimulation of preOB activate p62-ZZ domain signaling, which results in activation of downstream pathways involving NFκB and p38 MAPK. Further, p62-ZZ domain activation increases GFI1 levels, which subsequently translocates into the nucleus, binds the *Runx2* gene and recruits the chromatin modifier HDAC1 to deacetylate and repress the *Runx2-P1* promoter. Inhibition of the p62-ZZ domain by XRK3F2 may act in different ways to prevent transcriptional repression of *Runx2* by GFI1. First, by suppressing activation of transcription factors such as NFκB and/or C/*EBPβ*, thus preventing *Gfi1* transcription. Second, by inhibiting nuclear translocation of GFI1, thereby preventing its ability to target the *Runx2* promoter. In both scenarios XRK3F2 prevents GFI1 from instigating epigenetic suppression of *Runx2,* which allows for subsequent progression of osteoblastogenesis. Further, XRK3F2 blocks GFI1 maintenance of the epigenetic repression in the absence of MM, thereby allowing its reversal and rescuing the osteoblastogenesis potential.

experiments. While beyond the scope of this manuscript, due to the heterogeneity associated with MM, future experiments assessing the use of XRK3F2 in the context of additional MM cell lines will be instrumental. This will yield critical information about the requirement of p62 signaling activation within BMSCs triggered by interactions with other subtypes of MM cells.

Despite currently available treatments, the persistence of MM-induced skeletal lesions remains a relevant clinical problem for MM patients. Therefore, a better understanding of the molecular networks involved in sustaining MM-related bone disease is eagerly awaited. While epigenetic mechanisms in BMSCs in the context of MMBD are largely unexplored, here we demonstrate that targeting signal pathways that regulate epigenetic events using the small molecule inhibitor XRK3F2 is of great therapeutic potential, as it exhibits osteo-regenerative properties.

AUTHOR CONTRIBUTIONS

JA, RS, SM, GR, and DG conceived of the study and designed experiments, analyzed data, and interpreted results. JA, RS, SM, QS, JLA, and DZ performed experiments. RS, X-QX, and GR provided research materials. JA, RS, and DG wrote the manuscript. All contributing authors have agreed to submission of this manuscript for publication.

ACKNOWLEDGMENTS

This work was supported by funding from the American Cancer Society Institutional Research Grant (ACSIRG) Mechanism (RS), Multiple Myeloma Research Foundation (SM), US National Institutes of Health (NIH) National Center of Excellence for Computational Chemogenomics Drug Abuse Research (CDAR) P30 DA035778 (X-QX) from the National Institute on Drug Abuse (NIDA), VA Merit Review Award VA 2 I01 CX000623 (GR), NIH grant R01 AR059679 (GR and DG) from the National Institute of Arthritis and Musculoskeletal and Skin Diseases (NIAMS), the Commonwealth Universal Research Enhancement Program (CURE) SAP# 4100057687 (DG), and the Hematology-Oncology Division, Department of Medicine, University of Pittsburgh (DG). The authors gratefully thank the Veterans Administration Pittsburgh Healthcare System, Research and Development for use of the animal facilities.

Its contents are solely the responsibility of the authors and do not necessarily represent the official views of the NIAMS, NIDA, NIH, the Department of Veterans Affairs, or the United States Government.

REFERENCES

1. Greenberg AJ, Rajkumar SV, Therneau TM, Singh PP, Dispenzieri A, Kumar SK. Relationship between initial clinical presentation and the molecular cytogenetic classification of myeloma. *Leukemia* (2014) 28(2):398–403. doi: 10.1038/leu.2013.258
2. Siegel R, Ma J, Zou Z, Jemal A. Cancer statistics, 2014. *CA* (2014) 64:9–29. doi: 10.3322/caac.21208
3. Roodman GD. Pathogenesis of myeloma bone disease. *Blood Cells Mol Dis.* (2004) 32:290–2. doi: 10.1038/leu.2008.336
4. Saad F, Lipton A, Cook R, Chen YM, Smith M, Coleman R. Pathologic fractures correlate with reduced survival in patients with malignant bone disease. *Cancer* (2007) 110:1860–7. doi: 10.1002/cncr.22991
5. Terpos E, Berenson J, Raje N, Roodman GD. Management of bone disease in multiple myeloma. *Expert Rev Hematol.* (2014) 7:113–25. doi: 10.1586/17474086.2013.874943
6. Yaccoby S, Wezeman MJ, Henderson A, Cottler-Fox M, Yi Q, Barlogie B, et al. Cancer and the microenvironment: myeloma-osteoclast interactions as a model. *Cancer Res.* (2004) 64:2016–23. doi: 10.1158/0008-5472.CAN-03-1131
7. Taube T, Beneton MN, McCloskey EV, Rogers S, Greaves M, Kanis JA. Abnormal bone remodelling in patients with myelomatosis and normal biochemical indices of bone resorption. *Eur J Haematol.* (1992) 49(4):192–8.
8. Gainor BJ, Buchert P. Fracture healing in metastatic bone disease. *Clin Orthopaed Related Res.* (1983) (178):297–302.
9. Komori T. Regulation of osteoblast differentiation by Runx2. *Adv Exp Med Biol.* (2010) 658:43–9. doi: 10.1007/978-1-4419-1050-9_5
10. Kumar SK, Lee JH, Lahuerta JJ, Morgan G, Richardson PG, Crowley J, et al. Risk of progression and survival in multiple myeloma relapsing after therapy with IMiDs and bortezomib: a multicenter international myeloma working group study. *Leukemia* (2012) 26:149–57. doi: 10.1038/leu.2011.196
11. Accardi F, Toscani D, Bolzoni M, Dalla Palma B, Aversa F, Giuliani N. Mechanism of action of bortezomib and the new proteasome inhibitors on myeloma cells and the bone microenvironment: impact on myeloma-induced alterations of bone remodeling. *BioMed Res Int.* (2015) 2015:172458. doi: 10.1155/2015/172458
12. Reagan MR, Ghobrial IM. Multiple myeloma mesenchymal stem cells: characterization, origin, and tumor-promoting effects. *Clin Cancer Res.* (2012) 18:342–9. doi: 10.1158/1078-0432.CCR-11-2212
13. Qiang YW, Barlogie B, Rudikoff S, Shaughnessy JD, Jr. Dkk1-induced inhibition of Wnt signaling in osteoblast differentiation is an underlying mechanism of bone loss in multiple myeloma. *Bone* (2008) 42:669–80. doi: 10.1016/j.bone.2007.12.006
14. Colucci S, Brunetti G, Oranger A, Mori G, Sardone F, Specchia G, et al. Myeloma cells suppress osteoblasts through sclerostin secretion. *Blood Cancer J.* (2011) 1:e27. doi: 10.1038/bcj.2011.22
15. Giuliani N, Rizzoli V, Roodman GD. Multiple myeloma bone disease: pathophysiology of osteoblast inhibition. *Blood* (2006) 108(13):3992-6. doi: 10.1182/blood-2006-05-026112
16. Galson DL, Silbermann R, Roodman GD. Mechanisms of multiple myeloma bone disease. *BoneKEy Rep.* (2012) 1:135. doi: 10.1038/bonekey.2012.135
17. Fu R, Liu H, Zhao S, Wang Y, Li L, Gao S, et al. Osteoblast inhibition by chemokine cytokine ligand3 in myeloma-induced bone disease. *Cancer Cell Int.* (2014) 14:132. doi: 10.1186/s12935-014-0132-6
18. Roodman GD, Windle JJ. Paget disease of bone. *J Clin Invest.* (2005) 115:200–8. doi: 10.1172/JCI24281
19. Moscat J, Diaz-Meco MT, Wooten MW. Signal integration and diversification through the p62 scaffold protein. *Trends Biochem Sci.* (2007) 32:95–100. doi: 10.1016/j.tibs.2006.12.002
20. McManus S, Roux S. The adaptor protein p62/SQSTM1 in osteoclast signaling pathways. *J Mol Signal.* (2012) 7:1. doi: 10.1186/1750-2187-7-1
21. Milan E, Perini T, Resnati M, Orfanelli U, Oliva L, Raimondi A, et al. A plastic SQSTM1/p62-dependent autophagic reserve maintains proteostasis and determines proteasome inhibitor susceptibility in multiple myeloma cells. *Autophagy* (2015) 11:1161–78. doi: 10.1080/15548627.2015.1052928
22. Riz I, Hawley TS, Hawley RG. KLF4-SQSTM1/p62-associated prosurvival autophagy contributes to carfilzomib resistance in multiple myeloma models. *Oncotarget* (2015) 6:14814–31. doi: 10.18632/oncotarget.4530
23. Hiruma Y, Honjo T, Jelinek DF, Windle JJ, Shin J, Roodman GD, et al. Increased signaling through p62 in the marrow microenvironment increases myeloma cell growth and osteoclast formation. *Blood* (2009) 113:4894–902. doi: 10.1182/blood-2008-08-173948
24. Michigami T, Shimizu N, Williams PJ, Niewolna M, Dallas SL, Mundy GR, et al. Cell-cell contact between marrow stromal cells and myeloma cells via VCAM-1 and alpha(4)beta(1)-integrin enhances production of osteoclast-stimulating activity. *Blood* (2000) 96(5):1953–60. Available online at: http://www.bloodjournal.org/content/96/5/1953
25. Teoh HK, Chong PP, Abdullah M, Sekawi Z, Tan GC, Leong CF, et al. Small interfering RNA silencing of interleukin-6 in mesenchymal stromal cells inhibits multiple myeloma cell growth. *Leukemia Res.* (2016) 40:44–53. doi: 10.1016/j.leukres.2015.10.004
26. Dougall WC, Glaccum M, Charrier K, Rohrbach K, Brasel K, De Smedt T, et al. RANK is essential for osteoclast and lymph node development. *Genes Dev.* (1999) 13:2412–24.
27. Li J, Sarosi I, Yan XQ, Morony S, Capparelli C, Tan HL, et al. RANK is the intrinsic hematopoietic cell surface receptor that controls osteoclastogenesis and regulation of bone mass and calcium metabolism. *Proc Natl Acad Sci U S A.* (2000) 97(4):1566-71. doi: 10.1073/pnas.97.4.1566
28. Teramachi J, Windle JJ, Roodman GD, Kurihara N. The ZZ domain of sequestosome-1/p62 plays an important role in stromal cell support of myeloma cell growth and osteoclast formation. *ASH Annu Meet Abstr.* (2010) 116:128. Available online at: http://www.bloodjournal.org/content/116/21/128
29. Teramachi J, Silbermann R, Yang P, Zhao W, Mohammad KS, Guo J, et al. Blocking the ZZ domain of sequestosome1/p62 suppresses myeloma growth and osteoclast formation *in vitro* and induces dramatic bone formation in myeloma-bearing bones *in vivo*. *Leukemia* (2016) 30:390–8. doi: 10.1038/leu.2015.229
30. D'Souza S, del Prete D, Jin S, Sun Q, Huston AJ, Kostov FE, et al. Gfi1 expressed in bone marrow stromal cells is a novel osteoblast suppressor in patients with multiple myeloma bone disease. *Blood* (2011) 118:6871–80. doi: 10.1182/blood-2011-04-346775
31. Adamik J, Jin S, Sun Q, Zhang P, Weiss KR, Anderson JL, et al. EZH2 or HDAC1 inhibition reverses multiple myeloma-induced epigenetic suppression of osteoblast differentiation. *Mol Cancer Res.* (2017) 15:405–17. doi: 10.1158/1541-7786.MCR-16-0242-T
32. Wang YG, Qu XH, Yang Y, Han XG, Wang L, Qiao H, et al. AMPK promotes osteogenesis and inhibits adipogenesis through AMPK-Gfi1-OPN axis. *Cell Signal* (2016) 28:1270–82. doi: 10.1016/j.cellsig.2016.06.004
33. van der Meer LT, Jansen JH, van der Reijden BA. Gfi1 and Gfi1b: key regulators of hematopoiesis. *Leukemia* (2010) 24:1834–43. doi: 10.1038/leu.2010.195
34. Chiang C, Ayyanathan K. Snail/Gfi-1 (SNAG) family zinc finger proteins in transcription regulation, chromatin dynamics, cell signaling, development, and disease. *Cytokine Growth Factor Rev.* (2013) 24:123–31. doi: 10.1016/j.cytogfr.2012.09.002
35. Wang FM, Adamik J, Rushdan S, Jin S, Galson DL, Roodman GD. Increase of Gfi1 acetylation by HDAC inhibitors blocks Gfi1-mediated Runx2 repression in osteoblast precursors in multiple myeloma bone disease. *Blood* (2013) 122:753. Available online at: http://www.bloodjournal.org/content/122/21/753
36. Wilson NK, Timms RT, Kinston SJ, Cheng YH, Oram SH, Landry JR, et al. Gfi1 expression is controlled by five distinct regulatory regions spread over 100 kilobases, with Scl/Tal1, Gata2, PU.1, Erg, Meis1, and Runx1 acting as upstream regulators in early hematopoietic cells. *Mol Cell Biol.* (2010) 30:3853–63. doi: 10.1128/MCB.00032-10
37. Xiao G, Cui Y, Ducy P, Karsenty G, Franceschi RT. Ascorbic acid-dependent activation of the osteocalcin promoter in MC3T3-E1 preosteoblasts: requirement for collagen matrix synthesis and the presence of an intact OSE2 sequence. *Mol Endocrinol.* (1997) 11:1103–13. doi: 10.1210/mend.11.8.9955
38. Wang D, Christensen K, Chawla K, Xiao G, Krebsbach PH, Franceschi RT. Isolation and characterization of MC3T3-E1 preosteoblast subclones with distinct *in vitro* and *in vivo* differentiation/mineralization potential. *J Bone Miner Res.* (1999) 14:893–903. doi: 10.1359/jbmr.1999.14.6.893
39. Adamik J, Wang KZ, Unlu S, Su AJ, Tannahill GM, Galson DL, et al. Distinct mechanisms for induction and tolerance regulate the immediate early genes

encoding interleukin 1beta and tumor necrosis factor alpha. *PLoS ONE* (2013) 8:e70622. doi: 10.1371/journal.pone.0070622
40. Huang W, Yang S, Shao J, Li YP. Signaling and transcriptional regulation in osteoblast commitment and differentiation. *Front Biosci.* (2007) 12:3068–92. doi: 10.2741/2296
41. Jensen ED, Gopalakrishnan R, Westendorf JJ. Regulation of gene expression in osteoblasts. *BioFactors* (2010) 36:25–32. doi: 10.1002/biof.72
42. Sanz L, Sanchez P, Lallena MJ, Diaz-Meco MT, Moscat J. The interaction of p62 with RIP links the atypical PKCs to NF-kappaB activation. *EMBO J.* (1999) 18:3044–53. doi: 10.1093/emboj/18.11.3044
43. Yu HB, Kielczewska A, Rozek A, Takenaka S, Li Y, Thorson L, et al. Sequestosome-1/p62 is the key intracellular target of innate defense regulator peptide. *J Biol Chem.* (2009) 284:36007–11. doi: 10.1074/jbc.C109.073627
44. Saito A, Kawai K, Takayama H, Sudo T, Osada H. Improvement of photoaffinity SPR imaging platform and determination of the binding site of p62/SQSTM1 to p38 MAP kinase. *Chem Asian J.* (2008) 3:1607–12. doi: 10.1002/asia.200800099
45. Kawai K, Saito A, Sudo T, Osada H. Specific regulation of cytokine-dependent p38 MAP kinase activation by p62/SQSTM1. *J Biochem.* (2008) 143:765–72. doi: 10.1093/jb/mvn027
46. Lidonnici MR, Audia A, Soliera AR, Prisco M, Ferrari-Amorotti G, Waldron T, et al. Expression of the transcriptional repressor Gfi-1 is regulated by C/EBP{alpha} and is involved in its proliferation and colony formation-inhibitory effects in p210BCR/ABL-expressing cells. *Cancer Res.* (2010) 70:7949–59. doi: 10.1158/0008-5472.CAN-10-1667
47. Thambyrajah R, Mazan M, Patel R, Moignard V, Stefanska M, Marinopoulou E, et al. GFI1 proteins orchestrate the emergence of haematopoietic stem cells through recruitment of LSD1. *Nat Cell Biol.* (2016) 18:21–32. doi: 10.1038/ncb3276
48. Duan Z, Zarebski A, Montoya-Durango D, Grimes HL, Horwitz M. Gfi1 coordinates epigenetic repression of p21Cip/WAF1 by recruitment of histone lysine methyltransferase G9a and histone deacetylase 1. *Mol Cell Biol.* (2005) 25:10338–51. doi: 10.1128/MCB.25.23.10338-10351.2005
49. Adamik J, Ding J, Zhang P, Sun Q, Roodman GD, Galson DL. Lim-domain protein AJUBA is a required co-factor for Gfi1 suppression of Runx2 in pre-osteoblasts in multiple myeloma. *J Bone Miner Res.* (2015) 30(Suppl. 1):S331. Available online at: http://www.asbmr.org/education/AbstractDetail?aid=5168fa57-22d1-4f87-942e-f4bd2543e4e2
50. Montoya-Durango DE, Velu CS, Kazanjian A, Rojas ME, Jay CM, Longmore GD, et al. Ajuba functions as a histone deacetylase-dependent co-repressor for autoregulation of the growth factor-independent-1 transcription factor. *J Biol Chem.* (2008) 283:32056–65. doi: 10.1074/jbc.M802320200
51. Feng Y, Longmore GD. The LIM protein Ajuba influences interleukin-1-induced NF-kappaB activation by affecting the assembly and activity of the protein kinase Czeta/p62/TRAF6 signaling complex. *Mol Cell Biol.* (2005) 25:4010–22. doi: 10.1128/MCB.25.10.4010-4022.2005
52. Al Kaissi A, Scholl-Buergi S, Biedermann R, Maurer K, Hofstaetter JG, Klaushofer K, et al. The diagnosis and management of patients with idiopathic osteolysis. *Pediatr Rheumatol Online J.* (2011) 9:31. doi: 10.1186/1546-0096-9-31

Conflict of Interest Statement: GR serves as a consultant for Amgen. X-QX is the Founder of ID4Pharma and serves as a consultant for Oxis Biotech.

The remaining authors declare that the research was conducted in the absence of any commercial or financial relationships that could be construed as a potential conflict of interest.

frontiers in Endocrinology

ORIGINAL RESEARCH
published: 03 July 2018
doi: 10.3389/fendo.2018.00352

Mechanically-Loaded Breast Cancer Cells Modify Osteocyte Mechanosensitivity by Secreting Factors That Increase Osteocyte Dendrite Formation and Downstream Resorption

Wenbo Wang[1], *Blayne A. Sarazin*[1,2], *Gabriel Kornilowicz*[1] *and Maureen E. Lynch*[1,2]*

[1] *Department of Mechanical and Industrial Engineering, University of Massachusetts, Amherst, MA, United States,*
[2] *Department of Mechanical Engineering, University of Colorado, Boulder, CO, United States*

OPEN ACCESS

Edited by:
Julie A. Sterling,
Vanderbilt University, United States

Reviewed by:
Han Qiao,
Shanghai Ninth People's Hospital, Shanghai Jiao-Tong University School of Medicine, China
Jonathan Gooi,
University of Melbourne, Australia

***Correspondence:**
Maureen E. Lynch
Maureen.Lynch@colorado.edu

Specialty section:
This article was submitted to Bone Research, a section of the journal Frontiers in Endocrinology

Received: *10 February 2018*
Accepted: *11 June 2018*
Published: *03 July 2018*

Citation:
Wang W, Sarazin BA, Kornilowicz G and Lynch ME (2018) Mechanically-Loaded Breast Cancer Cells Modify Osteocyte Mechanosensitivity by Secreting Factors That Increase Osteocyte Dendrite Formation and Downstream Resorption. Front. Endocrinol. 9:352. doi: 10.3389/fendo.2018.00352

Advanced breast cancer predominantly metastasizes to the skeleton, at which point patient prognosis significantly declines concomitant with bone loss, pain, and heightened fracture risk. Given the skeleton's sensitivity to mechanical signals, increased mechanical loading is well-documented to increase bone mass, and it also inhibited bone metastatic tumor formation and progression *in vivo*, though the underlying mechanisms remain under investigation. Here, we focus on the role of the osteocyte because it is the primary skeletal mechanosensor and in turn directs the remodeling balance between formation and resoprtion. In particular, osteocytic dendrites are important for mechanosensing, but how this function is altered during bone metastatic breast cancer is unknown. To examine how breast cancer cells modulate dendrite formation and function, we exposed osteocytes (MLO-Y4) to medium conditioned by breast cancer cells (MDA-MB231) and to applied fluid flow (2 h per day for 3 days, shear stress 1.1 Pa). When loading was applied to MLOs, dendrite formation increased despite the presence of tumor-derived factors while overall MLO cell number was reduced. We then exposed MLOs to fluid flow as well as media conditioned by MDAs that had been similarly loaded. When nonloaded MLOs were treated with conditioned media from loaded MDAs, their dendrite formation increased in a manner similar to that observed due to loading alone. When MLOs simultaneously underwent loading and treatment with loaded conditioned media, dendrite formation was greatest. To understand potential molecular mechanisms, we then investigated expression of genes related to osteocyte maturation and dendrite formation (E11) and remodeling (RANKL, OPG) as well as osteocyte apoptosis. E11 expression increased with loading, consistent with increased dendrite formation. Though loaded conditioned media decreased MLO cell number, apoptosis was not detected via TUNEL staining, suggesting an inhibition of growth instead. OPG

expression was inhibited while RANKL expression was unaffected, leading to an overall increase in the RANKL/OPG ratio with conditioned media from loaded breast cancer cells. Taken together, our results suggest that skeletal mechanical loading stimulates breast cancer cells to alter osteocyte mechanosensing by increasing dendrite formation and downstream resorption.

Keywords: osteocyte, mechanical loading, fluid flow, bone, breast cancer, mechanobiology

INTRODUCTION

The skeleton is the most common site for breast cancer metastasis, where roughly 3 in 4 patients with advanced breast cancer develop incurable bone metastases (1). Once bone metastasis occurs, the lesions are overwhelmingly osteolytic, causing significant declines in prognosis (2) and severe skeletal complications such as bone pain and fracture (3). Once in bone, metastatic tumor cells dysregulate the normal bone remodeling process and initiate bone destruction to release vital growth factors from the bone matrix that literally "feed" the tumor cells (4). Thus, tumor growth and osteolysis are closely correlated. Currently, therapeutic strategies that target this relationship include both anti-osteoclastic and anti-tumorigenic effects [e.g., bisphosphonates (5, 6), denosumab (7)], and many new, more targeted approaches are being developed [e.g., nanomedicine that combines bisphosphonates with chemotherapies (8, 9)]. Despite these advances, most treatment options do not recover bone that has been lost with osteolysis, and improving the ability of these strategies to inhibit tumorigenesis and osteolysis long-term remains a goal.

Dynamic mechanical loading has recently been established as an important microenvironmental factor in bone metastatic cancer. In healthy bone, increased loading is well-documented to shift the remodeling balance toward bone formation by upregulating bone-forming osteoblasts and inhibiting bone-resorbing osteoclasts (10). Because this effect is the opposite of how bone metastatic tumors cells shift remodeling, loading is under investigation as a potential method of opposing cancer-induced bone disease. Supporting this hypothesis, increased mechanical loading in mouse models protected against bone metastatic breast cancer-induced osteolysis while increasing bone formation (11) and it inhibited multiple myeloma bone metastasis (12). In a 3D model of bone metastasis, applied mechanical loading inhibited breast cancer cell expression of genes interfering with remodeling (11). Furthermore, mechanical loading modulated interactions between breast cancer cells and mesenchymal stem cells (13), which are the progenitor cells that give rise to osteoblasts as well as to osteocytes, a specialized mechanosensory bone cell whose role in cancer-induced bone disease has only recently been recognized.

Osteocytes are the most abundant cell type in the skeleton, forming a complex, interconnected network throughout the skeleton. They are critical for sensing mechanical and chemical signals from all over the skeleton, and they integrate these signals to appropriately coordinate the downstream activities of osteoblasts and osteoclasts (14, 15). Despite this, little is known about their role in bone metastasis. In bone metastatic multiple myeloma patients, increased osteocyte apoptosis and circulating levels of pro-resorption osteocyte-specific proteins were found to correlate with increased osteolytic lesions, osteoclast formation, and bone loss (16). In preclinical models, physical connections between multiple myeloma cells and osteocytes occurred through dendrites, extensive processes used to connect osteocytes to themselves and other cells, and these connections facilitated osteolytic lesions and tumor cell growth (17). In the context of breast cancer, osteocytes secreted ATP through their dendrites in response to applied fluid flow, which inhibited breast cancer migration, proliferation, and metastasis to bone (18, 19). Based on these collective data, we speculate that osteocytes are the cellular link between mechanical loading and its inhibitory effects on bone metastatic cancer. However, whether osteocytes' mechanosensing ability is affected by bone metastasis is unknown.

We hypothesized that (i) soluble factors secreted by breast cancer cells alter the mechanoresponse of osteocytes to mechanical loading and (ii) mechanical loading of breast cancer cells modulates their effect on osteocyte mechanosensing. To this end, we first characterized the response of osteocytes to mechanical loading and to culture with tumor-conditioned media to determine the isolated effects of each of these two tumor microenvironmental factors. As dendrites are the most mechanosensitive part of the osteocyte (20, 21), and they increase in length (22) and number (23) in response to anabolic loading, particularly fluid flow (24), they are useful indicators of overall osteocyte mechanosensitivity. Next, to determine whether tumor-derived soluble factors modulated the osteocyte dendritic response to loading, osteocytes underwent mechanical loading in the presence of tumor-conditioned media. Finally, to model the more physiological situation in which both cell populations undergo loading, we exposed osteocytes to loading as well as media conditioned by breast cancer cells that had been similarly loaded. We evaluated dendrite formation and gene expression of E11/gp38, a marker of early osteocyte maturation that regulates dendrite formation during osteocyte differentiation (25). We also evaluated indicators that would point to changes to downstream remodeling, including osteocyte apoptosis, a trigger for downstream resorption (26), and gene expression of NF-κB ligand (RANKL) and its endogenous soluble inhibitor osteoprotegerin (OPG), the ratio of which is the critical factor controlling osteoclast differentiation and function (27).

MATERIALS AND METHODS

Cell Culture

MLO-Y4 cells (MLOs), a gift from Dr. Lynda Bonewald, were selected as our osteocyte model when investigating the role of mechanical loading because their mechano-response to applied fluid shear stress is very robust and well-characterized (22, 28–31). MLOs were cultured on collagen-coated tissue culture plastic [rat-tail collagen I (Fisher #CB-40236) diluted to 0.15 mg/ml in sterile 0.02 N acetic acid]. MLOs were maintained in Minimum Essential Medium Eagle—Alpha Modification (αMEM) supplemented with 2.5% fetal bovine serum (FBS), 1% Penicillin/Streptomycin (P/S) and 2.5% calf serum (CS) under standard cell culture conditions (37°C, 5% CO_2) (32). After cells reached ∼70% confluency, they were subsequently seeded onto collagen-coated coverslips (2,000 cells/cm^2) for experimentation.

Mechanical Loading

Osteocytes are particularly sensitive to fluid flow-induced shear stresses (24, 33), which changed expression of osteocyte-generated signals in favor of net bone formation, such as RANKL (34), OPG (35), and sclerostin (36). MLOs were exposed to oscillatory fluid shear stresses via a rocking see-saw platform, a simple, high-throughput system in which many standard culture dishes can be placed on a platform that rocks up and down in the vertical plane (37). This type of applied fluid flow set-up has elicited a strong anabolic response in osteocytes, including MLOs (29, 38, 39). The rocking parameters were adjusted to achieve a maximum characteristic shear stress of ∼1.1 Pa [calculated using equations from Zhou et. al. (40)], a stress level shown to increase dendrite formation and length in MLOs (22) and, when applied using steady flow, alter breast cancer migration dynamics in models of primary tumors (41, 42). Rocking was performed for 2 h per day at ∼1 Hz in the incubator for 3 days, after which cells were harvested for analysis.

Generation of Tumor-Conditioned Media

MDA-MB231 human breast cancer cells (MDA, ATCC) were maintained in complete Dulbecco's modified Eagle medium [DMEM (Invitrogen) supplemented with 10% FBS (Life Technologies) and 1% P/S (Invitrogen)] under standard cell culture conditions (37°C, 5% CO_2). To generate tumor conditioned media (TCM), MDAs were plated in T150 flasks and when they reached 90% confluency, their media was replaced with low serum DMEM (1% FBS, 1% P/S) for 24 h. TCM was collected, concentrated 10-fold in an Amicon centrifugal filter unit (MWCO 3kDa, EMD Millipore), and diluted to 2-fold final concentration in fresh MLO media, a level that previously affected other bone cells, including osteogenic differentiation in mesenchymal stem cells (13) and osteoclastogenesis in RAW 264.7 monocytes (43). Low serum DMEM with no cells was subjected to the same processing conditions and used for control. To generate loaded conditioned media, MDA cells were plated in T150 flasks, which were randomized into Loaded and Nonloaded TCM groups. Loaded TCM flasks received rocking for 6 h to match total loading exposure in MLOs, after which media was replaced with low serum DMEM and processed as previously described.

Fluorescent Staining

To quantify MLO dendrite number and cell number, we utilized phalloidin staining (Invitrogen, A34055) and DAPI (Sigma-Aldrich, D9542), respectively. To explore whether apoptosis contributed to loading-induced changes to the dendrite/osteocyte ratio, we utilized terminal deoxynucleotidyl transferase dUTP Nick-End Labeling (TUNEL) staining (DeadEnd Fluorometric TUNEL System, Promega, G3250) to assess MLO apoptosis. Briefly, for dendrite imaging, cells were fixed using 4% paraformaldehyde, washed with PBS, and permeabilized with 0.05% Triton-X. Cells were incubated with 1:5000 of DAPI and 1:200 of phalloidin for 1 h. For TUNEL staining, cells were incubated with 1:5000 of DAPI and 1:200 of phalloidin combined with recombinant terminal deoxynucleotidyl transferase enzyme per manufacturer's instructions. Cells were then imaged using spinning disk confocal microscopy (Zeiss Spinning Disk Cell Observer SD, Carl Zeiss). Seven fields of view were randomly selected for each coverslip, from which cell number, dendrite number, and TUNEL-positive cells were quantified using ImageJ (NIH). Data from all fields of view per sample were averaged for reporting.

Gene Expression

To explore additional potential mechanisms underlying loading-induced changes to physical dendrite formation, gene expression of E11/gp38, RANKL, and OPG were determined using quantitative real-time polymerase chain reaction (qPCR) and the comparative ΔCT method (44). Briefly, mRNA was isolated using the TRIzol extraction method in RNase-free conditions. RNA purity and quantity were tested using a spectrophotometer (NanoDrop 1000; Thermo Scientific). qPCR was performed using 25–50 ng of cDNA in a final volume of 20 μL containing 2X QuantiNova Probe PCR Master Mix (QuantiNova Probe PCR Kit, 208256, Qiagen). Predesigned qPCR probe assays were purchased for each of the genes of interest (E11, Mm.PT.58.42823717, Integrated DNA Technologies) (RANKL, Mm00441906_m1, ThermoFisher Scientific) (OPG, Mm00435454_m1, ThermoFisher Scientific). Results were normalized to the reference gene TATA-binding protein (TBP, Mm.PT.58.10867035, Integrated DNA Technologies) and presented as fold change.

Statistical Analysis

The effects of treating MLOs with mechanical loading (NonLoaded MLOs versus Loaded MLOs), tumor-conditioned media (TCM versus Control), and whether TCM was also loaded (NonLoaded TCM versus Loaded TCM) were all assessed using full factorial ANOVAs (JMP v8.0, SAS Institute Inc.). When the interaction factor was significant, a *post-hoc* Tukey-Kramer means comparisons test with a Bonferroni correction was conducted; otherwise, experimental groups were pooled for analysis as appropriate to evaluate main effects. Statistical significance was set at $p < 0.05$. All experiments were replicated 2–4 times. All data is represented as mean + standard deviation.

RESULTS

Mechanical Loading, but Not Breast Cancer-Conditioned Media, Increased Osteocyte Dendrite Formation

We first investigated the isolated effects of applied fluid flow and of tumor-conditioned media (TCM) treatment on MLO dendrite formation to provide a baseline response to these microenvironmental factors in our rocking system. Mechanical loading alone increased the number of dendrites per MLO primarily by boosting overall dendrite quantity (**Figures 1A,B**). MLO cell number was unaffected by applied fluid flow. In contrast, upon exposure to TCM, no change in dendrite/cell, cell number, or dendrite number was observed (**Figures 1C,D**).

Breast Cancer-Conditioned Media Increased Dendrite Formation in Osteocytes via a Decrease in Cell Growth

To determine how breast cancer cell-derived factors affected osteocytes' response to mechanical loading, we exposed MLOs to fluid shear stress in the presence and absence of TCM. In the TCM and Control treatment groups, loading increased the number of dendrites per osteocyte independent of TCM status (**Figures 2A,B**). Specifically, in the Control group, the loading-induced increase in dendrite/cell was driven by a rise in total number of dendrites and no loading-induced changes in MLO cell number (**Figure 2B**). In contrast, in the TCM group, the increase in dendrite/cell resulted from a reduction in MLO cell number and no loading-induced changes in total number of dendrites.

Mechanical Loading Applied to Breast Cancer Cells Modulated Their Effects on Loading-Induced Osteocyte Dendrite Formation

In vivo, both bone cells and cancer cells are exposed to the prevailing mechanical environment in the skeleton. To recapitulate this, we collected conditioned media from breast cancer cells that had been exposed to fluid flow, and then supplied it to MLOs during applied fluid flow. Loading increased dendrite number per MLO for both Loaded and NonLoaded TCM groups (**Figures 3A,B**), and this response was greatest with conditioned media from mechanically loaded MDAs, suggesting that loading applied to both MLOs and MDAs synergistically increases the number of dendrites formed in MLOs. Loading-induced increases to dendrite per cell occurred primarily through reduced MLO cell number

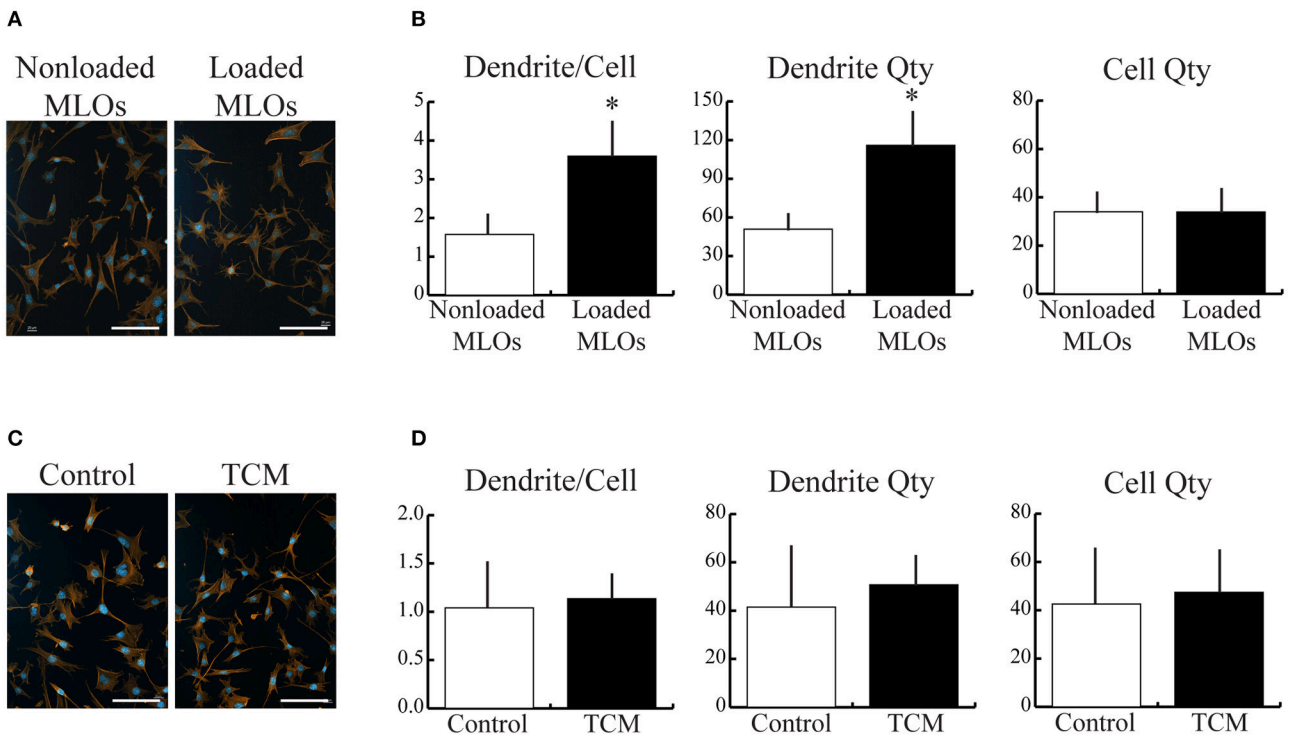

FIGURE 1 | Mechanical loading, but not breast cancer cell-derived soluble factors, increased MLO-Y4 dendrite formation**. (A,C)** Fluorescent images of MLOs suggested that fluid shear stress alone increased dendrite formation, but treatment with tumor-conditioned media (TCM) alone did not. (Scale bars = 100 μm; blue = DAPI, red = phalloidin) **(B)** Image analysis revealed that mechanical loading increased the number of dendrites per MLO, which was achieved via a similar increase in overall dendrite quantity. MLO cell number was not affected by loading. **(D)** In contrast, no detectable changes in dendrites per MLO, dendrite number, or MLO cell number were observed due to TCM treatment alone. Data are represented as mean + SD. *$p < 0.05$ relative to respective NonLoaded MLO group.

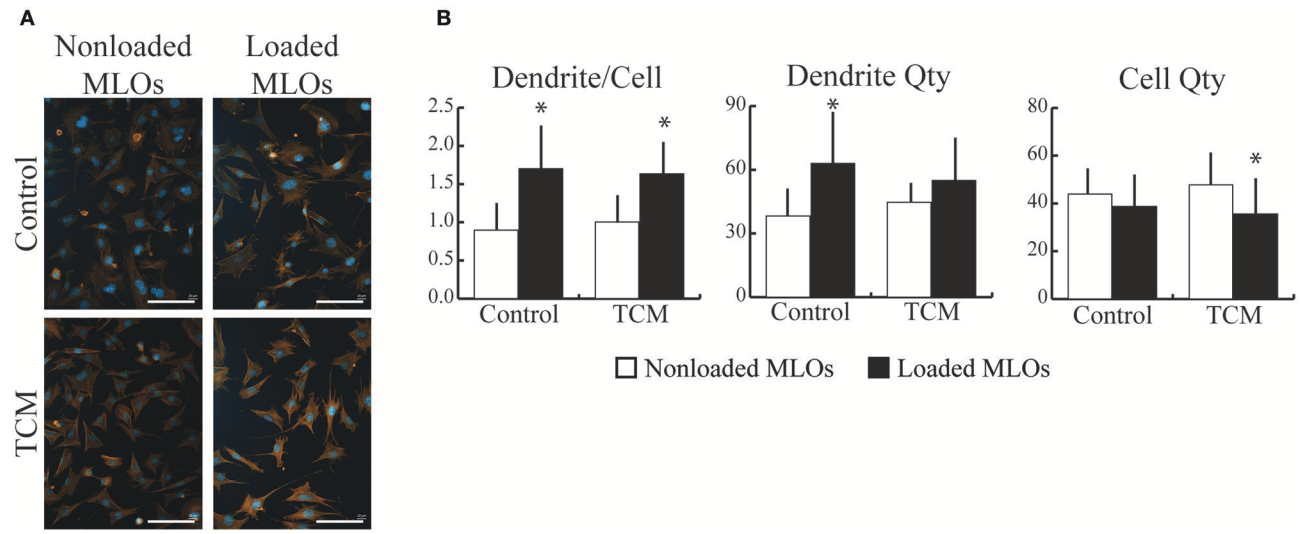

FIGURE 2 | Breast cancer-derived factors modulated MLO-Y4 cell growth during mechanical loading. **(A)** Fluorescent images of MLOs revealed that mechanical loading promoted dendrite formation independent of the presence of tumor-conditioned media (TCM). (Scale bars = 100 μm; blue = DAPI, red = phalloidin) **(B)** Mechanical loading increased the number of dendrites per MLO similarly in the absence (upper) and presence (lower) of TCM. In the Control group, loading-induced changes in dendrite/cell occurred due to an increase in overall dendrite quantity whereas in the TCM treatment group, changes occurred due to a decrease in MLO growth with loading. Data are represented as mean + SD. *$p < 0.05$ relative to respective NonLoaded MLO group.

(**Figure 3B**) as previously observed (**Figure 2B**), and these decreases in MLO cell number were maximal in the Loaded TCM group.

Applied Mechanical Loading Breast Cancer Cells Increased the RANKL/OPG Ratio in Osteocytes

To explore potential mechanisms underlying loading-induced changes to physical dendrite formation, we next quantified loading-induced changes in expression of E11, a gene related to osteocyte differentiation and dendrite formation. To further investigate osteocyte mechanosensitivity, we also quantified key genes that regulate downstream bone remodeling (RANKL, OPG). Corresponding to observed increases in dendrites per MLO, expression of E11 increased with applied fluid shear stress only in the Loaded TCM group, though a trend for loading-induced increases in the NonLoaded TCM group was present (**Figure 4A**). This result also suggests increased differentiation in MLOs with applied loading. No changes in RANKL gene expression occurred in response to any treatment (**Figure 4B**). However, treatment with Loaded TCM, though not applied loading, decreased OPG gene expression in MLOs (main effect of TCM treatment: pooled NonLoaded TCM vs. pooled Loaded TCM) (**Figure 4C**). This resulted in an overall increase in the RANKL/OPG ratio in MLOs (**Figure 4D**). Additionally, because we suspected the observed decreases in MLO cell number with TCM treatment could be due to apoptosis (17, 45), a known stimulant of resorption (26), we assessed osteocyte apoptosis via TUNEL staining, though we did not detect MLO apoptosis in any treatment group (**Supplementary Figure 1**).

DISCUSSION

To determine whether soluble signaling factors from breast cancer cells modulated osteocyte mechanosensing, we subjected osteocytes to applied fluid flow in combination with media conditioned by breast cancer cells that also underwent applied fluid flow. We found that breast cancer-derived soluble factors modulated fluid flow-induced dendrite formation in osteocytes, though they did not affect osteocytes in the absence of mechanical loading. Furthermore, when breast cancer cells underwent similar mechanical loading, their secretions impacted MLO cell growth and loading enhanced dendrite formation in the remaining osteocyte population. Soluble factors from mechanically-loading breast cancer cells increased the RANKL/OPG ratio and may also be stimulating osteocyte differentiation, as indicated by increased E11 expression. However, they do not stimulate resorption by inducing osteocyte apoptosis.

Based on our results, breast cancer cell-derived factors alone did not alter dendrite formation in MLO-Y4 cells. In a mouse model of bone metastatic multiple myeloma (MM), osteocytes and tumor cells physically interacted via dendrites, and this physical interaction was required for tumor cells to induce osteocyte apoptosis and increase levels of pro-resorption proteins RANKL and sclerostin (17). Here, we focused on paracrine signaling between breast cancer cells and osteocytes as the majority of osteocytes are deeply embedded in the bone matrix (46), although lack of physical contact could account for no observed changes to dendrite formation due to soluble factors alone and should be investigated in the future. In

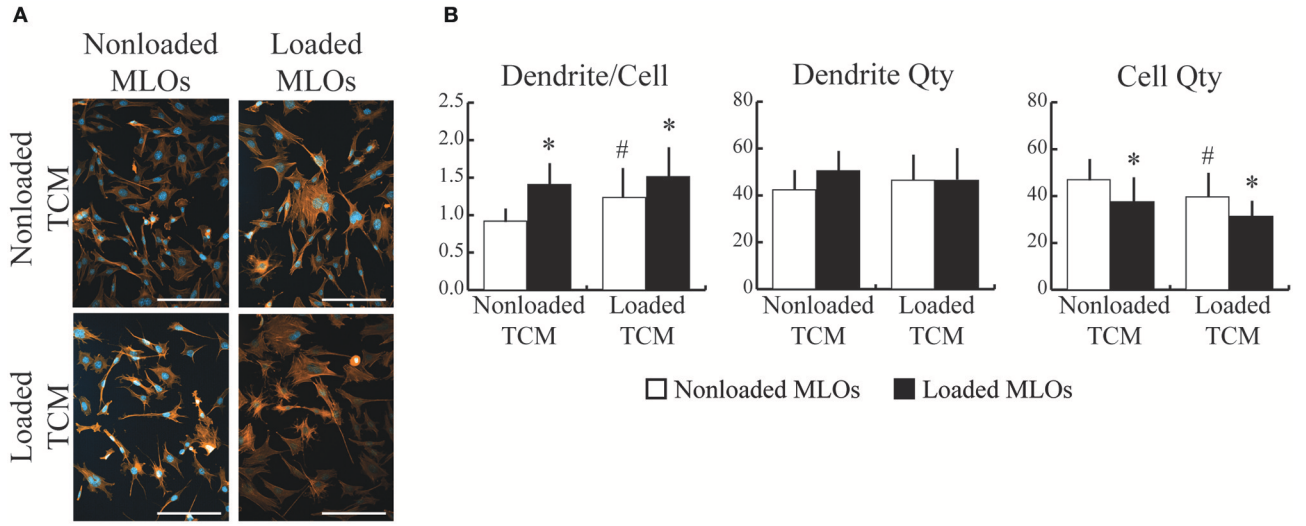

FIGURE 3 | Mechanically-loaded breast cancer cells altered loading-induced MLO-Y4 dendrite formation. **(A)** Fluorescent images of MLO cultured with conditioned media collected from NonLoaded MDAs (NonLoaded TCM, upper) and loaded MDAs (Loaded TCM, lower) suggested that mechanically-loaded tumor cells stimulated MLO to form more dendrites. (Scale bars = 100 μm; blue = DAPI, red = phalloidin) **(B)** Loading increased the number of dendrites per MLO for both N NonLoaded L and Loaded TCM groups. Furthermore, in the N NonLoaded L MLO groups, dendrite per cell was greater when MLOs were treated with Loaded TCM, suggesting that loading both cell types synergistically increased the number of dendrites per MLO. Loading-induced changes to dendrite per cell was achieved primarily via reductions in cell number irrespective of whether TCM came from Loaded or NonLoaded MDAs. Additionally, in NonLoaded MLO groups, MLO quantity was further reduced when treated with Loaded TCM relative to NonLoaded TCM, suggesting that loading applied to both cell types maximizes changes to cell quantity. Data are represented as mean + SD. $^{*}p < 0.05$ relative to respective NonLoaded (NL) MLO control group, $^{\#}p < 0.05$ relative to NonLoaded MLOs treated with NonLoaded TCM.

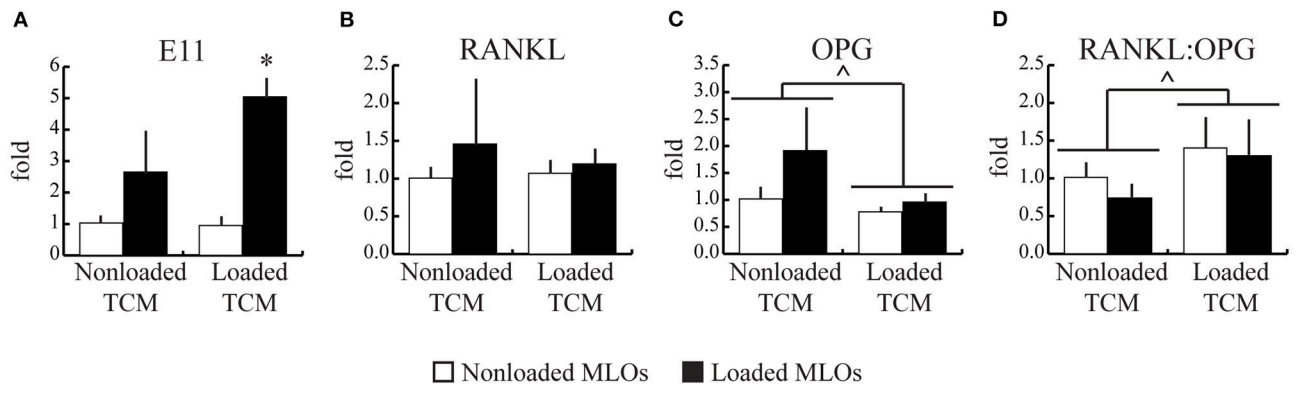

FIGURE 4 | Mechanically-loaded breast cancer cells enhanced E11 gene expression and increased the RANKL/OPG ratio in MLO-Y4s. **(A)** Mechanical loading in MLOs increased their expression of E11, which regulates dendrite formation, which parallels the increased dendrite formation observed histologically and suggests heightened MLO mechanosensivity. (a trend for changes with loading is noted for the NonLoaded TCM group). **(B–D)** RANKL gene expression was unaffected by loading in both NonLoaded TCM and Loaded TCM groups while OPG expression overall was lower in the Loaded TCM group relative to the NonLoaded TCM group (main effect of TCM treatment; NonLoaded and Loaded MLOs pooled for each TCM treatment), resulting in an overall higher RANKL:OPG ratio in the Loaded TCM group. This results suggests that downstream resorption is heightened when breast cancer cells experience mechanical loading in the skeleton. Data are represented as mean + SD. $^{*}p < 0.05$ relative to respective NonLoaded MLO control group, $^{\wedge}p < 0.05$ relative to the pooled NonLoaded TCM group (main effect of TCM treatment).

the context of breast cancer, when MDA-MB231 cells were treated with conditioned media collected from MLO-Y4 cells exposed to fluid shear stress (at a similar shear stress utilized in our study), the signaling molecular ATP that was secreted from dendritic hemichannels inhibited tumor cell migration, invasion, and growth (19). However, the reciprocal effects of tumor cells on osteocyte function was not investigated in that study.

When mechanical loading was applied to osteocytes in conjunction to treatment with conditioned media, loading-induced changes in dendrite formation were altered. In the control group, total dendrite number increased with loading,

as expected (23). As dendrites are the most mechanoresponsive part of the osteocyte (relative to the cell body) (20, 21), increased dendrite formation is expected to confer increased osteocyte mechanosensitivity overall. Similarly, as mechanical loading is well-documented to result in net bone formation via osteocyte signaling (10), we further expect that the observed increased dendrite formation would result in downstream net bone formation, which should be verified in future studies. Our results also suggest that osteocytes are able to respond to mechanical signals despite the presence of tumor-derived factors. Similarly, when mechanical loading was applied to a mouse model of breast cancer bone metastasis, significant increases in bone mass still occurred (11). Interestingly, increases in dendrite number per osteocyte occurred in a reduced osteocyte cell population whether tumor cell-secreted factors were collected from loaded or nonloaded breast cancer cells, and reductions were maximal with conditioned media from mechanically-loaded breast cancer cells. When bone marrow-derived mesenchymal stem cells (which are osteocyte progenitors) simultaneously underwent mechanical compression and exposure to conditioned media collected from loaded breast cancer cells, their growth profile did not change, though their osteogenic differentiation did (13). Similarly, we saw evidence for enhanced osteocyte differentiation via E11 gene expression. This may indicate that effects on cell growth depend on the stage of differentiation, at least in the osteoblastic lineage. Future work is needed to identify which tumor-secreted factors are modulating osteocyte cell growth. Taken together, our data show that despite tumor-mediated reduction in osteocyte cell number, dendrite formation due to loading increased in the existing population of osteocytes, indicative of heightened mechanosensitivity.

Changes in OPG, but not RANKL, were observed in response to mechanically-loading breast cancer cell secretions and applied fluid flow. The ratio of these two factors control downstream remodeling, rather than changes in one or the other (27). Based on gene expression, we observed an overall higher RANKL/OPG ratio when loading was applied to both tumor cells and osteocytes. This is expected to correlate with either the initiation of a remodeling cycle (as osteoclast formation and resorption occurs prior to formation) or result in net-resorption bone remodeling. Moreover, previous work applying fluid shear stress to MLOs demonstrated that changes to RANK/OPG at the gene level did not correlate with changes at the protein level (35). Two hours of fluid flow at similar levels of shear stress immediately increased RANKL and OPG gene expression in MLO-Y4 cells, but RANKL protein decreased while OPG protein increased. These changes to gene expression were detected immediately following a single bout of loading, but they returned to normal within 24 h. Here, we subjected osteocytes to mechanical loading for 3 consecutive days. In the future, how changes to osteocyte gene expression correlate to changes in downstream remodeling should be investigated.

We also determined that breast cancer-mediated changes in osteocyte cell growth was not due to osteocyte apoptosis. In contrast, bone metastatic MM has been associated with increased osteocyte apoptosis (17, 45), but this effect may require cell-cell contact as mentioned previously. It is possible that reducing osteocyte growth may constitute a mechanism by which breast cancer cells avoid osteocyte-mediated inhibition of their migration and proliferation, and that mechanical loading may augment the "intrinsic self-defense mechanism" of osteocytes against this (19).

In our current work, we utilized the MLO-Y4 osteocyte cell line to perform initial experiments investigating the role of loading on modulating breast cancer-mediated changes to osteocyte function because of its well-documented response to mechanical loading, especially to fluid flow (22, 28–31). However, it is likely that osteocyte interactions with cancer cells differ depending on their stage of differentiation. For example, expression of osteocytic proteins that are associated with multiple myeloma bone metastasis, such as sclerostin, are associated with mature osteocytes (47). Here, MLO-Y4s model early osteocytes and do not secrete such proteins (32). Future work should include osteocytes at varying stages of differentiation. For example, osteocyte cell lines such as IDG-SW3s (22, 28–31) and OCY454s (48) represent mature osteocytes that secrete sclerostin, while MLO-A5s represent mineralizing osteoid-osteocytes (49), all of which are useful models to utilize in future studies. Additionally, we combined human breast cancer cells with mouse osteocyte cells. However, both of these cells lines are extensively used and studied. In particular, the MDA-MB231 cell line is widely used in mouse models of breast cancer and bone metastasis. Previously, such a mouse model of bone metastatic breast cancer was combined with mechanical loading and demonstrated that increased mechanical loading interfered with the establishment of secondary tumors and bone osteolysis (11). *In vitro* models, such as the one utilized here, can be used to help elucidate the underlying cellular mechanisms of mechanical loading on bone metastasis.

Our current experiments with MLO-Y4s were performed using a 2D system. Even though osteocytes naturally reside in a 3D lacunar-canalicular network, our approach permitted comparison of our results with that from other MLO-Y4 flow studies, which are most commonly conducted in 2D. Furthermore, by applying fluid flow in the 2D rocking set-up, the resulting shear stress profile was more controllable and better characterized in terms of estimating the shear stresses applied to the cells (whereas comparing across 3D systems, which requires computational modeling to characterize the flow field, is usually unfeasible). Thus, we were able to reliably apply a shear stress ($\sim$1 Pa) known to affect osteocyte mechano-sensing ability (22) and breast cancer cell migration (under steady flow) (41, 42). To better represent the physiological environment of osteocytes, however, future studies should be conducted in 3D systems.

In summary, we have shown that mechanically-loaded breast cancer cells modify osteocyte mechanosensing and bone remodeling by increasing dendrite formation and inhibiting OPG expression. These results highlight that osteocytes serve

as the cellular link between mechanical loading and breast cancer-induced bone disease.

AUTHOR CONTRIBUTIONS

All contributing authors have agreed to submission of this manuscript for publication. ML conceived of the study. WW, BS, GK, and ML designed experiments, analyzed data, and interpreted results. WW, BS, and GK performed experiments. WW, BS, and ML wrote the manuscript.

FUNDING

We are thankful for funding from the University of Massachusetts Healy Endowment Grant and the Commonwealth Honors College.

ACKNOWLEDGMENTS

We thank Dr. Lynda Bonewald for advice and feedback; Drs. Paola Divieti Pajevic and Nora Springer for their advice on our fluorescent staining protocols; and Dr. Mary Hagen for her work in developing and validating qPCR assays.

SUPPLEMENTARY MATERIAL

The Supplementary Material for this article can be found online at: https://www.frontiersin.org/articles/10.3389/fendo.2018.00352/full#supplementary-material

Supplementary Figure 1 | Breast cancer-derived factors did not induce MLO-Y4 apoptosis. No evidence of osteocyte apoptosis was detected due to mechanical loading or treatment with conditioned media from mechanically-loaded breast cancer cells, as assessed by fluorometric TUNEL staining. (Scale bars = 100 μm; green = TUNEL, blue = DAPI, red = phalloidin).

REFERENCES

1. Harbeck N, Salem M, Nitz U, Gluz O, Liedtke C. Personalized treatment of early-stage breast cancer: present concepts and future directions. *Cancer Treat Rev*. (2010) 36:584–94. doi: 10.1016/j.ctrv.2010.04.007
2. Society AC. *Cancer Facts & Figures 2017*. Atlanta, GA: American Cancer Society (2017).
3. Coleman RE, Lipton A, Roodman GD, Guise TA, Boyce BF, Brufsky AM, et al. Metastasis and bone loss: advancing treatment and prevention. *Cancer Treat Rev*. (2010) 36:615–20. doi: 10.1016/j.ctrv.2010.04.003
4. Bussard KM, Gay CV, Mastro AM. The bone microenvironment in metastasis; what is special about bone? *Cancer Metastasis Rev*. (2008) 27:41–55. doi: 10.1007/s10555-007-9109-4
5. Green JR. Antitumor effects of bisphosphonates. *Cancer* (2003) 97(3 Suppl):840–7. doi: 10.1002/cncr.11128
6. Stresing V, Daubiné F, Benzaid I, Mönkkönen H, Clézardin P. Bisphosphonates in cancer therapy. *Cancer Lett*. (2007) 257:16–35. doi: 10.1016/j.canlet.2007.07.007
7. de Groot AF, Appelman-Dijkstra NM, van der Burg SH, Kroep JR. The anti-tumor effect of RANKL inhibition in malignant solid tumors - A systematic review. *Cancer Treat Rev*. (2018) 62:18–28. doi: 10.1016/j.ctrv.2017.10.010
8. Li C, Zhang Y, Chen G, Hu F, Zhao K, Wang Q. Engineered multifunctional nanomedicine for simultaneous stereotactic chemotherapy and inhibited osteolysis in an orthotopic model of bone metastasis. *Adv Mater*. (2017) 29:1605754. doi: 10.1002/adma.201605754
9. Qiao H, Cui Z, Yang S, Ji D, Wang Y, Yang Y, et al. Targeting osteocytes to attenuate early breast cancer bone metastasis by theranostic upconversion nanoparticles with responsive plumbagin release. *ACS Nano* (2017) 11:7259–73. doi: 10.1021/acsnano.7b03197
10. Thompson WR, Rubin CT, Rubin J. Mechanical regulation of signaling pathways in bone. *Gene* (2012) 503:179–93 doi: 10.1016/j.gene.2012.04.076
11. Lynch ME, Brooks D, Mohanan S, Lee MJ, Polamraju P, Dent K, et al. *In vivo* tibial compression decreases osteolysis and tumor formation in a human metastatic breast cancer model. *J Bone Miner Res*. (2013) 28:2357–67. doi: 10.1002/jbmr.1966
12. Pagnotti GM, Chan ME, Adler BJ, Shroyer KR, Rubin J, Bain SD, et al. Low intensity vibration mitigates tumor progression and protects bone quantity and quality in a murine model of myeloma. *Bone* (2016) 90:69–79. doi: 10.1016/j.bone.2016.05.014
13. Lynch ME, Chiou AE, Lee MJ, Marcott SC, Polamraju PV, Lee Y, et al. Three-dimensional mechanical loading modulates the osteogenic response of mesenchymal stem cells to tumor-derived soluble signals. *Tissue Eng Part A* (2016) 22:1006–15. doi: 10.1089/ten.tea.2016.0153
14. Schaffler MB, Cheung WY, Majeska R, Kennedy O. *Osteocytes: master* orchestrators of bone. *Calcif Tissue Int*. (2013) 94:5–24. doi: 10.1007/s00223-013-9790-y
15. Dallas SL, Prideaux M, Bonewald LF. The osteocyte: an endocrine cell and more. *Endocr Rev*. (2013) 34:658–90. doi: 10.1210/er.2012-1026
16. Terpos E, Christoulas D, Katodritou E, Bratengeier C, Gkotzamanidou M, Michalis E et al. Elevated circulating sclerostin correlates with advanced disease features and abnormal bone remodeling in symptomatic myeloma: reduction post-bortezomib monotherapy. *Int J Cancer* (2011) 131:1466–71. doi: 10.1002/ijc.27342
17. Delgado-Calle, J, Anderson J,Cregor MD,Hiasa M, Chirgwin, JM, Carlesso N, et al. Bidirectional notch signaling and osteocyte-derived factors in the bone marrow microenvironment promote tumor cell proliferation and bone destruction in multiple myeloma. *Cancer Res*. (2016) 76:1089–100. doi: 10.1158/0008-5472.CAN-15-1703
18. Zhou JZ, Anderson J, Cregor MD, Hiasa M, Chirgwin JM, Carlesso N, et al. Differential impact of adenosine nucleotides released by osteocytes on breast cancer growth and bone metastasis. *Oncogene* (2015) 34:1831–42. doi: 10.1038/onc.2014.113
19. Zhou JZ, Riquelme MA, Gu S, Kar R, Gao X, Sun L, et al. Osteocytic connexin hemichannels suppress breast cancer growth and bone metastasis. *Oncogene* (2016) 35:5597–607. doi: 10.1038/onc.2016.101
20. Thi MM, Suadicani SO, Schaffler MB, Weinbaum S, Spray DC. Mechanosensory responses of osteocytes to physiological forces occur along processes and not cell body and require alphaVbeta3 integrin. *Proc Natl Acad Sci USA*. (2013) 110:21012–7. doi: 10.1073/pnas.1321210110
21. Burra S, Nicolella DP, Fr ancis WL, Freitas CJ, Mueschke NJ, Poole K, et al. Dendritic processes of osteocytes are mechanotransducers that induce the opening of hemichannels. *Proc Natl Acad Sci USA*. (2010) 107:13648–53. doi: 10.1073/pnas.1009382107
22. Cheng B, Zhao S, Luo J, Sprague E, Bonewald LF, Jiang JX. Expression of functional gap junctions and regulation by fluid flow in osteocyte-like MLO-Y4 cells. *J Bone Miner Res*. (2001) 16:249–59. doi: 10.1359/jbmr.2001.16.2.249
23. Sasaki M, Kuroshima S, Aoki Y, Inaba N, Sawase T. Ultrastructural alterations of osteocyte morphology via loaded implants in rabbit tibiae. *J Biomech*. (2015) 48:4130–41. doi: 10.1016/j.jbiomech.2015.10.025
24. Price C, Zhou X, Li W, Wang L. Real-time measurement of solute transport within the lacunar-canalicular system of mechanically loaded bone: direct evidence for load-induced fluid flow. *J Bone Miner Res*. (2011) 26:277–85. doi: 10.1002/jbmr.211
25. Dallas SL, Bonewald LF. Dynamics of the transition from osteoblast to osteocyte. *Ann N Y Acad Sci*. (2010) 1192:437–43. doi: 10.1111/j.1749-6632.2009.05246.x

26. Plotkin LI. Apoptotic osteocytes and the control of targeted bone resorption. *Curr Osteoporos Rep*. (2014) 12:121–6. doi: 10.1007/s11914-014-0194-3
27. Boyce BF, Xing L. Functions of RANKL/RANK/OPG in bone modeling and remodeling. *Arch Biochem Biophys*. (2008) 473:139–46. doi: 10.1016/j.abb.2008.03.018
28. Fahlgren A, Bratengeier C, Semeins CM, Klein-Nulend J, Bakker AD. Supraphysiological loading induces osteocyte-mediated osteoclastogenesis in a novel *in vitro* model for bone implant loosening. *J Orthop Res*. (2017) 36:1425–34. doi: 10.1002/jor.23780
29. Brady RT, O'Brien FJ, Hoey DA. Mechanically stimulated bone cells secrete paracrine factors that regulate osteoprogenitor recruitment, proliferation, and differentiation. *Biochem Biophys Res Commun*. (2015) 459:118–23. doi: 10.1016/j.bbrc.2015.02.080
30. Genetos DC, Kephart CJ, Zhang Y, Yellowley CE, Donahue HJ. Oscillating fluid flow activation of gap junction hemichannels induces ATP release from MLO-Y4 osteocytes. *J Cell Physiol*. (2007) 212:207–14. doi: 10.1002/jcp.21021
31. Middleton K, Al-Dujaili S, Mei X, Günther A, You L. Microfluidic co-culture platform for investigating osteocyte-osteoclast signalling during fluid shear stress mechanostimulation. *J Biomech*. (2017) 59:35–42. doi: 10.1016/j.jbiomech.2017.05.012
32. Bonewald LF. Establishment and characterization of an osteocyte-like cell line, MLO-Y4. *J Bone Miner Metab*. (1999) 17:61–5. doi: 10.1007/s007740050066
33. You J, Yellowley CE, Donahue HJ, Zhang Y, Chen Q, Jacobs CR. Substrate deformation levels associated with routine physical activity are less stimulatory to bone cells relative to loading-induced oscillatory fluid flow. *J Biomech Eng*. (2000) 122:387–93. doi: 10.1115/1.1287161
34. Xiong J, Onal M, Jilka RL, Weinstein RS, Manolagas SC, O'Brien CA. Matrix-embedded cells control osteoclast formation. *Nat Med*. (2011) 17:1235–41. doi: 10.1038/nm.2448
35. You L, Onal M, Jilka RL, Weinstein RS, Manolagas SC, O'Brien CA. Osteocytes as mechanosensors in the inhibition of bone resorption due to mechanical loading. *Bone* (2008) 42:172–9. doi: 10.1016/j.bone.2007.09.047
36. Nguyen J, Tang SY, Nguyen D, Alliston T. Load regulates bone formation and Sclerostin expression through a TGFbeta-dependent mechanism. *PLoS ONE* (2013) 8:e53813. doi: 10.1371/journal.pone.0053813
37. Michael Delaine-Smith R, Javaheri B, Helen Edwards J, Vazquez M, Rumney RM. Preclinical models for *in vitro* mechanical loading of bone-derived cells. *Bonekey Rep*. (2015) 4:728. doi: 10.1038/bonekey.2015.97
38. Hoey DA, Kelly DJ, Jacobs CR. A role for the primary cilium in paracrine signaling between mechanically stimulated osteocytes and mesenchymal stem cells. *Biochem Biophys Res Commun*. (2011) 412:182–7. doi: 10.1016/j.bbrc.2011.07.072
39. Delaine-Smith RM, MacNeil' S, Reilly GC. Matrix production and collagen structure are enhanced in two types of osteogenic progenitor cells by a simple fluid shear stress stimulus. *Eur Cell Mater*. (2012) 24:162–74. doi: 10.22203/eCM.v024a12
40. Zhou X, Liu D, You L, Wang L. Quantifying fluid shear stress in a rocking culture dish. *J Biomech*. (2010) 43:1598–602. doi: 10.1016/j.jbiomech.2009.12.028
41. Polacheck WJ, Charest JL, Kamm RD. Interstitial flow influences direction of tumor cell migration through competing mechanisms. *Proc Natl Acad Sci U S A*. (2011) 108:11115–20. doi: 10.1073/pnas.1103581108
42. Polacheck WJ, German AE, Mammoto A, Ingber DE, Kamm RD. Mechanotransduction of fluid stresses governs 3D cell migration. *Proc Natl Acad Sci USA*. (2014) 111:2447–52. doi: 10.1073/pnas.1316848111
43. Pathi SP, Kowalczewski C, Tadipatri R, Fischbach C. A novel 3-D mineralized tumor model to study breast cancer bone metastasis. *PLoS ONE* (2010) 5:e8849. doi: 10.1371/journal.pone.0008849
44. Schmittgen TD, Livak KJ. Analyzing real-time PCR data by the comparative C(T) method. *Nat Protoc*. (2008) 3:1101–8. doi: 10.1038/nprot.2008.73
45. Giuliani N, Ferretti M, Bolzoni M, Storti P, Lazzaretti M, Dalla Palma B et al. Increased osteocyte death in multiple myeloma patients: role in myeloma-induced osteoclast formation. *Leukemia* (2012) 26:1391–401. doi: 10.1038/leu.2011.381
46. Kamioka H, Honjo T, Takano-Yamamoto T. A three-dimensional distribution of osteocyte processes revealed by the combination of confocal laser scanning microscopy and differential interference contrast microscopy. *Bone* (2001) 28:145–9. doi: 10.1016/S8756-3282(00)00421-X
47. Delgado-Calle J, Sato AY, Bellido T. Role and mechanism of action of sclerostin in bone. *Bone* (2017) 96:29–37. doi: 10.1016/j.bone.2016.10.007
48. Spatz JM, Wein MN, Gooi JH, Qu Y, Garr JL, Liu S, et al. The Wnt Inhibitor Sclerostin Is Up-regulated by Mechanical Unloading in Osteocytes *in Vitro*. *J Biol Chem*. (2015) 290:16744-58. doi: 10.1074/jbc.M114.628313
49. Kato Y, Boskey A, Spevak L, Dallas M, Hori M, Bonewald LF. Establishment of an osteoid preosteocyte-like cell MLO-A5 that spontaneously mineralizes in culture. *J Bone Miner Res*. (2001) 16:1622–33. doi: 10.1359/jbmr.2001.16.9.1622

Conflict of Interest Statement: The authors declare that the research was conducted in the absence of any commercial or financial relationships that could be construed as a potential conflict of interest.

frontiers in Endocrinology

MINI REVIEW
published: 07 August 2018
doi: 10.3389/fendo.2018.00436

Advanced Imaging of Multiple Myeloma Bone Disease

Barry G. Hansford[1] *and Rebecca Silbermann*[2]*

[1] *Department of Diagnostic Radiology, Oregon Health and Sciences University, Portland, OR, United States,* [2] *Division of Hematology and Medical Oncology, Oregon Health and Sciences University, Knight Cancer Institute, Portland, OR, United States*

Multiple myeloma (MM), a malignancy of mature plasma cells, is the second most common hematologic malignancy and the most frequent cancer to involve the skeleton (1, 2). Bone disease in MM patients is characterized by lytic bone lesions that can result in pathologic fractures and severe pain. While recent advances in MM therapy have significantly increased the median survival of newly diagnosed patients (3), skeletal lesions and their sequelae continue to be a major source of patient morbidity and mortality and bone pain is the most frequent presenting symptom of MM patients (4). Rapid improvements in imaging technology now allow physicians to identify ever smaller skeletal and bone marrow abnormalities, however the clinical value of subtle radiographic findings is not always clear. This review summarizes currently available technologies for assessing MM bone disease and provides guidance for how to choose between imaging modalities.

Keywords: myeloma bone disease, MRI imaging, PET imaging, CT imaging, lytic bone disease

OPEN ACCESS

Edited by:
Julie A. Sterling, Vanderbilt University, United States

Reviewed by:
Laurent Garderet, Assistance Publique Hopitaux De Paris (AP-HP), France
Babatunde Olukayode Oyajobi, The University of Texas Health Science Center at San Antonio, United States
Damien Huglo, Université Lille Nord de France, France

***Correspondence:**
Rebecca Silbermann
silbermr@ohsu.edu

Specialty section:
This article was submitted to Bone Research, a section of the journal Frontiers in Endocrinology

Received: *21 March 2018*
Accepted: *16 July 2018*
Published: *07 August 2018*

Citation:
Hansford BG and Silbermann R (2018) Advanced Imaging of Multiple Myeloma Bone Disease. Front. Endocrinol. 9:436. doi: 10.3389/fendo.2018.00436

INTRODUCTION

Multiple myeloma (MM) bone disease continues to be one of the most devastating complications of MM and is characterized by an uncoupling of the normal bone remodeling process. In contrast to physiologic bone remodeling, where bone formation occurs at sites of bone resorption, MM bone disease (MMBD) is marked by local areas of increased osteolysis in areas adjacent to MM cells and highly suppressed or absent osteoblast function. This combination leads to lytic bone lesions that do not heal and generalized bone loss. Pain related to bone destruction occurs in more than two-thirds of patients and is the most frequent symptom at disease presentation. In addition, MMBD results in enhanced tumor growth and fractures, all of which impact survival. Approximately 70% of MM patients have skeletal disease at diagnosis and up to 85% develop bone lesions after diagnosis. Importantly, it is estimated that 60% of patients develop pathologic fractures over their disease course (5, 6), and MM patients with pathologic fractures have a 20% increased risk of death compared to other patients (7). Despite this high prevalence, not all MM patients develop MMBD. For those that do, management of MM bone disease remains a crucial part of their long-term care as MM bone lesions persist in the absence of active disease in the majority of patients.

Skeletal imaging is a critical component of both the initial diagnostic evaluation and the long-term management of patients with plasma cell disorders. MM is preceded by the well-defined conditions monoclonal gammopathy of undetermined significance (MGUS) and smoldering MM (SMM), both of which are currently managed with surveillance. Active (symptomatic) MM is treated with antineoplastic therapy and has historically been diagnosed based on the presence of >10% clonal bone marrow plasma cells or biopsy-proven plasmacytoma in combination with one

or more myeloma-defining events: hypercalcemia, renal dysfunction, anemia, and lytic bone disease (referred to as CRAB criteria). The definition of active MM was broadened by the International Myeloma Working Group in 2014 to include patients with a high disease burden based on percentage of monoclonal plasma cell infiltration in the bone marrow or a high serum involved to uninvolved free light chain ratio (>100), as patients with these laboratory biomarkers have a high risk of progression to active disease (8). Importantly, the definition of MM bone disease was clarified to exclude osteoporosis or vertebral compression fractures identified in the absence of other lytic lesions (8). Updated MM diagnostic criteria also included allowance of advanced imaging technology including CT, PET, and MRI for the identification of focal bone lesions, however the decision of which imaging modality to use for which patient remains at the discretion of the provider.

MGUS is an asymptomatic condition defined by the presence of a low concentration (<3 g/dL) serum monoclonal protein, a bone marrow with <10% monoclonal plasma cells, and the absence of CRAB criteria. SMM is defined by the presence of a serum monoclonal protein >3 g/dL and/or 10–60% monoclonal bone marrow plasma cells in addition to the absence of CRAB criteria and an involved to uninvolved serum free light chain ratio <100. MGUS and SMM are premalignant conditions with variable courses. Patients with MGUS and SMM have an overall risk of progression to MM of 1 and 10% per year, respectively (9), however individuals within each group have variable risks of disease progression. Validated multivariate risk models allow prognostic stratification of MGUS and SMM patients into risk categories with 5 year probabilities of MM progression of 2, 10, and 46% for MGUS and 4, 46, and 72% for SMM (10). Interestingly, MGUS and SMM are both associated with osteopenia, altered bone microstructure, and an increased fracture risk (11, 12).

PATHOPHYSIOLOGY OF MYELOMA BONE DISEASE

The tightly regulated osteoclast—osteoblast activity of normal physiologic bone remodeling is uncoupled in MM bone disease. MM cells physically disrupt the bone-remodeling compartment, allowing cell-cell contact between MM cells and bone cells and the exchange of soluble factors that mediate the enhanced bone destruction and absent bone formation characteristic of MM bone disease (13). Cellular components of the bone marrow microenvironment, such as osteoclasts, osteocytes, immune cells, and bone marrow stromal cells stimulate the growth and chemoresistance of MM cells in the marrow space through the production of both membrane-bound and soluble growth factors that enhance MM cell growth and increase marrow angiogenesis (14, 15). MM-cell derived cytokines in turn increase osteoclast formation and bone resorption both systemically and in areas of tumor infiltration (16), creating a "vicious cycle" of increased bone resorption leading to increased tumor burden. The bone resorption process itself also results in the release and activation of bone matrix-derived growth factors that further enhance MM cell growth (17). Osteoblast function, in contrast, is highly suppressed or absent, resulting in purely lytic bone lesions.

Skeletal remodeling is abnormal in patients with MGUS and SMM. In retrospective studies, MGUS is associated with a 6 times greater risk of vertebral fracture and 1.4–2.5 times greater risk of any fracture when compared to control populations (11, 18). Limited prospective evaluations of skeletal abnormalities in MGUS have been completed to date, but those that have confirm the high prevalence of vertebral fractures in MGUS and suggest an association between non-traumatic vertebral fractures and a clonal lambda light chain predominance (19). MGUS and SMM are associated with osteopenia, altered bone microstructure, and an increased rate of bone resorption and overall fracture risk (11, 12, 20). Biochemical markers of bone resorption such as serum carboxy-terminal telopeptide of type-I collagen (CTX-1) and urine deoxypyridinoline (DPD) correlate with disease burden in patients with MGUS as compared with MM (21, 22), and MGUS patients have reduced levels of bone-specific alkaline phosphatase, a cell membrane-associated enzyme produced by osteoblasts, as compared to patients with non-malignant osteoporosis (23).

IMAGING TECHNIQUES FOR MULTIPLE MYELOMA

Currently available imaging modalities allow characterization of lytic bone disease, bone marrow infiltration, bone mineral density (BMD), and extra-medullary disease involvement in MM. The primary purpose of skeletal imaging in MM has historically been identification of lytic bone disease, which allows classification of a patient as having smoldering or active disease, identification of bone lesions at risk of fracture and requiring acute management, and surveillance for new skeletal lesions based on patient symptoms and as evidence of disease progression. Recently however, the prognostic value of early identification of focal bone marrow involvement in MM, both at diagnosis and in response to antimyeloma therapy, has been evaluated.

Identification of Lytic Bone Lesions

Lytic bone disease is classically identified in MM using whole body radiography (skeletal survey, SS), which consists of conventional x-rays of the skull, spine, pelvis, chest, femora, and humeri, and was a component of the Durie-Salmon MM staging system (24, 25). SS remains the traditional gold standard for identification of lytic bone lesions, however standard radiography cannot detect early lytic bone lesions and therefore underestimates bone marrow involvement. Identification of lytic bone lesions using standard radiography requires loss of a minimum of 30% of trabecular bone volume (26), and a systematic review comparing imaging modalities for detection of lytic bone lesions concluded that low-dose, whole-body computed tomography, magnetic resonance imaging (MRI), and positron emission tomography (PET)-CT are all superior to SS for the detection of myeloma bone disease, except for in the ribs and skull (27). The updated International Myeloma Working Group (IMWG) criteria for the diagnosis of active multiple

myeloma (8) reflect this data, and acknowledge that newer and highly sensitive imaging modalities, including low-dose whole-body CT and PET-CT may be used to satisfy CRAB criteria if lesions are >5 mm in size and even if lesions cannot be visualized by standard x-rays. At this time, the primary advantages of SS as a screening tool in MM are its low cost and widespread availability.

Dedicated low-dose, whole-body computed tomography (WBCT) is an increasingly common imaging modality to screen for lytic bone disease in MM. Several studies have confirmed that WBCT is more sensitive than SS for the detection of lytic bone lesions, particularly in the axial skeleton, with some reporting that bone lesions were detected by WBCT in 20–25% of patients with negative SS, as well as fractures (28, 29). (**Figures 1A,B** provide examples of skeletal lesions identified on WBCT that are not visible on standard radiographs). In addition, WBCT can detect osteopenia and extraosseous disease. Based on these findings and the short scan time as compared to SS, many centers have moved to WBCT for initial screening for lytic disease. WBCT is less useful for monitoring response to therapy, as bone marrow lesions are poorly visualized with CT and lytic reactions persist after therapy. WBCT radiation doses vary according to individual institutions' WBCT protocols and are generally higher for WBCT than SS. However with the increasingly common adoption of low dose WBCT techniques the dose difference as compared to SS may be negligible. Additionally, the time required for radiologic review of WBCT images is greater than that required for SS, and clinically significant and insignificant incidental findings can be identified which may unnecessarily raise patient anxieties and lead to increased healthcare costs (30).

Identification of Focal Bone Marrow Infiltration

MRI allows assessment of bone marrow involvement in MM and can reveal both diffuse bone marrow abnormalities and focal lesions. MRI has historically been coupled with SS to assess the spine and pelvis when determining if a patient has smoldering or active disease, for staging and response evaluation in patients with non-secretory MM, and in evaluation of suspected solitary plasmacytoma (24, 31). However, it has been reported that nearly 50% of patients with MGUS and MM have skeletal lesions detectable on MRI outside of the axial skeleton (32). In contrast to SS and CT, which are primarily used to identify cortical bone lesions in MM, MRI allows detailed evaluation of the bone marrow space and identification of varying patterns of bone marrow heterogeneity. Five patterns of marrow involvement in MM have been described and associated with tumor burden: normal marrow appearance, focal involvement (a focal lesion is defined by a diameter >5 mm), homogeneous diffuse infiltration, combined diffuse and focal infiltration, and a variegated pattern with inhomogenous marrow (**Figures 1C,D** compare CT and MRI imaging of bone marrow infiltration) (33, 34). High tumor burden is suspected in cases with diffuse hypointensity on T1-weighted images and diffuse hyperintensity on T2-weighted images, such as in **Figures 1E,F**. Cases with low tumor burden are usually associated with a normal MRI pattern (34).

Conventional MRI protocols are now increasingly used for whole body imaging (WBMRI), and revised IMWG diagnostic criteria for MM include the presence of more than one focal lesion (>5 mm) on MRI studies as a biomarker of malignancy (8, 34). MM lesions typically demonstrate low signal intensity on T1-weighted images, due to absence of intralesional fat and high signal intensity on fat-suppressed T2-weighted images, due to high cellularity and water content. Functional MRI techniques, such as dynamic contrast-enhanced MRI and diffusion weighted imaging provide further diagnostic sensitivity that can improve the detection of bone marrow infiltration. Dynamic contrast-enhanced MRI, which is not yet widely available in the clinic, assesses the distribution of contrast within and outside of blood vessels, providing data on vessel permeability that can be correlated with marrow angiogenesis, including the angiogenic response to therapy (35). Diffusion weighted imaging (DWI) measures the random motion of water molecules in tissue, providing information on tissue cellularity, cellular membrane integrity, and the extracellular space (36), and allows qualitative assessment of the bone marrow space in MM. Normal yellow marrow appears hypointense on DWI. As marrow cellularity increases, due to malignant infiltration or red bone marrow hypertrophy, signal hyperintensity increases corresponding to greater restricted diffusion (33).

The combination of WBCT with ^{18}F-fluoro-deoxyglucose (FDG) positron emission tomography (PET-CT) provides an alternative method of visualizing bone marrow infiltration while also allowing visualization of total body tumor burden. Metabolic activity of lesions of interest is calculated based on FDG uptake in cells with high glucose demand and compared with standardized uptake values. CT images are then combined with PET images to provide anatomic localization. Importantly, hypermetabolic bone lesions can be identified in the absence of underlying lytic lesions. Active MM is FDG-PET-CT positive in the marrow space, although FDG-PET-CT is less sensitive than MRI for evaluation of diffuse marrow infiltration (36, 37). FDG-PET-CT is negative in patients with MGUS and SMM with low disease burden (38). Therapeutic response to treatment is characterized by a reduction or elimination of FDG accumulation in involved bone structures.

Multiple studies comparing whole body (WB)MRI or SS with MRI of the spine and pelvis to FDG-PET-CT in patients with active MM have demonstrated that MRI is superior to CT for detection of skeletal lesions (39). Results of studies comparing WBMRI to FDG-PET-CT, however, are mixed, and it is likely that the imaging modalities are of equal sensitivity (40), except for when evaluating the spine, where MRI is preferred (34). PET-MRI is a promising new hybrid technology, which in initial investigations appears to be at least as sensitive as PET-CT (41, 42).

An important caveat to these findings, however, is that standardized rubrics for interpreting MRI and PET-CT in MM continue to evolve (43, 44). In some cases the adoption of the imaging technology itself precedes the standardization of image interpretation, creating a challenging situation for treating clinicians. In addition, false positive bone marrow

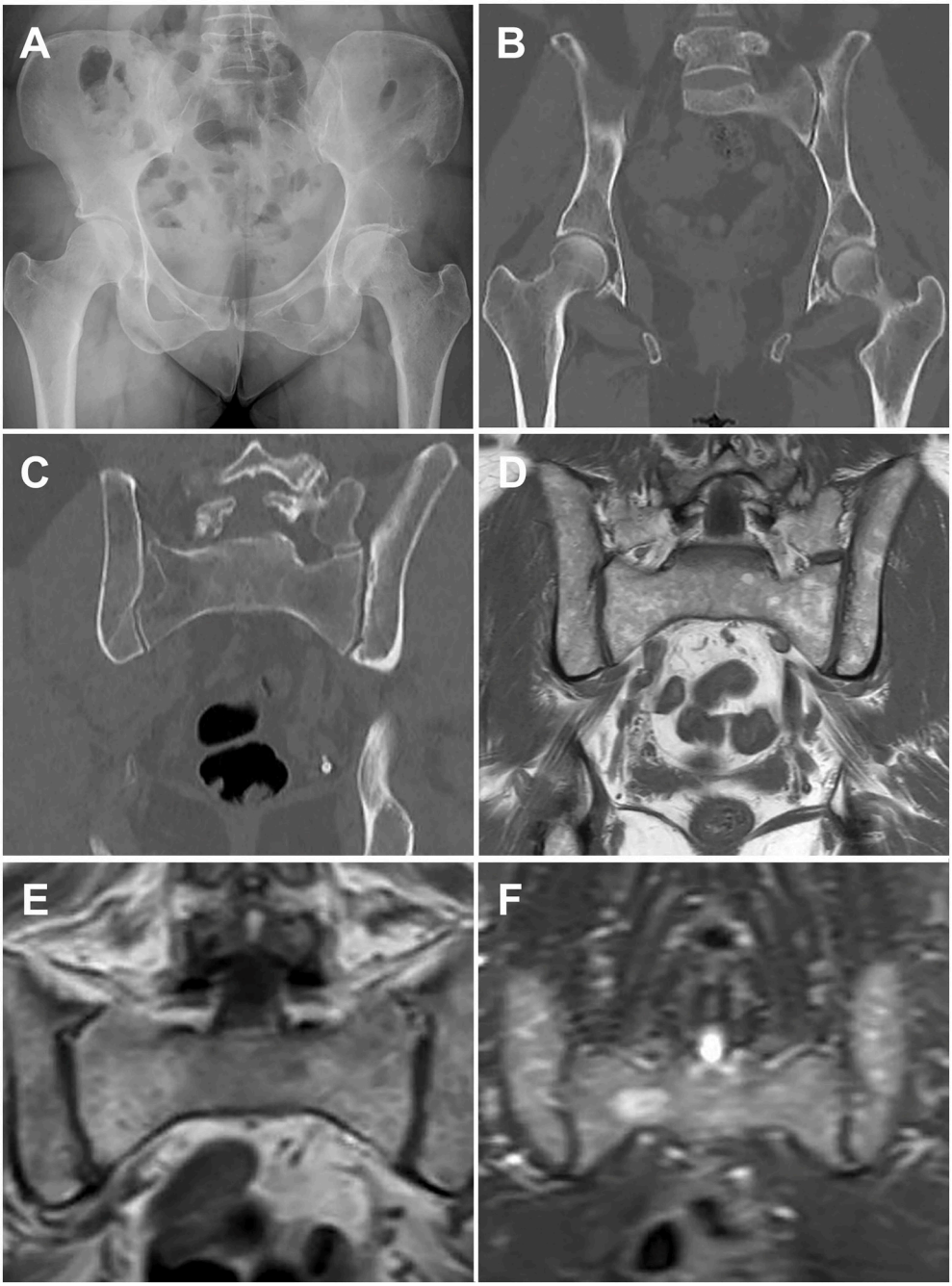

FIGURE 1 | Paired images from patients illustrating different imaging modalities. Image pairs **(A,B)** and **(E,F)** are patients with active multiple myeloma. Image pair **(C,D)** is a patient with smoldering multiple myeloma. **(A)** Frontal pelvis radiograph demonstrates diffuse osteopenia with a dominant destructive osteolytic myelomatous deposit at the left supra-acetabular region as well as multiple smaller subtle lucent foci of disease. **(B)** Coronal reformat CT of the pelvis from a whole-body CT multiple myeloma protocol again demonstrates the dominant destructive left supra-acetabular lesion as well as multiple additional foci of smaller osteolytic myelomatous disease throughout the imaged osseous structures. Many of the smaller lesions identified on CT were occult on the comparison radiographs. **(C)** Coronal reformat CT of the pelvis from a whole-body CT multiple myeloma protocol demonstrates diffuse heterogeneity of the bone marrow including regions of mixed lucency and slightly increased density with a representative lucent focus at the superior aspect of the right iliac bone. **(D)** Coronal T1-weighted non-fat saturated image from a whole-body MRI multiple myeloma protocol demonstrates a diffusely heterogeneous appearance of the bone marrow without evidence for macroscopic myelomatous disease. **(E)** Coronal T1-weighted non-fat saturated image from a whole-body MRI multiple myeloma protocol demonstrates a diffuse micronodular pattern of myelomatous disease, also commonly referred to as a variegated or salt-and-pepper appearance. **(F)** Coronal STIR image from a whole-body MRI multiple myeloma protocol demonstrates diffuse heterogeneity of the bone marrow with a dominant hyperintense right hemisacral lesion compatible with macroscopic myelomatous disease.

TABLE 1 | Summary of advanced imaging modalities commonly used in the management of multiple myeloma.

	Radiation dose	Examination time	Sensitivity for detection of focal bone lesions	Key references evaluating the efficacy of cross-sectional imaging modalities	Key references evaluating the prognostic utility of cross-sectional imaging modalities
Digital Skeletal Survey (SS) (Chest; antero-posterior (AP) and laterval views of the spine, humera, femora; lateral views of the skull; AP view of the pelvis)	1.5–2.5 mSv	10 min. (Patients are repositioned during the examination)	Low, compared to cross-sectional imaging techniques.		
Whole body low dose CT (Vertex to mid- thighs), without iv contrast	4–7 mSv	5 min.	Superior to SS, particularly in the axial skeleton. Less sensitive	(28, 29)	
FDG-PET-CT (Vertex to mid-thighs)	Variable, based on institutional practice*	60–90 min. wait time following tracer injection, then 20 min. scan time	Similar to MRI	(36, 38–40)	(46, 50, 53, 54, 63)
Axial MRI (Spine and pelvis)	None	90 min.	Similar to PET-CT, limited by imaging field.	(32, 34)	(52)
Whole body MRI (Vertex to knees)	None	90 min.	Similar to PET-CT.	(34–36, 39, 40)	(51, 54, 64, 65)

**Some institutional protocols obtain the CT portion of a PET-CT scan for the purpose of attenuation correction only.*

infiltrative findings are observed in both MRI and PET-CT studies. It is also difficult to distinguish red bone marrow from bone marrow infiltrated with MM on MRI with DWI, complicating interpretation of MRI bone marrow findings in younger patients (45), and PET-CT images can be falsely positive in the setting of trauma (including recent fracture), recent chemotherapy, radiotherapy and growth factors, and falsely negative following administration of high-dose steroids (46).

^{18}F-sodium fluoride (NaF), a PET radiotracer which accumulates in both osteoblastic and osteolytic lesions, reflecting bone remodeling, has been investigated to a limited extent in MMBD (47). A recent small study prospectively compared SS, whole body MRI, FDG-PET-CT, and NaF-PET-CT in patients with newly diagnosed MM (48). MRI was superior to SS, FDG-PET-CT, and NaF-PET-CT. Detection of skeletal abnormalities by NaF-PET-CT was equivalent to SS, a finding consistent with other evaluations of NaF-PET-CT in MM patients (49).

Imaging to Assess Disease Response

Improvement in imaging technology has accelerated interest in the use of imaging to monitor disease response in MM. Historically, skeletal imaging with SS was performed at suspected disease relapse or in the setting of new skeletal symptoms with the goal of identification of progressive disease as evidenced by new lytic bone lesions. The utility of FDG-PET-CT for evaluation of disease response in MM has been extensively studied in both a prospective and retrospective fashion (46). Suppression of FDG-PET-CT focal lesions correlates well with disease response to therapy, and precedes resolution of lesions observed on MRI (50). Interestingly, it has been suggested that MRI-assessment of bone marrow infiltration, perhaps in combination with functional MRI techniques, may have utility as a measure of minimal residual disease (51).

Imaging as a Prognostic Tool

The prognostic value of both MRI and PET-CT has been evaluated in MM patients. While the clinical significance of focal bone lesions that do not meet IMWG criteria for MM bone disease is not yet clear, serial WBMRI or FDG-PET-CT imaging can be used to follow the progression of these lesions. Focal bone lesions identified on axial MRI and not identified on SS correlated with overall survival in a large study of MM patients who received tandem autologous stem cell transplants. Sixty percent of patients studied had resolution of these lesions following treatment and superior survival (52). The presence of three or more FDG-avid focal lesions has been shown to be an independent predictor of overall survival (50, 53). Additionally, the persistence of three FDG-avid lesions after induction therapy for MM is associated with decreased overall survival (53). This data is supported by the IMAJEM study, a subgroup analysis of the Intergroupe Francophone du Myélome (IFM)/Dana Farber Cancer Institute (DFCI) 2009 trial (54). PET-CT and MRI were performed at diagnosis, following induction therapy and prior to maintenance therapy. Bone lesion identification at diagnosis did not differ significantly between imaging modalities. Normalization of PET-CT prior to initiation of maintenance therapy was associated with an improved 2-year progression free and overall survival. Interestingly, normalization of MRI before

maintenance was not predictive of progression free or overall survival.

Evaluation of Bone Mineral Density

Age-related bone loss is traditionally characterized using dual-energy x-ray absorptiometry (DXA). While areal BMD is an established predictor of fracture risk (55), sequential measures of BMD are not routinely performed in MM and are challenging to interpret due to the heterogeneous BMD changes in MM (56). In addition, the revised IMWG criteria for the diagnosis of MM excludes osteoporosis in the absence of lytic lesions as sufficient to fulfill CRAB requirements of bone disease because many myeloma patients are elderly and have pre-existing osteoporosis and clarifies that bone densitometry studies are not sufficient to determine the presence of multiple myeloma (8). Despite this, it is important to recognize that the majority of systemic therapies for MM include glucocorticoids, which are themselves associated with increased fracture risk, and are included in the World Health Organization Fracture Risk Assessment Tool (FRAX) (55). Therefore DXA screening should be considered in patients undergoing active MM therapy who are not treated with bisphosphonates (due to intolerance or patient preference), or those requiring reinitiation of therapy who previously completed their bisphosphonate treatment.

Interestingly, MGUS is associated with skeletal fragility and MGUS patients have an increased risk of fracture, particularly axial fracture, as compared to age-matched controls (11, 18, 57). Recent studies employing quantitative computerized tomography (QCT) and high-resolution peripheral QCT (HRpQCT), imaging technology primarily used in osteoporosis research, have reported an overall increase in bone size with an increased endocortical area of the distal radius and diminished cortical thickness and bone strength in MGUS patients (12, 57, 58). The natural history of these findings in MGUS is not known, and it is not known if these abnormalities persist or change during progression to active myeloma.

SELECTION OF IMAGING MODALITIES FOR MM

The International Myeloma Working Group (IMWG), European Myeloma Network, National Comprehensive Cancer Network (NCCN), the European Society for Medical Oncology (ESMO), and the British Society for Hematology Guidelines have all published guidelines to assist clinicians in choosing between available imaging modalities (24, 34, 46, 59–62). In all guidelines, WBCT is preferred for the diagnosis of lytic bone disease as compared to SS. The choice of imaging technology for patients without clear-cut myeloma bone disease, however, is more challenging, and dependent on available imaging technology and radiologic expertise. WBMRI, when available, provides excellent diagnostic and potentially prognostic information, however appropriate interpretation of the marrow changes that may be seen on images requires institutional experience. When WBMRI is not available, axial MRI should be performed when vertebral body involvement is suspected. PET/CT provides an excellent alternative to WBMRI when determining if a patient has active or smoldering MM. Key characteristics of the imaging techniques that are currently used most frequently for the identification of MMBD and clinical management of MM patients are summarized in the **Table 1**.

In conclusion, technology for assessing MM bone disease is rapidly evolving. Therapeutic clinical trials are beginning to routinely incorporate serial imaging assessments into their design, allowing investigators to evaluate the utility of these advanced imaging technologies to monitor response to treatment and disease progression.

AUTHOR CONTRIBUTIONS

RS wrote the manuscript and reviewed the scientific literature. BH selected the images included in the figure, wrote the figure legends, and provided detailed comments and input.

REFERENCES

1. Roodman GD. Pathogenesis of myeloma bone disease. *J Cell Biochem*. (2010) 109:283–91. doi: 10.1038/leu.2008.336
2. Siegel R, Ma J, Zou Z, Jemal A. Cancer statistics, 2014. *CA Cancer J Clin*. (2014) 64:9–29. doi: 10.3322/caac.21208
3. Kyle RA, Durie BG, Rajkumar SV, Landgren O, Blade J, Merlini G, et al. Monoclonal gammopathy of undetermined significance (MGUS) and smoldering (asymptomatic) multiple myeloma: IMWG consensus perspectives risk factors for progression and guidelines for monitoring and management. *Leukemia* (2010) 24:1121–7. doi: 10.1038/leu.2010.60
4. Roodman G, Diagnosis and treatment of myeloma bone disease. In: Rajkumar S, Kyle R, editors. *Treatment of Multiple Myeloma and Related Disorders*. New York, NY: Cambridge University Press (2009). p. 64–76.
5. Greenberg AJ, Rajkumar SV, Therneau TM, Singh PP, Dispenzieri A, Kumar SK. Relationship between initial clinical presentation and the molecular cytogenetic classification of myeloma. *Leukemia* (2014) 28:398–403. doi: 10.1038/leu.2013.258
6. Melton LJ III, Kyle RA, Achenbach SJ, Oberg AL, Rajkumar SV. Fracture risk with multiple myeloma: a population-based study. *J Bone Miner Res.* (2005) 20:487–93. doi: 10.1359/JBMR.041131
7. Saad F, Lipton A, Cook R, Chen YM, Smith M, Coleman R. Pathologic fractures correlate with reduced survival in patients with malignant bone disease. *Cancer* (2007) 110:1860–7. doi: 10.1002/cncr.22991
8. Rajkumar SV, Dimopoulos MA, Palumbo A, Blade J, Merlini G, Mateos MV, et al. International Myeloma Working Group updated criteria for the diagnosis of multiple myeloma. *Lancet Oncol*. (2014) 15:e538–48. doi: 10.1016/S1470-2045(14)70442-5
9. Kyle RA, Therneau TM, Rajkumar SV, Offord JR, Larson DR, Plevak MF, et al. A long-term study of prognosis in monoclonal gammopathy of undetermined significance. *N Engl J Med*. (2002) 346:564–9. doi: 10.1056/NEJMoa01133202
10. Perez-Persona E, Mateo G, Garcia-Sanz R, Mateos MV, de Las Heras N, de Coca AG, et al. Risk of progression in smouldering myeloma and monoclonal gammopathies of unknown significance: comparative analysis of the evolution of monoclonal component and multiparameter flow cytometry of bone marrow plasma cells. *Br J Haematol.* (2010) 148:110–4. doi: 10.1111/j.1365-2141.2009.07929.x

11. Melton LJ III, Rajkumar SV, Khosla S, Achenbach SJ, Oberg AL, Kyle RA. Fracture risk in monoclonal gammopathy of undetermined significance. *J Bone Miner Res.* (2004) 19:25–30. doi: 10.1359/jbmr.0301212
12. Ng AC, Khosla S, Charatcharoenwitthaya N, Kumar SK, Achenbach SJ, Holets MF, et al. Bone microstructural changes revealed by high-resolution peripheral quantitative computed tomography imaging and elevated DKK1 and MIP-1 α levels in patients with MGUS. *Blood* (2011) 118:6529–34. doi: 10.1182/blood-2011-04-351437
13. Andersen TL, Sondergaard TE, Skorzynska KE, Dagnaes-Hansen F, Plesner TL, Hauge EM, et al. A physical mechanism for coupling bone resorption and formation in adult human bone. *Am J Pathol.* (2009) 174:239–47. doi: 10.2353/ajpath.2009.080627
14. Mitsiades CS, McMillin DW, Klippel S, Hideshima T, Chauhan D, Richardson PG, et al. The role of the bone marrow microenvironment in the pathophysiology of myeloma and its significance in the development of more effective therapies. *Hematol Oncol Clin North Am.* (2007) 21:1007–34, vii–viii. doi: 10.1016/j.hoc.2007.08.007
15. Cackowski FC, Anderson JL, Patrene KD, Choksi RJ, Shapiro SD, Windle JJ, et al. Osteoclasts are important for bone angiogenesis. *Blood* (2010) 115:140–9. doi: 10.1182/blood-2009-08-237628
16. Galson DL, Silbermann R, Roodman GD. Mechanisms of multiple myeloma bone disease. *Bonekey Rep.* (2012) 1:135. doi: 10.1038/bonekey.2012.135
17. Dallas SL, Rosser JL, Mundy GR, Bonewald LF. Proteolysis of latent transforming growth factor-beta (TGF-beta) -binding protein-1 by osteoclasts. A cellular mechanism for release of TGF-beta from bone matrix. *J Biol Chem.* (2002) 277:21352–60. doi: 10.1074/jbc.M111663200
18. Gregersen H, Jensen P, Gislum M, Jorgensen B, Sorensen HT, Norgaard M. Fracture risk in patients with monoclonal gammopathy of undetermined significance. *Br J Haematol.* (2006) 135:62–7. doi: 10.1111/j.1365-2141.2006.06269.x
19. Piot JM, Royer M, Schmidt-Tanguy A, Hoppe E, Gardembas M, Bourree T, et al. Factors associated with an increased risk of vertebral fracture in monoclonal gammopathies of undetermined significance. *Blood Cancer J.* (2015) 5:e345. doi: 10.1038/bcj.2015.71
20. Berenson JR, Rosen LS, Howell A, Porter L, Coleman RE, Morley W, et al. Zoledronic acid reduces skeletal-related events in patients with osteolytic metastases. *Cancer* (2001) 91:1191–200. doi: 10.1002/1097-0142(20010401)91:7<1191::AID-CNCR1119>3.0.CO;2-0
21. Jakob C, Zavrski I, Heider U, Brux B, Eucker J, Langelotz C, et al. Bone resorption parameters [carboxy-terminal telopeptide of type-I collagen (ICTP), amino-terminal collagen type-I telopeptide (NTx), and deoxypyridinoline (Dpd)] in MGUS and multiple myeloma. *Eur J Haematol.* (2002) 69:37–42. doi: 10.1034/j.1600-0609.2002.00505.x
22. Ting KR, Brady JJ, Hameed A, Le G, Meiller J, Verburgh E, et al.Clinical utility of C-terminal telopeptide of type 1 collagen in multiple myeloma. *Br J Haematol.* (2016) 173:82–8. doi: 10.1111/bjh.13928
23. Woitge HW, Horn E, Keck AV, Auler B, Seibel MJ, Pecherstorfer M. Biochemical markers of bone formation in patients with plasma cell dyscrasias and benign osteoporosis. *Clin Chem.* (2001) 47:686–93.
24. Dimopoulos M, Terpos E, Comenzo RL, Tosi P, Beksac M, Sezer O, et al. International myeloma working group consensus statement and guidelines regarding the current role of imaging techniques in the diagnosis and monitoring of multiple Myeloma. *Leukemia* (2009) 23:1545–56. doi: 10.1038/leu.2009.89
25. Durie BG, Salmon SE. A clinical staging system for multiple myeloma. Correlation of measured myeloma cell mass with presenting clinical features, response to treatment, and survival. *Cancer* (1975) 36:842–54. doi: 10.1002/1097-0142(197509)36:3<842::AID-CNCR2820360303>3.0.CO;2-U
26. Edelstyn GA, Gillespie PJ, Grebbell FS. The radiological demonstration of osseous metastases. Experimental observations. *Clin Radiol.* (1967) 18:158–62. doi: 10.1016/S0009-9260(67)80010-2
27. Regelink JC, Minnema MC, Terpos E, Kamphuis MH, Raijmakers PG. Pieters-van den Bos IC, et al. Comparison of modern and conventional imaging techniques in establishing multiple myeloma-related bone disease: a systematic review. *Br J Haematol.* (2013) 162:50–61. doi: 10.1111/bjh.12346
28. Pianko MJ, Terpos E, Roodman GD, Divgi CR, Zweegman S, Hillengass J, et al. Whole-body low-dose computed tomography and advanced imaging techniques for multiple myeloma bone disease. *Clin Cancer Res.* (2014) 20:5888–97. doi: 10.1158/1078-0432.CCR-14-1692
29. Hillengass J, Moulopoulos LA, Delorme S, Koutoulidis V, Mosebach J, Hielscher T, et al. Whole-body computed tomography versus conventional skeletal survey in patients with multiple myeloma: a study of the International Myeloma Working Group. *Blood Cancer J.* (2017) 7:e599. doi: 10.1038/bcj.2017.78
30. Surov A, Bach AG, Tcherkes A, Schramm D. Non-osseous incidental findings in low-dose whole-body CT in patients with multiple myeloma. *Br J Radiol.* (2014) 87:20140185. doi: 10.1259/bjr.20140185
31. Moulopoulos LA, Dimopoulos MA, Weber D, Fuller L, Libshitz HI, Alexanian R. Magnetic resonance imaging in the staging of solitary plasmacytoma of bone. *J Clin Oncol.* (1993) 11:1311–5. doi: 10.1200/JCO.1993.11.7.1311
32. Bauerle T, Hillengass J, Fechtner K, Zechmann CM, Grenacher L, Moehler TM, et al. Multiple myeloma and monoclonal gammopathy of undetermined significance: importance of whole-body versus spinal MR imaging. *Radiology* (2009) 252:477–85. doi: 10.1148/radiol.2522081756
33. Dutoit JC, Claus E, Offner F, Noens L, Delanghe J, Verstraete KL. Combined evaluation of conventional MRI, dynamic contrast-enhanced MRI and diffusion weighted imaging for response evaluation of patients with multiple myeloma. *Eur J Radiol.* (2016) 85:373–82. doi: 10.1016/j.ejrad.2015.11.040
34. Dimopoulos MA, Hillengass J, Usmani S, Zamagni E, Lentzsch S, Davies FE, et al. Role of magnetic resonance imaging in the management of patients with multiple myeloma: a consensus statement. *J Clin Oncol.* (2015) 33:657–64. doi: 10.1200/JCO.2014.57.9961
35. Huang SY, Chen BB, Lu HY, Lin HH, Wei SY, Hsu SC, et al. Correlation among DCE-MRI measurements of bone marrow angiogenesis, microvessel density, and extramedullary disease in patients with multiple myeloma. *Am J Hematol.* (2012) 87:837–9. doi: 10.1002/ajh.23256
36. Dutoit JC, Verstraete KL. Whole-body MRI, dynamic contrast-enhanced MRI, and diffusion-weighted imaging for the staging of multiple myeloma. *Skeletal Radiol.* (2017) 46:733–50. doi: 10.1007/s00256-017-2609-6
37. Lu YY, Chen JH, Lin WY, Liang JA, Wang HY, Tsai SC et al. FDG PET or PET/CT for detecting intramedullary and extramedullary lesions in multiple Myeloma: a systematic review and meta-analysis. *Clin Nucl Med.* (2012) 37:833–7. doi: 10.1097/RLU.0b013e31825b2071
38. Adam Z, Bolcak K, Stanicek J, Buchler T, Pour L, Krejci M, et al. Fluorodeoxyglucose positron emission tomography in multiple myeloma, solitary plasmocytoma and monoclonal gammapathy of unknown significance. *Neoplasma* (2007) 54:536–40.
39. Baur-Melnyk A, Buhmann S, Becker C, Schoenberg SO, Lang N, Bartl R, et al. Whole-body MRI versus whole-body MDCT for staging of multiple myeloma. *AJR Am J Roentgenol.* (2008) 190:1097–104. doi: 10.2214/AJR.07.2635
40. Waheed S, Mitchell A, Usmani S, Epstein J, Yaccoby S, Nair B, et al. Standard and novel imaging methods for multiple myeloma: correlates with prognostic laboratory variables including gene expression profiling data. *Haematologica* (2013) 98:71–8. doi: 10.3324/haematol.2012.066555
41. Shah SN, Oldan JD. PET/MR Imaging of Multiple Myeloma. *Magn Reson Imaging Clin N Am.* (2017) 25:351–65. doi: 10.1016/j.mric.2017.01.003
42. Sachpekidis C, Hillengass J, Goldschmidt H, Mosebach J, Pan L, Schlemmer HP, et al. Comparison of (18)F-FDG PET/CT and PET/MRI in patients with multiple myeloma. *Am J Nucl Med Mol Imaging* (2015) 5:469–78.
43. Dutoit JC, Verstraete KL. MRI in multiple myeloma: a pictorial review of diagnostic and post-treatment findings. *Insights Imaging* (2016) 7:553–69. doi: 10.1007/s13244-016-0492-7
44. Nanni C, Zamagni E, Versari A, Chauvie S, Bianchi A, Rensi M, et al. Image interpretation criteria for FDG PET/CT in multiple myeloma: a new proposal from an Italian expert panel. IMPeTUs (Italian Myeloma criteria for PET USe). *Eur J Nucl Med Mol Imaging* (2016) 43:414–21. doi: 10.1007/s00259-015-3200-9
45. Khoo MM, Tyler PA, Saifuddin A, Padhani AR. Diffusion-weighted imaging (DWI) in musculoskeletal MRI: a critical review. *Skeletal Radiol.* (2011) 40:665–81. doi: 10.1007/s00256-011-1106-6
46. Cavo M, Terpos E, Nanni C, Moreau P, Lentzsch S, Zweegman S, et al. Role of (18)F-FDG PET/CT in the diagnosis and management of multiple myeloma and other plasma cell disorders: a consensus statement by the International Myeloma Working Group. *Lancet Oncol.* (2017) 18:e206–17. doi: 10.1016/S1470-2045(17)30189-4

47. Sachpekidis C, Goldschmidt H, Hose D, Pan L, Cheng C, Kopka K, et al. PET/CT studies of multiple myeloma using (18) F-FDG and (18) F-NaF: comparison of distribution patterns and tracers' pharmacokinetics. *Eur J Nucl Med Mol Imaging* (2014) 41:1343–53. doi: 10.1007/s00259-014-2721-y
48. Dyrberg E, Hendel HW, Al-Farra G, Balding L, Logager VB, Madsen C, et al. A prospective study comparing whole-body skeletal X-ray survey with 18F-FDG-PET/CT, 18F-NaF-PET/CT and whole-body MRI in the detection of bone lesions in multiple myeloma patients. *Acta Radiol Open* (2017) 6:2058460117738809. doi: 10.1177/2058460117738809
49. Ak I, Onner H, Akay OM. Is there any complimentary role of F-18 NaF PET/CT in detecting of osseous involvement of multiple myeloma? A comparative study for F-18 FDG PET/CT and F-18 FDG NaF PET/CT. *Ann Hematol.* (2015) 94:1567–75. doi: 10.1007/s00277-015-2410-3
50. Usmani SZ, Mitchell A, Waheed S, Crowley J, Hoering A, Petty N, et al. Prognostic implications of serial 18-fluoro-deoxyglucose emission tomography in multiple myeloma treated with total therapy 3. *Blood* (2013) 121:1819–23. doi: 10.1182/blood-2012-08-451690
51. Hillengass J, Merz M, Delorme S. Minimal residual disease in multiple myeloma: use of magnetic resonance imaging. *Semin Hematol.* (2018) 55:19–21. doi: 10.1053/j.seminhematol.2018.02.001
52. Walker R, Barlogie B, Haessler J, Tricot G, Anaissie E, Shaughnessy JD Jr, et al. Magnetic resonance imaging in multiple myeloma: diagnostic and clinical implications. *J Clin Oncol.* (2007) 25:1121–8. doi: 10.1200/JCO.2006.08.5803
53. Bartel TB, Haessler J, Brown TL, Shaughnessy JD Jr, van Rhee F, Anaissie E, et al. F18-fluorodeoxyglucose positron emission tomography in the context of other imaging techniques and prognostic factors in multiple myeloma. *Blood* (2009) 114:2068–76. doi: 10.1182/blood-2009-03-213280
54. Moreau P, Attal M, Caillot D, Macro M, Karlin L, Garderet L, et al. Prospective evaluation of magnetic resonance imaging and [(18)F]fluorodeoxyglucose positron emission tomography-computed tomography at diagnosis and before maintenance therapy in symptomatic patients with multiple myeloma included in the IFM/DFCI 2009 trial: results of the IMAJEM study. *J Clin Oncol.* (2017) 35:2911–8. doi: 10.1200/JCO.2017.72.2975
55. Kanis JA, Diagnosis of osteoporosis and assessment of fracture risk. *Lancet* (2002) 359:1929–36. doi: 10.1016/S0140-6736(02)08761-5
56. Abildgaard N, Brixen K, Eriksen EF, Kristensen JE, Nielsen JL, Heickendorff L. Sequential analysis of biochemical markers of bone resorption and bone densitometry in multiple myeloma. *Haematologica* (2004) 89:567–77.
57. Thorsteinsdottir S, Lund SH, Lindqvist EK, Thordardottir M, Sigurdsson G, Costello R, et al. Bone disease in monoclonal gammopathy of undetermined significance: results from a screened population-based study. *Blood Adv.* (2017) 1:2790–8. doi: 10.1182/bloodadvances.2017010454
58. Farr JN, Zhang W, Kumar SK, Jacques RM, Ng AC, McCready LK, et al. Altered cortical microarchitecture in patients with monoclonal gammopathy of undetermined significance. *Blood* (2014) 123:647–9. doi: 10.1182/blood-2013-05-505776
59. Moreau P, San Miguel J, Sonneveld P, Mateos MV, Zamagni E, Avet-Loiseau H, et al. Multiple myeloma: ESMO clinical practice guidelines for diagnosis, treatment and follow-up. *Ann Oncol.* (2017) 28:iv52–61. doi: 10.1093/annonc/mdx096
60. Terpos E, Kleber M, Engelhardt M, Zweegman S, Gay F, Kastritis E, et al. European Myeloma Network guidelines for the management of multiple myeloma-related complications. *Haematologica* (2015) 100:1254–66. doi: 10.3324/haematol.2014.117176
61. Kumar SK, Callander NS, Alsina M, Atanackovic D, Biermann JS, Chandler JC, et al. Multiple Myeloma, Version 3.2017, NCCN Clinical Practice Guidelines in Oncology. *J Natl Compr Canc Netw.* (2017) 15:230–69. doi: 10.6004/jnccn.2017.0023
62. Chantry A, Kazmi M, Barrington S, Goh V, Mulholland N, Streetly M, et al. British Society for Haematology, Guidelines for the use of imaging in the management of patients with myeloma. *Br J Haematol.* (2017) 178:380–93. doi: 10.1111/bjh.14827
63. Zamagni E, Patriarca F, Nanni C, Zannetti B, Englaro E, Pezzi A, et al. Prognostic relevance of 18-F FDG PET/CT in newly diagnosed multiple myeloma patients treated with up-front autologous transplantation. *Blood* (2011) 118:5989–95. doi: 10.1182/blood-2011-06-361386
64. Hillengass J, Fechtner K, Weber MA, Bauerle T, Ayyaz S, Heiss C, Hielscher T, et al. Prognostic significance of focal lesions in whole-body magnetic resonance imaging in patients with asymptomatic multiple myeloma. *J Clin Oncol.* (2010) 28:1606–10. doi: 10.1200/JCO.2009.25.5356
65. Hillengass J, Weber MA, Kilk K, Listl K, Wagner-Gund B, Hillengass M, et al. Prognostic significance of whole-body MRI in patients with monoclonal gammopathy of undetermined significance. *Leukemia* (2014) 28:174–8. doi: 10.1038/leu.2013.244

Conflict of Interest Statement: The authors declare that the research was conducted in the absence of any commercial or financial relationships that could be construed as a potential conflict of interest.

frontiers in Endocrinology

REVIEW
published: 07 September 2018
doi: 10.3389/fendo.2018.00518

Multimodal Treatment of Bone Metastasis—A Surgical Perspective

Henry Soeharno [1,2], Lorenzo Povegliano [1,3] and Peter F. Choong [1,4]*

[1] Department of Orthopedics, St Vincent's Hospital Melbourne, Melbourne, VIC, Australia, [2] Department of Orthopedics, Singapore General Hospital, Singapore, Singapore, [3] Clinica Orthopedica, Universita di Udine, Azienda Sanitaria Universitaria Integrata di Udine, Udine, Italy, [4] Department of Surgery, University of Melbourne, Melbourne, VIC, Australia

Over the past decades there has been an increase in the incidence of cancer worldwide. With the advancement in treatment, patient survival has improved in tandem with the increasing incidence. This, together with the availability of advanced modern diagnostic modalities, has resulted in more cases of metastatic bone disease being identified. Bone metastasis is an ongoing problem and has significant morbidity implications for patients affected. Multimodal treatment strategies are required in dealing with metastatic bone disease, which include both surgical and non-surgical treatment options. In the multidisciplinary team, orthopedic surgeons play an important role in improving the quality of life of cancer patients. Surgical intervention in this setting is aimed at pain relief, restoration of function and improvement in functional independence. In selected cases with resectable solitary metastasis, surgical treatment may be curative. With the advancement of surgical technique and improvement in implant design and manufacture, a vast array of surgical options are available in the modern orthopedic arena. In the majority of cases, limb salvage procedures have become the standard of care in the treatment of metastatic bone disease. Non-surgical adjuvant treatment also contributes significantly to the improvement of cancer patient care. A multidisciplinary approach in this setting is of paramount importance.

Keywords: bone metastasis, metastases, metastatic, prophylactic surgery, multimodal, metastatic bone disease

OPEN ACCESS

Edited by:
Chandi C. Mandal, Central University of Rajasthan, India

Reviewed by:
Jawed Akhtar Siddiqui, University of Nebraska Medical Center, United States
David M. Findlay, University of Adelaide, Australia

****Correspondence:***
Henry Soeharno
ninja0038@gmail.com

Specialty section:
This article was submitted to Bone Research, a section of the journal Frontiers in Endocrinology

Received: *08 March 2018*
Accepted: *17 August 2018*
Published: *07 September 2018*

Citation:
Soeharno H, Povegliano L and Choong PF (2018) Multimodal Treatment of Bone Metastasis—A Surgical Perspective. Front. Endocrinol. 9:518. doi: 10.3389/fendo.2018.00518

INTRODUCTION

The Scandinavian Skeletal Metastasis registry reported an 18% increase in the incidence of cancer over the past decade (1). This is thought to be the result of an increase in the incidence of cancer as well as the improvement in diagnosis. Bone metastasis carries significant morbidity for afflicted patients and negatively impacts their quality of life. Following the lung and liver, bone is the third most likely affected site in metastatic cancer (2). Breast and prostate carcinomas have the greatest tendency to metastasize to bone (65–75%), followed by thyroid (60%), lung (30–40%), and renal (20–25%) carcinomas (3–5). The spine and the pelvis are the sites most frequently affected by metastasis (6). Long bones, such as the humerus and femur are also common sites for metastases (4).

Through the advances of modern cancer treatment options, we see a general improvement in the longevity of cancer patients, and hence an increase in the risk of bone metastasis (7). The management of patients with metastatic bone disease requires a multidisciplinary approach to ensure thorough diagnostic workup and treatment planning. A multi-modal treatment strategy, which includes medical therapy, radiotherapy and surgery, is encouraged in order to optimize

treatment outcomes. In the setting of metastatic disease, surgical treatment is aimed at alleviating pain, restoring functional independence, and improving the overall quality of life of patients (8).

In the current modern orthopedic surgery arena, complex reconstructive surgery is made possible with the availability of advanced implant technology. Through better understanding of biomechanics and tribology, as well as better implant manufacturing processes, orthopedic surgeons now have a wide array of reliable implant options. Extensive bony defects can be resected and reconstructed with modern modular endoprosthesis (9). Advanced implant technologies, including modern locking plates and intramedullary nails have provided treating surgeons with a more robust reconstructive option (10). In the setting of metastatic bone disease construct fixation should be stable and strong enough to allow patients to immediately weight bear. In this regard, the modern implant repertoire allows individualization of treatment and a more predictable outcome.

PRINCIPLES OF MANAGEMENT AND INDICATION FOR SURGERY

Diagnosis

Bone metastases can be asymptomatic and often present as an incidental finding during initial staging investigations. In some cases, they may be detected later during follow up in the setting of adjuvant treatment. It is important to note that about 75% of patients with bone metastases present with pain, which warrants further workup (11). Pain in bone metastases is unfortunately nonspecific; although certain characteristics such as rest pain, night pain or activity-related pain may raise the index of suspicion and indicate the need for further workup.

Metastatic bone disease typically involves multiple sites, which makes diagnosis relatively straightforward. A solitary bone lesion in the setting of a known primary carcinoma, on the other hand, can present a significant diagnostic dilemma. In these cases it is safe to assume the possibility of a malignant primary bone tumor, unless proven otherwise.

Adams et al. (12) reported on the consequences and prevention of inadvertent internal fixation of primary osseous sarcomas. In their study, 8 patients assumed to have metastatic disease underwent internal fixation and were later found to have primary bone sarcoma. As a consequence, 6 out of the 8 patients underwent an amputation. They concluded that inadequate history taking, incomplete staging imaging studies and improper biopsy resulted in these unfortunate incidences. Catastrophic inadvertent intramedullary nailing of a malignant primary bone tumor carries with it significant morbidity, since the majority of patients in such cases will require a high amputation for local disease control (12).

Investigations

Plain Radiography (X-ray)

Orthogonal plain radiographs of the entire bone in question should be obtained, including the joint above and below. The radiographic appearances of metastatic lesions are usually described as osteolytic (**Figure 1**), osteoblastic, or mixed lytic-sclerotic (13). Prostate cancer classically gives rise to osteoblastic lesions, whereas renal carcinoma, lung carcinoma and multiple myeloma are osteolytic in appearance (13). Breast cancer often has a mixture of both lytic and sclerotic disease (13, 14). It is estimated that by the time a lesion becomes radiographically detectable, around 25–75% loss of bone mineral has occurred (15). For this reason, by the time a lesion is detectable on radiographs, the bone involved has weakened significantly (15, 16).

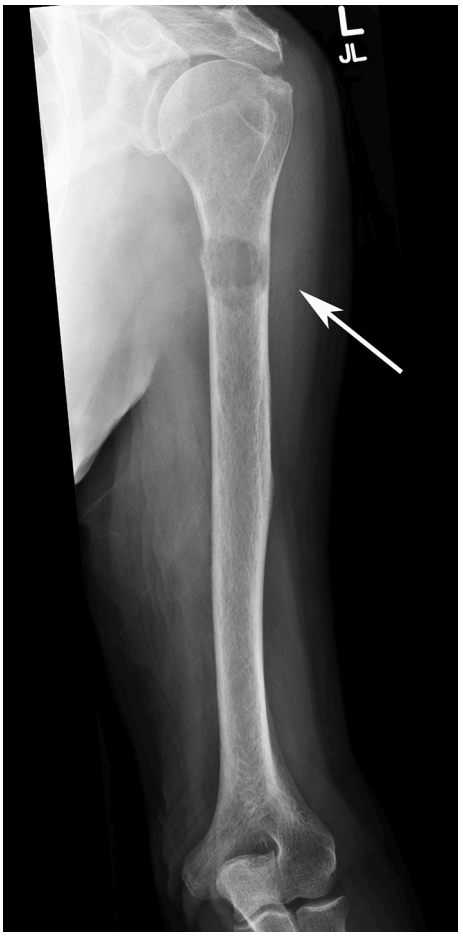

FIGURE 1 | AP radiograph of a left humerus demonstrating a lytic metastatic lesion (arrow) in the proximal diaphysis. Note the extensive cortical involvement, predisposing it to a pathological fracture.

Computed Tomography (CT Scan)

CT scan is the most sensitive imaging modality available for evaluating the extent of cortical bone destruction (**Figure 2**) (17). It is also useful in image guidance during percutaneous biopsy of metastatic lesions. CT scan has a sensitivity of 74% and specificity of 56% in the detection of skeletal metastasis (18).

Magnetic Resonance Imaging (MRI)

MRI has a high sensitivity in detecting small metastatic lesions that are otherwise undetectable by other modalities such as CT scan and bone scan. Yang et al., in their meta-analysis comparing four imaging modalities (CT, MRI, FDG-PET, and

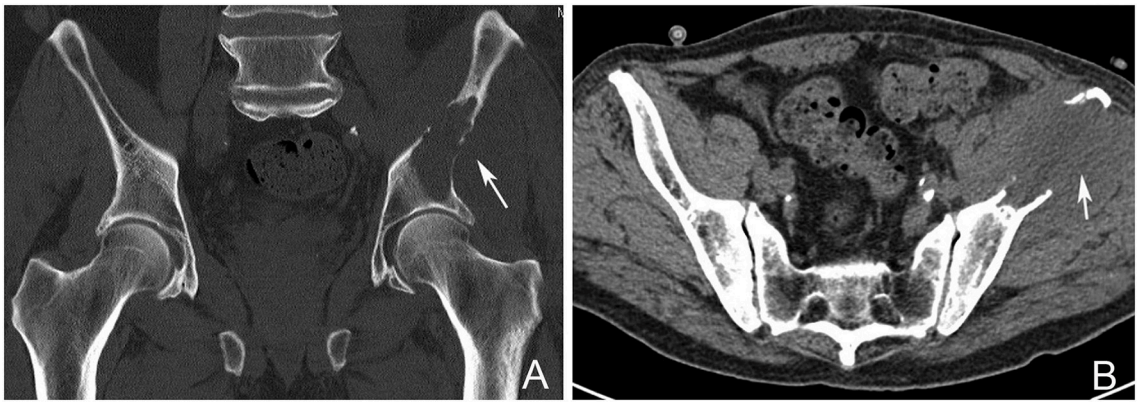

FIGURE 2 | Pelvic CT Scan showing a left sided periacetabular renal cell carcinoma metastasis. **(A)** Involvement of the left supraacetabular region by a large lytic metastatic lesion (arrow). **(B)** Note the extensive extraosseous involvement (arrow).

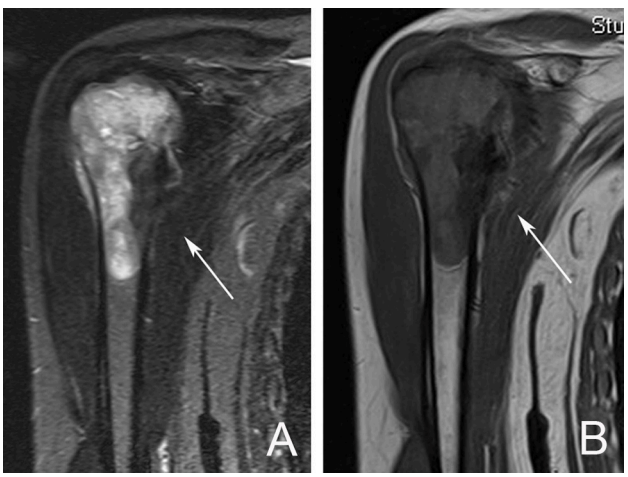

FIGURE 3 | MRI scan demonstrating a right proximal humerus metastatic lesion. **(A)** T2 weighted MRI sequence showing the extent of intramedullary involvement (arrow). **(B)** T1 weighted MRI sequence showing complete involvement of the proximal humerus with cortical breach at the medial calcar region (arrow).

bone scintigraphy) in the detection of bone metastases, found MRI to have a sensitivity of 91% and specificity of 95% (19).

MRI is considered to be the most sensitive imaging modality for assessing the extent of intramedullary and extraosseous soft tissue involvement (**Figure 3**) (20). In the spine, the use of MRI allows the differentiation between osteoporotic and pathological fractures, since edema in osteoporotic compression fractures usually subsides by around 10–12 weeks (18).

Bone Scan (99mTc Bone Scintigraphy)

Bone scan is a radionuclide-based imaging modality that measures osteoblastic activity and skeletal vascularity, hence its ability to detect osteoblastic metastases. It is also useful in determining whether a metastatic lesion is solitary or widespread, since the whole skeleton is captured during imaging (**Figure 4**). In rapidly growing lytic tumors, such as multiple myeloma, the bone scan may appear "cold" since minimal osteoblastic activity is present. In contrast false positive readings are common in areas with high bone turnover, such as seen in trauma and infection (21). The sensitivity and specificity of bone scan in detecting bone metastases has been reported as 78 and 48%, respectively (20).

Positron Emission Tomography (PET)

Fluorodeoxyglucose-positron emission tomography (FDG-PET) is a nuclear imaging modality that detects the metabolic activity of tumors. It relies on the glucose uptake by tumor cells, hence its ability to detect early metastasis prior to any detectable bony destruction (20). Although highly sensitive (98%), FDG-PET on its own has low specificity (56%) since it is a functional rather than anatomic imaging modality (19). The combination of FDG-PET with anatomic imaging modality, such as CT scan, increases its specificity significantly (up to 97%) (**Figure 5**) (22).

Tumor Markers

Apart from routine blood testing, such as full blood count, renal and liver panels, tumor markers are used as part of the systemic staging process in cancer patients. Tumor markers are proteins that represent unique genetic signatures of a particular tumor histotype (**Table 1**), hence their role as diagnostic adjuncts. Tumor markers are also used in monitoring treatment response and in disease surveillance.

Biopsy

Adequate tumor tissue is the key to diagnosis. Biopsies should only be undertaken after all other staging studies are completed. Biopsy may be taken intra-operatively during fracture fixation of a pathological fracture or as a staged procedure during the staging process. Core needle biopsy has been shown to be reliable and adequate for diagnosis in over 90% of cases (23–25). Image-guided core needle biopsy is usually utilized in order to accurately target the lesion and minimize the risk of a false negative reading (26). In areas that are difficult to access, such as the periacetabular

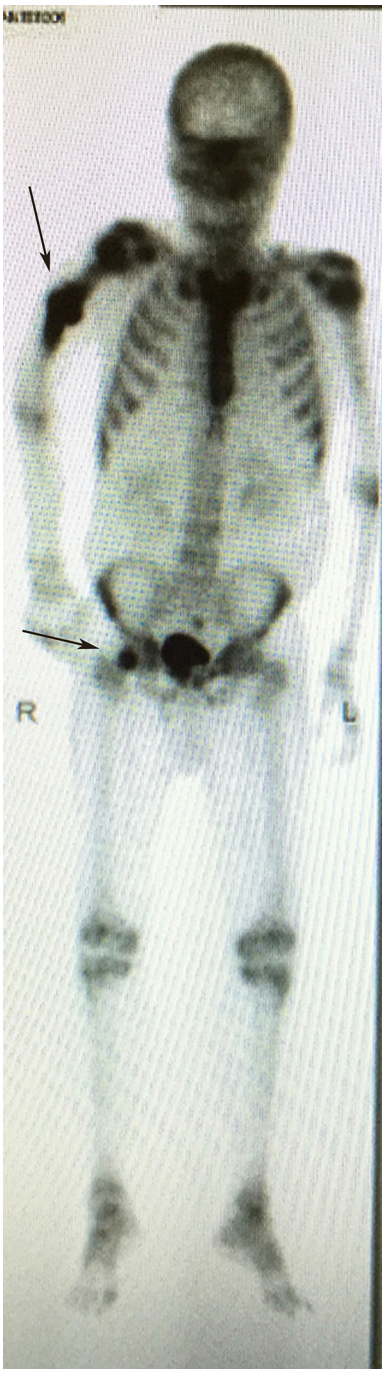

FIGURE 4 | Bone scan demonstrating increase uptake at the right humerus diaphysis and right femoral head (arrows), highlighting the sites of bone metastasis.

area, percutaneous image-guided core needle biopsy has largely replaced the need for open biopsies. Since most impending or pathological fractures are non-emergency cases, surgical fixation should not be performed until a definitive diagnosis has been confirmed (12, 27).

Prognosis and Surgical Decision-Making

The aim of surgical intervention in the setting of metastatic bone disease is to improve the quality of life of patients. Surgery allows pain control by achieving local control of the tumor, and at the same time, restoring the patient's functional independence. Following a thorough staging process to delineate the local and systemic extent of disease, a decision needs to be made as to whether treatment is aimed at palliative or curative intent. In the majority of metastatic conditions, surgical treatment is aimed at palliation, however, in selected cases such as resectable renal cell carcinoma with solitary metastasis, curative wide resection and reconstruction may be considered (**Figure 6**). Fottner et al. (28) in their retrospective review of 101 patients, who were treated surgically for skeletal metastasis of renal cell carcinoma, reported significantly better survival in patients with solitary metastatic lesions who underwent surgical wide resection. They also concluded that other factors contributing to higher survival include, age <65 years, absence of pathologic fractures and tumor-free resection margins.

Les et al. (29) in their retrospective review on 78 patients treated surgically for bone metastasis of renal cell carcinoma compared the rate of local progression between patients treated with local resection versus those who received intralesional procedures. Forty-one percent of patients in the intralesional procedure group required further procedures due to local progression. In contrast, only 1 out of the 37 patients who were treated with marginal or wide resection, required additional surgical intervention for local progression. They concluded that patients who receive intralesional procedures are at a much higher risk of local progression and therefore recommend surgical resection in order to minimize the risk of local progression.

The prognosis associated with a known primary cancer is a major deciding factor in determining the appropriate type of surgical treatment in metastatic bone disease. Longer survival is associated with an increased risk of disease progression or recurrence, hence more aggressive surgical treatment is often warranted. Kirkinis et al. (30) in their review on survival, prognostic factors, and outcomes after surgical treatment of appendicular skeleton bone metastases found several factors to be important predictors of prognosis. These include the primary tumor histoptype and the presence of visceral metastasis, pathological fractures, and multiple metastases. Patients with metastatic disease from renal cell and breast carcinoma were found to have the longest survival, whereas lung carcinoma and myeloma patients were shown to have the worse prognosis.

Given the numerous factors that contribute to the overall survival of patients, making a prognostic prediction is a major challenge. Over the years, several predictive tools have been designed to aid in the treatment decision-making process. Forsberg et al. (31) reviewed the Bayesian Belief Network (BBN) as a model for predicting patient survival. The model is designed to calculate the predicted survival at 3 and 12 months and subsequently guide surgical treatment options. They suggested that an estimated survival of <3 months does not

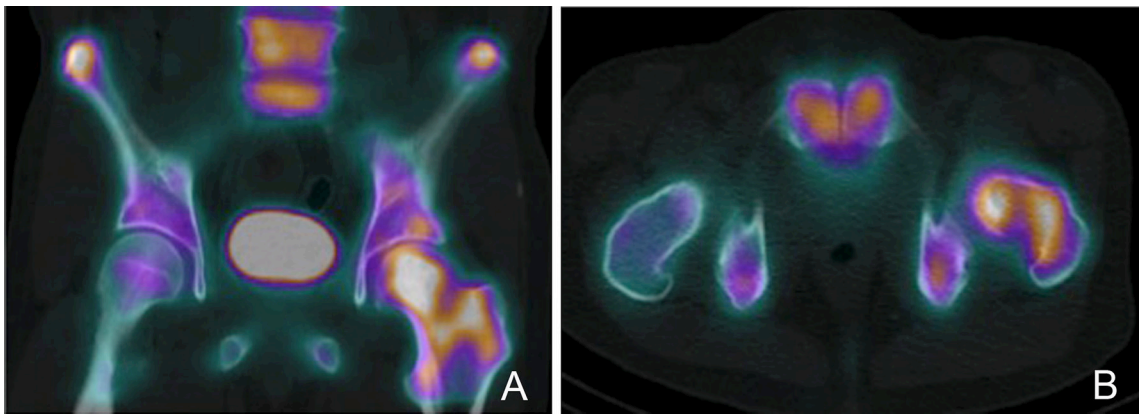

FIGURE 5 | PET-CT scan demonstrating a left proximal femur metastatic lesion. **(A)** Coronal and **(B)** axial cuts of the PET-CT images demonstrating intense FDG uptake at the left femoral head, neck and intertrochanteric region.

TABLE 1 | Examples of commonly used tumor markers.

Tumor marker	Disease
CEA	Colorectal cancer
PSA	Prostate cancer
CA 15-3	Breast cancer
CA 125	Ovarian cancer
CA 19-9	Pancreatic cancer
Beta 2 microglobulin	Multiple myeloma

support surgical treatment of impending pathological fractures. Patients with an estimated survival between 3 and 12 months were recommended for less invasive surgical management not associated with prolonged rehabilitation. When the predicted survival was more than 12 months, a more robust surgical option, such as tumor resection with endoprosthetic reconstruction was recommended.

Predictive models such as the BBN are invaluable in deciding the most appropriate surgical options, however the ultimate surgical treatment modality should be individualized for each patient. The general rule still applies, that any surgical fixation in metastatic bone disease should be sufficiently robust to allow early weight bearing while minimizing any potential complications. The type of fixation needs to have adequate durability to last patients for their remaining lifespan.

Pre-operative Planning

Careful pre-operative planning and the use of appropriate implants are fundamental in oncology surgery. Patients with malignancy should be managed by a multidisciplinary team, as these patients tend to be physiologically compromised and have elevated surgical risk. Meticulous coordination between multidisciplinary team members (medical oncologist, radiation oncologist, orthopedic surgeons, physiotherapist, nursing staff) is paramount in ensuring high quality care.

The role of surgery for bone metastasis can be divided into (i) prophylactic fixation to prevent impending pathological fractures, (ii) stabilization of a pathological fractures, (iii) segmental resection of tumors, and (iv) arthroplasty for replacing joints that have been destroyed by tumor. To this end, orthopedic surgeons have a vast array of surgical devices and implants in their surgical armamentarium at their disposal. These include plates and screws, intramedullary fixation devices, and tumor endoprostheses. The use of percutaneous intralesional injection of polymethylmethacrylate acid (PMMA) in osteoplasty, offers a minimally invasive management option for some contained tumors, e.g., vertebral metastases (4).

Assessing Risk of Fracture

The definition of an impending pathological fracture remains ambiguous and it is the role of treating orthopedic surgeons to recognize them in a timely manner so that appropriate intervention can be administered. When a metastatic lesion has destroyed 30–50% of bone, usually it is deemed that a fracture is impending (32). Treatment strategies are strongly based on the risk of fracture and expected survival of the patient.

Several radiographic-based guidelines have been proposed in the past to aid in the decision-making regarding the need for prophylactic fixation. Fidler (33) proposed prophylactic fixation of long bones with more than 50% destruction by metastasis. Harrington (34) amended Fidler's guide, adding the criteria of: length of lesion of more than 2.5 cm, fractures around the femoral lesser trochanter region and persistent pain post radiation therapy. These guidelines, although useful, were somewhat oversimplified for actual clinical practice application.

In 1989, Mirels (35) developed a scoring system to predict the risk of impending fractures. This system offers a general guideline regarding when to intervene and remains one of the most widely system used. The Mirels scoring system (**Table 2**) is based on a point system that incorporates four criteria (nature of lesion, location, size of cortical involvement and pain), with each criteria carrying a score from 1 to 3 with increasing

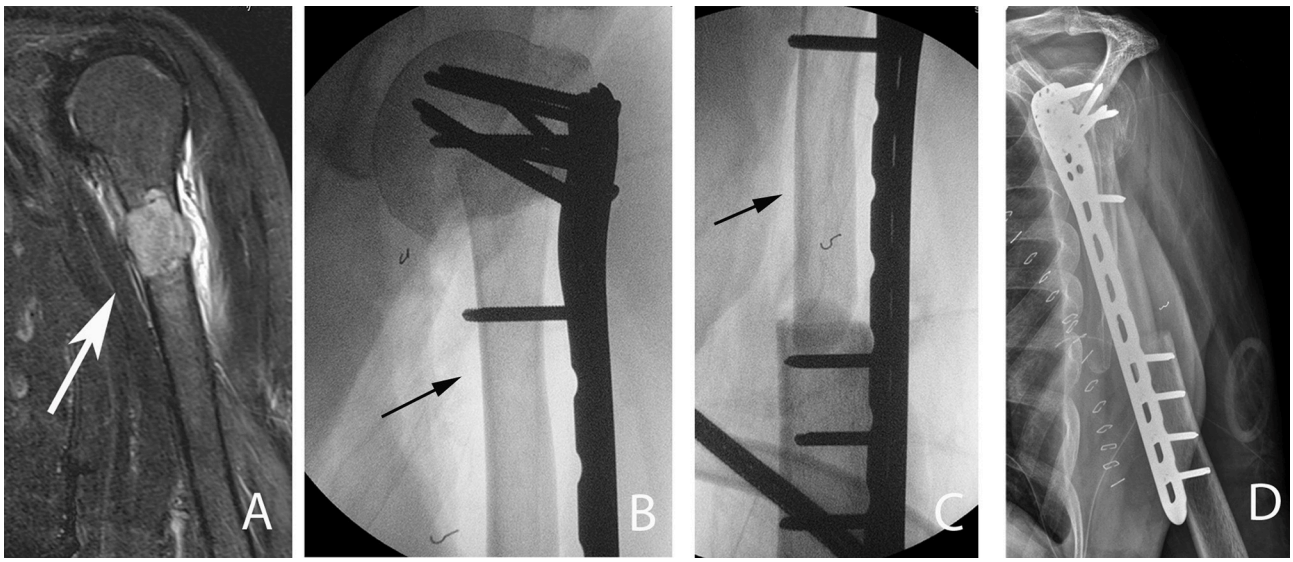

FIGURE 6 | A 54-year-old patient with a left proximal humeral diaphyseal renal cell solitary metastasis treated with wide resection and reconstruction using a fibular allograft and locking plate internal fixation. **(A)** MRI of left humerus showing a metastatic lesion (arrow). **(B,C)** Intraoperative fluoroscopic images after intercalary resection of the proximal humerus diaphysis and reconstruction using a fibular strut graft (arrows). **(D)** Note the preservation of the native humeral head and the locking plate fixation.

TABLE 2 | Mirels score.

Score	Site	Pain	Lesion	Size
1	Upper limb	Mild	Blastic	<1/3
2	Lower limb	Moderate	Mixed	1/3–2/3
3	Peritrochanteric	Functional	Lytic	>2/3

Mirels score ≥ 9 High risk, 8 Intermediate, ≤7 Low risk for fracture.

severity. Non-surgical treatment is recommended for scores of ≤7 and radiation therapy is usually considered as a means of local control. Scores >9 carry a strong recommendation for prophylactic fixation. Scores between 7 and 9 are open to debate as to whether surgery is indicated, and this is where institutional experience prevails. Despite being more comprehensive, the Mirels scoring system has some limitations. The amount of cortical destruction is determined based on two-dimensional orthogonal radiographs, which limits accuracy in the estimation of cortical involvement. The Mirels scoring system has low sensitivity and specificity, moreover, there is uncertainty regarding treatment for patients with a score of 8 (35).

Nazarian et al. (36) developed and validated a CT-based rigidity analysis (CTRA) utilizing the quantification of changes in bone geometry and density. The system allowed for calculation of bone resistance to uniaxial loads, bending moment and torsional moment. In their multicenter prospective study, orthopedic tumor surgeons selected treatment plans for 124 patients with metastatic bone disease based on the Mirels scoring system. In the study, 36 patients had their treatment plan changed by their treating surgeon after CTRA results were provided. Their study concluded that CTRA had a sensitivity of 100% and specificity of 90% in predicting pathological fractures in comparison to the Mirels score (71% sensitive and 50% specific) (36).

The biology of pathological bone differs from that of normal bone. In pathological bone, the inherent ability to heal is impaired, hence most of these fractures require surgical fixation for stabilization (37). Standard fracture fixation techniques are often inadequate in dealing with pathological bone, hence rigid fixation techniques and strategies that account for the abnormal healing response and progressive nature of metastatic disease (locally and systemically) are required (38, 39).

In suitable cases, curettage of large lesions followed by cementing and supplementary plate fixation can provide a sufficiently robust construct to allow for early weight bearing. The ability to perform curettage on lesions prior to filling with bone cement allows for reduction in disease burden, which has been shown to reduce pain significantly (39). Leggon et al. (40) examined the torsional strength of canine femur bone that had simulated tumor defects treated with either bone cement and/or compression plating. Their result showed that the combination of bone cement and plating resulted in a construct that was 2.6 times stronger in torsional strength when compared to those with plate fixation alone (40).

Bone Metastasis by Region and Technical Consideration

Long bones

Only around 10% of all skeletal metastasis affects the long bones as opposed to the axial skeleton, which accounts for up to 70% (41, 42). In long bone metastasis, the two most common sites

are the proximal femur and proximal humerus (2). With the exception of lung carcinoma, metastatic carcinoma rarely affects areas distal to the elbows and knees (42). Due to its tendency to metastasize via the systemic arterial blood supply, lung cancer metastasis tends to be more widespread and may affect distant sites such as the hands and feet (43). Although the majority of bone metastases occur in the axial skeleton, most pathological fractures occur in the long bones (42).

Pathological fractures of the lower limb have a significant impact on a patient's mobility, whereas upper limb pathological fractures will greatly affect a patient's functional independence. Surgical management of lower limb long bone impending and pathological fractures is recommended as non-surgical management has been shown to have inferior results in controlling pain and restoring limb function (44).

Various surgical options are available, such as internal fixation with extra or intramedullary devices to endoprosthetic arthroplasty options. Bone cement (PMMA) is frequently used to fill large bone defects in order to augment fixation constructs (45). It has the advantage of immediate stability due to its high compressive strength (**Figure 7**). The use of bone graft for void filling in metastatic disease is not usually recommended, since graft incorporation is less likely in post-irradiated bone (46, 47). Moreover, the effect of adjuvant chemotherapy delays graft healing and the shortened survival of patients with metastatic disease would make prolonged immobility of the limb, while waiting for the graft to heal, untenable (42).

The choice of fixation technique is largely guided by the location of the lesion, amount of bony involvement and disease response to systemic treatment (39). It is important to choose a fixation construct with the assumption that pathological bone will not heal and that a second revision surgery may not be tolerated by patients with metastatic bone disease. The construct of choice should be robust enough to allow immediate weight bearing for the likely survival time of the patient (48).

Femur

The proximal femur is one of the most common areas for pathological fractures to occur. One third of such fractures occur at the femoral neck. Internal fixation of pathological fractures at the femoral neck generally results in an unfavorable outcome with high fixation failure rates due to poor healing potential of pathological bone (49).

Arthroplasty/endoprosthetic replacement procedures have a more reliable outcome in dealing with proximal femur pathological fractures, as it does not rely on bone healing which is necessary following treatment with internal fixation Steensma et al. compared failure rates between endoprosthetic reconstruction, intramedullary nailing and open reduction-internal fixation, in their retrospective study of 298 patients with proximal femur pathological fractures. They found that the endoprosthetic replacement group had a significantly lower failure rate (3.1%) when compared to the intramedullary nailing (6.1%) and open reduction-internal fixation (42.1%) groups (50).

In pathologic bone, the innate healing ability is impaired, which renders implant bony on-growth or in-growth unreliable. This healing impairment is even more significant in post-irradiated bone, hence cemented stem implants are recommended in this scenario (50). Cemented stems offer immediate stability while minimizing the risk of subsequent

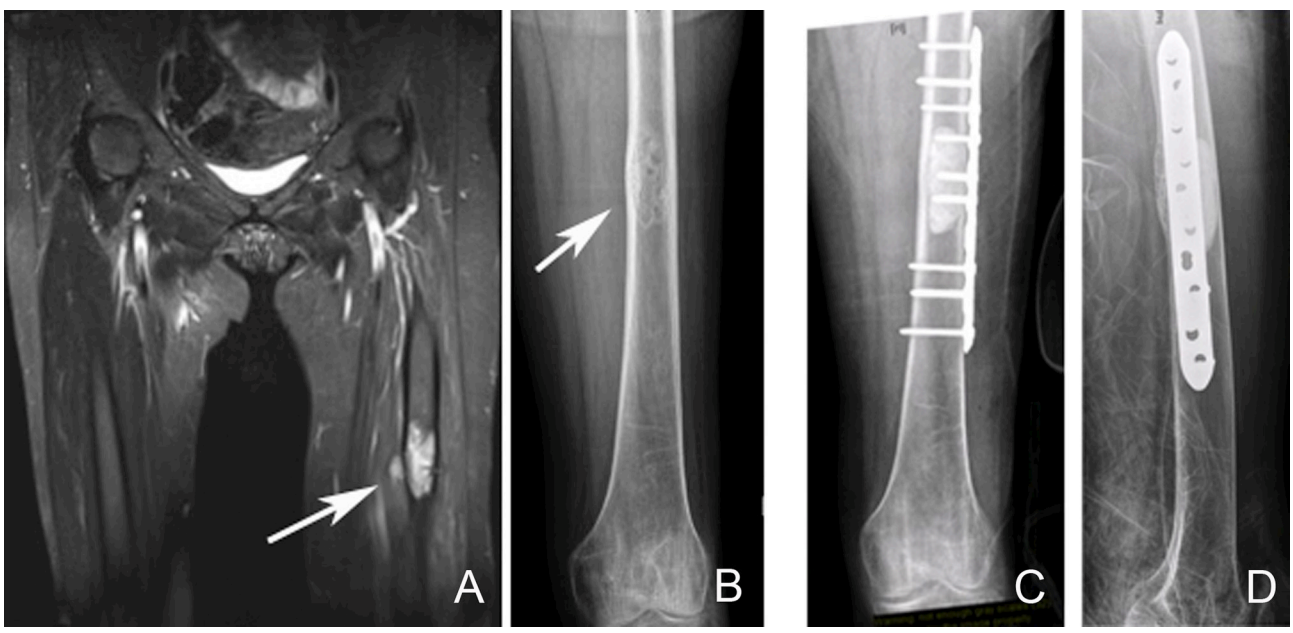

FIGURE 7 | Left femoral diaphyseal metastatic lesion from breast carcinoma treated with curettage followed by cement-plate surgical fixation. **(A)** MRI showing a left femur diaphyseal intramedullary metastatic lesion. **(B)** The same lesion seen on plain X-ray. Note the mixed lytic sclerotic appearance of the lesion. **(C,D)** AP and lateral post-operative X-rays after curettage and cement-plate surgical fixation.

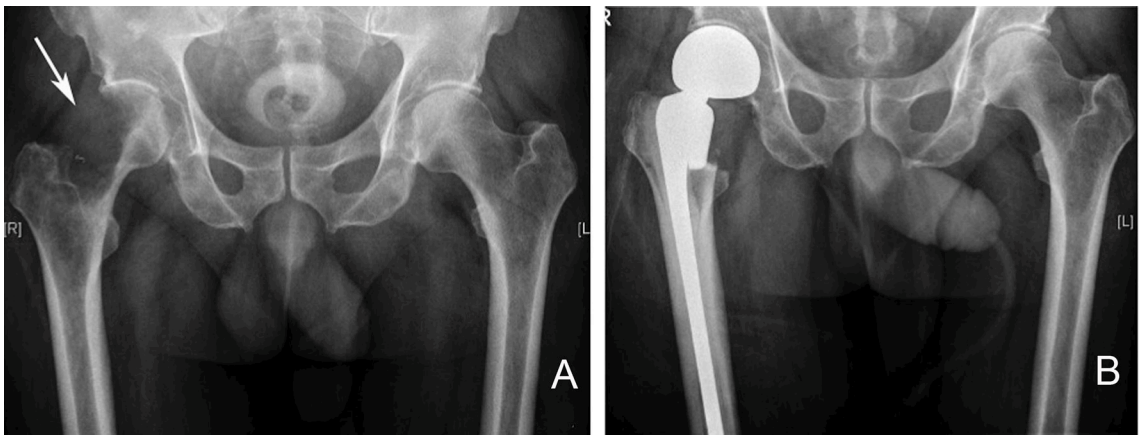

FIGURE 8 | Right proximal femur metastatic melanoma treated with a calcar replacing hemiarthroplasty. **(A)** Large destructive lytic metastatic lesion involving the head and neck of the right femur. **(B)** X-ray post reconstruction with a calcar replacing hemiarthroplasty implant.

loosening. An important consideration is the use long-stem prosthesis in order to protect the remaining femoral shaft that may be affected by future metastatic deposits due to disease progression (51).

The options of hemiarthroplasty and total hip replacement are both available, the choice of which depends on the presence of acetabular involvement. In cases where the acetabulum is spared, a hemiarthroplasty is adequate (50, 51). Involvement of the calcar femorale will necessitate the use of a femoral stem with a calcar replacing option (**Figure 8**). When there is extensive bony involvement, a proximal femur endoprosthesis is usually required (**Figure 9**). As a general rule, the femoral stem of the arthroplasty implant of choice should bypass the most distal aspect of the metastatic lesion by at least two cortical widths. This is to minimize the risk of subsequent periprosthetic fractures (52).

Peritrochanteric fractures or lesions may be addressed using plates and screws construct, such as a sliding hip screw, or a cephalomedullary device (**Figure 10**); the later has the advantage of being a load sharing device with superior biomechanical properties (53). Tanaka et al. in their retrospective study of 80 intramedullary nailing procedures for femoral metastases, reported implant survival rate of 94% at both 2 and 3 years. Three intramedullary nail implant failures occurred in those with subtrochanteric metastases (3 of 46 patients), which were subsequently revised with endoprosthetic reconstruction. They concluded that intramedullary nailing for femoral metastases is an adequate fixation method and allows for a less invasive method of fixation at a lower cost. They also emphasized that in the event of implant failure, endoprosthetic replacement is a viable salvage option (54).

Adjuncts such as PMMA (bone cement) may be used to augment the construct following tumor debulking via curettage. Since internal fixation in this region relies on bony purchase at the femoral head and neck region, it is important to rule out metastatic involvement in these areas preoperatively. In cases where there is involvement of the femoral head or neck, the use of proximal femur replacement endoprosthesis offers a more reliable solution (55).

Subtrochanteric and diaphyseal femoral involvement are most commonly addressed using locked intramedullary nails. Prophylactic fixation of impending pathological fractures is preferred, as fixation of an actual pathological fracture has been shown to result in inferior functional outcome and longer hospital stay. Arvinius et al. (56) in their retrospective study of 65 patients with metastasis to the femur, compared those who received surgical treatment prophylactically for impending fractures (21 patients) versus those who required treatment for pathological fractures (44 patients). All patients underwent fixation using a cephalomedullary device. In their study, 100% of patients who underwent prophylactic fixation for impending fracture were able to ambulate postoperatively, as compared to only 75.9% in the pathological fracture group. They concluded that patients who underwent prophylactic nailing required less postoperative blood transfusion, were able to ambulate earlier (day 4 vs. 9.7) and required shorter hospital stay (8 vs. 16 days) (56). Intramedullary nailing allows for a minimally invasive surgical approach, which minimizes intraoperative blood loss and surgical time significantly. This is particularly favorable in cases where patients are physiologically unfit to undergo lengthy surgical procedures.

The femoral subtrochanteric region undergoes tremendous amounts of stress during weight bearing, with loads up to 4–6 times body weight. Locked intramedullary nail spanning the whole femur with proximal fixation to the femoral head and neck is recommended (57). Careful perioperative workup and intraoperative monitoring is required to minimize the risk of pulmonary embolic phenomena, which may be life-threatening. Large subtrochanteric metastatic lesions may render intramedullary fixation inadequate since the implant are subjected to tremendous load-bearing stresses in such cases. This predisposes the implant to early failure and in these circumstances, proximal femoral replacement with a tumor endoprosthesis offers a more reliable solution (52, 57).

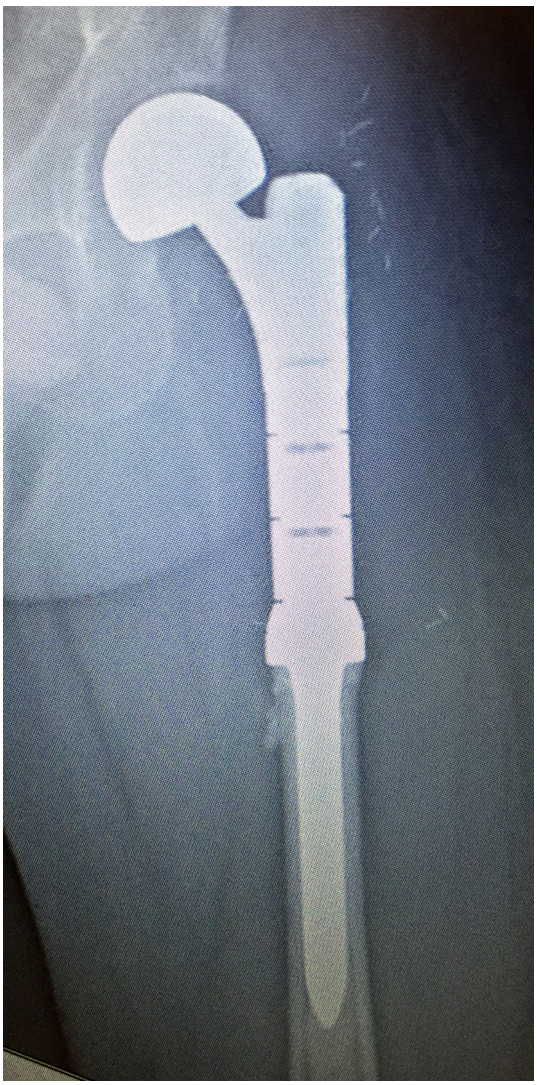

FIGURE 9 | Reconstruction using a left proximal femur replacement endoprosthesis following resection. The modularity of these implants allow for accurate restoration of limb length.

Postoperative adjuvant radiotherapy should be given to the entire bone following fixation with a locked intramedullary nail, as soon as surgical wound healing has occurred (57).

Distal femur involvement by metastatic disease may pose a challenge in deciding the most appropriate implant choice due to its periarticular location. In cases where there is joint sparring with adequate bone stock, the use of curettage and PMMA augmented plate fixation or retrograde intramedullary nailing may provide adequate fixation (2). Ahmadi et al. (58) performed biomechanical testing on 15 synthetic femurs, comparing the mechanical stiffness and strength of retrograde nail, lateral locking plate and lateral non-locking plate. In their testing, a tumor-like defect was created at the lateral metaphyseal region, which was then filled with bone cement prior to fixation. Their results show that all three fixation types were similar in terms of axial stiffness, however retrograde nail was found to be superior to non-locking plates in terms of torsional and sagittal bending stiffness. They concluded that having the advantage of less soft tissue dissection, retrograde intramedullary nailing may be a sound option in dealing with distal femoral metastatic disease (58). It is important to note that their study was conducted using synthetic femur models which lacks the anisotropic property of biological bone. The other limitation of their study is that no comparison was made with retrograde nailing without bone cement augmentation. The addition of curettage and bone cement filling would somewhat negate the less invasive advantage that retrograde nail has over other open fixation methods.

In cases where lesions involve a large part of the distal femur, resection, and reconstruction using a distal femoral replacement endoprosthesis is preferred (**Figure 11**). Guzik et al. reported their findings on 67 patients with metastatic bone disease who underwent radical resection and modular prosthesis replacement. They concluded that radical resection of the area affected by tumor followed by reconstruction using modular prosthesis provided patients with significant improvement in pain and function. They also concluded that radical resection of the tumor prevents local recurrence and future implant loosening (9).

Humerus

Following the femur, the humerus is the second most common site for bony metastasis. As with the femur, the proximal region of the humerus is the most frequently affected area, followed by the diaphysis (44). Being a non-weight bearing bone, majority of traumatic humeral fractures are amenable to conservative treatment with acceptable outcome. This is not the case in the setting of metastatic bone disease, as healing without surgical intervention is less likely. A painful, non-united humeral pathological fracture has a significant negative impact on a patient's functional independence and quality of life (44).

For lesions involving the humeral head and metaphysis, replacement with an endoprosthesis using a long cemented stem has shown reliable results. Kumar et al. in their retrospective review of 100 patients who underwent proximal humerus endoprosthesis replacement, showed reasonable functional outcome with good implant survivorship (86.5% at 20 years). They found that the length of the resected bone segment affected the functional outcome (59). Of note, their study included patients who underwent proximal humerus resection and reconstruction for primary bone sarcoma rather than metastasis.

In selected cases where the lesion is still contained within reasonable bone stock, locking plate fixation with bone cement augmentation may be sufficient (10).

Intramedullary nails are frequently used for diaphyseal lesions or pathological fractures. The ability to insert intramedullary nails via a minimally invasive approach, minimizes intraoperative blood loss and operative time significantly. The other advantage of intramedullary nail over plate fixation is the ability to span the whole bone, which minimizes the risk of future periprosthetic fractures due to disease progression.

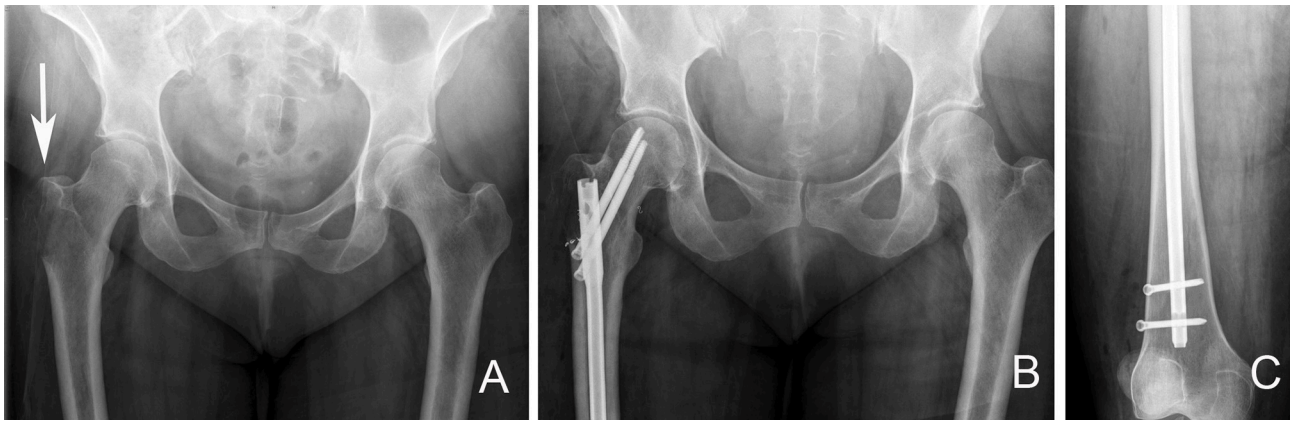

FIGURE 10 | Right proximal femur bone metastasis treated with a locked intramedullary nail. **(A)**. Destructive lytic lesion involving the proximal femur greater trochanter area (arrow). **(B)** Postoperative X-ray after fixation with a cephalomedullary nail. Note the proximal fixation spanning the femoral head and neck. **(C)** Distal locking bolt fixation to ensure axial and rotational stability.

Bone metastasis in the distal humerus can be challenging to manage. Distal periarticular lesions may require an elbow joint sacrificing procedure, such as local resection followed by reconstruction using a total elbow endoprosthesis (**Figure 12**) (60).

Tibia

Although rare, involvement of the tibia in metastatic bone disease can have a major impact on patient's mobility and quality of life. Resection of extensive proximal tibial metastasis with endoprosthesis reconstruction is a viable option, however careful planning is required, as resection around this region is associated with high rates of wound complications, often requiring additional soft tissue coverage procedures. In smaller lesions where there is no joint involvement, the option of locking plate fixation with bone cement augmentation may suffice (2). As with the femur and the humerus, diaphyseal lesions are best treated with locked intramedullary nails. This usually provides significant pain relief and allows early weight bearing (61).

The options for addressing lesions involving the distal tibia or ankle joint are more limited. Fixation using locking plates with cement augmentation may be suitable for extraarticular involvement, however involvement of the ankle joint usually requires a below knee amputation (62).

Pelvis

The pelvis and spine are the most common sites affected by metastases (6, 63–65). The pelvic region undergoes significant amounts of mechanical stress, which predisposes it to pathological fractures in the setting of bone metastasis. Surgical treatment of pelvic metastases can be challenging because of its complex bony anatomy and neighboring vital structures. Enneking et al. devised a classification system to divide the pelvis into four anatomic regions (**Figure 13**). This classification system was developed to provide a commonality of language when describing pelvic tumors and location of surgery (63).

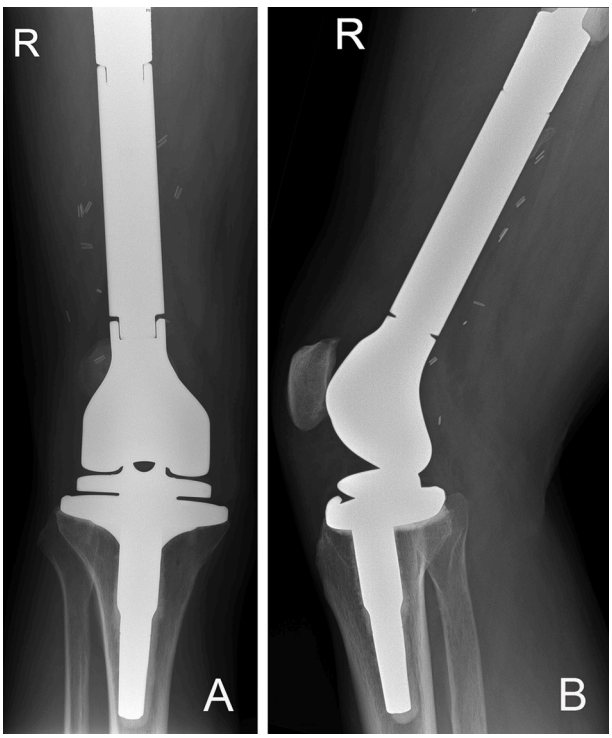

FIGURE 11 | (A) AP and **(B)** lateral radiographs of a right distal femur modular endoprosthesis. The modularity of these implants allow for reconstruction of long segments of bone defects.

Zone 1 and 3 are non-weight-bearing zones, whereas zone 2 is the articular zone through which weight bearing occurs, and zone 4 is where stress transfer occurs between the spine and the pelvis. Of note, although Zone 1 is not directly involved in weight bearing, it is an important part of the stress transfer zone in the pelvis. Fractures may occur anywhere in the pelvis but the periacetabular region (zone 2) is the

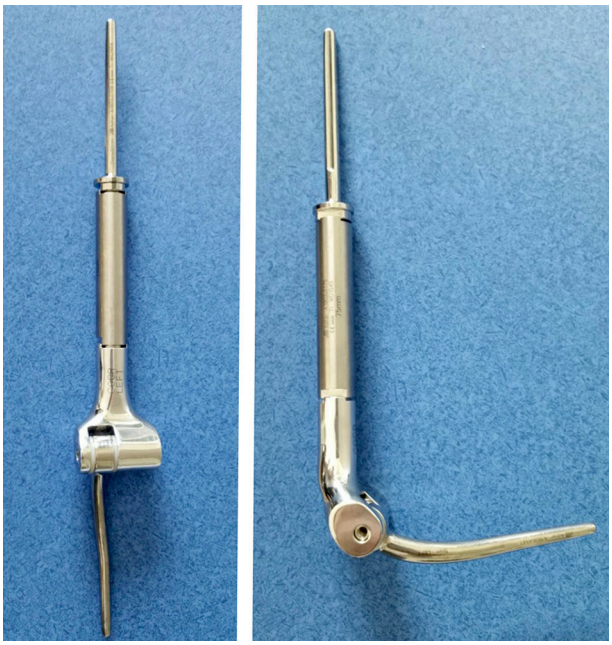

FIGURE 12 | Modular total elbow endoprosthesis implant. These implants allow for reconstruction of a large segment of bone defect while preserving some elbow function.

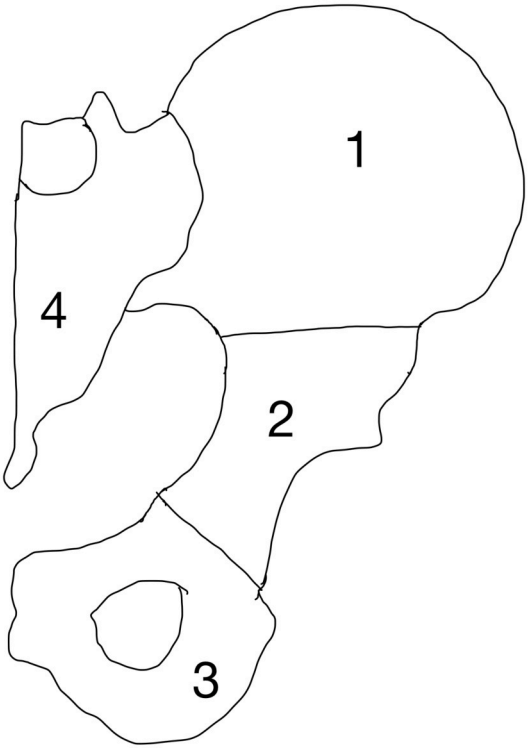

FIGURE 13 | Enneking classification system of the pelvis (Zone 1–4).

most vulnerable due to high mechanical stresses during weight bearing.

Harrington specifically classified metastases in relation to the acetabulum because of the importance of this anatomical structure. He described 4 types: Type 1 is where the subchondral bone of the acetabulum is still intact. Type 2 has medial wall involvement but an intact superior part (acetabular roof) and lateral wall. Type 3 has medial wall, lateral rim and acetabular roof involvement and Type 4 is when the acetabulum is collapsed completely (64).

Capanna et al. introduced an algorithm that divided patients into 4 classes (**Table 3**) based on the nature of the metastatic disease and its location (6).

Muller and Capanna published a guideline for the surgical treatment of metastatic pelvic lesions, taking into consideration the Enneking and Harrington classification for acetabular defects (65).

All patients in Capanna class 1, 2, and 3 should be considered for surgical treatment. Patients in class 1 may be treated aggressively with curative intent. If the lesion is in zone 1 or 3, reconstruction may not always be necessary. For lesions in zone 2, reconstruction with prosthetic or biologic construct is required (64).

The option of treatment for patients in class 2 and 3 is to provide a durable construct, although surgery may not be performed with curative intent. The aim is to achieve a marginal or intralesional resection followed by reconstruction options according to the amount of the periacetabular bone loss. Harrington Type 1 defects are usually addressed by curettage and cementation or conventional arthroplasty. In Type 2 defects, where there is medial acetabular wall involvement, joint replacement with the use of reinforcement ring is necessary. In Type 3 defects, total hip replacement with cementation of bone defects reinforced with transosseous pins is the recommended surgical option. In Type 4 defects, the options include pelvic megaprosthesis, saddle femoral prosthesis or massive allograft with joint replacement.

TABLE 3 | Capanna classification.

Capanna class	Pelvis
Class 1	Solitary metastatic lesion Primary with good prognosis Interval over 3 years since detection of primary tumor
Class 2	Pathological fracture in the periacetabular region
Class 3	Supra-acetabular osteolytic lesion
Class 4	Multiple osteoblastic lesions at all sites Osteolytic or mixed lesions in iliac wing and anterior pelvis Small periacetabular osteolytic lesions

Patients in Capanna class 4 should be treated conservatively (chemotherapy, radiotherapy or hormonal therapy). The aim of treatment in this class is to palliate pain in order to improve quality of life (65).

In dealing with highly vascular metastatic lesions, such as that from renal and thyroid carcinoma, it is recommended that preoperative angiographic selective arterial embolization be performed in order to minimize intraoperative blood loss (**Figure 14**) (66–68). Chatziioannou et al. conducted

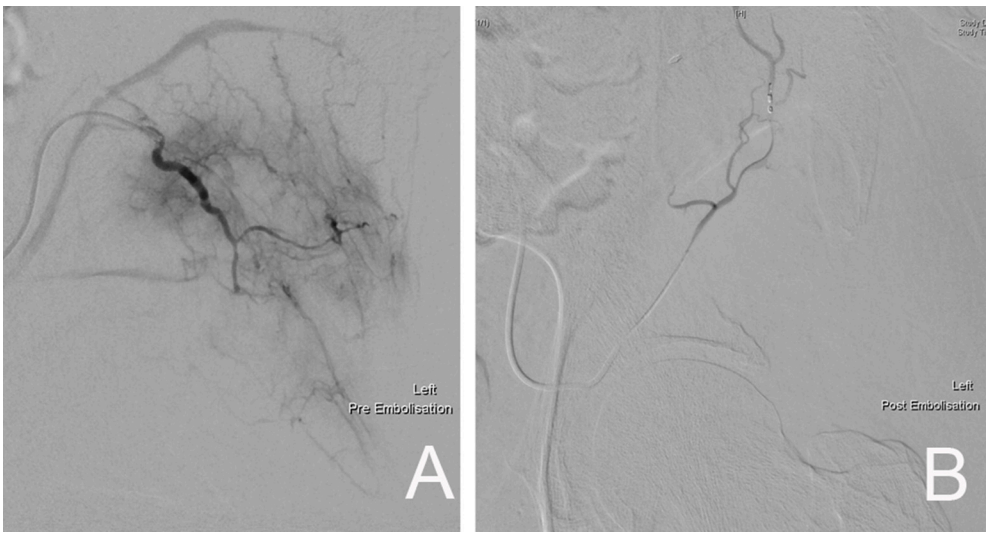

FIGURE 14 | (A) Pre-embolization angiography demonstrating the rich blood supply to the left pelvic metastatic lesion. **(B)** Post-embolization fluoroscopic image showing complete devascularization of the metastatic lesion.

a retrospective study on the effectiveness of preoperative embolization in bone metastasis from renal cell carcinoma. Their study included 28 preoperative embolization procedures, which were divided into those with complete and incomplete revascularization of lesions post-embolization. Their findings show that complete devascularization of metastatic lesions resulted in significantly less intraoperative mean blood loss (535 $\pm$ 390 vs. 1.247 $\pm$ 1.047 ml) and transfusion requirements (1.3 $\pm$ 1 vs. 2.4 $\pm$ 1.2 units). They highlighted the importance of embolizing every feeder vessel to the metastatic lesion to achieve complete devascularization, since an incomplete result significantly increased intraoperative blood loss and transfusion requirements (67).

ADJUNCTIVE MANAGEMENT

Radiation Therapy

Radiation therapy plays an important role in the treatment of skeletal metastasis, both as an adjunct to other treatments and as monotherapy (69). Its uses have been shown to be effective in reducing pain, preventing pathological fractures and minimizing the need for further surgery (70).

Radiation therapy is commonly administered as a single or multiple fraction therapy. The type of tumor and the general condition of the patient usually dictates which method of radiation therapy is to be administered (69, 70). De Felice et al. suggested that in uncomplicated painful bone metastases, a single fraction of 8 Gy for three-dimensional conformal radiation therapy (3D-CRT) or 15–24 Gy stereotactic body radiation should be given; in cases of pathological fractures, the same authors suggested 5 fractions of 20 Gy or 10 fractions of 30 Gy for 3D-CRT to be administered (69). Lutz et al. (71) in their ASTRO Evidence-Base Guideline in 2011, update in 2016, recommended a single dose of 8 Gy fraction for targeted bone lesion. Should radiation therapy be deemed necessary as a post-operative adjunct, they suggested the use of multifractionated radiation therapy over single-fraction therapy. They concluded that the need for re-irradiation in those undergoing single-fraction therapy is up to 20% in contrast to only 8% in those who received multi-fraction therapy (72).

Despite its effectiveness as a treatment modality in the treatment of metastatic bone disease, it is important to consider the dose-dependent toxicity associated with radiation therapy. Both systemic and local side effects have been reported (2–40%), which may include nausea, vomiting and local soft tissue generated pain (69, 70). The presence of multiple symptomatic metastases and the proximity of the metastases to critical structures may render radiation therapy unsuitable in certain cases (73).

Antiresorptives

Antiresorptive therapies are commonly used for the treatment of osteoporosis. The five main classes of antiresorptives used clinically include: Bisphosphonates, estrogens, calcitonin, selective estrogen receptor modulators (SERMs), and monoclonal antibodies such as Denosumab.

Bisphosphonates are potent inhibitors of osteoclast-mediated bone resorption (74, 75). In recent years it has become standard of treatment for lytic lesions, such as found in multiple myeloma and breast cancer (75). Bisphosphonate use in the setting of metastatic bone disease has been shown to cause recalcification of lytic metastasis (74, 75), which in turn reduces pain and minimizes the development of further lesions (76). Some of the most common Bisphosphonates used include Zolendronic acid, Clodronate, and Pamidronate (77, 78).

Bisphosphonates, in particular Zolendronic acid has been shown to have anti-tumor effects through the inhibition of

tumor cell proliferation, induction of apoptosis, inhibition of angiogenesis and other important effects (79–81). Terpos et al. in their recent analysis comparing Bisphosphonates vs. either placebo or no treatment, demonstrated that the use of Bisphosphonates in the treatment of patients with multiple myeloma had reduced the rate of pathological fractures. They also concluded that Zolendronic acid appeared to be superior when compared to other Bisphosphonates (76).

O'Carrigan et al. reviewed 44 randomized controlled trials which included 37.302 patients with breast cancer. Included were patients with early breast cancer, advanced breast cancer without metastasis and those with metastatic disease. They compared the effects of Bisphosphonates to placebo, other Bisphosphonates, other antiresorptive agents, and also examined the effect of early versus delayed treatment with Bisphosphonates. They concluded that in patients with early breast cancer, Bisphosphonates reduced the risk of bone metastasis and improved overall survival when compared to placebo or no treatment. In patients who have metastatic disease, Bisphosphonates were found to reduce the risk of skeletal related events (SRE) and appeared to reduce bone pain when compared to placebo or no Bisphosphonates (82).

In breast cancer, the role of Bisphosphonates has been well established, however there is a lack of consensus regarding the duration of treatment and whether all metastatic breast cancer patients should receive Bisphosphonates. Hillner et al. in their American Society of Clinical Oncology guideline on the role of Bisphosphonates in breast cancer, acknowledged that the duration of treatment is not well defined, however reported that the majority of patients tolerated treatment beyond 2 years. They recommended that once treatment is commenced, it should be continued until there is a decline in patient's performance status. They also concluded that patients who have multiple painful metastasis and metastases to weight-bearing bones, should be commenced on Bisphosphonates (83).

Denosumab is a fully human IgG2 monoclonal antibody that blocks RANKL with subsequent reduction in osteoclastic bone resorption, giving a Bisphosphonate-like action. Numerous studies have demonstrated that the use of Denosumab in metastatic bone disease have significantly reduced the development of skeletal-related events associated with bone metastases (84–86). Recent studies have also shown that blocking RANKL action on tumor cells had an inhibitory effect on tumor cells in *in vitro* and animal models, although the exact mechanism is not fully understood (87, 88). Gonzalez-Suarez et al. published their study on the role of RANKL on RANK expressing tumor cells in mice. They demonstrated that the inhibition of RANKL in breast cancer had resulted in a decrease in associated lung metastasis (89).

CONCLUSION

Despite advances in medical treatment in cancer and the steady improvement in overall survival of cancer patients, the management of metastatic bone disease remains challenging. The treatment of metastatic bone disease is multi-modal and often includes a combination of medical therapy, radiation therapy, or surgery.

Advances in modern medical diagnostic imaging have allowed earlier detection of bone metastasis in the course of disease, enabling treating surgeons to intervene before pathological fractures occur. A vast array of implants and treatment options are available in our current modern orthopedic surgery arena, and these enhance the role of orthopedic surgeons in decision making when considering the best surgical treatment strategy. The goal of surgical treatment is to alleviate pain, restore function, and ultimately improve the quality of life of patients. The complexity of the management of patients with metastatic bone disease mandates a multidisciplinary approach with careful planning, in order to achieve the best and safest outcome for patients.

AUTHOR'S NOTE

All deidentified images used in figures are from the image database of St. Vincent's Hospital, Melbourne, Australia.

AUTHOR CONTRIBUTIONS

HS, LP, and PC: article conception and structuration. HS and LP: literature search and manuscript drafting. HS, LP, and PC: critical revision of manuscript content. PC: approving final version of manuscript.

REFERENCES

1. Ratasvuori M, Wedin R, Keller J, Nottrott M, Zaikova O, Bergh P, et al. Insight opinion to surgically treated metastatic bone disease: Scandinavian Sarcoma Group Skeletal Metastasis Registry report of 1195 operated skeletal metastasis. *Surg Oncol.* (2013) 22:132–38. doi: 10.1016/j.suronc.2013.02.008
2. Ashford RU, Benjamin L, Pendlebury S, Stalley PD. The modern surgical and non-surgical management of appendicular skeletal metastases. *Orthop Trauma* (2012) 26:184–99. doi: 10.1016/j.mporth.2012.02.002
3. Coleman RE. Metastatic bone disease: clinical features, pathophysiology and treatment strategies. *Cancer Treat Rev.* (2001) 27:165–76. doi: 10.1053/ctrv.2000.0210
4. Bauer HC. Controversies in the surgical management of skeletal metastases. *J Bone Joint Surg Br.* (2005) 87:608–17. doi: 10.1302/0301-620X.87B5.16021
5. Janjan N. Bone metastases: approaches to management. *Semin Oncol.* (2001) 28:28–34. doi: 10.1016/S0093-7754(01)90229-5
6. Capanna R, Campanacci DA. The treatment of metastases in the appendicular skeleton. *J Bone Joint Surg Br.* (2001) 83:471–81. doi: 10.1302/0301-620X.83B4.12202
7. Lichtenberg FR. The impact of pharmaceutical innovation on premature mortality, hospital separations, and cancer survival in Australia. *Econ Rec.* (2017) 93:353–78. doi: 10.1111/1475-4932.12332
8. Jacofsky DJ, Papagelopoulos PJ, Sim FH. Advances and challenges in the surgical treatment of metastatic bone disease. *Clin Orthop.* (2003) (415S):14–8. doi: 10.1097/01.blo0000093046.96273.07
9. Guzik G. Results of the treatment of bone metastases with modular prosthetic replacement—analysis of 67 patients. *J. Orthop Surg Res.* (2016) 11:20. doi: 10.1186/s13018-016-0353-6
10. Gregory JJ, Ockendon M, Cribb GL, Cool PW, Williams DH. The outcome of locking plate fixation for the treatment of periarticular metastases. *Acta Orthop Belg.* (2011) 77:362–70. doi: 10.1302/1358-992X.94BSUPP_XXX.BOOS2011-012

11. British Association of Surgical Oncology Guidelines. The management of metastatic bone disease in the United Kingdom. The Breast Specialty Group of the British Association of Surgical Oncology. *Eur J Surg Oncol*. (1999) 25:3–23
12. Adams SC, Potter BK, Mahmood Z, Pitcher JD, Temple HT. Consequences and prevention of inadvertent internal fixation of primary osseous sarcomas. *Clin Orthop Relat Res*. (2009) 467:519–25. doi: 10.1007/s11999-008-0546-3
13. Guise TA, Mohammad KS, Clines G, Stebbins EG, Wong DH, Higgins LS, et al. Basic mechanism responsible for osteolytic and osteoblastic bone metastases. *Clin Cancer Res*. (2006) 12:6213s−6s. doi: 10.1158/1078-0432.CCR-06-1007
14. Boyce BF, Yoneda. T, Guise TA. Factors regulating the growth of metastatic cancer in bone. *Endocr Realt Cancer* (1999) 6:333–47. doi: 10.1677/erc.0.0060333
15. Rosenthal DI. Radiologic diagnosis of bone metastases. *Cancer* (1997) 80(Suppl. 8):1595–607.
16. Even-Sapir E. Imaging of malignant bone involvement by morphologic, scintigraphic, and hybrid modalities. *J Nucl Med*. (2005) 46:1356–67
17. Bristow AR, Agrawal A, Evans AJ, Burrell HC, Cornford EJ, James JJ, et al. Can computerized tomography replace bone scintigraphy in detecting bone metastases from breast cancer? A prospective study. *Breast* (2008) 17:98–103. doi: 10.1016/j.breast.2007.07.042
18. Yu HH, Tsai YY, Hoffe SE. Overview of diagnosis and management of metastatic disease to bone. *Cancer Control* (2012) 19:84–91. doi: 10.1177/107327481201900202
19. Yang HL, Liu T, Wang XM, Xu Y, Deng SM. Diagnosis of bone metastases: a meta-analysis comparing 1^8FDG PET, CT, MRI and bone scintigraphy. *Eur Radiol*. (2011) 21:2604–17. doi: 10.1016/j.ejrad.2011.01.126.
20. Choi J, Raghavan M. Diagnostic imaging and image-guided therapy of skeletal metastases. *Cancer Control* (2012) 19:102–12. doi: 10.1177/107327481201900204
21. Heindel W, Gübitz R, Vieth V, Weckesser M, Schober O, Schäfers M. The diagnostic imaging of bone metastases. *Dtsch Arztebl Int*. (2014) 111:741–47. doi: 10.3238/arztebl.2014.0741
22. Beheshti M, Vali R, Waldenberger P, Fitz F, Nader M, Hammer J, et al. The use of F-18 choline PET in the assessment of bone metastases in prostate cancer: correlation with morphological changes on CT. *Mol Imaging Biol*. (2010) 12:98–107. doi: 10.1007/s11307-009-0239-7
23. Ball AB, Fisher C, Pittam M, Watkins RM, Westbury G. Diagnosis of soft tissue tumours by tru-cut biopsy. *Br J Surg*. (1990) 77:756–8. doi: 10.1002/bjs.1800770713
24. Kissin MW, Fisher C, Carter RL, Horton LW, Westbury G. Value of tru-cut biopsy in the diagnosis of soft tissue tumours. *Br J Surg*. (1986) 73:742–4. doi: 10.1002/bjs.1800730921
25. Pramesh CS, Deshpande MS, Pardiwala DN, Agarwal MG, Puri A. Core needle biopsy for bone tumours. *Eur J Surg Oncol*. (2001) 27:668–71. doi: 10.1053/ejso.2001.1198
26. Lin YC, Wu JS, Kung JW. Image guided biopsy of musculoskeletal lesions with low diagnostic yield. *Curr Med Imaging Rev*. (2017) 13:260–67. doi: 10.2174/1573405612666160610090233
27. Spence GM, Dunning MT, Cannon SR, Briggs TW. The hazard of retrograde nailing in pathological fractures: three cases involving primary musculoskeletal malignancy. *Injury* (2002) 33:533–38. doi: 10.1016/S0020-1383(02)00035-9
28. Fottner A, Szalantzy M, Wirthmann L, Stähler M, Baur-Melnyk A, Jansson V, et al. Bone metastases from renal cell carcinoma: patient survival after surgical treatment. *BMC Musculoskelet Disord*. (2010) 11:145. doi: 10.1186/1471-2474-11-145
29. Les KA, Nicholas RW, Rougraff B. Local progression after operative treatment of metastatic kidney cancer. *Clin Orthop Relat Res*. (2001) 390:206–11. doi: 10.1097/00003086-200109000-00023
30. Kirkinis MN, Lyne CJ, Wilson MD, Choong PFM. Metastatic bone disease: a review of survival, prognostic factors and outcomes following surgical treatment of the appendicular skeleton. *Eur J Surg Oncol*. (2016) 42:1787–97. doi: 10.1016/j.ejso.2016.03.036
31. Forsberg JA, Eberhardt J, Boland PJ, Wedin R, Healey JH. Estimating survival in patients with operable skeletal metastases: an application of a Bayesian belief network. *PLoS ONE* (2011) 6:e19956. doi: 10.1371/journal.pone.0019956
32. Beals RK, Lawton GD, Snell WE. Prophylactic internal fixation of the femur in metastatic breast cancer. *Cancer* (1971) 28:1350–4.
33. Fidler M. Prophylactic internal fixation of secondary neoplastic deposits in long bones. *Br Med J*. (1973) 1:341–3. doi: 10.1136/bmj.1.5849.341
34. Harrington KD. New trends in the management of lower extremity metastases. *Clin Orthop Relat Res*. (1982) 169:53–61. doi: 10.1097/00003086-198209000-00008
35. Mirels H. Metastatic disease in long bones. a proposed scoring system for diagnosing impending pathologic fractures. *Clin Orthop Relat Res*. (1989) 249:256–64. doi: 10.1097/00003086-198912000-00027
36. Nazarian A, Entezari V, Zurakowski D, Calderon N, Hipp JA, Villa-Camacho JC, et al. Treatment planning and fracture prediction in patients with skeletalmetastasis with CT-based rigidity analysis *Clin Cancer Res*. (2015) 21:2514–9. doi: 10.1158/1078-0432.CCR-14-2668
37. Gainor BJ, Buchert P. Fracture healing in metastatic bone disease. *Clin Orthop Relat Res*. (1983) 178:297–302. doi: 10.1097/00003086-198309000-00041
38. Scolaro AJ, Lackman RD. Surgical management of metastatic long bone fracture: principles and techniques. *J Am Acad Orthop Surg*. (2014) 22:90–100. doi: 10.5435/JAAOS-22-02-90
39. Aboulafia AJ, Levine AM, Schmidt D, Aboulafia D. Surgical therapy of bone metastases. *Semin Oncol*. (2007) 34:206–14. doi: 10.1053/j.seminoncol.2007.03.002
40. Leggon RE, Lindsey RW, Panjabi MM. Strength reduction and the effects of treatment of long bones with diaphyseal defects involving 50% of the cortex. *J Orthop Res*. (1988) 6:540–6.
41. Coleman RE. Clinical features of metastatic bone disease and risk of skeletal morbidity. *Clin Cancer Res*. (2006) 12:6243s−9s. doi: 10.1158/1078-0432.CCR-06-0931
42. Hage WD, Aboulafia AJ, Aboulafia DM. Incidence, location, and diagnostic evaluation of metastatic bone disease. *Orthop Clin North Am*. (2000) 31:515–28. doi: 10.1016/S0030-5898(05)70171-1
43. Sherry HS, Levy RN, Siffert RS. Metastatic disease of bone in orthopedic surgery. *Clin Orthop*. (1982) 169:44–52.
44. Tillman RM. The role of the orthopaedic surgeon in metastatic disease of the appendicular skeleton. Working party on metastatic bone disease in breast cancer in the UK. *J Bone Joint Surg Br*. (1999) 81:1–2.
45. Harrington KD, Johnston JO, Turner RH, Green DL. The use of methylmethacrylate as an adjunct in the internal fixation of malignant neoplastic fractures. *J Bone Joint Surg Am*. (1972) 54:1665–76.
46. Hornicek FJ, Gebhardt MC, Tomford WW, Sorger JI, Zavatta M, Menzner JP, et al. Factors affecting nonunion of the allograft-host junction. *Clin Orthop Relat Res*. (2001) 382:87–98. doi: 10.1097/00003086-200101000-00014
47. Ehrhart NP, Eurell JA, Constable PD, Gaddy D, Nicholas RW. The effect of host tissue irradiation on large-segment allograft incorporation. *Clin Orthop Relat Res*. (2005) 435:43–51. doi: 10.1097/01.blo.0000165732.64757.bb
48. Aaron AD. Current concepts review-treatment of metastatic adenocarcinoma of the pelvis and the extremities. *J Bone Joint Surg*. (1997) 79:917–32.
49. Damron TA, Sim FH. Surgical treatment for metastatic disease of the pelvis and proximal end of the femur. *J Bone Joint Surg Am*. (2000) 49:114–26. doi: 10.2106/00004623-200001000-00015
50. Steensma M, Boland PJ, Morris CD. Athanasian E, Healey JH. Endoprosthetic treatment is more durable for pathologic proximal femur fractures. *Clin Orthop Relat Res*. (2012) 470:920–6. doi: 10.1007/s11999-011-2047-z
51. Morris HG, Capanna R, Del Ben M, Campanacci D. Prosthetic reconstruction of the proximal femur after resection for bone tumors. *J Arthroplasty* (1995) 10:293–9.
52. Ashford RU, Hanna SA, Park DH, Pollock RC, Skinner JA, Briggs TW, et al. Proximal femoral replacements for metastatic bone disease: financial implications for sarcoma units. *Int Orthop*. (2010) 34:709–13. doi: 10.1007/s00264-009-0838-6
53. Weber KL, Randall RL, Grossman S, Parvizi J. Management of lower-extremity bone metastases. *J Bone Joint Surg Am*. (2006) 88(Suppl. 4):11–9. doi: 10.2106/JBJS.F.00635
54. Takaaki T, Imanishi J, Charoenlap C, Choong PFM. Intramedullary nailing has sufficient durability for metastatic femoral fractures. *World J Surg Oncol*. (2016) 14:80. doi: 10.1186/s12957-016-0836-2

55. Wedin R, Bauer HC. Surgical treatment of skeletal metastatic lesions of the proximal femur: endoprosthesis or reconstruction nail? *J Bone Joint Surg Br*. (2005) 87B:1653–7. doi: 10.1302/0301-620X.87B12.16629
56. Arvinius C, Parra JL, Mateo LS, Maroto RG, Borrego AF, Stern LL. Benefits of early intramedullary nailing in femoral metastases. *Int Orthop*. (2014) 38:129–32. doi: 10.1007/s00264-013-2108-x
57. Ramakrishnan M, Prasad SS, Parkinson RW, Kaye JC. Management of sub-trochanteric femoral fractures and metastases using long proximal femoral nail. *Injury* (2004) 35:184–90. doi: 10.1016/S0020-1383(03)00101-3
58. Ahmadi S, Shah S, Wunder JS, Schemitsch EH, Ferguson PC, Zdero R. The biomechanics of three different fracture fixation implants for distal femur repair in the presence of a tumor-like defect. *Proc Inst Mech Eng H* (2013) 227:78–86. doi: 10.1177/0954411912454368
59. Kumar D, Grimer RJ, Abudu A, Carter SR, Tillman RM. Endoprosthetic replacement of the proximal humerus: long term results. *J Bone Joint Surg Br*. (2003) 85:717–22. doi: 10.1302/0301-620X.85B5.13838
60. Hanna SA, David LA, Aston WJ, Gikas PD, Blunn GW, Cannon SR, et al. Endoprosthetic replacement of the distal humerus following resection of bone tumours. *J Bone Joint Surg Br*. (2007) 89:1498–503. doi: 10.1302/0301-620X.89B11.19577
61. De Geeter K, Reynders P, Samson I. Metastatic fractures of the tibia. *Acta Orthop Belg*. (2001) 67:54–9.
62. Ashford RU. Palliative orthopaedic surgery for skeletal metastases. *Eur Oncol*. (2009) 51:30–4. doi: 10.17925/EOH.2009.05.1.30
63. Enneking W, Dunham W, Gebhardt M, Malawar M, Pritchard D. A system for the classification of skeletal resections. *La Chirurgia degli Organi di Movimento* (1990) 75:217–40.
64. Harrington KD. The management of acetabular insufficiency secondary to metastatic malignant disease. *J Bone Joint Surg Am*. (1981) 63:653–4.
65. Daniel AM, Capanna R. The surgical treatment of pelvic bone metastases. *Adv Orthop*. (2015) 2015:525363. doi: 10.1155/2015/525363
66. Robial N, Charles YP, Bogorin I, Godet J, Beaujeux R, Boujan F. Is preoperative embolization a prerequisite for spinal metastases surgical management? *Orthop Traumatol Surg Res*. (2012) 98:536–42. doi: 10.1016/j.otsr.2012.03.008
67. Chatziioannou AN, Johnson ME, Pneumaticos SG, Lawrence DD, Carrasco CH. Preoperative embolization of bone metastases from renal cell carcinoma. *Eur Radiol*. (2000) 10:593–96. doi: 10.1007/s003300050969
68. Rossi G, Mavrogenis AF, Casadei R, Bianchi G, Romagnoli C, Rimondi E, et al. Embolisation of bone metastases from renal cancer. Radiol Med. (2013) 118:291–302. doi: 10.1007/s11547-012-0802-4
69. Francesca DF, Andrea P, Daniela M, Vincenzo T. The role of radiation therapy in bone metastases management. *Oncotarget* (2017) 8:25691–9. doi: 10.18632/oncotarget.14823
70. Howell DD, James JL, Hartsell WF, Suntharalingam M, Machtay M, Suh JH, et al. Single-fraction radiotherapy versus multifraction radiotherapy for palliation of painful vertebral bone metastases-equivalent efficacy, less toxicity, more convenient: a subset analysis of Radiation Therapy Oncology Group trial 97–14. *Cancer* (2013) 119:888–96. doi: 10.1002/cncr.27616
71. Lutz S, Berk L, Chang E, Chow E, Hahn C, Hoskin P. et al. Palliative radiotherapy for bone metastases: an ASTRO evidence-based guideline. *Int J Radiat Oncol Biol Phys*. (2011) 79:965–76. doi: 10.1016/j.ijrobp.2010.11.026
72. Lutz S, Balboni T, Jones J, Lo S, Petit J, Rich SE, Wong R, Hahn C. Palliative radiation therapy for bone metastases: update of an ASTRO Evidence-Based Guideline. *Pract Radiat Oncol*. (2017) 7:4–2. doi: 10.1016/j.prro.2016.08.001
73. Paice JA, Ferrell B. The management of cancer pain. *CA Cancer J Clin*. (2011) 61:157–82. doi: 10.3322/caac.20112
74. Coleman R, Body JJ, Aapro M, Hadji P, Herrstedt J, ESMO Guidelines Working Group. Bone health in cancer patients: ESMO clinical practice guidelines. *Ann Oncol*. (2014) 25:124–137. doi: 10.1093/annonc/mdu103
75. Boely JJ, Mancini I. Bisphoosphonate for cancer patients: why, hox and when? *Support Care Cancer* (2002) 10:10399–407. doi: 10.1007/s005200100292
76. Terpos E1, Berenson J, Raje N, Roodman GD. Management of bone disease in multiple myeloma. *Expert Rev Hematol*. (2014) 7:113–25. doi: 10.1586/17474086.2013.874943
77. Morgan GJ, Davies FE, Gregory WM, Szubert AJ, Bell SE, Drayson MT, et al. Effects of induction and maintenance plus long-term bisphosphonates on bone disease in patients with multiple myeloma: the Medical Research Council Myeloma IX Trial. *Blood* (2012) 119:5374–83. doi: 10.1182/blood-2011-11-392522
78. Morgan GJ, Davies FE, Gregory WM, Cocks K, Bell SE, Szubert AJ, et al. First-line treatment with zoledronic acid as compared with clodronic acid in multiple myeloma (MRC Myeloma IX): a randomised controlled trial. *Lancet* (2010) 376:1989–99. doi: 10.1016/S0140-6736(10)62051-X
79. Comito G, Pons Segura C, Taddei ML, Lanciotti M, Serni S, Morandi A. et al. Zoledronic acid impairs stromal reactivity by inhibiting M2-macrophages polarization and prostate cancer-associated fibroblasts. *Oncotarget* (2017) 8:118–32. doi: 10.18632/oncotarget.9497
80. Zekri J, Mansour M, Karim SM. The anti-tumour effects of zoledronic acid. *J Bone Oncol*. (2014) 3:25–35. doi: 10.1016/j.jbo.2013.12.001
81. Bosch-Barrera J, Merajver SD, Menéndez JA, Van Poznak C. Direct antitumour activity of zoledronic acid: preclinical and clinical data .*Clin Transl Oncol*. (2011) 13:148–55. doi: 10.1007/s12094-011-0634-9
82. O'Carrigan B, Wong MH, Willson ML, Stockler MR, Pavlakis N, Goodwin A. Bisphosphonates and other bone agents for breast cancer. *Cochrane Database Syst Rev*. (2017) 10:CD003474. doi: 10.1002/14651858.CD003474
83. Hillner BE, Ingle JN, Berenson JR, Janjan NA, Albain KS, Lipton A. et al. American Society of Clinical Oncology guideline on the role of bisphosphonates in breast cancer. *J Clin Oncol*. (2000) 18:1378–91. doi: 10.1200/JCO.2000.18.6.1378
84. Gnant M, Pfeiler G, Dubsky PC, Hubalek M, Greil R, Jakesz R, et al. Abstract S2–02: the impact of adjuvant denosumab on diseasefree survival: results from 3,425 postmenopausal patients of the ABCSG-18 trial. *Cancer Res.* (2016) 76(Suppl. 4):S2. doi: 10.1158/1538-7445.SABCS15-S2-02
85. Goss PE, Barrios CH, Bell R, Finkelstein D, Iwata H, Martin M, et al. A randomized, double-blind, placebo-controlled multicenter phase III study comparing denosumab with placebo as adjuvant treatment for women with early-stage breast cancer who are at high risk of disease recurrence (D-CARE). *J Clin Oncol*. (2011) 29(suppl. 15):TPS152. doi: 10.1200/jco.2011.29.15_suppl.tps152
86. Smith MR, Saad F, Coleman R, Shore N, Fizazi K, Tombal B. et al. Denosumab and bone-metastasis-free survival in men with castration-resistant prostate cancer: results of a phase 3, randomised, placebo controlled trial. *Lancet* (2012) 379:39–46. doi: 10.1016/S0140-6736(11)61226-9
87. Armstrong AP, Miller RE, Jones JC, Zhang J, Keller ET, Dougall WC. RANKL acts directly on RANK-expressing prostate tumor cells and mediates migration and expression of tumor metastasis genes. *Prostate* (2008) 68:92–104. doi: 10.1002/pros.20678
88. Jones DH, Nakashima T, Sanchez OH, Kozieradzki I, Komarova SV, Sarosi I. et al. Regulation of cancer cell migration and bone metastasis by RANKL. *Nature* (2006) 440:692–6. doi: 10.1038/nature04524
89. Gonzalez-Suarez E, Jacob AP, Jones J, Miller R, Roudier-Meyer MP, Erwert R, et al. RANK ligand mediates progestin-induced mammary epithelial proliferation and carcinogenesis. *Nature* (2010) 468:103–7. doi: 10.1038/nature09495

Conflict of Interest Statement: The authors declare that the research was conducted in the absence of any commercial or financial relationships that could be construed as a potential conflict of interest.

Advantages of publishing in Frontiers

OPEN ACCESS
Articles are free to read for greatest visibility and readership

FAST PUBLICATION
Around 90 days from submission to decision

HIGH QUALITY PEER-REVIEW
Rigorous, collaborative, and constructive peer-review

TRANSPARENT PEER-REVIEW
Editors and reviewers acknowledged by name on published articles

Frontiers
Avenue du Tribunal-Fédéral 34
1005 Lausanne | Switzerland

Visit us: www.frontiersin.org
Contact us: info@frontiersin.org | +41 21 510 17 00

REPRODUCIBILITY OF RESEARCH
Support open data and methods to enhance research reproducibility

DIGITAL PUBLISHING
Articles designed for optimal readership across devices

FOLLOW US
@frontiersin

IMPACT METRICS
Advanced article metrics track visibility across digital media

EXTENSIVE PROMOTION
Marketing and promotion of impactful research

LOOP RESEARCH NETWORK
Our network increases your article's readership